PHYSIOLOGICAL AND PHARMACOLOGICAL EFFECTS OF ZINC ON RAT HIPPOCAMPAL PYRAMIDAL NEURONES *IN VITRO*

A thesis submitted for the Degree of Doctor of Philosophy
in the University of London, Faculty of Science

by

Xinmin Xie, B.Sc. (Hons.), M.Sc., M.D.

Department of Pharmacology,
School of Pharmacy,
29/39, Brunswick Square,
London WC1N 1AX.

March 1992

ABSTRACT

The mammalian brain contains an abundance of zinc and stimulation of the mossy fibres in the hippocampus can induce Zn^{2+} release. However, a physiological role for endogenous zinc in synaptic transmission has not been shown. The present study was undertaken to address this fundamental issue by using electrophysiological techniques, including intracellular and simultaneous extracellular recordings from rat hippocampal brain slices *in vitro*. Pyramidal neurones were identified by histological methods using intracellular labelling based on the avidin-biotin system.

Exogenous zinc (50-300μM) induced the appearance of rhythmically occurring giant depolarizing synaptic potentials (GDPs) in adult hippocampal neurones (n=245). These zinc-induced GDPs were mediated by $GABA_A$ receptors and appeared similar to spontaneous large depolarizing potentials which occur naturally in immature CA3 neurones (n=160) from young rats (postnatal days 2-12). Selective zinc-chelating agents (CP94 and CP40) based on heterocyclic pyridinones reversibly inhibited these innate GDPs in young neurones in a concentration (1-400μM) dependent manner.

The mechanism underlying GDP generation was investigated by examining the effect of zinc on membrane properties and synaptic neurotransmission in adult neurones. Zinc had a wide variety of actions on voltage-operated and/or ligand-gated channels, including i) increasing the membrane input resistance and enhancing cell excitability; ii) augmenting postsynaptic $GABA_A$ responses; iii) inhibiting postsynaptic $GABA_B$ receptors; iv) increasing the release of GABA; v) inhibiting N-methyl-D-aspartate (NMDA) receptors; vi) potentiating non-NMDA receptor mediated responses; and vii) depressing stimulus-evoked excitatory postsynaptic potentials and population spikes. The long-term potentiation in CA1 and CA3 regions induced by high frequency stimulation was also blocked by zinc. Zinc-induced GDPs occurred in the apparent absence of any functional excitatory synaptic transmission but could be reversibly inhibited by the specific adrenergic β_1-receptor antagonist, atenolol. The action of zinc in inducing GDPs was not reproduced by other cations, such as Ba^{2+}, Cd^{2+}, Co^{2+}, Cu^{2+}, Fe^{2+}, Mn^{2+}, Al^{3+} and a K^+ channel blocker 4-aminopyridine. These results provide the first evidence of a physiological role for endogenous zinc in immature hippocampal synaptic neurotransmission and suggest that exogenous zinc can differentially modulate inhibitory and excitatory synaptic transmission in the adult hippocampus.

PHYSIOLOGICAL AND PHARMACOLOGICAL EFFECTS OF ZINC ON RAT HIPPOCAMPAL PYRAMIDAL NEURONES *IN VITRO*

Chapter 1
GENERAL INTRODUCTION

The first evidence that the transition metal, zinc was an essential component in the diet of animals was provided by Todd et al. in 1934 using the rat as an experimental model. Since then, the nutritional requirement for zinc in both health and disease states has been extensively documented (Chvapil, 1973; Dreosti et al., 1981; Iyengar, 1987; Prasad, 1988; Frederickson 1989; Sandyk, 1991).

The presence of an abundance of this trace element in the mammalian central nervous system (CNS) was discovered by Maske (1955) who observed an intense reaction between hippocampal tissue and dithizone (diphenylthiocarbazone), a metal-chelating intravital stain. Since tissues stained intravitally by dithizone are unsuitable for high power light-microscopy, Timm (1958) developed a histochemical method of silver sulphide staining with a resolution superior to the dithizone method and found that the heavy metals, zinc, copper, iron and lead were unevenly distributed in the brain. The giant boutons of the hippocampal mossy fibre system in particular, are strongly stained by this method. This discovery was subsequently confirmed by modified histochemical studies (Danscher et al., 1973; Pérez-Clausell & Danscher, 1985; Frederickson et al., 1987) and by ^{65}Zn autoradiographic studies, which are specific for determining the distribution of zinc (von Euler, 1961; Hassler & Söremark, 1968; Dencker & Tjalve, 1979). These observations indicated that much of the zinc in the hippocampus is associated with the mossy fibre axons which project from the granule cells in the dentate area (regio inferior) to the pyramidal neurones in the CA3 subfield.

At an ultrastructural level, electron microscopic histochemical research demonstrated that the presence of zinc is primarily connected with synaptic vesicle structures located within the mossy fibre nerve terminals (Haug, 1967, 1973; Ibata & Otsuka, 1969; Pérez-Clausell & Danscher, 1985; Holm et al., 1988; Claiborne, Rea & Terrian, 1989).

Quantitative chemical analyses, such as atomic absorption spectrophotometry and quantitative histofluorescence techniques, have consistently supported the histochemical evidence that zinc is differentially distributed in the CNS (Frederickson et al., 1983,

1987; Szerdahelyi & Kása, 1983; Savage, Montano & Kasarski, 1989). Although estimation of the zinc content in the brain may vary substantially (Crawford, 1983), the zinc distribution pattern is consistent with the highest levels (>65μg/g dry weight) occurring in the hippocampus and the lowest (<25μg/g) in the thalamus-hypothalamus and medulla oblongata. Intermediate amounts of zinc can be found in the olfactory bulbs, cerebellum, striatum, cortex and throughout the mid-brain (Crawford & Connor, 1972; Donaldson et al., 1973). The average concentration in the brain of most species appears to be a little over 25μg/g dry weight, (Crawford & Connor, 1972). After magnesium, calcium and iron, zinc is the fourth most abundant divalent metal ion in the brain. In the rat hippocampus, the order of trace elements is Zn> Fe> Cu> Mn (Szerdahelyi & Kása, 1983). This zinc distribution pattern in the CNS determined mostly in rats, is also found in humans (Hu & Friede, 1968; Frederickson et al., 1983).

Developmental studies show that in the rat, unlike most other brain regions which at birth generally have similar concentrations of zinc to the adult, hippocampal zinc levels increase substantially during the first 3 postnatal weeks (Szerdahelyi & Kása, 1983). Simultaneously with the electrophysiological maturation of granule cells and their axons, the mossy fibres, the metal appears to be accumulated into the granule cell and spreads out of the perikarya and shifts into the terminal boutons by axoplasmic transport (Crawford & Connor, 1972; Frederickson, Howell, & Frederickson, 1981; Wolf, Schütte & Römhild, 1984). However, it has been reported that the mossy fibre termination in CA3 also has a positive Timm stain, indicating that the presence of zinc occurs at much earlier times including 2-3 days after birth (Zimmer & Haug, 1978).

Furthermore, neurochemical studies demonstrate that zinc can be actively taken up (Wolf, Schütte & Römhild, 1984; Wensink et al., 1988) into synaptic vesicles throughout the telencephalon (Ibata & Otsuka, 1969; Pérez-Clausell & Danscher, 1985; Holm et al., 1988). When uptake into the mossy fibre region is examined directly by assaying microdissected hilar tissue, the mossy fibre region exhibits significantly greater uptake of ^{65}Zn than other hippocampal regions, particularly when the tissue is electrophysiologically active (Howell, Welch & Frederickson, 1984).

The close relationship between mossy fibres and zinc has been further reaffirmed by the demonstration that zinc can be released or co-released with glutamate, a major excitatory transmitter in the CNS (Crawford & Connor, 1973), into the synaptic cleft

following stimulation. The zinc release is calcium-dependent and can be evoked by either electrical or high potassium-induced stimulation in adult hippocampal slices *in vitro* (Assaf & Chung, 1984; Howell, Welch & Frederickson, 1984). These studies revealed the presence of a unique pool of 'releasable' zinc ions (Zn^{2+}). It was estimated that the zinc concentration in the extracellular space may be as high as 300μM following high intensity stimulation (Assaf & Chung, 1984).

Spontaneous and evoked release of endogenous zinc has also been found in the rat hippocampal mossy fibre zone *in situ*, particularly following high frequency electrical stimulation (>10Hz), or kainate-induced stimulation (Charlton et al., 1985; Aniksztejn, Charton & Ben-Ari, 1987). It has also been reported that zinc (sulphide) can be released into synaptic clefts after *in vivo* injection of sodium sulphide (Pérez-Clausell & Danscher, 1986).

The ubiquitous distribution of zinc in the brain may be taken as an indication that the endogenous metal performs a specialized function(s) in the region of high concentration. The evidence of zinc release further raises the possibility that zinc may subsequently interact with pre- and postsynaptic membrane proteins, perhaps acting as a neuromodulator controlling cell excitability and synaptic activity. The zinc ion is a small cation (hydrated radius 0.44nm) with a double positive charge ensuring a high field strength around the ion. These properties indicate that zinc may be capable of interacting with membrane proteins (Smart, 1990). Indeed, pharmacological studies have shown that zinc inhibits the binding of opioid peptides, glutamate and aspartate to their respective receptors (Stengaard-Pedersen, Fredens & Larsson, 1981; Slevin and Kasarskis, 1985). Also a functional interaction of zinc with the major excitatory and inhibitory amino acid neurotransmitter receptors in the CNS has been demonstrated. Zinc selectively inhibits responses mediated by N-methyl-D-aspartate (NMDA) receptors and slightly potentiates responses on non-NMDA receptors in cultured embryonic neurones and cortical brain slices (Peters, Koh & Choi, 1987; Westbrook & Mayer, 1987; Hori, Galeno & Carpenter, 1987). On the vertebrate $GABA_A$-receptor complex, zinc can have differential effects depending on the stage of neuronal development which may be related to the subunit composition of the $GABA_A$ receptor (Smart & Constanti, 1990; Draguhn et al., 1990; Smart et al., 1991).

Overall this suggests that zinc may play a physiological role in synaptic transmission at the mossy fibre terminals, rather than just be related to structural development (Bettger & O'Dell, 1981; Ochiai, 1988). To address this fundamental issue, von Euler (1961) initiated studies on the effect of chelating zinc in the adult rat mossy fibre pathway. He presented evidence for an irreversible block of transmission in the mossy fibre system following local treatment with hydrogen sulphide (H_2S). However, H_2S is a very toxic agent and such irreversible blockade could well have resulted from a non-specific effect. Crawford and his colleagues (1973, 1975) studied transmission in adult rat mossy fibre-CA3 synapses after first reducing the systemic availability of zinc with dithizone, a non-selective metal chelator. They reported that population spikes evoked by mossy fibre stimulation were initially enhanced and then slightly reduced following repetitive stimuli (10Hz). However, Danscher et al. (1975) reported only transient and non-specific effects on synaptic transmission after direct hippocampal injection of diethyldithiocarbamate (DEDTC, antabuse), although treatment with this chelating agent could cause partial depletion and also alter the distribution of zinc in the adult rat hippocampus (Szerdahelyi & Kása, 1987).

An involvement of zinc in hippocampal electrophysiology was originally proposed by Hesse (1979) who demonstrated that in zinc-deficient adult rats, low-frequency electrical stimulation of the mossy fibres produced synaptic responses declining abnormally in amplitude with successive stimuli. Hesse suggested that the deposits of zinc in the mossy fibre nerve terminal boutons might be important for synaptic transmission. However, zinc is known to be a structural or catalytic component of 200-300 metalloenzymes in a variety of species. The synthesis of the excitatory neurotransmitter, glutamate is dependent on the activity of glutamate dehydrogenase, which is also a zinc-containing enzyme (Vallee & Galdes, 1984; Vallee & Auld, 1990). Thus, the involvement of zinc-containing metalloenzymes in this phenomenon cannot be entirely excluded. Since zinc also contributes to the stability of biological membranes (Bettger & O'Dell, 1981; Pasternak, 1988), feeding adult animals with a zinc deficient diet is likely to cause complex changes to the whole animal physiology (Hesse, Hesse & Catalanotlo, 1979; Wallwork & Crawford, 1987).

Since these studies, there has been little progress in establishing a physiological role for endogenous zinc in the CNS. This has been partly due to the lack of any

demonstrated action which could be attributed to **endogenous** zinc. Also, a **selective** and potent zinc chelating agent was not available until quite recently (Hider et al., 1990). However, **exogenous** zinc has been well established as a blocker of many species of voltage-gated ion channels in a variety of preparations as summarized in the Table 1.1. These effects of zinc are described in more detail in the appropriate chapters.

Table 1.1. Inhibition of voltage-gated ion channels by zinc

Species of Ion Channel	Zinc concentration	Type of Preparation	Reference
POTASSIUM			
Transient (I_A)	100-250μM	Rat sympathetic ganglia (SCG)	Constanti & Smart, 1987
Ca^{2+}-activated			
(I_C)	100-250μM	SCG	Constanti & Smart, 1987
(I_{AHP})	0.5-1μM	Rat hippocampi	Sim & Cherubini, 1990
Delayed (I_K)	2-200μM	Frog muscle	Stanfield, 1975
CALCIUM (I_{Ca})			
Slow inactivating	0.5-1μM	Rat hippocampi	Sim & Cherubini, 1990
Dihydroyridine-sensitive	100μM-1mM	Mouse myotubes	Winegar & Lansman, 1990
SODIUM (I_{Na})	15μM-2mM	Calf Purkinje fibres	Visentin et al, 1990
CHLORIDE (I_{Cl})	100-500μM	Frog muscle	Hutter & Warner, 1967*

* Hutter, O.F. & Warner, A.E. (1967). Action of some foreign cations and anions on the chloride permeability of frog muscle. J. Physiol. **189**, 445-460.

Finally, as Dreosti (1989) pointed out, ..."Of particular interest must be the emerging role of zinc in synaptic transmission and its proposed involvement in neuroreceptor modulation, a research area which promises to hold the focus on zinc in the brain into the twenty-first century". The main goal of the present study was to address this fundamental question, whether endogenous zinc in the mossy fibre nerve terminals participated at all in synaptic signalling directly, for example by control of the amount of neurotransmitter released and/or by modulating postsynaptic receptor sensitivity. Another motivation for this work was to examine in greater detail the pharmacological action of zinc on inhibitory and excitatory synaptic activity in the **intact** hippocampus, by using mostly intracellular and occasionally simultaneous extracellular recording from adult and young rat hippocampal brain slices *in vitro*.

Chapter 2
MATERIALS AND METHODS

1. Hippocampal brain slice preparation

Hippocampal brain slices were prepared from Wistar rats. Adult animals were at least postnatal age 90 days (P>90, 200-300g mass), and young rats were P2-21. Rats were anaesthetized by ether inhalation and decapitated. The brain was rapidly removed into ice-cold Krebs solution (*vide infra*). Transverse hippocampal slices were cut using a McIlwain tissue chopper, producing 400μm thick adult slices and 600μm thick young postnatal slices. In some experiments the connections between CA1 and CA3 were disrupted by sectioning using a razor blade (Schwartzkroin & Prince, 1978).

The slices were immediately incubated by suspension on a Nylon mesh submerged in a large volume of oxygenated Krebs solution (250ml) at ambient temperature (20-25°C) until required. Recordings were usually made within 1-10 hours after brain slice preparation. Occasionally, some slices were used after 24 hours following removal from the animal. These slices were quite viable and the data collected from '24hr-old' neurones was not apparently different from that obtained from fresh slices. These data were therefore pooled. Increasing the incubation time of brain slices *in vitro* to over 35 hours proved unsuccessful with very few viable neurones.

2. Composition of superfusing media

The extracellular medium was based on a Krebs solution containing (mM): NaCl, 118; KCl, 3; $CaCl_2$, 2.5 (reduced to 2 for young slices); $MgCl_2$, 2; $NaHCO_3$, 25; D-glucose, 11, bubbled with 95% O_2/5%CO_2, pH 7.4. Previous workers have demonstrated the advantage of using higher Ca^{2+} and Mg^{2+} concentrations (usually 1mM for each) for maintaining the slice viability and for recording stability (Alger & Nicoll, 1980; Haas & Greene, 1986). Since Zn^{2+} ions may be precipitated in the presence of phosphate, the Krebs was devoid of both HPO_4^{2-} and SO_4^{2-} salts (Smart & Constanti, 1982). All neuronal impalements were obtained in normal Krebs before any pharmacological

manipulation. To enhance the activation of N-methyl-D-aspartate (NMDA) receptors, nominally zero magnesium Krebs (Mg-free) solution containing 10μM glycine was used (Nowak et al., 1984; Mayer, Westbrook & Guthrie, 1984; Johnson & Ascher, 1987). To inhibit the action of NMDA the extracellular concentration of magnesium was raised to 4-6mM, with nominally zero glycine concentration.

3. Electrophysiological techniques

3.1. Intracellular recording

After equilibration for approximately 1 hour, a single slice was held suspended between two pieces of nylon mesh submerged in a recording chamber (Fig. 2.1) and fully superfused with oxygenated Krebs solution maintained at 30±1°C. Intracellular recordings were obtained from pyramidal neurones in CA1 and CA3 subfields using a single microelectrode current-voltage clamp amplifier (Dagan 8100). This amplifier allows voltage-recording and current-passing to be performed by the same electrode on a time-share basis (Wilson & Goldner, 1975). The simplified recording circuits are illustrated in Fig 2.2. The switching frequency was 2-3KHz (25% duty cycle) after adjustment of the capacity neutralization in the switch clamp operating mode. Intracellular recordings were performed using either current clamp or voltage clamp.

Microelectrodes were constructed from borosilicate filamented glass tubes (GC 100F-15, Clark Electromedical Co.) using a horizontal microelectrode puller. This produced a short rigid shank enabling stable impalement of a single pyramidal cell. Microelectrodes were filled with either 3M-KCl or 4M-potassium acetate (buffered to pH 7±0.2 with 0.5% acetic acid). The microelectrode resistances ranged from 30 to 80MΩ for adult neurones and 60-100MΩ for young immature neurones and depended upon the recording mode. These microelectrodes could pass up to ±1nA current without serious rectification.

The microelectrode was lowered into the CA1 or CA3 pyramidal cell layer under visual control using a three-dimensional Prior micromanipulator (Fig.2.1 and 2.3). Pyramidal neurones were usually impaled at a depth of 60-150μm below the slice surface. The most satisfactory method for neuronal impalement was by high frequency electrical oscillation and by rapid capacity compensation adjustment. Cell penetration was

immediately followed by negative D.C. current injection to take the cell membrane potential to around -80mV. As the cell input resistance increased, indicating the impalement improved, the D.C. current was slowly removed. Membrane potentials were estimated from the potential observed upon withdrawal of the electrode from the cell after recording. Hyperpolarizing current pulses (-0.3 to -0.5nA, 200-300ms, 0.2-0.5Hz) were routinely applied to monitor the membrane input resistance. Intracellular recordings were stable for 1-9 hours.

3.2. Simultaneous extracellular recording

In some experiments, simultaneous extracellular recordings of dendritic or somatic field potentials were made with 2M-NaCl filled microelectrodes (resistance 1-5MΩ), using a high impedance amplifier. The extracellular electrodes were placed in the vicinity of the impaled cell in stratum pyramidale to record orthodromically-evoked population spikes (OPS), or positioned in stratum radiatum to record the population excitatory postsynaptic potential (pEPSP). As an indicator of healthy synaptic inhibition, experiments were only performed on slices where orthodromic stimulation in the standard Krebs solution evoked a single population spike (Haas, Xie & Lui, 1986; Davies, Davies & Collingridge, 1990).

3.3. Electrical stimulation

Synaptic responses were evoked by electrical stimulation. Bipolar stimulating electrodes made from stainless steel with a separation of <50μm, were located under visual control in stratum lucidum or in the hilar region of the dentate gyrus for stimulating the mossy fibre input to CA3 neurones. Electrodes were placed in stratum radiatum for stimulating the Schaffer collateral afferents to the CA1 subfield. Intact synaptic responses, excitatory and inhibitory postsynaptic potentials (EPSP-IPSPs) were evoked by orthodromic stimulation of input afferents using remotely placed stimulating electrodes (S_1, in Fig. 2.3). Monosynaptic $GABA_B$-mediated IPSPs ($IPSP_B$s) were elicited by localized stimulation in stratum lucidum or stratum radiatum with stimulating electrodes placed close to the recording site, <0.5mm (S_2, Fig. 2.2) in the presence of $GABA_A$ antagonists, bicuculline (20μM) picrotoxin (40μM) and excitatory amino acid (EAA) receptor antagonists, D-2-amino-5-phosphonovalerate (APV, 40μM) and 6-cyano-

7-nitro-quinoxaline-2,3-dione (CNQX, 20μM) (see Davies, Davies & Collingridge, 1990). For antidromic stimulation applied to CA1 neurones, stimulating electrodes were placed in the stratum oriens or alveus.

Stimuli were composed of square-wave pulses (5-50V, 60-100μs) delivered every 10-120s. High frequency stimulation for inducing long term potentiation (LTP) consisted of two 100Hz/1s duration trains separated by 30s (Malenka, Madison & Nicoll, 1986).

4. Data recording and analysis

Sampled currents and membrane voltage, or field potentials, were continuously recorded on a ink-pen chart recorder (Brush-Gould 2200) and selectively photographed from a storage oscilloscope. Signals were also stored on a Racal store 4D FM tape recorder (band width D.C. to 2.5kHz) for later analysis using a Mission 286-based computer system. Evoked synaptic responses were averaged and analyzed by a synaptic current analysis program (SCAN, version 3.0, provided by J. Dempster, University of Strathclyde). Dose-response curves and current-voltage (I-V) relationships were plotted using Fig-P (Biosoft). Data are presented as means ± standard deviation (S.D.) and statistical significance was assessed using *t*-tests.

Neurones were selected for studies if the membrane potential was at least -60mV with action potential amplitudes of 80-100mV. Some passive membrane properties of young and adult pyramidal neurones are summarized in Table 2.1.

Table 2.1. Analysis of resting membrane potential, input resistance and spike amplitude of pyramidal neurones

	Young (P<21)	n	Adult	n	P
Membrane potential (mV)	-66±6	43	-68±5	70	>0.1
Input resistance (MΩ)	83±39	43	42±12	70	<0.01
Spike amplitude (mV)	65-96	160	80-120	245	

Data were obtained from young neurones in region CA3 and for adult cells, both CA1 and CA3 regions are pooled. Recordings were made using 3M KCl or 4M K-acetate filled microelectrodes. Data of membrane potential and input resistance are presented as mean ± S.D. n, number of cells. The significant difference between young and adult neurones was assessed using a *t*-test.

Typical current clamp records of membrane potential responding to direct current injection are shown in Fig. 2.4. No significant difference in passive membrane properties was found between the recordings with KCl and K-acetate filled microelectrodes, although spontaneous IPSPs became depolarizing when recorded with KCl-filled microelectrodes. Any recordings from CA3 pyramidal neurones, or the use of microelectrodes filled with K-acetate are specified in the appropriate figure legends, otherwise all recordings were made from adult CA1 neurones using KCl-filled microelectrodes.

5. Identification of neurones

Neurones were always impaled in stratum pyramidale (Fig. 2.3) and identified according to their position (CA1 or CA3), their morphology (Fitch, Juraska & Washington, 1989) and also electrophysiological properties (Schwartzkroin, 1975, 1977; Schwartzkroin & Kunkel, 1982; Haas & Greene, 1986; Lacaille & Schwartzkroin, 1988a). Previous studies have indicated that non-pyramidal neurones are also present within the pyramidal cell layer (Seress & Ribak, 1985; Scharfman & Schwartzkroin, 1988; Nitsch, Soriano & Frotscher, 1990). In some selected neurones, to establish that intracellular recordings were definitely obtained from pyramidal neurones, cells were stained using the avidin-biotin complex system (Horikawa & Armstrong, 1988; Kawaguchi, Wilson & Emson, 1989) to allow additional morphological characterization.

Neurones were impaled in 400μm thick slices with microelectrodes containing 2M-potassium chloride and 2% w/v N-(2-aminoethyl) biotinamide hydrochloride (Neurobiotin, Vector Labs; resistances 60-80MΩ). The neurobiotin was injected into the neurones by passing depolarizing current pulses (1-2nA, 300ms, 3.3Hz) for 5-10min. Usually 1-3 neurones in each slice were injected with neurobiotin and subsequently processed using a method modified from Kita & Armstrong (1991).

Slices were fixed by submersion in 4% paraformaldehyde in a 0.15M phosphate buffered saline (PBS, pH 7.4) for 30min at room temperature, or at 4°C overnight. Without further sectioning on a vibratome, fixed slices were rinsed three times for 15min in 70% ethanol. To quench endogenous peroxidase activity (which might be present in red blood cells), slices were preincubated in 0.3% H_2O_2 diluted with 100% methanol for

30min, and rinsed with PBS several times. The tissues were then incubated for 10-15 hours on a shaking water bath at 30°C with an avidin-biotin-horseradish peroxidase (HRP) complex (ABC solution, Vector Labs) diluted 1 in 100 using 0.5% v/v solution of Triton-X-100 in PBS (Triton increases the permeability of the neuronal membrane to HRP). Slices were rinsed several times in PBS and then reacted with 0.05% v/v diaminobenzidine (DAB, Vector Labs) and 0.003% v/v H_2O_2 in PBS for 2-10min. The time was adjusted to control the staining intensity (brown stain) within the injected cell under 40-100X magnification. Slices were washed for 5min in PBS (3 times) to reduce the background staining, and then dehydrated following standard histological procedures. Slices were treated sequentially with 50%, 70%, and 98% v/v ethanol and citroclear, with each step taking 10-15min. Dried slices were subsequently mounted onto microscope slides for permanent storage.

Neurones were visualized at 100-400X with a Nikon alphaphot microscope and photographed using Kodak vericolor film. Figure 2.5 is a photomicrograph of a typical pyramidal neurone in the CA1 subfield with a conical cell soma of diameter approximately 20μm (measured at the base), a large apical dendrite (diameter 5μm) and some thinner basal dendrites (<2μm). Neurones injected with neurobiotin for up to 15min, did not exhibit any electrophysiological properties which were clearly different from those previously recorded in untreated cells.

6. Drugs and their application

Most drugs were dissolved in distilled water as stock solutions (concentrations ranged 10-100mM), and freshly diluted with Krebs solution when applied via superfusion. The recording chamber volume was approximately 0.3ml, and the reservoir used for bubble trapping contained 1ml. The solution flow rate was 7±0.2ml/min and the bath exchange time was about 10s. Drugs were usually applied in at least a 15ml volume achieving a tissue contact time of approximately 2min, which was a sufficient time to obtain an equilibrium response.

Drugs were also applied by ionophoresis using single- or double-barrelled ionophoretic electrodes. Agents applied in this manner included, GABA (1M, pH4, dissolved in distilled water), glutamate (200mM, pH7, dissolved in 0.9% w/v sodium

chloride solution), kainate (50mM, pH7, dissolved in 0.9% w/v sodium chloride solution) and picrotoxin (5mM, pH7, dissolved in 0.9% w/v sodium chloride solution). All ionophoretic pipettes were positioned in the apical dendritic field for both CA1 and CA3 neurones.

Zinc chelators, 1,2-diethyl-3-hydroxypyridine-4-one (CP94) and 1-hydroxyethyl-3-hydroxy-2-methylpyridin-4-one (CP40) were gifts kindly provided by Prof. R.C. Hider (Kings College, London).

(-)- and (+)-isomer-baclofen, and p-[3-aminopropyl]-p-diethoxymethyl-phosphinic acid (CGP 35348) were kindly provided by CIBA-GEIGY (Switzerland). Flurazepam was obtained from Hoffmann-La Roche AG (Switzerland).

Zinc chloride ($ZnCl_2$) and all reagents used for the Krebs solutions were of 'Analar' grade and supplied by BDH.

γ-Aminobutyric acid (GABA), aspartic acid (Asp), (+)-bicuculline (BIC), diethyldithiocarbamate (DEDTC), ethylene glycol-bis(β-aminoethylether)-N-N'-tetraacetic acid (EGTA), 4-aminopyridine (4-AP), glycine (Gly), 5-hydroxytryptamine (5-HT), pentobarbitone (PB), picrotoxin (PTX), quisqualic acid (QU) and tetrodotoxin (TTX) were obtained from Sigma.

α-Amino-3-hydroxy-5-methyl-4-isoxazole propionate (AMPA), bromowillardiine (BRW), 6-cyano-7-nitro-quinoxaline-2,3-dione (CNQX), D-2-amino-5-phosphonovalerate (APV), kainic acid (KA), kynurenic acid (KYN), and N-methyl-D-aspartic acid (NMDA), trans-1-amino-cyclopentyl-1,3,-dicarboxylate (tACPD) were supplied by Tocris Neuramin (Cambridge).

(±)-8-hydroxy-2-(di-N-propylamino)tetralin hydrobromide (DPAT) was obtained from Research Biochemical Incorporated (MA, USA).

Aluminium chloride hexahydrate ($AlCl_3$), cadmium chloride ($CdCl_2$), cobalt chloride hexahydrate [$Co(II)Cl_2$], copper chloride dihydrate [$Cu(II)Cl_2$], iron(II) chloride tetrahydrate [$Fe(II)Cl_2$], manganese chloride anhydrous [$Mn(II)Cl_2$] and histidine (His) were of purum grade and supplied by Fluka (Switzerland).

Fig 2.1. Photographs of the experimental set-up for intracellular and extracellular recording. **A**, An overall view of the set-up illustrating the microscope, recording chamber, two three-dimensional Prior micromanipulators and a temperature controller (left of the chamber). Above the righthand micromanipulator a gauge was used to ascertain the depth of the microelectrode in the tissue. **B**, Enlarged photograph showing details of the recording chamber. Solution flow inlet (1) and outlet (2) of the bath perfusion system, also extracellular (3) and intracellular (4) recording microeletrodes, and stimulating electrodes (6). The Nylon wire grid (5) used for holding the hippocampal slice is also shown.

A

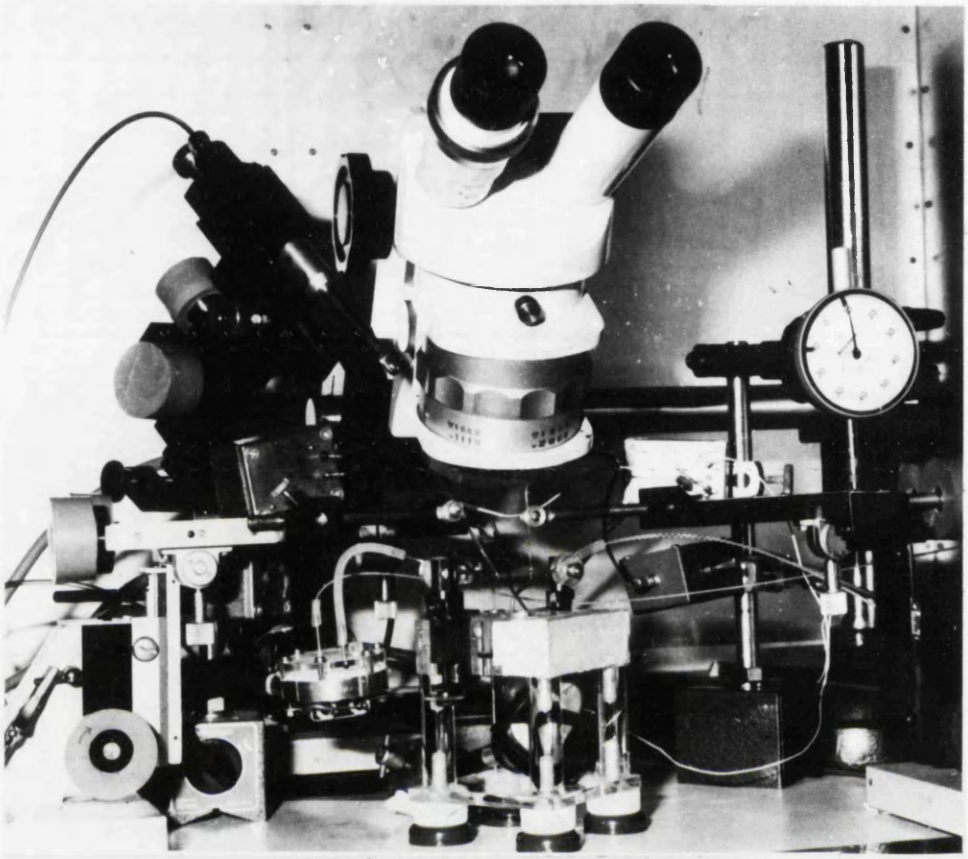

B

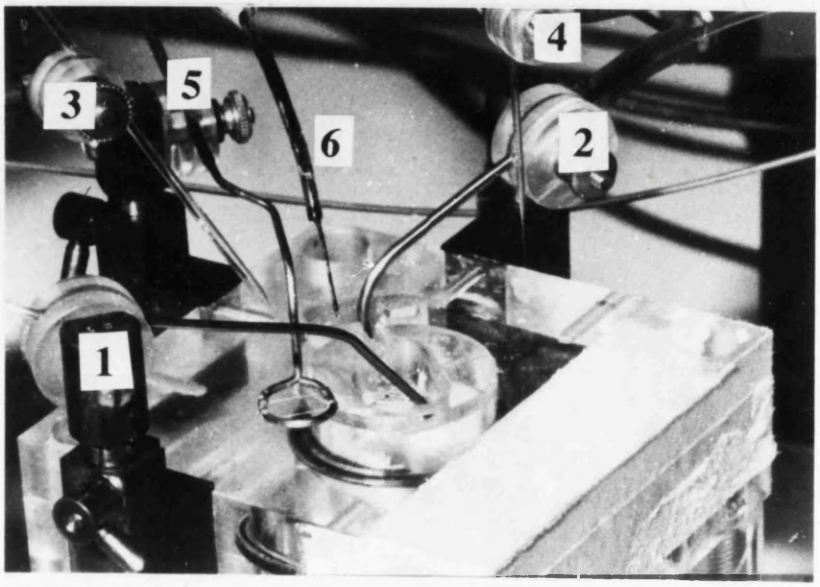

Fig. 2.2. **A**, Schematic diagram of single microelectrode intracellular recording switch clamp circuit. A_1, a high input-impedance amplifier. A_2, the clamp feedback amplifier. Cc, current command. CCS, a controlled current source. I_0, current injected into the cell. S_1, a switch to control the output of CCS. S_2, a switch between voltage and current clamp. SH1 and SH2, two sample and hold devices. V_c, voltage command. V_{in}, input voltage comprising the membrane potential (V_m) plus the voltage drop (V_e) across the resistance of the microelectrode caused by I_0. **B**, Diagram showing the relative timing of the states of switch S1 between current passing and voltage recording and the corresponding signals from voltage and current recording after the respective periods of signal sampling. 0 indicates the zero voltage reference line.

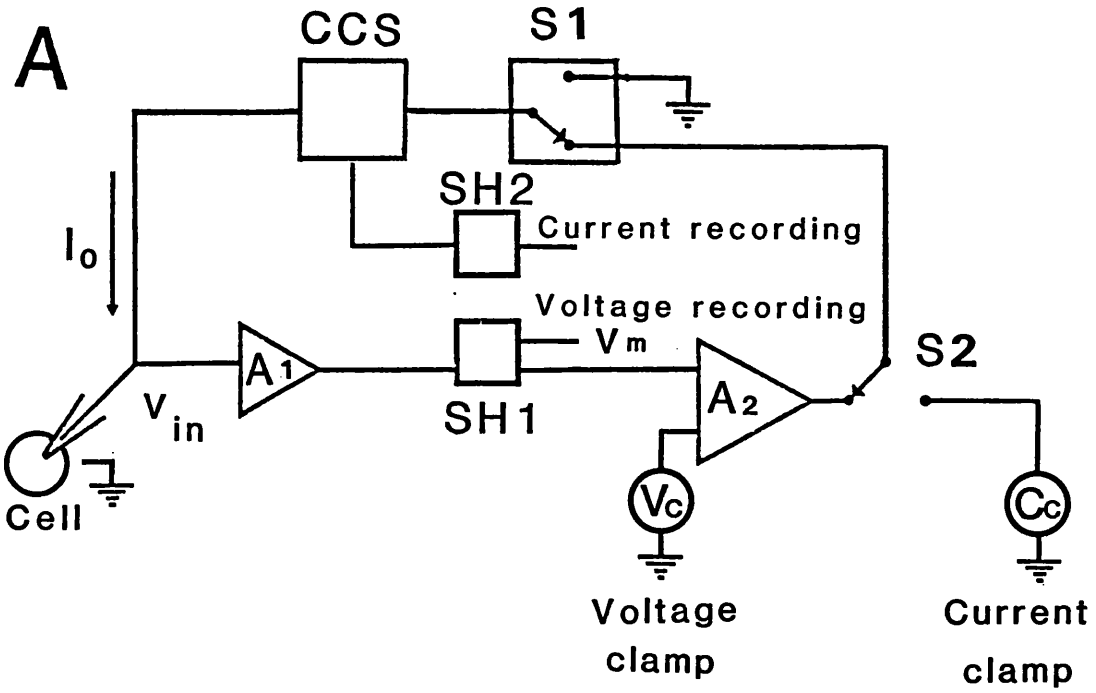
A
CCS
S1
SH2
Current recording
I_o
Voltage recording
V_m
S2
A1
A2
V_{in}
SH1
Cell
Vc
Cc
Voltage clamp
Current clamp

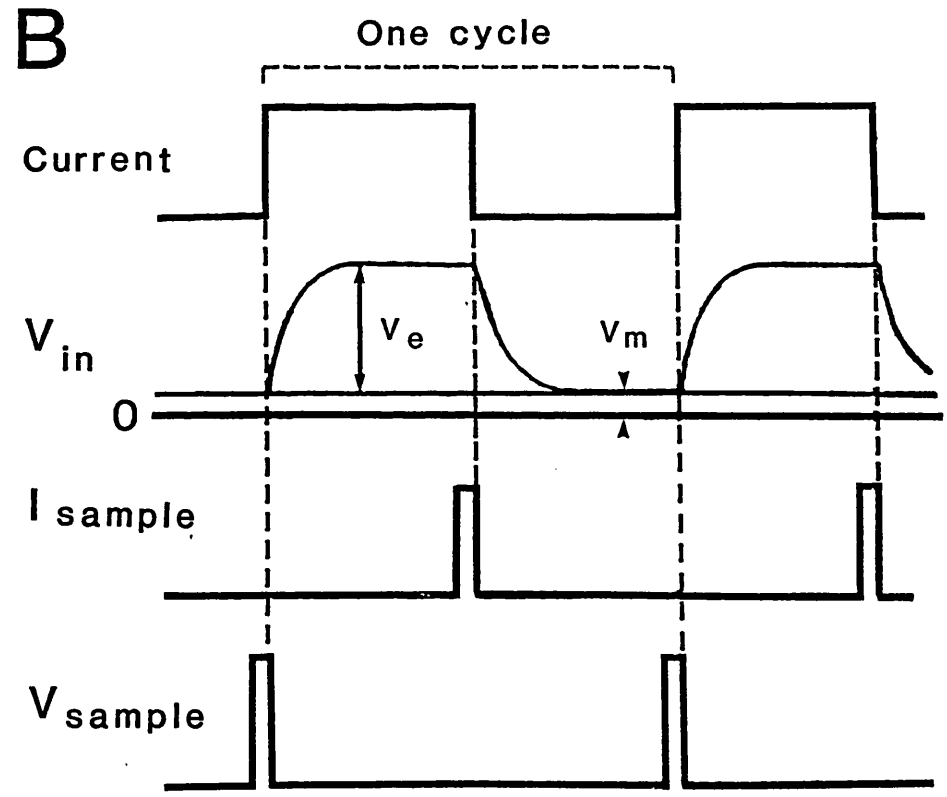
B
One cycle
Current
V_{in}
V_e
V_m
0
I sample
V sample

Fig. 2.3. **A**, Diagram of hippocampal network and the arrangement of the recording microelectrode and stimulating electrodes. ALV, alveus; EC, entorhinal cortex; DG, dentate gyrus; FI, fimbria; LAC-MOL, lacunosum-moleculare; LAT, late entorhinal cortex; MF, mossy fibres; OR, oriens; RAD, radiatum; PP, perforant pathway; PYR, pyramidale; SCH, Schaffer collateral; S_1 and S_2, two stimulating electrodes, positioned far away and close to the recording cell. CA1 and CA3 indicate the pyramidal cell subfields. **B**, Actual hippocampal brain slice cut from an adult rat brain at a thickness of 400μm stained with diaminobenzidine. The slice is shown with with the imprint by the nylon mesh as seen *in situ* under a microscope at 30x magnification. The slice is orientated similar to the schema shown in A. The Arrow indicates an intracellular labelled pyramidal neurone in the CA1 region (enlarged photograph shown in Fig. 2.5).

A

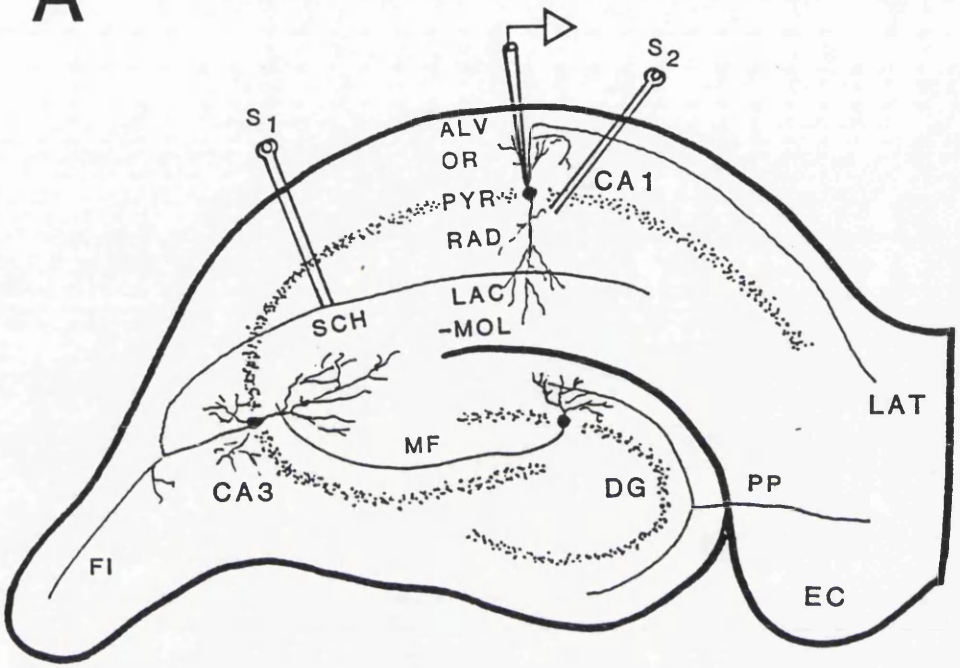

B

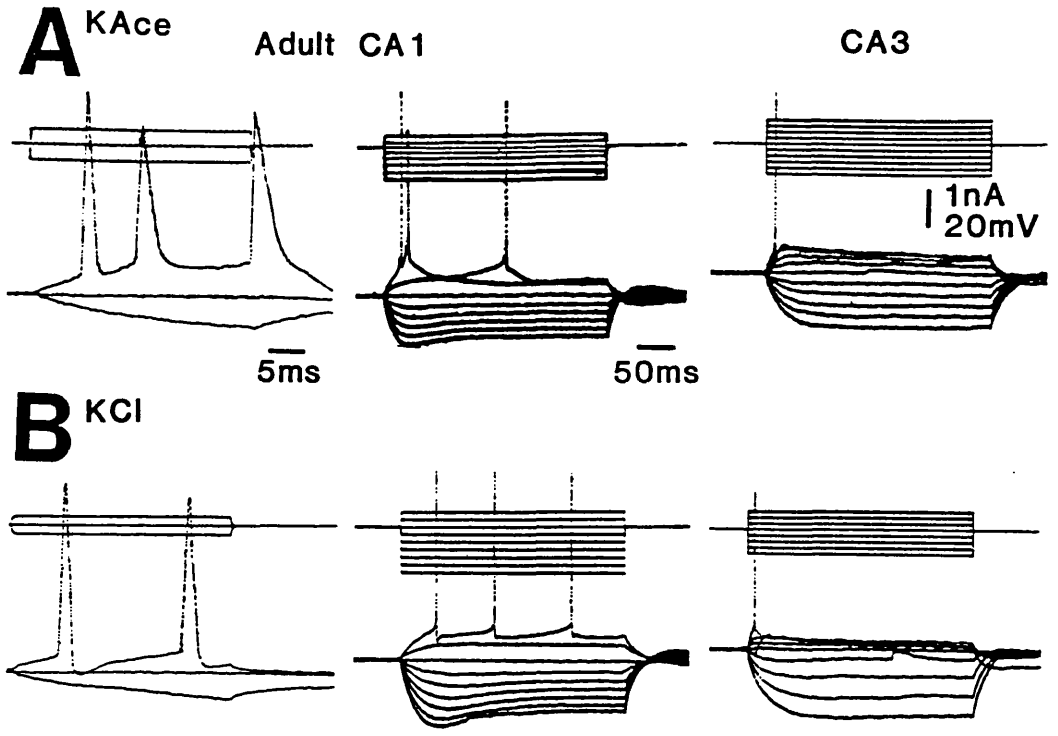

Fig. 2.4. Responses of adult CA1 and CA3 neurones to direct current injection. Current clamp records of membrane potential (lower traces) show superimposed electrotonic potentials produced by depolarizing and hyperpolarizing current pulses (30 or 300ms, 0.5Hz, upper traces). **A**, Recordings using 4M K acetate-filled microelectrodes. The resting potential for the CA1 cell was -73mV and for the CA3 cell, -68mV. **B**, Recordings using 3M KCl-filled microelectrodes. The resting potential for the CA1 cell was -67mV and for the CA3 cell, -63mV.

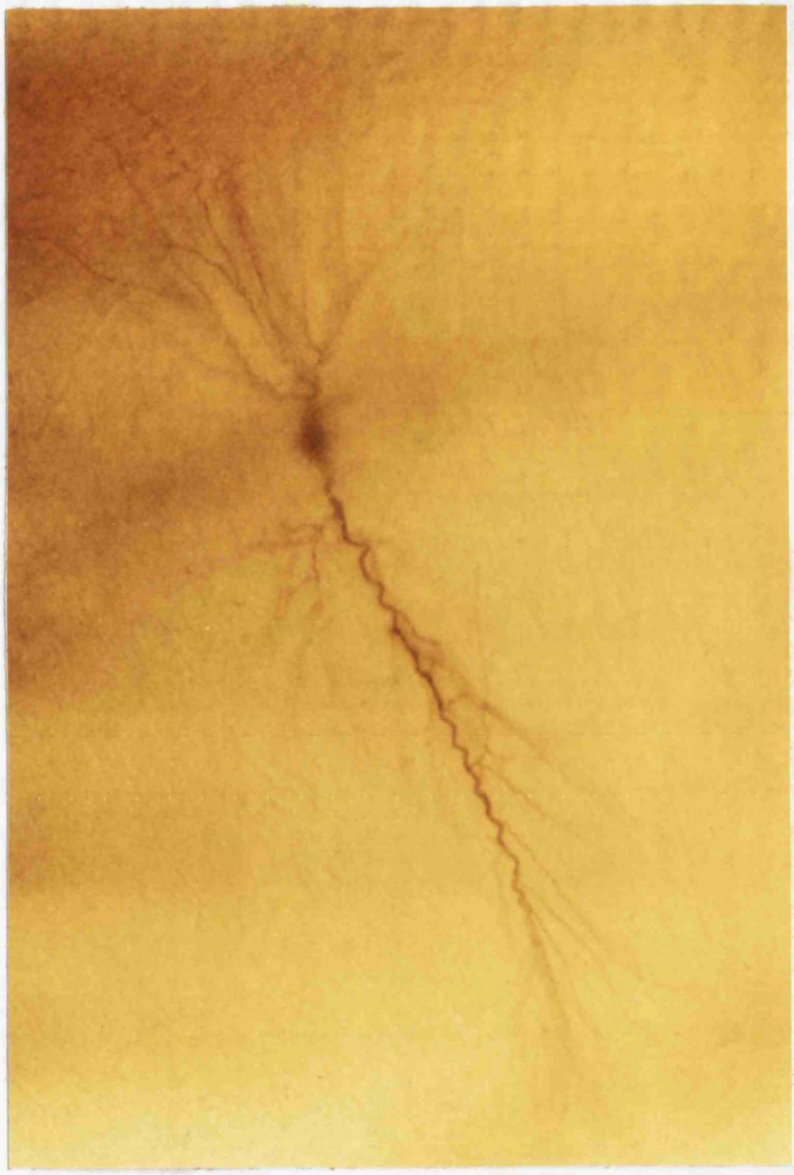

50 μM

Fig. 2.5. A photomicrograph of a pyramidal neurone in region CA1 taken from a 400μm thick adult hippocampal brain slice (see arrow in Fig. 2.3B). The neurone was injected with neurobiotin using constant current pulses (+1nA, 300ms, 3Hz) for 10min and subsequently reacted with a conjugated avidin-biotin-horseradish peroxidase complex and finally stained with diaminobenzidine.

Chapter 3

ZINC INDUCES GIANT SYNAPTIC POTENTIALS IN ADULT HIPPOCAMPAL PYRAMIDAL NEURONES

INTRODUCTION

The transition metal zinc is an essential nutritive requirement with a widespread role in both animal and human metabolism (Todel et al., 1934; Frederickson et al., 1987; Dreosti, 1989). However, an excess of zinc in the brain has been related to the development of epilepsy (Barbeau & Donaldson, 1974; Ebadi & Pfeiffer, 1984). Zinc induced both seizures and convulsions when injected intracerebroventricularly, intrahippocampally or by intracranial infusions in several animal models (Donaldson et al., 1971; Itoh & Ebadi, 1982; Pei et al., 1983), implying that Zn^{2+} has a predominantly proconvulsant action in the CNS. However, systemic administration of zinc salts can produce complex and contradictory effects. An inhibition of seizure development has been observed in some paradigms (Porsche, 1983; Sterman et al., 1986; Morton et al., 1990), whereas facilitation (Tokuoka et al., 1967; Chung & Johson, 1983a,b; Mody & Miller, 1984), or sometimes no effect, was reported in other experimental models (Itoh & Ebadi, 1982; Morton et al., 1990). Similarly, a dietary zinc deficiency can either potentiate (Sterman et al., 1986) or depress (Tokuoka et al., 1967; Fukahori & Itoh, 1990) seizures, whereas other studies have reported no significant effects (Hesse, 1979; Hesse et al., 1979; Wallwork & Crawford, 1987). Electrophysiological studies using ionophoretically applied zinc to rat cortical neurones reported that 45% of extracellularly recorded cells exhibited an increased firing rate, whereas 45% of cells were not affected and 10% showed a depressed level of firing (Wright, 1984). Intracellular studies in olfactory cortex *in vitro* demonstrated that zinc increased cortical neuronal excitability and prolonged EPSPs (Smart & Constanti 1983, 1990). In cultured embryonic hippocampal neurones zinc also produced a prolonged period of increased synaptic activity and concurrent action potential discharges (Mayer & Vyklicky, 1989).

However, in all these *in vitro* preparations zinc failed to induce an epileptic-like burst discharge. The underlying type of activity which may be involved in the epileptogenic effect of zinc, or alternatively, the cellular events induced by zinc which can contribute to the inhibition of seizure development, remains unknown. Also the action of zinc on hippocampal synaptic transmission in intact brain slices has not been studied in detail. The present experiments were undertaken to study these questions using intracellular recordings from hippocampal slices of adult rats *in vitro*.

Since the CA3 subfield of the hippocampus contains a higher amount of endogenous zinc (Haug, 1967; Crawford & Connor, 1972; Frederickson et al., 1987; Savage, Montano & Kasarskis, 1989) and is susceptible to spontaneous and synchronized bursting (Schwartzkroin & Prince, 1978; Wong & Traub, 1983; Johnston & Brown, 1981, 1984; Miles & Wong, 1986), most of the pyramidal neurones studied were recorded from the CA1 subfield. Occasionally, some of the CA1 neurones were disconnected from the CA3 subfield by sectioning the slice between CA1 and CA3 regions (Schwartzkroin & Prince 1978). In comparison some recordings were also made from the CA3 subfield.

RESULTS

1. Induction of spontaneous giant depolarizing potentials (GDPs) by zinc in pyramidal neurones

Intracellular recording from hippocampal neurones in the CA1 or CA3 subfield revealed a continuous synaptic "noise" composed of largely spontaneous inhibitory postsynaptic potentials (IPSPs) supplemented by the occasional firing of spontaneous action potentials (Fig. 3.1A). Spontaneous bursting (defined as a spontaneous depolarization with a superimposed cluster of action potentials, cf. Schwartzkroin & Prince, 1978; Wong & Traub, 1983; Johnston & Brown, 1984) in the CA1 or CA3 region was not been observed in any of the cells superfused with the normal Krebs solution.

Bath application of zinc (50-1000μM) induced a gradual hyperpolarization (3-10mV) of the resting membrane potential (-68±5mV, n=70) and slightly increased the membrane input resistance. After application for 3-8min, zinc caused the appearance of large and long-lasting spontaneous depolarizing potentials (29±6mV amplitude, and 1-4s duration). In addition bursts of action potentials were superimposed upon the depolarization when the recording electrode was filled with 3 M KCl (Fig. 3.1A). Smaller amplitude depolarizations (20±4mV) and often without superimposed action potential firing were observed when recording with electrodes filled with 4 M K acetate. Such large depolarizations, defined as giant depolarizing potentials (GDPs) were associated with at least a 100 % increase in the membrane input conductance at the peak of the depolarization. A small (2-6mV) afterhyperpolarization (AHP) usually followed these events (Fig. 1B). These paroxysmal depolarizations recurred with a mean interval of approximately 2min (117±62s, n=52), and were quite regular in any one individual neurone (Fig. 3.1A). The frequency of spontaneous GDPs was not apparently dependent on membrane potential over the range -50 to -100mV. However, the GDP amplitude increased with membrane hyperpolarization and was reduced with depolarization (Fig. 3.2), presumably due to a change in the driving force for the ions mediating the GDPs as the membrane potential approached the reversal potential for these events (*vide infra*). At depolarized membrane potentials (-50mV), an increased level of spontaneous action potential firing occurred, which made accurate measurements of frequency difficult. In

the single CA1 neurone depicted in Fig. 3.2, the GDPs occurred at a frequency of approximately 0.05Hz at -100mV, decreasing to 0.02Hz at -50mV. At more depolarised membrane potentials (<-70mV), spontaneous GDPs were associated with small AHPs which disappeared near the potassium equilibrium potential (-80 to -90mV; cf. Alger & Nicoll, 1980; Nicoll & Alger, 1981).

Spontaneous GDPs disappeared within 2min following the washout of zinc. If the exposure to zinc was for a prolonged period, over 40-80min, then eventually the spontaneous depolarizations would wane and disappear. The first indication of waning was a decrease in the frequency of appearance, and then the duration of these potentials was also reduced. Following a prolonged wash with control Krebs after a long exposure to zinc, a second application of zinc would not reveal any further spontaneous GDPs. This might be associated with a toxicological effect of zinc (cf. Yokoyama, Koh & Choi, 1986).

2. Zinc induces evoked GDPs: stimulus interval analysis

The periodic appearance of spontaneous depolarizations induced by zinc, suggested that they may be of synaptic origin or possibly due to zinc affecting the membrane properties of the postsynaptic cell. Depolarizing current pulses were injected into both CA1 and CA3 neurones with variable widths and amplitudes to try to induce spontaneous depolarizations in the absence of zinc. This protocol produced depolarizations coupled with action potential trains but failed to initiate any large depolarizations similar to those observed in the presence of zinc (Fig. 3.3A). Also orthodromic stimulation of variable intensity (10-35V) applied to the Schaffer-collaterals when recording from CA1 neurones, or the mossy fibres for CA3 cells, only evoked consistent EPSP-IPSP complexes usually with superimposed action potentials (Fig. 3.3B). However, after superfusion of zinc (300μM), subsequent stimulation of the nerve fibre pathways induced the appearance of GDPs following the EPSP and spontaneous GDPs also appeared on continued exposure to zinc (Fig. 3.3C).

The zinc-induced depolarizing potentials were probably produced as a result of activity in synaptic pathways, since the addition of tetrodotoxin (TTX, 1μM), which blocks sodium-dependent action potentials and therefore synaptic transmission, caused

the cessation of spontaneous GDPs (Fig. 3.4A). The evoked responses following nerve fibre stimulation was also reversibly abolished in the presence of TTX (Fig. 3.4B). The generation of the zinc-induced evoked potentials was apparently in an all-or-none manner. In the presence of 300μM zinc, subthreshold stimuli (6V, 0.1ms) applied to the Schaffer-collaterals did not reveal evoked GDPs in CA1 neurones (Fig. 3.5A). Increasing the stimulus strength from 7 to 15V produced an EPSP followed by an evoked GDP with constant amplitude and duration (Fig. 3.5B) and quite similar in profile to the spontaneous GDP occurring in the same cell (Fig. 3.5A). Increasing the stimulus strength did not apparently affect the zinc-induced depolarizing potential. A paired-pulse stimulation protocol was applied to the Schaffer-collaterals in the presence of 300μM zinc to assess the degree of interaction between the successive evoked GDPs. An evoked response was not produced in many neurones by the second stimulus if the interval between two successive stimuli was less than approximately 90s (Fig. 3.6A). Following the first stimulation, there was for each neurone a well defined time interval during which repeated stimulation, even at increased stimulus strength, would not evoke a second response. If a minimum time of approximately 90s was allowed between successive stimuli, the probability of obtaining a second response equal in amplitude and duration to the first was increased; however, a spontaneous GDP intervening between the two stimuli was also capable of inhibiting any further evoked potentials for the next 90s (Fig. 3.6A). The minimum time required between successive stimuli to ensure a high probability of producing a second evoked response in zinc was 145±92s (n=26; Fig. 3.6B). This was close to the mean time interval (117±62s, n=52) occurring between spontaneous GDPs. During this interval a cluster of action potentials could still be elicited in the neurone by a direct injection of depolarizing current.

Antidromic stimulation to CA1 neurones (the stimulating electrodes were placed in stratum oriens or alvenus) could also evoke GDPs in the presence of 300μM zinc (not shown).

3. Generation of GDPs is dependent on zinc concentration

The minimum zinc concentration causing the induction of spontaneous and evoked depolarizing events was variable between different pyramidal neurones, even within the

same hippocampal slice. Usually 15 min was allowed to elapse between bath application of zinc and the appearance of the depolarizing events. If no such events were observed, this particular concentration of zinc was deemed ineffective. In some neurones, up to three different concentrations of zinc were applied, always following a recovery from the effect of the preceding dose of zinc. The relationship between zinc concentration (10-1000μM; n=168) and the induction of the synaptic events was well described by a sigmoid curve and revealed a threshold concentration for zinc at 20-30μM, with an EC_{50} of approximately 100μM. Increasing the zinc concentration to 200-300μM resulted in a near maximal effect with most cells exhibiting depolarizing events (Fig. 3.7). These concentrations of zinc may be achieved by the release of endogenous zinc from the mossy fibre terminals into the synaptic space during peaks of convulsive activity (Assaf & Chung, 1984). There were no notable differences between exogenous zinc-induced GDPs in CA1 (n=126) and CA3 neurones (n=42), following assessment of the threshold zinc concentration, the latency of onset of GDPs and the frequency of spontaneous depolarizing events. Therefore, results obtained from these two populations of neurones have now been pooled unless specified otherwise.

In experiments (n=3) where a cut was made through the slice between CA1 and CA3 regions severing the usual connections via the Schaffer collateral fibres, spontaneous GDPs were still induced by 300 μM zinc in CA1 neurones. Thus the CA1 neurones in isolation are capable of generating GDPs in the presence of zinc. This is quite unlike the penicillin-induced paroxysmal depolarizing shift (PDS) observed in the hippocampus, which preferentially occurred in the CA3 region and required intact synaptic connection between CA1 and CA3 subfields (Schwartzkroin, & Prince, 1978; Mesher & Schwartzkroin, 1980; Johnston & Brown, 1981). The mechanism underlying the zinc-induced depolarizing events was quite robust, since they also occurred in slices maintained *in vitro* for over 24 hours and was therefore probably not due to acute damage following the preparation of 'fresh' brain slices.

4. Influence of excitatory synaptic transmission on zinc-induced GDPs

As zinc-induced GDPs required intact synaptic transmission, it was of interest to identify which receptors mediated such large depolarizing potentials. In the hippocampus

glutamate is known to be an important excitatory neurotransmitter and underlies both fast and slow EPSPs via non-NMDA receptors and NMDA receptors respectively (Watkins & Evans, 1981; Mayer & Westbrook, 1984; Davies & Collingridge, 1989). These receptors are also often involved in the generation of epileptic-like activity in hippocampal brain slices which have been used as experimental models following exposure to bicuculline, penicillin, or NMDA and kainate (Curtis and Felix, 1971; Croucher, Collins & Meldrum, 1982; Wong & Traub, 1983; Thomson & West, 1986; Neuman, Cherubini & Ben-Ari, 1988).

The possible involvement of NMDA or non-NMDA receptors in the generation of zinc-induced GDPs was studied using the selective excitatory amino acid (EAA) antagonists. Neither DL-2-amino-5-phosphonovalerate (APV; 40μM, n=3), an NMDA antagonist (Davies at al., 1981; Peet et al., 1986), nor 6-cyano-7-nitroquinoxaline-2,3-dione (CNQX; 10μM, n=4), a non-NMDA receptor antagonist (Honoré et al., 1988) were able to block either spontaneous or evoked synaptic events in the presence of 300μM zinc (Fig. 3.8A,B & 3.9). A role for NMDA receptors in controlling or initiating the zinc-induced events was also largely discounted following the lack of effect of superfusing the hippocampal slices with 4mM Mg^{2+} and nominally zero glycine containing Krebs (n=15, Fig. 3.8C). The concentration range employed for the NMDA and non-NMDA antagonists to inhibit the zinc-induced events would normally inhibit directly-evoked responses using bath or ionophoretically-applied EAA agonists (Chapter 7). This suggests that zinc-induced GDPs are not directly mediated by EAA receptors and they do not require functional excitatory synaptic activity. Furthermore, the non-specific EAA antagonist kynurenic acid (Stone & Connick, 1985) was also ineffective at inhibiting the depolarizing events using concentrations up to 2mM. In addition, using a combination of 20μM CNQX, 40μM APV and high Mg^{2+} (4mM) which completely blocked evoked EPSPs, zinc (300μM) was still capable of inducing spontaneous GDPs (n=6; Fig. 3.10).

5. GDPs are mediated by $GABA_A$ receptors

Since zinc-induced GDPs are not mediated by EAA receptors, the contribution of inhibitory transmitter receptors to the generation of GDPs was assessed. Most central

inhibitory synaptic transmission is mediated by GABA (Krnjević, 1976; Andersen et al., 1980; Alger & Nicoll, 1982).

Bath application of the traditional $GABA_A$ antagonist (+)-bicuculline (10μM) to the superfusing medium completely inhibited both the spontaneous and evoked depolarizing potentials in the presence of 300μM zinc in both CA1 and CA3 neurones. The spontaneous synaptic 'noise' caused by IPSPs were also inhibited by bicuculline leaving a quiescent neurone. Only a partial recovery was possible following a prolonged washout of bicuculline (Fig. 3.11, n=14). Furthermore, neurones could be prevented from generating GDPs in the presence of 300μM zinc by preincubation with 10μM bicuculline (n=8). It was noted that the dose of bicuculline used to block or prevent the GDP had no effect on the resting membrane potential and did not induce epileptic-like activity in normal Krebs containing less than 4mM K^+ (cf. Rutecki, Lebeda & Johnston, 1987). However, this concentration would inhibit $GABA_A$-mediated responses and IPSPs. The pharmacological similarity between GABA responses and the zinc- induced depolarizing events could be further extended by affecting $GABA_A$ receptor function using allosteric modulators, e.g., barbiturates and benzodiazepines. Both classes of compound have separate binding sites on the $GABA_A$ receptor complex (Study & Barker, 1981). In a CA1 neurone, following stimulation of the Schaffer-collateral pathway, pentobarbitone (100μM) substantially enhanced the amplitude and prolonged the duration of the zinc-induced GDP in a reversible manner (Fig. 3.12A). Bath-applied flurazepam (2-20μM) also prolonged the duration of the spontaneous GDP in 300μM zinc, but had little effect on the amplitude (Fig. 3.12B). Both drugs had no influence on the frequency of spontaneous depolarizing events induced by zinc. These features of the zinc-induced depolarizations are consistent with such events being mediated by $GABA_A$ receptors.

The dependence of these depolarizing potentials on $GABA_A$ receptors was further emphasized by measuring the reversal potential for GABA-evoked responses and the zinc-induced depolarizations. GABA was applied by ionophoresis to the apical dendrites of a CA1 neurone superfused with 300μM zinc. The GABA response was typically biphasic at -60mV membrane potential with an initial short latency depolarization followed by a long latency hyperpolarization (Fig. 3.13A). Both responses were associated with an increase in the membrane conductance. Previous studies indicated that the short latency depolarizing response may represent the activation of dendritic $GABA_A$

receptors, whereas the hyperpolarizing response occurs after activation of somatic $GABA_A$ receptors (Andersen et al., 1980; Alger & Nicoll, 1982). The reversal potentials for the short and long latency GABA responses, in addition to the zinc-induced GDPs were determined by injecting constant D.C. current into the cell and changing the membrane potential over the range -40 to -90mV. The reversal potentials for the short and long latency GABA responses were -56±5 and -66±8mV (mean±S.D.; n=4) respectively. Similarly, the reversal potential for the zinc-induced GDPs was estimated at -53±7mV (n=3) and closely correlated with the reversal of the short latency GABA response (Fig. 3.13B). The GDP reversal potential was more depolarized at -30±3mV (n=3) when recording with 3M KCl-filled microelectrodes. Again the zinc-induced events reversed at the same membrane potential as the GABA-evoked response (not shown). This suggested that the GDP events were mediated by $GABA_A$ receptors.

The increase in amplitude and a shift in the reversal potential of GDPs when using 3M KCl-filled microelectrodes suggested that underlying the depolarization was a chloride-mediated current. It is well known that $GABA_A$ receptor activation is linked to an increased Cl^- conductance (Krnjević, 1976; Andersen et al., 1980, Alger & Nicoll, 1982). To further determine if the Cl^- conductance underlying the GDP is the same as that activated by GABA, responses to GABA were evoked during a spontaneous GDP. Since the frequency of the depolarizing events was reasonably regular in any one neurone, it was possible to simultaneously apply GABA during a zinc-induced event. GABA responses evoked following ionophoresis to the dendrites of CA1 neurones were not additive when they occurred simultaneously with spontaneously depolarizing events induced by zinc (Fig. 3.14A). Furthermore, ionophoretically-applied bicuculline (5mM, +200nA) or picrotoxin (50μM, +200nA) into the apical dendrites of CA1 neurones inhibited both the GABA response and the GDP. (Fig. 3.14B). These results suggest that both the GABA response and the zinc-induced depolarization are probably mediated by the same receptor population in the dendrites and utilise the same chloride conductance.

6. Zinc-induced GDPs are enhanced by 4-aminopyridine

The aminopyridines, particularly 4-aminopyridine (4-AP) are known to produce convulsions in man (Spyker et al., 1980) and epileptiform activity in both *in vivo*

(Baranyi & Fehér, 1979) and *in vitro* experimental models (Thesleff, 1980; Buckle & Haas, 1982; Rutecki, Lebeda & Johnston, 1987; Avoli & Perreault, 1987; Perreault & Avoli, 1989; Ives & Jefferys, 1990). A common feature of 4-AP-induced paroxysmal depolarizing shifts (PDSs) and the late depolarizing potential evoked by stimulation in the hippocampus is the activation of EAA receptors as well as $GABA_A$ receptors. The later characteristic is also common to zinc-induced GDPs, therefore both zinc and 4-AP induced depolarizations were compared.

Bath application of 4-AP (50-100μM) produced spontaneous and evoked PDS in CA1 neurones accompanied with a slight hyperpolarization and marked increase in synaptic 'noise' and action potential firing (Fig. 3.15A,B). 4-AP also increased the cell excitability in response to direct current injection manifested by a reduction in the spike threshold and a slight reduction in the accommodation of firing (Fig. 3.15C). Spontaneous PDSs were blocked by 20μM bicuculline, but for the evoked PDS, only the late depolarizing component was inhibited (Fig. 3.15B). These results confirm that epileptiform activity produced by 4-AP is, at least in part, a consequence of enhanced inhibitory and excitatory synaptic transmission (Buckle & Haas, 1982; Rutecki, Lebeda & Johnston, 1987; Aram, Michelson & Wong, 1991). The duration of spontaneous or evoked GDPs induced by zinc were prolonged by the addition of 4-AP (50μM), but the frequency of spontaneous GDPs was unchanged (Fig. 3.16).

DISCUSSION

This study has attempted to explore the cellular basis for zinc producing proconvulsant or depressant effects on CNS neurones. The major novel finding was the observation of spontaneous and stimulus-evoked giant depolarizing potentials induced by zinc in CA1 and CA3 hippocampal neurones. These large potentials were found to be mediated by synaptically released GABA acting on postsynaptic $GABA_A$ receptors.

1. Zinc-induced GDPs are polysynaptic events

Two types of bursts have been classified in hippocampal neurones defined as network and endogenous bursts (Johnston & Brown, 1981, 1984). The evidence for GDPs being generated by a polysynaptic circuit came from the following results: (i) spontaneous and evoked GDPs were abolished by blockade of synaptic transmission with TTX; (ii) the frequency and probability of occurrence of spontaneous GDPs were unaltered by changes in the postsynaptic neuronal membrane potential; (iii) the evoked GDPs were not graded, but responded to orthodromic stimulation of the Schaffer-collateral or mossy fibres with different stimulus intensities or stimulus-intervals in an all-or-none manner. All these characteristics of zinc-induced GDPs satisfy the criteria for network-type events as previously defined in many studies (Johnston & Brown, 1981, 1984; Ben-Ari et al., 1989). Such characteristics indicate that an intact neuronal circuitry is required for the generation of these potentials. The lack of intact circuitry in tissue cultured hippocampal neurones may be one reason why such events have eluded previous investigations (Mayer & Vyklicky, 1989; Mayer, Vyklicky & Westbrook, 1989). Curiously, these zinc-induced large synaptic potentials were not seen when recording intracellularly from pyramidal neurones in the olfactory cortex brain slices in the presence of 300-500μM zinc (Smart & Constanti, 1983, 1990).

2. Zinc-induced synaptic potentials are $GABA_A$-mediated giant IPSPs

Intracellular recordings from pyramidal neurones in hippocampal brain slices are routinely characterised by a continuous background 'noise' due to spontaneous synaptic

potentials (Miles & Wong, 1984). When the recording electrode contains 3M KCl, these potentials are usually 2-8mV in amplitude at a membrane potential of approximately -70mV, and are largely composed of depolarizing IPSPs mediated by $GABA_A$ receptor activation. Zinc did not apparently affect these IPSPs, but within 5-10min of application, large depolarizing potentials appeared. In some neurones, a cyclical sequence of events was associated with the zinc-induced potentials. The spontaneous background IPSPs increased in frequency and amplitude immediately prior to the discharge of a large depolarization. Furthermore, after the depolarization, there was a period of quiescence during which there were few IPSPs and GDPs could not be evoked by stimulation. Eventually the IPSPs frequency returned to near basal level.

The zinc-induced large synaptic potentials were generated with a markedly increased conductance and could be readily inhibited by bicuculline or picrotoxin and enhanced by pentobarbitone or flurazepam, suggesting that $GABA_A$ receptors mediated the giant IPSPs. Zinc-induced depolarizing potentials could also be observed when recording with microelectrodes filled with 4M potassium acetate, although their amplitudes were smaller, suggesting these events are probably mediated by an increased chloride conductance mechanism. The GDP reversal potential correlated closely with the reversal potential for the depolarizing GABA responses, which are thought to represent activation of dendritic $GABA_A$ receptors (Andersen et al., 1980, Alger & Nicoll, 1982). GABA evoked responses by local ionophoresis to the dendritic region exhibited no additivity with the GDP. Furthermore, ionophoretically-applied bicuculline or picrotoxin to the apical dendritic field was capable of blocking the GDP. All these features indicated that GDPs are probably generated by the activation of $GABA_A$ receptors localized in the dendritic region of CA1 or CA3 subfields, which is presumably why zinc-induced synaptic potentials mediated by GABA are always depolarizing at the resting membrane potential, irrespective of the type of microelectrode electrolytes (K acetate or KCl) employed.

3. Origin of GABA-mediated synaptic potentials

In the hippocampal CA1 subfield, GABAergic inhibition of the pyramidal cells is principally mediated by local interneurones (Andersen, Eccles & Løyning, 1964; Alger

& Nicoll, 1982; Turner, 1990). Electromicroscopic studies have provide evidence that axons originating from interneurones mostly form synapses with the dendritic region of pyramidal cells in the hippocampus (Schwartzkroin, Kunkel, & Mathers, 1982; Schwartzkroin & Kunkel, 1982). The most likely site of GABA release is in the dendritic area for the pyramidal neurones. The local interneurones are activated by the Schaffer collaterals from area CA3 and commissural fibres from the contralateral hippocampus (feed-forward inhibition) (Alger & Nicoll, 1982; Turner, 1990) and by collaterals from the pyramidal cells in area CA1 (feedback inhibition) (Andersen, Eccles & Løyning, 1964). Activation of these interneurones by excitatory synaptic transmission leads to generation of IPSPs, mainly mediated by $GABA_A$ receptors in the pyramidal cells. However, the inability of APV and CNQX to block the production of the zinc-induced giant IPSPs suggests that zinc inducing the release of GABA may either directly affect the interneurones, or other transmitter systems are also involved in the mediation of the giant IPSPs (*vide infra*, Chapter 6).

The amplitude of the giant IPSPs induced by zinc is much larger than the mean amplitude of the background IPSPs, suggesting that either a distinct inhibitory cell population is responsible for their generation, or that many interneurones are synchronously discharging to produce giant IPSPs. There are many types of inhibitory interneurones in the hippocampus, including basket cells, oriens/alveus and stratum lacunosum-moleculare interneurones (Lacaille & Schwartzkroin, 1988a,b). The release of GABA inducing the giant IPSPs recorded in the pyramidal neurones in the presence of zinc may occur from one or more of these cells. In addition, for CA3 neurones, the mossy fibre projections are known to arborize into the dendritic field of basket neurones as well as to form large proximal synaptic connections with pyramidal neurones (Frotscher, 1985). Recent immunohistochemical evidence suggests that in addition to glutamate, the mossy fibre nerve terminals also contain GABA (Sandler & Smith, 1991) which if co-released might suggest that this pathway can have an inhibitory and excitatory function. Furthermore, hilar neurones are also suggested to project directly to pyramidal neurones and could be a source of GABA underlying the giant IPSPs induced by zinc and 4-AP (Muller & Misgeld, 1991).

4. Activity-dependent depression of zinc-induced giant IPSPs

An interesting feature of these zinc-induced potentials concerns the interval between two successive spontaneous depolarizations. In a single pyramidal neurone, the inter-depolarization intervals were usually quite similar, but varied between different neurones. The failure of transmission between spontaneous or evoked GDPs could be designated as an apparent 'activity-dependent' depression (cf. McArren & Alger, 1985; Thompson & Gähwiler, 1989a). The significance of these intervals was demonstrated by repeated stimulation of the Schaffer-collateral or mossy fibre pathways in the presence of zinc. If the stimulus interval was reduced between successive stimuli, the second GDP was labile and a failure of transmission would occur. After delaying stimulation for a period not less than that observed between two spontaneous events, simulation of the fibre tracts would now evoke a giant potential. This apparent 'activity-dependent disinhibition' was not followed by any excitatory or epileptic-type discharges. A use-dependent depression of IPSPs in the hippocampus has been reported previously *in vivo* (Ben-Ari, Krnjević & Reinhardt, 1979) and *in vitro* (McCarren & Alger, 1985; Thompson & Gähwiler, 1989a; Davies, Davies & Collingridge, 1990). However, usually a train of repetitive stimuli are required for a clear depression, although some depression can be seen after only one stimulus (McCarren & Alger, 1985). A failure of transmission could be due to: (i) $GABA_A$ receptor desensitization, or a shift in the reversal potential for the $GABA_A$ receptor-gated Cl- mediated response (E_{GABA}) or E_{Cl}, would cause a reduction in the amplitude of GABA responses (Thompson & Gähwiler, 1989b,c). These possibilities are considered unlikely since in the period immediately following an evoked GDP, the postsynaptic membrane was still responsive to GABA suggesting that there was little or no receptor desensitization. Also there was no small decrement in the amplitude of the GDPs but a complete failure of transmission. Furthermore, this phenomenon was observed when using KCl-filled microelectrodes rendering any subsequent large shift in E_{GABA} or E_{Cl} unlikely; (ii) An increased level of released GABA could activate presynaptic $GABA_B$ receptors and thereby inhibit transmission until the excess GABA is removed via uptake processes (Deisz & Prince, 1989; Thompson & Gähwiler, 1989b; Davies, Davies & Collingridge, 1990). However, CGP 35348, a $GABA_B$ antagonist, does not substantially affect the generation or the frequency of GDPs. Additional mechanisms

would involve, for example, an acute depletion of neurotransmitter or a prolonged inactivation of presynaptic calcium channels. Both would lead to a temporary failure of transmission (cf. Watson, Rader & Lanthorn, 1989). The present results suggest that the failure of transmission is probably a presynaptic phenomenon.

5. Comparison of zinc-induced GDPs with other giant synaptic potentials

The most extensively studied animal models of epilepsy *in vivo* and *in vitro* were developed by application of penicillin, bicuculline or picrotoxin (Curtis & Felix, 1971; Ayala et al., 1973; Schwartzkroin & Prince, 1978; Dingledine & Gjerstad, 1980; Swann & Brady, 1984; Tancredi & Avoli, 1987). The intracellular correlate of the interictal event associated with epilepsy consists of a sudden large depolarization which was originally termed a PDS (Matsumoto & Ajmone-marsan, 1964). The PDS is a giant synaptic potential and apparently mediated by excitatory amino acid transmitter(s), since the PDS potentials reverse at 0-10mV and are blocked by CNQX and APV (Johnston & Brown, 1981; Dingledine, Hynes & King, 1986; Ben-Ari, Cherubini & Krnjević, 1988; Lee & Hablitz, 1989). Zinc-induced giant depolarizing potentials resemble to a certain extent of the PDS. But one characteristic which is common to several of the convulsants capable of inducing PDSs is the ability to antagonize GABAergic potentials and cause a consequent reduction in the efficacy of GABAergic inhibition (Krnjević, 1976; Swartzwelder, Anderson & Wilson, 1988; Avoli, 1988; Chamberlin & Dingledine, 1988). This is in contrast to zinc-induced depolarizing potentials which are mediated by the release of **inhibitory** transmitter.

GABA-mediated large depolarizing synaptic potentials have been reported previously in hippocampal and cortical neurones; including, an innate occurrence in immature postnatal hippocampal neurones (Mueller, Taube & Schwartzkroin, 1984; Ben-Ari et al., 1989; Xie & Smart, 1991a), or induced in the adult hippocampus following either high intensity afferent stimuli (Perreault & Avoli, 1988), or after pharmacological manipulation with pentobarbitone (Alger & Nicoll, 1980), or 4-AP (Buckle & Haas, 1982; Rutecki, Lebeda & Johnston, 1987; Avoli & Perreault, 1987; Avoli, 1988; Muller & Misgeld, 1991), or guanosine-5'-o-(3-thio)triphosphate (GTP-γ-S; Thalmann, 1988), a non-hydrolysable analog of GTP. The induction of large depolarizing potentials

following incubation with 4-AP shows striking similarities with the potentials induced by zinc. These potentials are also generated without requiring intact excitatory synaptic transmission (Aram, Michelson & Wong, 1991). However, 4-AP also induces a large increase in excitatory transmitter release (Fig. 3.15, see also Buckle & Haas, 1982; Rutecki, Lebeda & Johnston, 1987), whereas zinc seems to result in an apparently specific increase in the release of GABA (*vide infra*, Chapter 7).

The significance of these results is that giant $GABA_A$-mediated potentials have only been induced by compounds usually not found in the CNS. Zinc is a naturally occurring trace element in neuronal tissues and is particularly concentrated in the hippocampus. The observation that zinc appears to have uncovered a novel inhibitory mechanism to modulate cell excitability adds to the established feedback and feed-forward inhibitory networks (Andersen et al., 1980; Alger & Nicoll, 1982). Since zinc increases GABA release it is doubtful whether this giant depolarizing potential has any relevance to the epileptogenic effect of zinc observed in previous studies (Donaldson et al., 1971; Itoh & Ebadi, 1982; Pei et al., 1983).

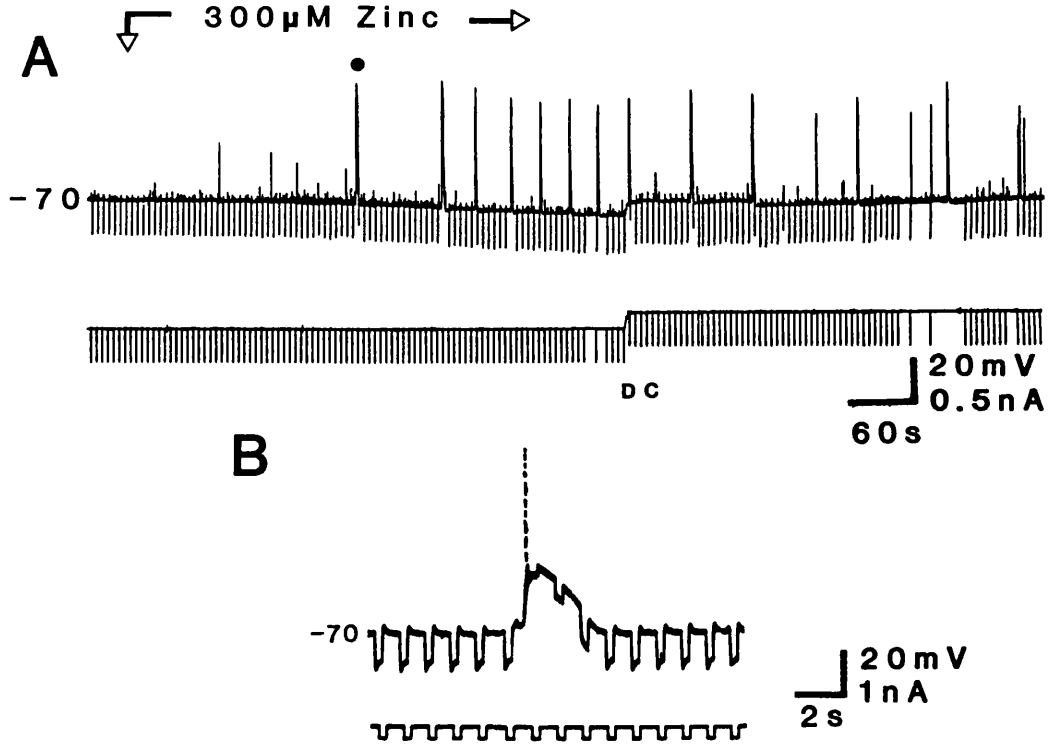

Fig. 3.1. Zinc induces giant depolarizing potentials (GDPs) in adult hippocampal neurones. **A**, Chart record of an intracellular recording from a CA1 neurone at a membrane potential of -70mV adjusted with DC current injection. Hyperpolarizing electrotonic potentials (downward deflections) were evoked by 0.3nA, 300ms, 0.5Hz constant current pulses. The small amplitude (2-7mV) depolarizing potentials are due to synaptic activity, mainly IPSPs. Application of 300µM zinc (open triangles) hyperpolarized the membrane potential with a small increase in the input resistance. After 4 min, spontaneous GDPs (●) appeared. Note that stopping the hyperpolarizing current injections did not affect the GDPs. **B**, A spontaneous GDP (upper trace) induced by zinc (300µM) was associated with a large increase in the input conductance (measured from the electrotonic potentials induced by -0.3nA, 300ms, 1Hz current pulses; lower trace). Recording was obtained from another CA1 neurone using a 4 M K acetate-filled microelectrode.

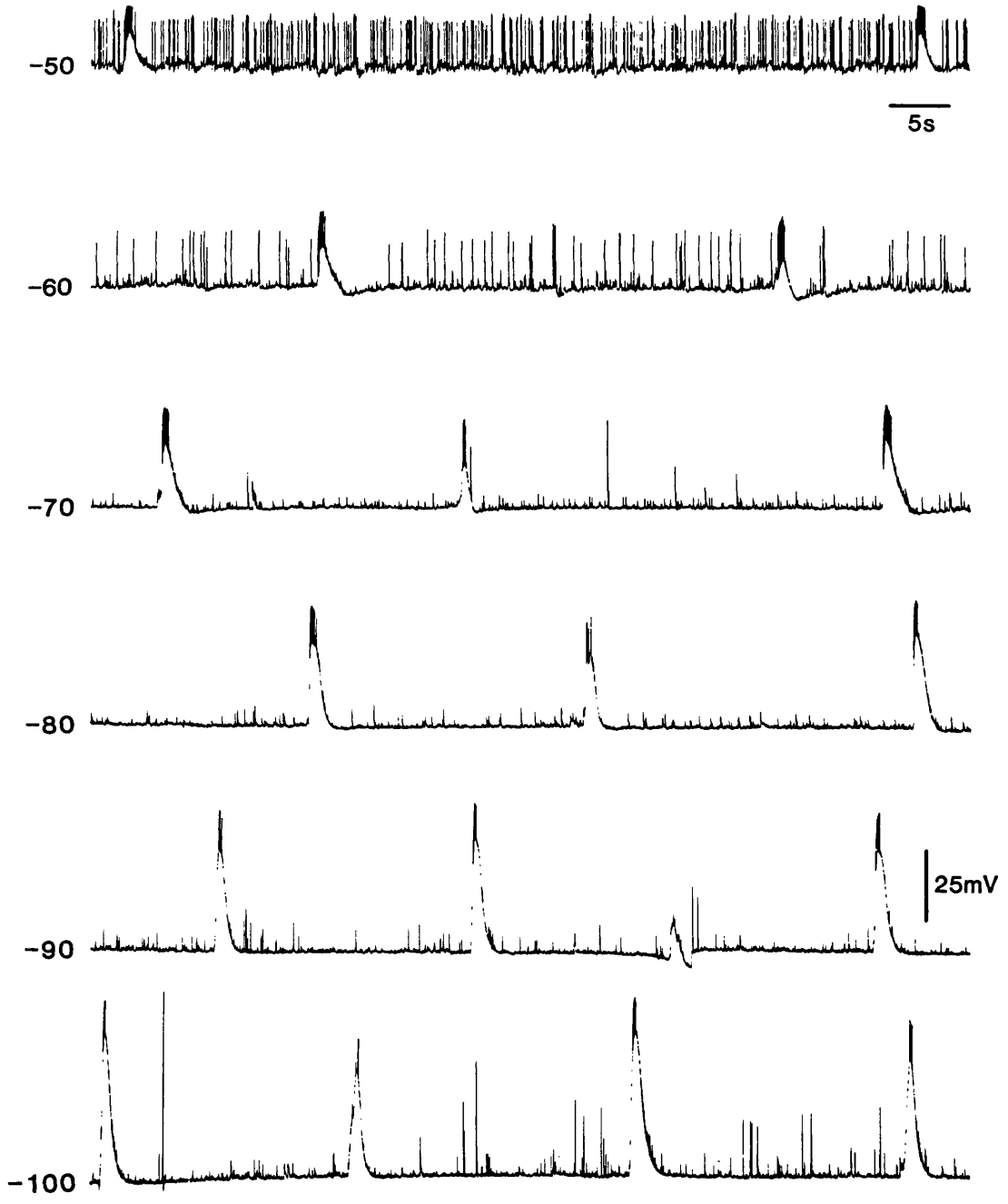

Fig. 3.2. The frequency of spontaneous GDPs is independent of the membrane potential. Chart records taken from a CA1 neurone with a resting membrane potential of -64mV. Spontaneous GDPs were induced by 300μM zinc, and the membrane potential was altered to the values indicated by DC current injection. Note membrane potentials above -60mV caused an increased spontaneous action potential firing.

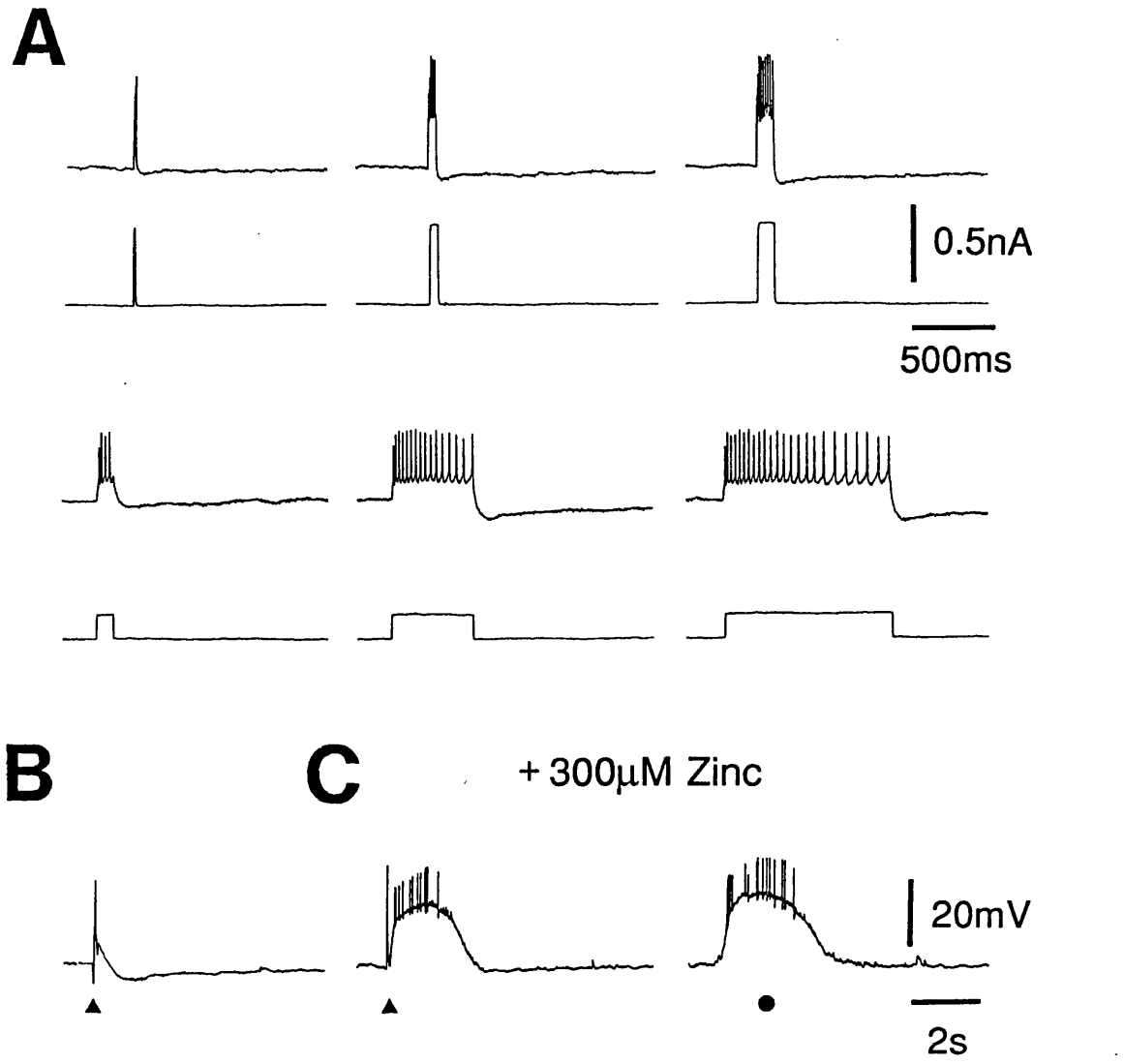

Fig. 3.3. Large depolarizations are not elicited by direct membrane excitation with depolarizing current. **A**, Varying either the amplitude (1nA, upper traces, or 0.3nA, lower traces) or the duration (10, 50, and 100ms, upper traces; 100, 500, and 1000ms, lower traces) of depolarizing current pulses elicited only action potentials and graded afterhyperpolarizations. **B**, In the same cell, orthodromic stimulation of the Schaffer-collateral pathway (▲, 10V, 0.1ms) evoked an EPSP-IPSP complex with a superimposed action potential. **C**, After bath-application of 300μM zinc, stimulation now induced an evoked GDP. Spontaneous GDPs (●) also appeared with a similar time course to the evoked potential. Membrane potential -70mV adjusted with DC current injection. Time calibration in A applies to B.

Fig. 3.4. Zinc-induced spontaneous and stimulus-evoked GDPs are blocked by tetrodotoxin (TTX). Intracellular recording from a CA1 neurone at a resting membrane potential of -66mV. **A**, Bath-applied 300μM zinc (open arrow) throughout the experiment induced spontaneous GDPs (●), which were blocked by 1μM TTX (solid line) and partly recovered after washing with zinc containing Krebs for 20min (W+Zn 20). **B**, In the same cell, stimulation of Schaffer collateral fibres (▲, 10V, 0.1ms) evoked an EPSP in the absence of zinc (control). In the presence of 300μM zinc, the same stimulus intensity evoked a GDP which was also reversibly blocked by 1μM TTX (TTX/Zn). Hyperpolarizing current pulses (-0.3nA, 300ms) were applied to monitor the cell input resistance.

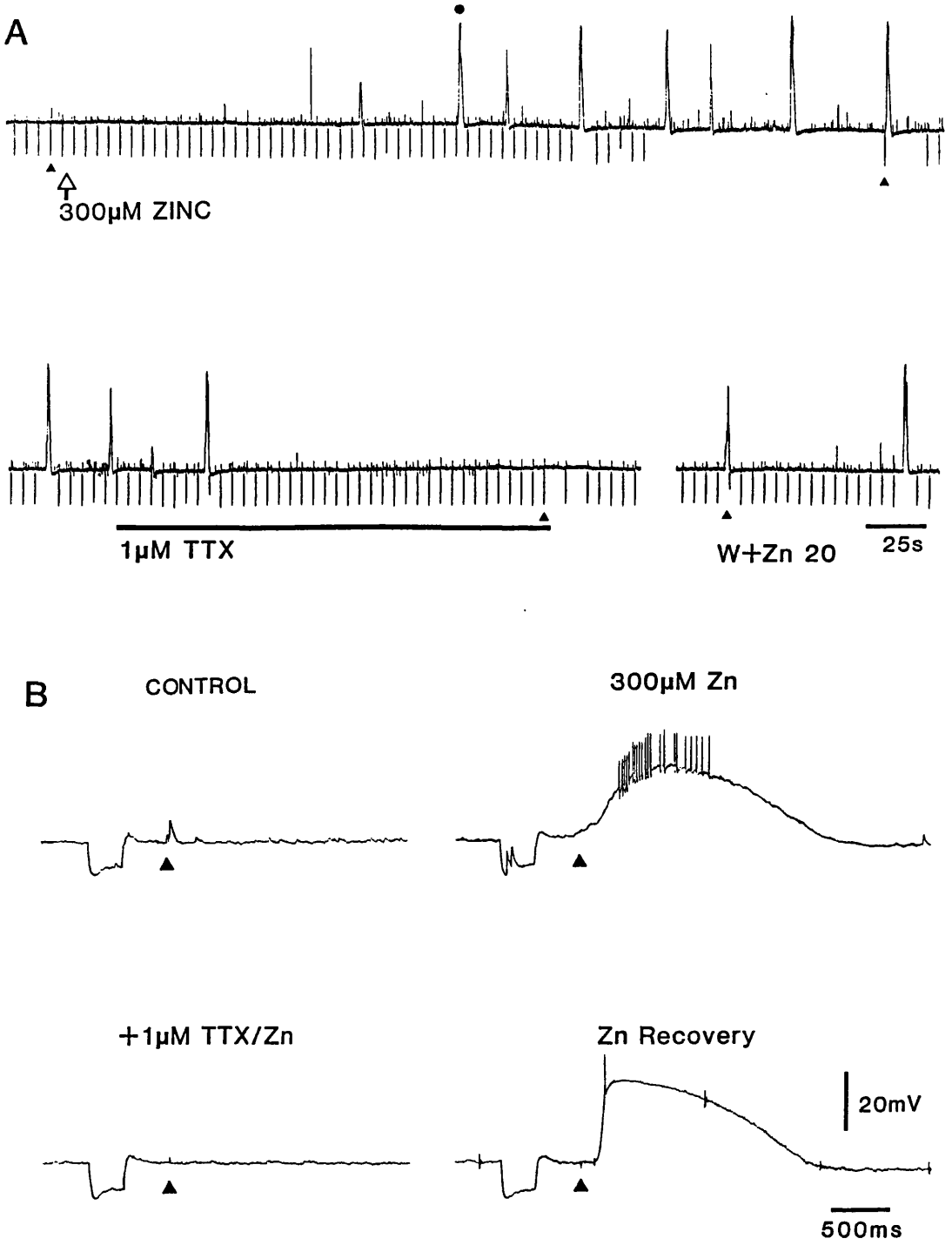
A
300μM ZINC
1μM TTX
W+Zn 20
25s
B
CONTROL
300μM Zn
+1μM TTX/Zn
Zn Recovery
20mV
500ms

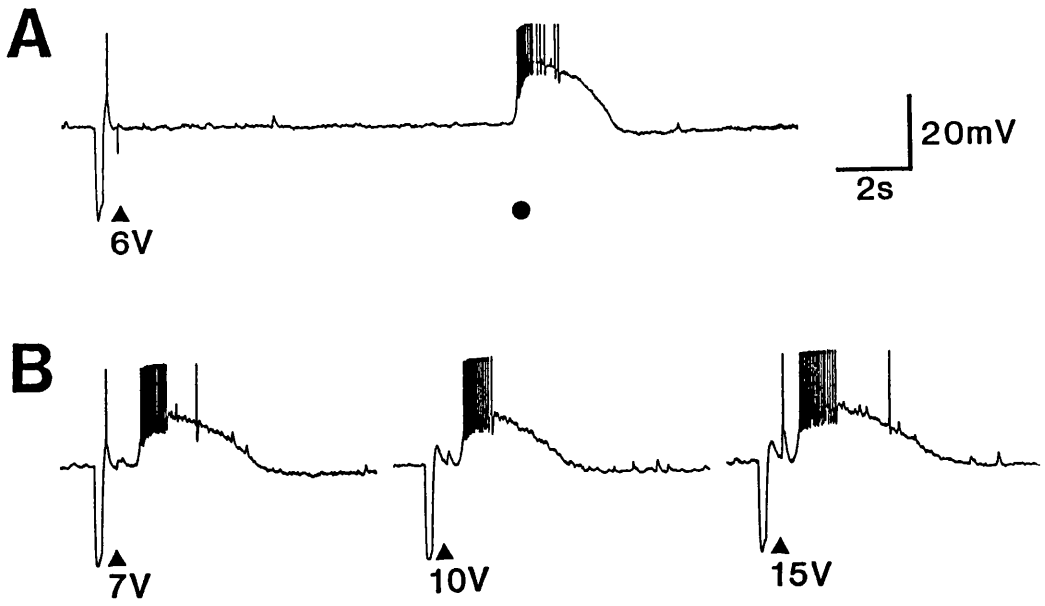

Fig. 3.5. Zinc-induced evoked GDPs in an all-or-none manner. Intracellular recording from a CA1 neurone in the presence of 300μM zinc. Schaffer collateral fibres were stimulated at different intensities (▲, 6-15V, 0.1ms). The filled circle (●) indicates a spontaneous GDP (**A**). Increasing the stimulus intensity evoked GDPs in an all-or-none manner (**B**). Membrane potential -70mV, adjusted by DC current injection. Membrane resistance was monitored using hyperpolarizing current pulses (-0.5nA, 300ms, 1 pulse per 90s).

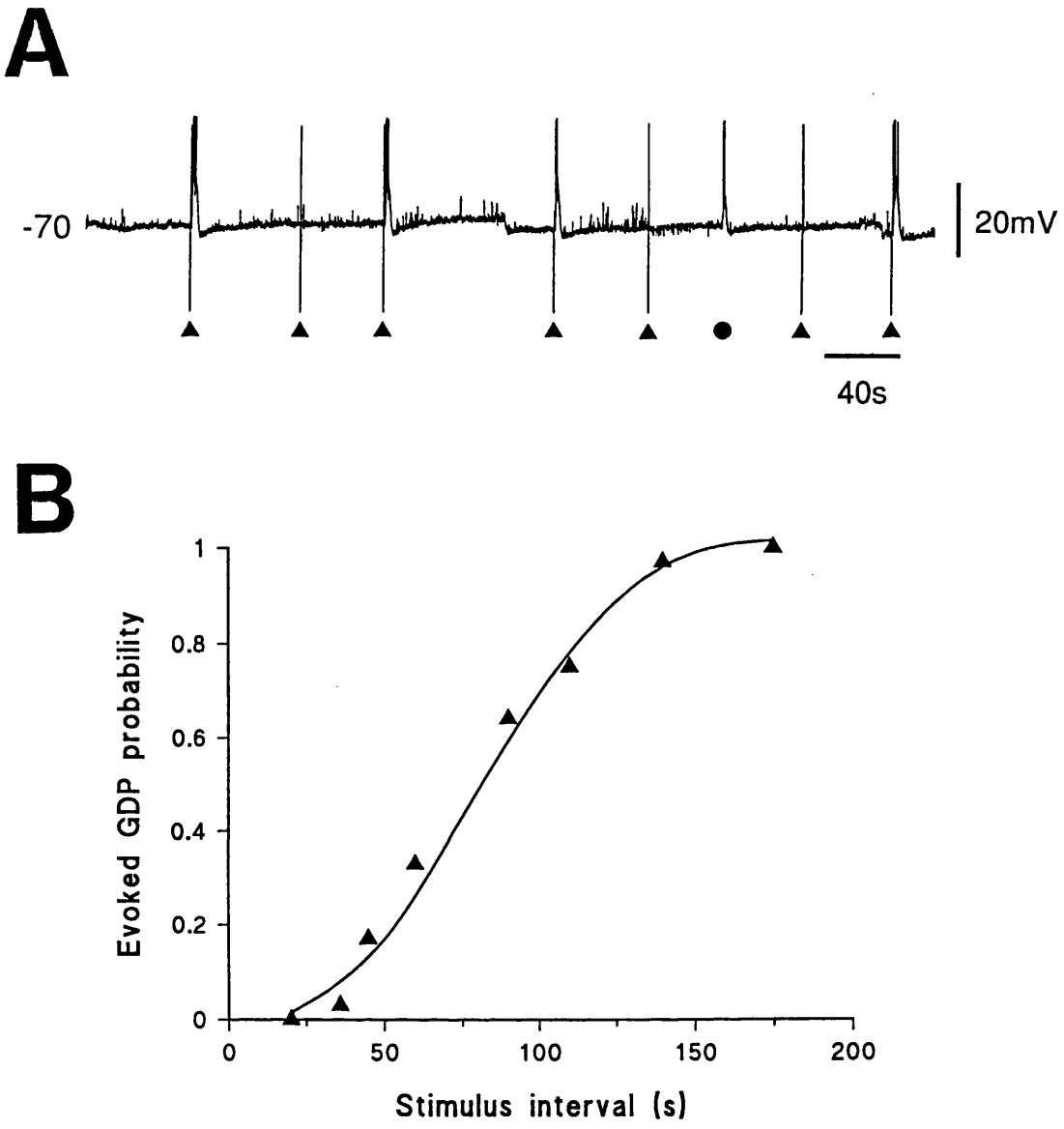

Fig. 3.6. Paired-pulse interval analysis for evoking GDPs. **A**, GDPs in a CA1 cell following stimulation of the Schaffer-collateral pathway (▲, 15V, 0.1ms) in the presence of zinc. Stimuli applied at intervals less than approximately 90s from the previous GDP (evoked ▲ or spontaneous ●) failed to trigger an evoked GDP. Membrane potential was -70mV was adjusted with DC current injection. A hyperpolarizing electrotonic potential (-0.5nA, 300ms) was applied prior to each stimulation to monitor the input resistance. **B**, Relationship between the probability of evoking a GDP and the stimulus interval. To ensure successful generation of an evoked GDP, a mean interval of 145±92s was required between successive stimuli. Data was collected from 88 stimuli monitored in 26 cells.

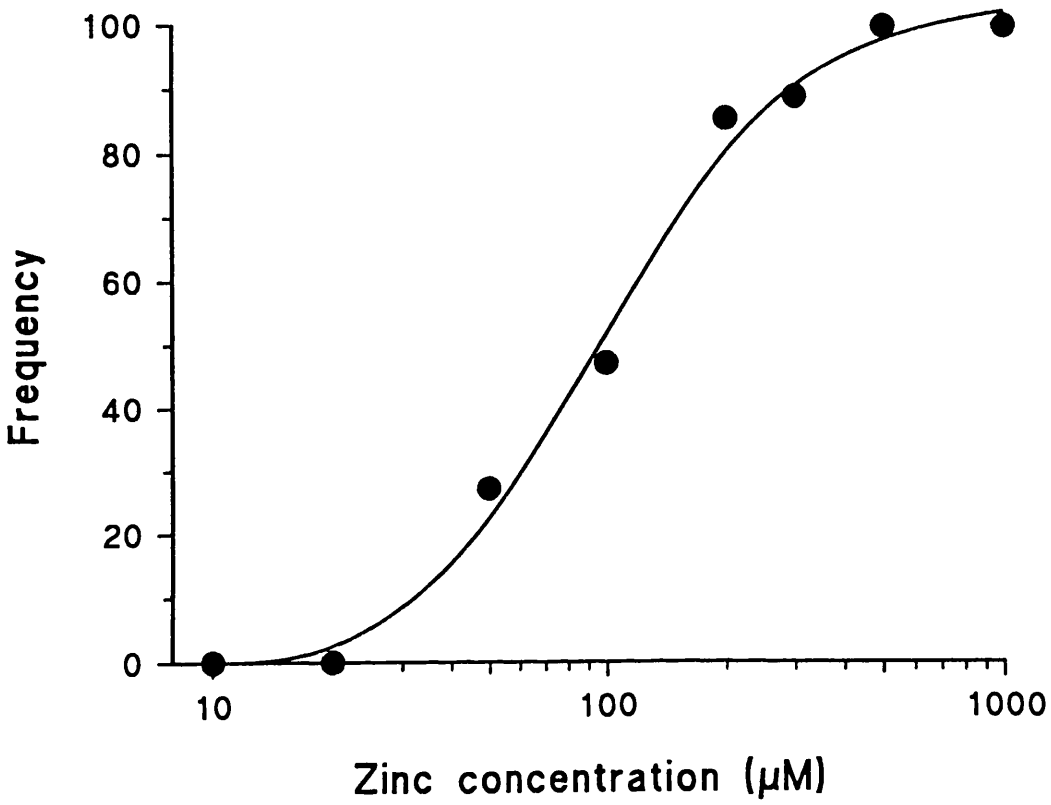

Fig. 3.7. Frequency of spontaneous and evoked GDPs in pyramidal neurones are dependent on zinc concentration. Points are the percentage (%) of cells exhibiting both spontaneous and evoked GDPs and plotted against the zinc concentration. The semilogarithmic dose-response curve reveals an EC_{50} of approximately 100μM. Data were collected from 168 applications of different zinc concentrations to CA1 (n=126) and CA3 cells (n=42).

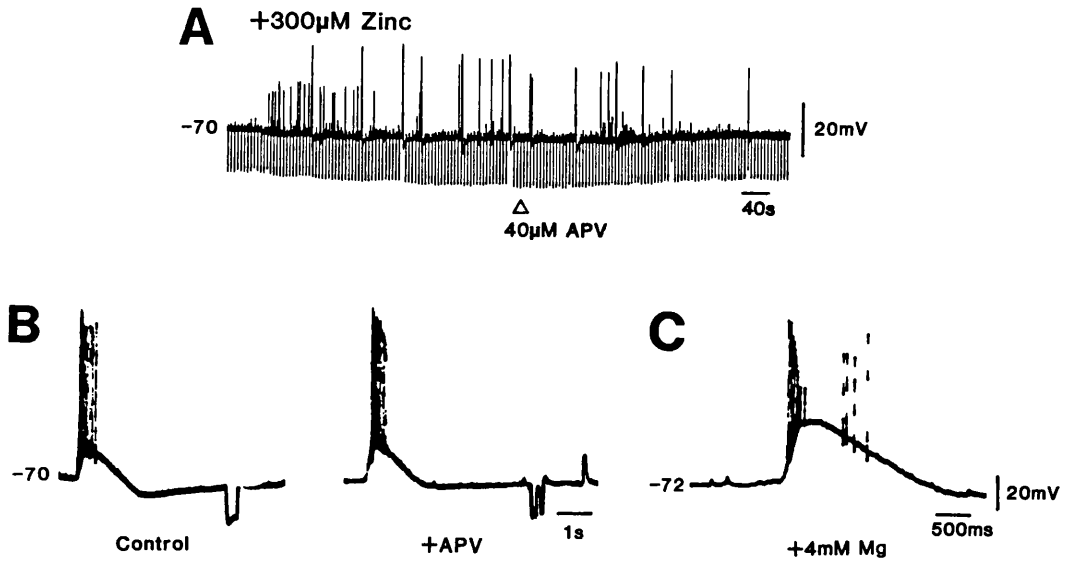

Fig. 3.8. Effect of DL-2-amino-5-phosphonovalerate (APV) on zinc-induced GDPs. **A**, Intracellular recording of a CA1 neurone at a membrane potential -70mV (adjusted with DC current injection) in the presence of 300μM zinc. Upward deflections are spontaneous action potentials and zinc-induced GDPs; downward deflections are hyperpolarizing electrotonic potentials evoked by constant current pulses (-0.3nA, 300ms, 0.3Hz). Application of 40μM APV (open triangle) did not block spontaneous GDPs. **B**, Oscilloscope records illustrate two GDPs selected from trace A in the absence and in the presence of APV on an expanded timescale. **C**. In Krebs containing 4mM Mg^{2+}, 300μM zinc still induced spontaneous GDPs recorded from another CA1 cell, resting membrane potential -72mV.

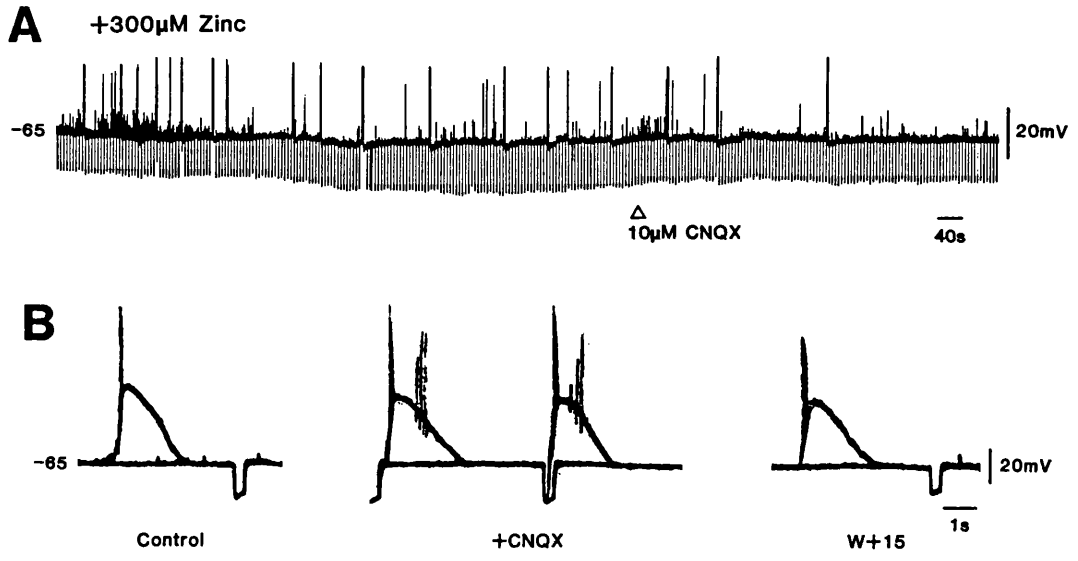

Fig. 3.9. Effect of 6-cyano-7-nitroquinoxaline-2,3-dione (CNQX) on zinc-induced spontaneous GDPs. **A** Intracellular recording from a CA1 neurone with resting membrane potential -65mV in the presence of 300μM zinc. Upward deflections are spontaneous action potentials and zinc-induced GDPs; downward deflections are hyperpolarizing electrotonic potentials evoked by constant current pulses (-0.3nA, 300ms, 0.3Hz). Application of 10μM CNQX (open triangle) slightly reduced the GDP frequency but did not block spontaneous GDPs. **B**, Oscilloscope records illustrate four GDPs on an expanded timescale taken from trace A before, during and after application of CNQX (washing for 15min, W+15).

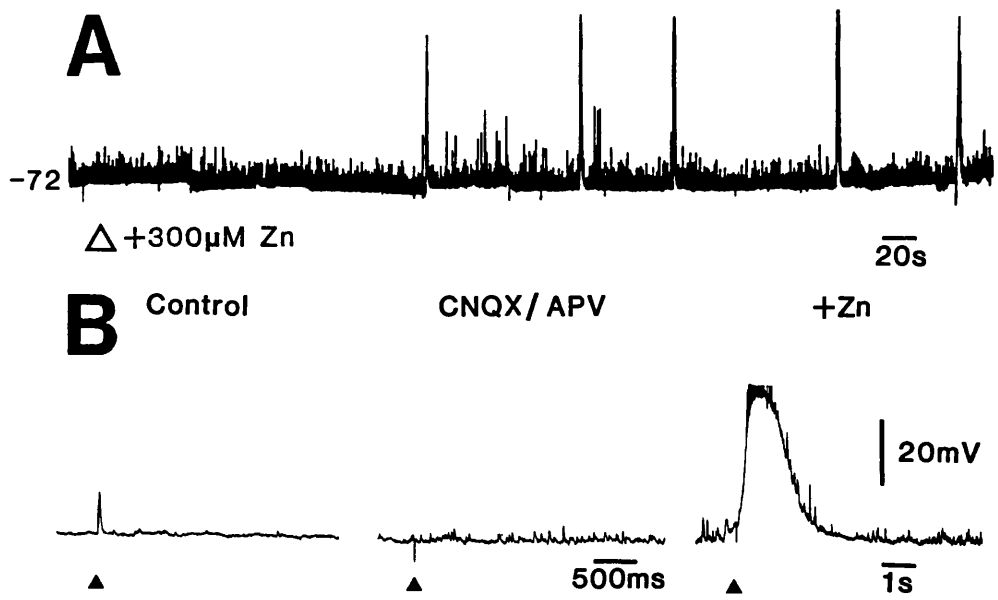

Fig. 3.10. Zinc induces spontaneous GDPs in the apparent absence of functional excitatory synaptic activity. The presence of 20μM CNQX, 40μM APV and 4mM Mg^{2+} completely blocked evoked EPSPs following stimulation of the Schaffer-collateral pathways (▲, 20V, 0.1ms) as shown in the middle trace of **B**. Bath-applied 300μM zinc (open triangle) was still capable of inducing spontaneous GDPs (**A**) and evoked GDPs (▲, in **B**) in a CA1 neurone. Note the continuously active background level of IPSPs in A. The resting membrane potential was -72mV.

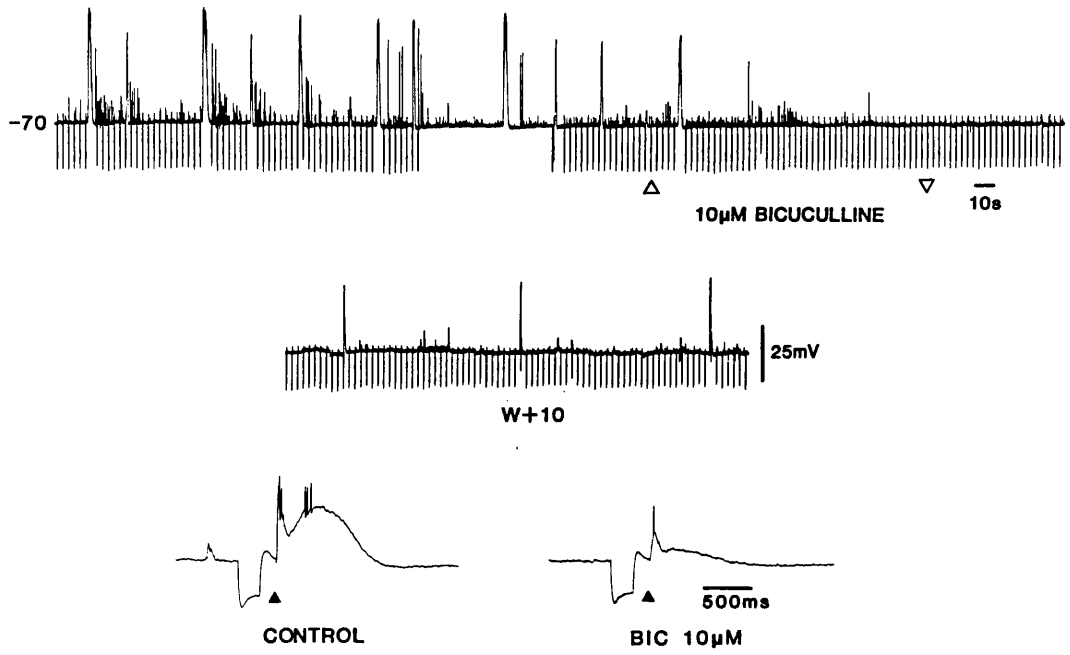

Fig. 3.11. Zinc-induced GDPs are blocked by a $GABA_A$ antagonist. Intracellular recording from a CA1 neurone at a membrane potential -70mV (adjusted with DC current injection) in the presence of 300μM zinc. Upward deflections are spontaneous action potentials and zinc-induced GDPs; downward deflections are hyperpolarizing electrotonic potentials evoked by constant current pulses (-0.3nA, 300ms, 0.2Hz). Zinc-induced GDPs were inhibited by bath-applied 10μM bicuculline (BIC, open triangle). Note BIC also inhibited spontaneous synaptic 'noise'. A partial recovery followed after a 10min washout of BIC (W+10, middle trace). Bottom traces illustrate two evoked GDPs on an expanded timescale following stimulation of the Schaffer-collateral pathway (▲, 10V, 0.1ms) in the absence and presence of 10μM BIC.

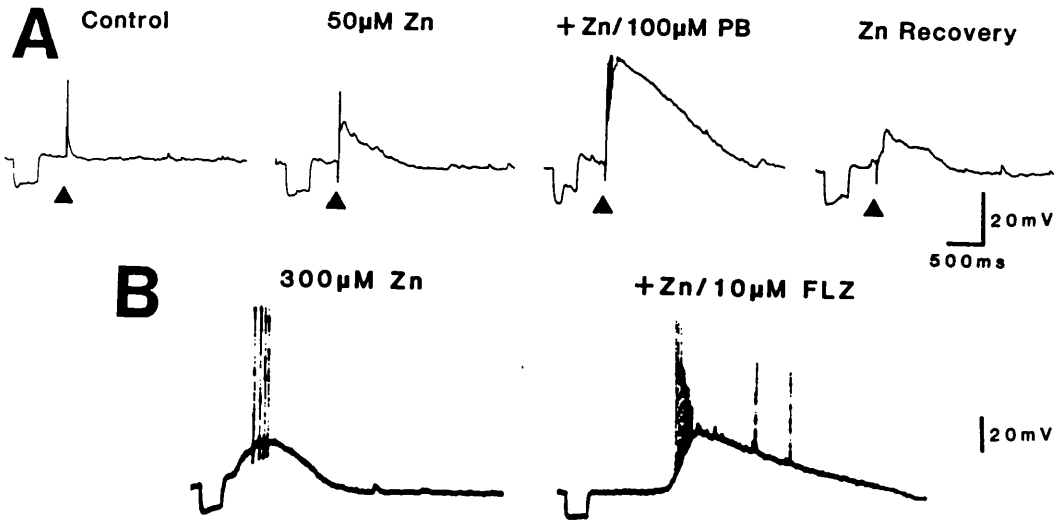

Fig. 3.12. Zinc-induced GDPs are augmented by pentobarbitone or flurazepam. **A**, Intracellular recording from a CA1 neurone with a resting membrane potential of -60mV. In the presence of a low concentration of zinc (50μM), orthodromic stimulation of the Schaffer-collateral fibres (▲, 8V, 0.1ms) evoked a small GDP. Hyperpolarizing electrotonic potentials were elicited by constant current pulses (-0.3nA, 300ms, 1 pulse per 2min). Following co-application of 100μM pentobarbitone (PB) and zinc (50μM), the evoked GDP is markedly enhanced, which was recoverable on washing for 30min in zinc containing Krebs. **B**, Recording from another CA1 cell, 10μM flurazepam (FLZ) prolongs the duration of a spontaneous GDP induced by 300μM zinc. Hyperpolarizing electrotonic potentials were elicited by constant current pulses (-0.3nA, 300ms, 0.2Hz). Resting membrane potential -73mV.

Fig. 3.13. Zinc-induced GDPs reverse at the same membrane potential as GABA-evoked responses. **A**, Biphasic membrane responses were evoked by ionophoretically-applied GABA (1M, +150nA, solid bar) to the apical dendrites of a CA1 neurone. GDPs (●) were induced by bath-applied 300μM zinc. The reversal potentials for the GDPs and the biphasic GABA responses were determined by varying the membrane potential using DC current injection. Hyperpolarizing electrotonic potentials were evoked by constant current pulses (-0.5nA, 300ms, 0.5Hz). To increase clarity constant current pulses were temporarily stopped at -40mV and the chart recorder speed increased at -50mV. **B**, The peak amplitudes of the GDPs (●) and biphasic GABA responses measured at fixed latencies from the beginning of GABA application (short latency ■ 10s, long latency □ 15s), are plotted against the membrane potential. Note the GDP reversal potential correlated closely with the reversal potential for the depolarizing (short latency) GABA response. Resting membrane potential -64mV, using a K-acetate filled microelectrode.

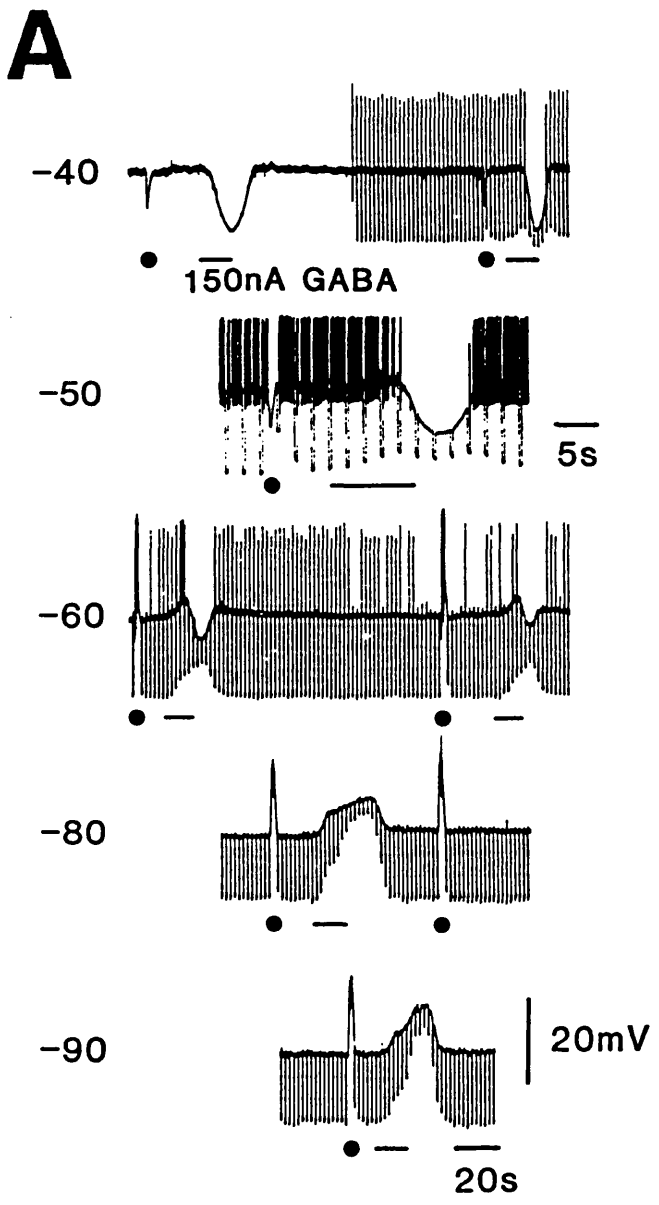
A
-40
150nA GABA
-50
5s
-60
-80
-90
20mV
20s

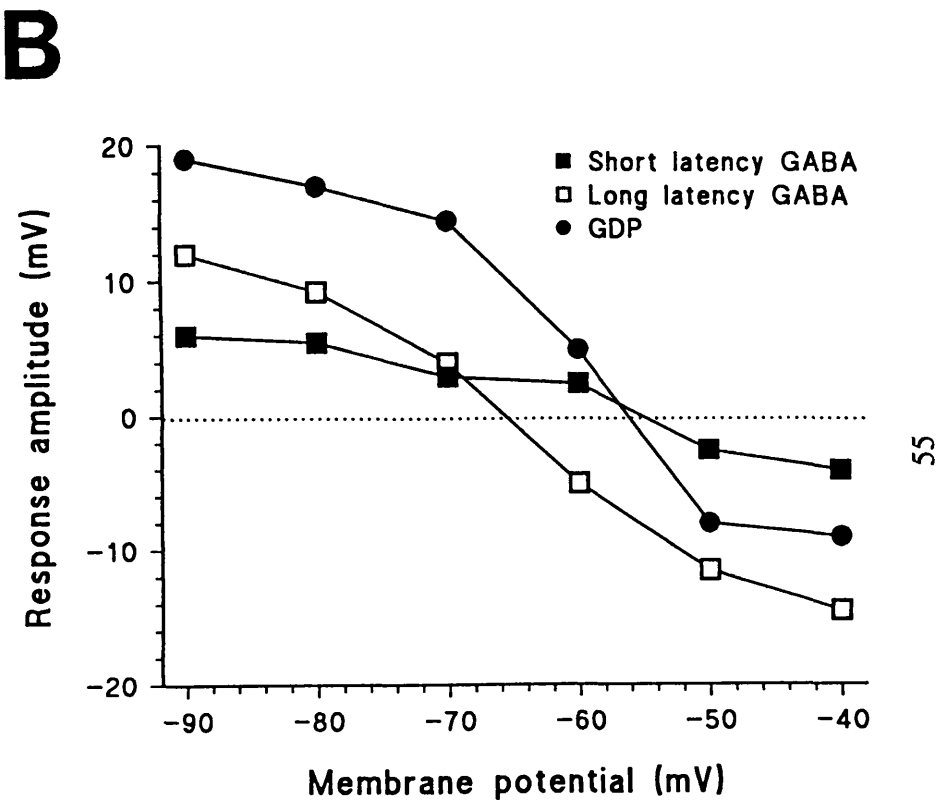
B
Short latency GABA
Long latency GABA
GDP
Response amplitude (mV)
20
10
0
-10
-20
-90
-80
-70
-60
-50
-40
Membrane potential (mV)

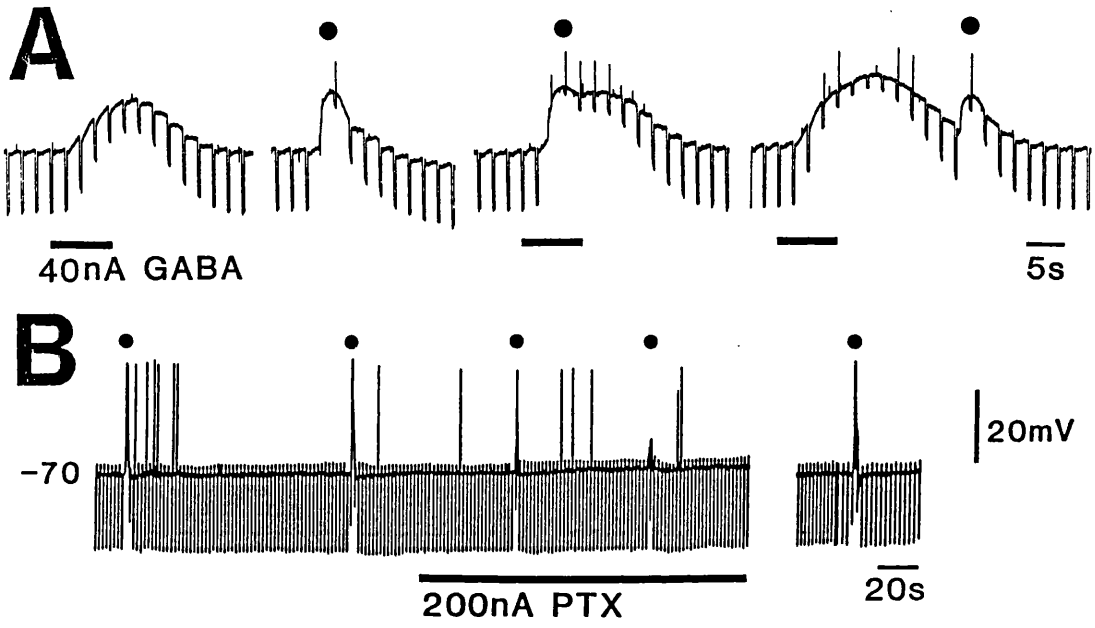

Fig. 3.14. GABA responses are evoked during zinc-induced GDPs and inhibited by picrotoxin. **A**, GABA (1M, +40nA, solid bar) was applied by ionophoresis in the apical dendritic region of the CA1 subfield. GDPs (●) were induced by bath-applied 300μM zinc. Note that the maximal activation induced by exogenous GABA is the same as the GDP and when both potentials occur at the same time, they are not additive. Membrane potential was -70mV adjusted with DC current injection. Hyperpolarizing electrotonic potentials (-0.5nA, 200ms, 0.5Hz) were applied throughout to monitor the membrane input conductance. **B**, Recording from another CA1 neurone, exhibiting spontaneous GDPs (●) induced by zinc (300μM). Ionophoretically-applied picrotoxin (PTX, 50mM, +200nA, solid line) to the apical dendrites inhibited the GDPs in a reversible manner. Membrane potential -70mV (adjusted with DC current injection) with hyperpolarizing electrotonic potentials evoked by constant current pulses (-0.5nA, 200ms, 0.5Hz).

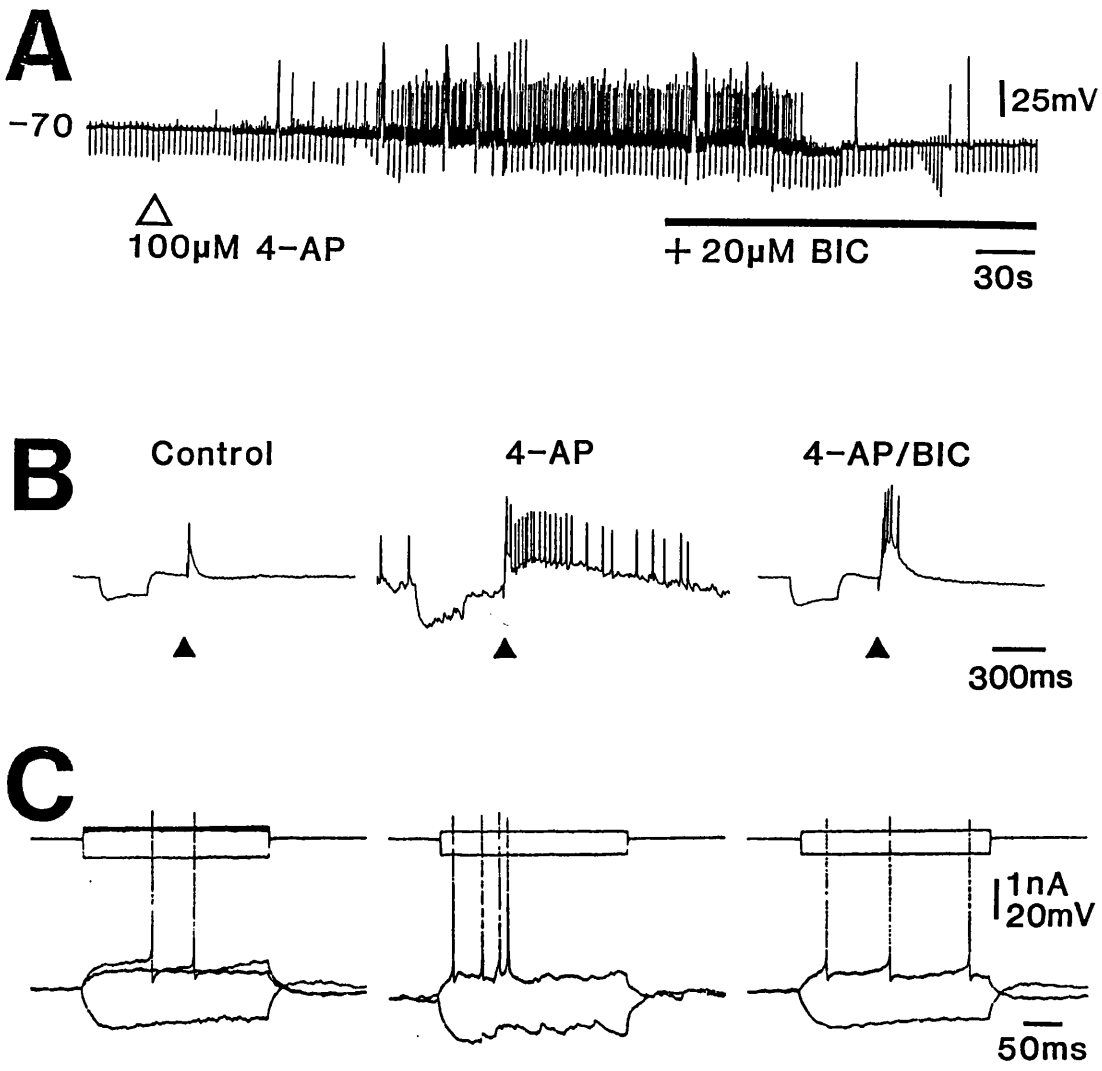

Fig. 3.15. 4-aminopyridine (4-AP) induces spontaneous and evoked paroxysmal depolarizing shifts (PDS) in CA1 neurones. **A**, Intracellular recording from a CA1 neurone at a membrane potential of -70mV, shows the effects of 4-AP (100μM, open triangle) on membrane potential, input conductance and spontaneous potentials. The spontaneous PDS were blocked by 20μM bicuculline (BIC, solid line). **B**, In the same cell, stimulation of the Schaffer-collaterals (▲, 10V, 0.1ms) evoked an EPSP and action potential (in control). 4-AP induced an evoked PDS including a late depolarizing potential which was blocked by 20μM BIC. **C**, Superimposed oscilloscope traces illustrate effects of 4-AP and 4-AP plus BIC on electrotonic responses to positive and negative current injection. Note 4-AP increased cell excitability (middle trace). Hyperpolarizing electrotonic potentials (-0.3nA, 300ms, 0.3Hz, top traces in C) were applied to monitor the membrane input conductance.

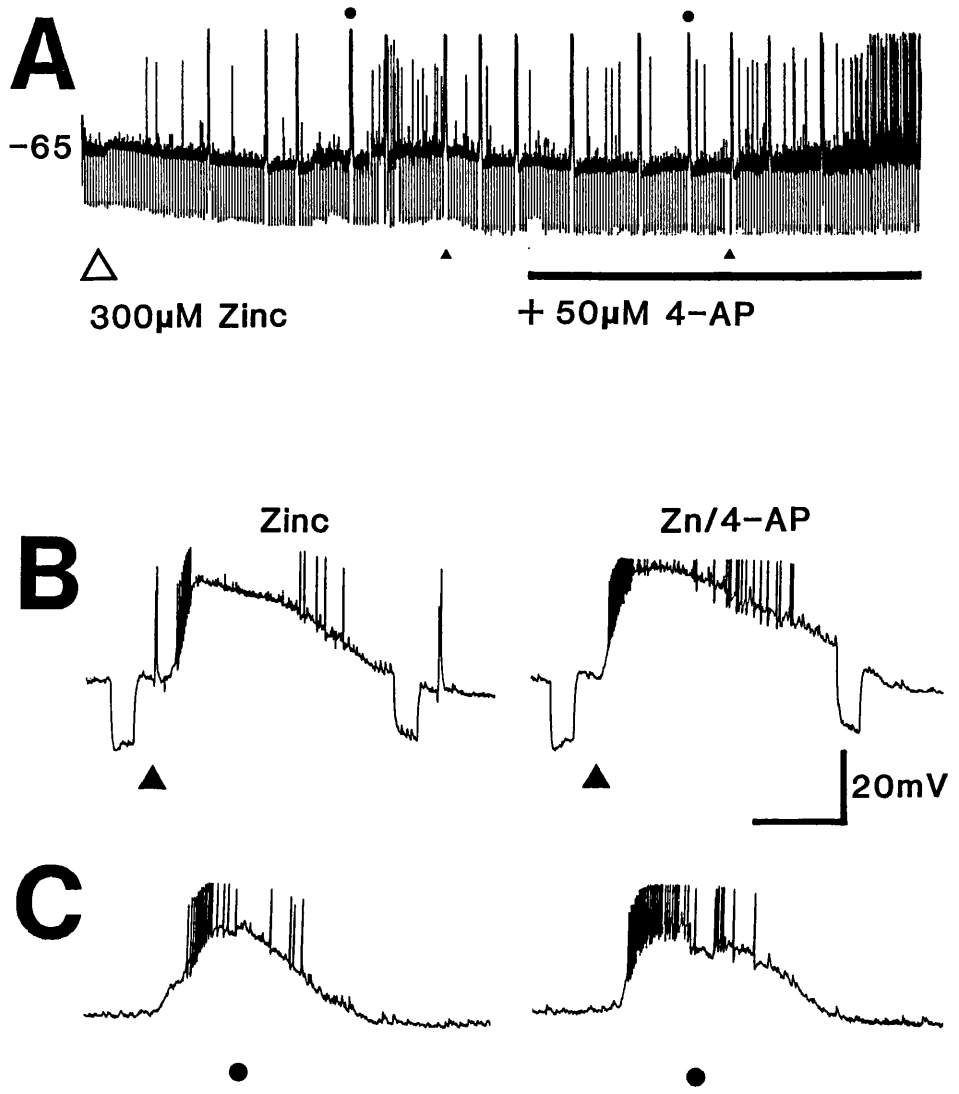

Fig. 3.16. Effect of 4-aminopyridine (4-AP) on the zinc-induced GDPs. **A**, Intracellular recording from a CA1 neurone with a resting membrane potential of -65mV. Hyperpolarizing electrotonic potentials (-0.3nA, 300ms, 0.3Hz) were applied to monitor the membrane input conductance. Application of 300μM zinc (open triangle) throughout the experiment induced the appearance of spontaneous and evoked GDPs following stimulation of the Schaffer-collaterals (▲, 10V, 0.1ms). The addition of 4-AP (50μM, solid line) slightly prolonged the duration of evoked (▲) and spontaneous (●) GDPs as shown on an expanded timescale in **B** and **C** respectively. Time calibration in A is 1min, in B and C, 1s.

Chapter 4

A PHYSIOLOGICAL ROLE FOR ENDOGENOUS ZINC IN IMMATURE HIPPOCAMPAL SYNAPTIC TRANSMISSION

INTRODUCTION

The large pool of zinc in the CNS is not ubiquitously distributed throughout the entire telencephalon. It is found principally in the cortex, hippocampus, cerebral hemisphere and pineal body with the hippocampus containing the highest concentration of zinc (Crawford & Connor, 1972; Donaldson et al., 1973; Frederickson et al., 1983, 1987). Zinc is actively uptaken (Howell, Welch & Frederickson, 1984; Wolf et al., 1984; Wensink et al., 1988) and stored in synaptic vesicles in nerve terminals (Ibata & Otsuka, 1969; Perez-Clausell & Danscher, 1985; Holm et al., 1988). Stimulation of nerve fibre tracts that contain large amounts of zinc, such as the hippocampal mossy fibre system, can induce its release into the synaptic cleft (Assaf & Chung, 1984; Howell, Welch & Frederickson, 1984; Charlton et al. 1985), suggesting that it may act as a neuromodulater. The known interaction of zinc with the major excitatory and inhibitory amino acid neurotransmitter receptors in the CNS supports this notion (Peters, Koh & Choi, 1987; Westbrook & Mayer, 1987; Hori et al., 1987; Smart & Constanti, 1990).

At present, most studies of zinc in the CNS have revealed both the pharmacological and pathological effects of **exogenous** zinc. However, whether **endogenous** zinc has a physiological role in CNS synaptic transmission, has so far not been demonstrated.

Interestingly, the zinc-induced giant depolarizing potentials observed in adult hippocampus appeared very similar to the spontaneous depolarizations which occur naturally in immature CA3 pyramidal neurones from young postnatal rats (P1-12). These large regular depolarizations, referred to as GDPs (Ben-Ari et al., 1989), occur in pyramidal neurones not subjected to any prior pharmacological manipulation. Such GDPs are also mediated by GABA acting on $GABA_A$ receptors; however, the mechanism(s) underlying the generation of GDPs was unknown. It seemed plausible, following the

similarity between the innate GDPs in young neurones and the zinc-induced depolarizing potentials in adult hippocampal slices, that endogenous zinc in the hippocampus might be responsible for the generation of spontaneous GDPs in the immature hippocampus. This aspect was investigated by using new, selective zinc chelating agents, based on heterocyclic pyridinones (Hider et al., 1990), to remove the influence of endogenous zinc on the young CA3 pyramidal cells.

RESULTS

1. Innate GDPs in immature CA3 neurones

Intracellular recordings from hippocampal CA3 neurones of P2-P12 rats displayed spontaneous GDPs in normal Krebs. This activity consisted of a large, long-lasting depolarization (20 - 50mV amplitude, and 200 - 600ms duration) from the resting membrane potential (-66±6mV, n=43), with a superimposed burst of action potentials (Fig. 4.1). The peak amplitude of the GDPs was associated with at least a 100 % increase in the resting input conductance (Fig. 4.1B). Afterhyperpolarizations usually followed the termination of the depolarization and were 2-12mV in amplitude and 1-2s in duration. The mean frequency of GDPs was 0.05±0.006 Hz, (n=56) and usually quite regular in any one individual cell (Fig. 4.1B).

The frequency of spontaneous GDPs was independent of the membrane potential from -105 to -30mV, but the GDP amplitude increased with hyperpolarization and decreased with depolarization (Fig. 4.1A). Unlike exogenous zinc-induced GDPs in adult hippocampus, these regular potentials did not wane or run down during the intracellular recording (1-9 hours).

However, the occurrence of GDPs gradually waned with neuronal development. As shown in Fig. 4.2, from P2 to P8 most neurones (80-100%, n=72) exhibited GDPs. There was a transitional period between P9-13, during which GDPs progressively disappeared until P14 when GDPs were quite rare.

Stimulation of the hilar region or the mossy fibre pathway in immature slices (P2-12), produced an EPSP immediately followed by an evoked GDP which was almost

identical to the spontaneous GDP (Fig. 4.3A). The evoked GDPs usually responded to different stimulus intensities in an all-or-none manner, however the latency of onset for a GDP was usually reduced and the duration was prolonged at high stimulus intensities (Fig. 4.3B). The minimum time required between two successive stimuli was approximately 10s to enable the generation of a second full-sized GDP. This interval was close to the spontaneous inter-GDP interval observed in the same cells. Repeated stimulation at different intervals ranging from 50 to 2000ms revealed that the amplitude of the second GDP was graded (Fig. 4.3C). It was of interest to closely compare these evoked innate GDPs in young cells with the zinc-induced evoked GDPs found in adult neurones. Both responded to different stimulus intensities in an all-or-none manner; however, the spontaneous inter-GDP intervals and the time required for generation of a second full amplitude evoked GDP in immature CA3 neurones was approximately 10 times shorter than those in adult cells (10s vs 120s). Interestingly, the GDP durations in young animals are also approximately 10-fold shorter than those in adult slices (300ms vs 3s). This indicated that there might be a relationship between the amplitude and duration of GDPs and the transmitter(s) release. In some cells, both young and adult, GDPs appeared following a gradual increase in the amplitude and frequency of synaptic noise, (mainly spontaneous IPSPs), just prior to the GDP occurring.

The involvement of neurotransmitter release in generating spontaneous and evoked GDPs was also demonstrated by their blockade in the presence of 1μM TTX, or by raising extracellular Ca^{2+} (4mM) and Mg^{2+} (6mM) concentrations, which blocks polysynaptic transmission (Berry & Pentreath, 1976) (Fig. 4.4).

These spontaneous GDPs in young CA3 neurones were reversibly inhibited by the $GABA_A$ antagonist bicuculline (5-10μM; Fig. 4.5A). In addition to blocking the spontaneous GDPs, bicuculline could also induce seizure-like activity which consisted of a sudden depolarization associated with firing action potentials lasting for 15-30s in 8 out of 15 CA3 neurones (P5-12). The evoked synaptic potential using threshold stimulation was also blocked in the presence of bicuculline. However, synaptic potentials evoked by supra-threshold stimuli were resistant to inhibition by bicuculline, but were partially suppressed by APV (40μM) and completely blocked with a combination of APV and CNQX (20μM; Fig. 4.5B). The results suggest that spontaneous GDPs and the threshold stimulus evoked synaptic potential are mainly mediated by the release of GABA acting

on $GABA_A$ receptors; whereas the supra-threshold stimulus evoked large depolarizing potentials which persist in the presence of $GABA_A$ antagonists and are mediated by EAA receptors. The frequency of spontaneous GDPs was increased and the duration of the evoked GDP was prolonged by pentobarbitone (50μM, n=3; Fig. 4.6). Interestingly, flurazepam (10-20μM, n=4) was apparently unable to affect the GDP.

Unlike the exogenous zinc-induced GDPs in adult hippocampus, the generation of GDPs in young CA3 neurones apparently relied upon functional excitatory synaptic transmission. The GDPs could be effectively blocked by 10μM CNQX (Fig. 4.8A and B; n=6) but only partially inhibited by 50μM APV (Fig. 4.7C and D; n=5), suggesting the involvement of mainly non-NMDA receptors.

2. Spontaneous and evoked GDPs are inhibited by zinc-chelators

Zinc-chelating agents, based on heterocyclic pyridinones (Fig. 4.8; Hider et al., 1990), were selected according to their partition coefficients to be either capable of permeating the cell membrane, or to remain exclusively extracellular. Bath application to young slices of 1,2-diethyl-3-hydroxypyridin-4-one (CP94, 1-400μM), which can permeate into cells, reduced the amplitude and frequency of spontaneously occurring GDPs, with eventual abolition after 5min application (Fig. 4.9; n=35). The inhibition was fully and rapidly reversible on washout of CP94. Spontaneous action potential firing was unaffected by CP94, suggesting that this agent was not interfering with action potential generation and therefore blocking the production of the GDP (Fig. 4.9). Spontaneous GDPs were inhibited by CP94 in a dose-dependent fashion. At 0.5μM, CP94 had virtually no effect, but at 1-10μM a reduced frequency and amplitude of spontaneous GDPs became obvious. Figure 4.10A illustrates a typical record from the same cell, where 10μM CP94 reversibly inhibited spontaneous GDPs and as CP94 concentrations increased to 100μM, GDPs were completely abolished. Analysis of the zinc chelator-GDP inhibition curve revealed that the threshold concentration was 2-5μM and an IC_{50} of approximately 15μM (Fig. 4.10B).

Evoked GDPs following stimulation of the mossy fibre pathway were also inhibited in a reversible manner by CP94 (Fig. 4.11). As previously indicated, the evoked GDP which was triggered by supra-threshold stimulation and resistant to bicuculline

inhibition was only slightly suppressed by the zinc chelator. The residual potential which persisted in the presence of CP94 was completely blocked by the addition of CNQX (10μM; Fig. 4.11B).

A different zinc chelating agent, 1-hydroxyethyl-3-hydroxy-2-methylpyridin-4-one (CP40, 400μM), which does not permeate into cells (Fig. 4.8B), also readily inhibited spontaneous GDPs (n=3, not shown). This suggests that endogenous zinc is probably exerting its effect extracellularly to induce GDPs. However, the evoked GDP triggered by threshold stimulation was only slightly reduced in duration by CP40. These results indicate that CP94, which can permeate cell membranes to presumably form complexes with intracellular Zn^{2+} prior to being released (Assaf & Chung, 1984; Howell et al., 1984), is more potent than CP40 which is poor in membrane penetration and would only have an extracellular effect.

Conversely, the addition of **exogenous** zinc (50-200μM, n=14) to young slices increased the frequency of spontaneous GDPs naturally occurring in immature CA3 neurones (Fig. 4.12A). Zinc also prolonged the duration of evoked GDPs, but did not change the stimulation threshold (Fig. 4.12B).

As the occurrence of GDPs gradually waned with neuronal development (Fig. 4.2), hippocampal CA3 neurones taken from P13-15 animals usually did not exhibit any spontaneous GDPs, but occasionally a small evoked GDP could still be triggered by mossy fibre stimulation. In these neurones, it was possible to induce spontaneous GDPs which reproduced the properties of innate GDPs recorded from younger neurones, by the addition of zinc (50-200μM; Fig. 4.13). The duration of the evoked GDP was also increased by zinc, but subsequent application of CP94 blocked both the spontaneous and evoked GDPs. This occurred concurrently with a small membrane depolarization and input conductance increase, probably due to the complexation of the exogenous zinc. The cell hyperpolarized and spontaneous GDPs quickly returned following a washout of CP94 in the presence of zinc. Furthermore, the evoked GDP displayed an 'over-recovery', which often occurred following washout of the chelator. This may be due to an increased release of zinc into the extracellular space, since the Zn^{2+}-chelator complex could not permeate the cell membrane (Hider, personal communication) and thus zinc would be accumulated within the mossy fibre terminals. On washing out CP94, the Zn^{2+}-chelator complex would dissociate and more free Zn^{2+} could be subsequently released upon

stimulation. Alternatively, 'over-recovery' may be due to an increase in the release of neurotransmitter, since GABA may also accumulate during the period when GDPs were absent. It is more likely that a combination of both factors contributed to this phenomenon.

3. Comparison of selective zinc chelators with other metal chelating agents

One question which arose during this study was whether the action of the specific zinc-chelating agents is unique? It was of interest therefore to test whether other metal chelators can reproduce the effects of the pyridinone-based chelators.

3.1. Diethyldithiocarbamate (DEDTC, antabuse)

Previous studies have shown that local injection of DEDTC into the hippocampus, renders the metal in the mossy fibre pathway of the hippocampus unstainable by the Timm-sulphide silver method (Danscher et al. 1975). Bath application of DEDTC (100-400μM) for 10-60min abolished spontaneous action potentials and slightly reduced the duration of evoked GDPs in young CA3 neurones, but had no obvious effect on the frequency of spontaneous GDPs (Fig. 4.14; n=3).

3.2. Ethylene glycol-bis(β-aminoethylether)-N-N'-tetraacetic acid (EGTA)

EGTA is a divalent cation chelator and widely used in the complexation of Ca^{2+}. Bath application of EGTA (100-400μM, n=3) to young hippocampal CA3 neurones, quickly caused a membrane depolarization (4-8mV) and markedly **increased** the frequency of spontaneous GDPs. Following washout of EGTA spontaneous GDPs returned to their original frequency (Fig. 4.15).

4. Selectivity of zinc chelating action

Although CP94 and CP40 are highly selective zinc-chelating agents (Hider et al., 1990), and have a profound effect on the innate GDPs in the young hippocampus compared with other metal chelators, e.g. EGTA and DEDTA, it was still essential to establish that its action was selective.

The generation of GDPs in young CA3 neurones were mediated by GABA acting on postsynaptic $GABA_A$ receptors and the release of GABA relied upon functional excitatory synaptic activity. It was conceivable that the zinc chelating agents might abolish the GDPs by blocking $GABA_A$ receptors or ion channels, or by interfering with excitatory synaptic activity. However, CP94 (400μM) did not block ionophoretically- or bath-applied GABA or glutamate responses in CA3 neurones, despite markedly reducing the frequency of spontaneous GDPs (Fig. 4.16A, B and C; n=4).

Both CP94 and CP40 had no direct effect on the resting membrane potential, input resistance or the firing rate of spontaneous action potentials in young CA3 neurones (Fig. 4.9 and 4.10). Any significant effect on underlying membrane currents would have been manifest as a change in the current-voltage properties of the cell, but this was not observed (Fig. 4.16D).

Alternatively, any reduction in the concentration of extracellular Ca^{2+} by chelation, could have a profound influence on transmitter release (Berry & Pentreath, 1976) and thus affect the GDPs. This mechanism was unlikely, as the chelating agents are selective for complexing Zn^{2+} over monovalent and other divalent cations, e.g., Na^+, K^+, Ca^{2+} and Mg^{2+} (R.C. Hider, personal communication). Also, by reducing extracellular Ca^{2+} or Mg^{2+} from 2mM to 1.5mM, to simulate complexation of Ca^{2+} or Mg^{2+} by a high dose of CP94 (1mM), the frequency of spontaneous GDPs increased markedly and the duration of the evoked GDP was prolonged rather than inhibited (Fig. 4.17). Indeed, complexation of Ca^{2+}/Mg^{2+} (but not a complete elimination of extracellular Ca^{2+}) did not cause an inhibition, but an increase in the frequency of spontaneous GDPs when using the non-selective chelator EGTA (Fig. 4.15).

In addition, there was no any evidence that CP94 (1-400μM) interfered with neurotransmitter release. We would expect CP94 to affect orthodromic transmission in adult slices if release was generally reduced, but this did not occur. Figure 4.18 illustrates that the zinc chelator, CP94 (400μM), had no effect on the membrane properties, or excitability of an **adult** CA3 neurone. Also there was no detectable change in the mossy fibre stimulation-evoked EPSP-IPSP sequence, or the shape of the evoked action potential and the corresponding population spikes, which were recorded simultaneously and reflected the extracellular electrical activity of a population of pyramidal cells.

DISCUSSION

As originally suspected, spontaneous and evoked GDPs naturally occurring in the immature CA3 neurones were reversibly inhibited by zinc-chelating agents, CP94 and CP40. This is the first demonstration of a physiological role for endogenous zinc in synaptic neurotransmission in the immature CNS.

1. Innate GDPs in immature CA3 neurones are induced by endogenous zinc

In young hippocampal slices, typical "normal" neurotransmission is that which is associated with the spontaneous or evoked GDPs. These occur naturally and can be recorded in CA3 neurones (Ben-Ari, et al., 1989; Xie & Smart, 1991a). The evoked GDPs occurred in an all-or-none manner following different stimulus intensities, but only the spontaneous and threshold stimulus evoked GDPs were mainly mediated by $GABA_A$ receptors. Using supra-threshold stimulation, the evoked large potential persisted in the presence of bicuculline but was blocked by the EAA receptor antagonists (APV and CNQX), suggesting they were mediated by the release of glutamate acting on EAA receptors. Spontaneous bursts mediated by NMDA receptors have been reported in the immature rat entorhinal cortex (Jones & Heinemann, 1989).

The selective zinc-chelating agents, CP94 and CP40 reversibly inhibited the $GABA_A$-mediated spontaneous potentials and the threshold evoked GDPs, without interfering with the neuronal membrane properties or excitability. The rapid onset and reversible inhibition of the zinc chelators is also compatible with the complexation of free Zn^{2+} instead of bound zinc and therefore renders the involvement of zinc-containing metalloenzymes in this phenomenon unlikely (cf. Vallee & Galdes, 1984). The results presented thus far indicate that activation of $GABA_A$ receptors mediates the GDPs in immature hippocampal neurones and these potentials are probably generated by endogenous Zn^{2+} in the hippocampus. These recurrent GDP events no doubt reflect some functional role for endogenous zinc in the immature CNS. By P14 and older rats, CA3 neurones do not display any spontaneous or evoked GDPs. This electrophysiological maturation of the hippocampal synaptic transmission suggests one possible role for zinc in synaptic function is limited to the developing CNS. Developmental changes in synaptic

properties in the hippocampus of neonatal rats have been noted previously (Mueller, Taube & Schwartckroin, 1983; Muller, Oliver & Lynch, 1989). Before mature synaptogenesis (Schwartzkroin, 1982), GABA release from immature CNS synaptosomes occurs in a calcium-independent manner and apparently devoid of vesicles (Taylor & Gordon-Weeks, 1989; Taylor, Docherty & Gordon-Weeks, 1990). It is possible that the generation of GDPs in neurones of this age could be dependent on zinc for the release of GABA.

2. Interactions between Zn^{2+} and Ca^{2+}/Mg^{2+}

Clearly the zinc-chelating agents, CP94 and CP40, inhibited GDPs not by blocking $GABA_A$ receptors/ion channels, or by interfering with excitatory neurotransmission. However, there may be some interaction between Zn^{2+} and Ca^{2+}/Mg^{2+}. Normally raising Mg^{2+} alone will increase the spike threshold and decrease transmitter release (Berry & Pentreath, 1976) and increased Ca^{2+} levels will also increase the spike threshold. The protocol of using high Ca^{2+}/Mg^{2+} has been shown to be particularly effective at reducing transmission through polysynaptic synapses in the CNS (Berry & Pentreath, 1976). Indeed spontaneous and evoked GDPs are completely abolished when the perfusing media contained high calcium (4mM) and magnesium concentrations (6mM). This confirmed that the GDPs in young CA3 neurones are polysynaptic events (Ben-Ari et al., 1989).

Conversely, a reduction of Ca^{2+}/Mg^{2+} concentrations (but not Ca^{2+}-free) would decrease the spike threshold and therefore increase the transmitter release through polysynaptic synapses. An increase of the frequency of spontaneous GDPs was demonstrated by reducing calcium and/or magnesium levels in the perfusion medium. Since transmitter release depends on the presence of calcium (Berry & Pentreath, 1976), the postsynaptic potential will be reduced and eventually disappear in Ca^{2+}-free solution. However, the doses of chelators used here are unlikely to result in a Ca^{2+}-free solution. The zinc chelators, CP94 or CP40, at appropriate concentrations (1-400μM) selectively complex Zn^{2+} effectively inhibiting the GDPs without apparently interfering with the functional role of Ca^{2+}/Mg^{2+}. Whereas non-selective metal chelators, e.g. DEDTC have less inhibitory effect on the GDPs. EGTA did not inhibit but increased the frequency of

spontaneous GDPs. One possible explanation for this result was the complexation of extracellular Ca^{2+}/Mg^{2+} thereby reducing their concentrations.

3. Endogenous extracellular Zn^{2+} levels and the release of zinc

Chemical studies have shown that two molecules of the zinc-chelating agents (CP94 or CP40) complex one free Zn^{2+} ion (Hider et al., 1990). CP94 at 1μM began to have a threshold inhibitory effect on the frequency and amplitude of spontaneous GDPs and at 10μM was capable of blocking GDPs in some cells (n=3). This enabled an estimation of the endogenous extracellular free Zn^{2+} levels in the hippocampus which may range from 0.5 to 5μM. Previously, quantitative chemical analyses using atomic absorption spectrophotometry revealed the zinc content in the hippocampus to be >65μg/g dry weight and the average concentration in the brain of to be approximately 25μg/g (Crawford & Connor, 1972; Donaldson et al., 1973; Crawford, 1983). However the extracellular free Zn^{2+} concentrations are not accurately known. It has been estimated that the total amount of zinc released from the mossy fibre of adult hippocampus following stimulation could achieve local extracellular concentrations of up to 300μM. Interestingly, studies on the adult hippocampus described in Chapter 3 showed that following the addition of 300μM zinc, virtually 90% of cells displayed GDPs. However, both the estimated zinc concentration and the dose of zinc used to induce GDPs in adult neurones are likely to include free and bound zinc. Neurochemical studies indicate that most zinc becomes quickly bound to proteins (there are many zinc-binding proteins, e.g. metallothioneins etc.), amino acids and other organic substances in the CNS (Itoh, Ebadi & Swanson, 1983). The threshold concentration of exogenous zinc (30-50μM) required to induce the GDPs in adult neurones is likely to be distorted by such zinc-binding compounds and also probably by the diffusion pathways in the hippocampal brain slice. Thus the amount of 'active' free Zn^{2+} ions may be much less than 50μM. Therefore, from the chelation studies, the estimate of endogenous free Zn^{2+} levels in the interstitial fluid of 0.5-5μM may not be unreasonable. The implication that zinc is released in young rats can also be correlated with a previous morphological study indicating that in P2-3 neonates, a mossy fibre termination and positive Timm stain can be observed in the CA3 subfield (Zimmer & Haug, 1978).

Chelation of zinc with CP40, an agent that does not permeate into the cell membrane, also reduced the GDP frequency. This suggested that free Zn^{2+} ions in extracellular space are responsible for the induction of the GDPs. As extracellular zinc is accumulated into the mossy fibre system (granule cells and their axons, the mossy fibres) during early postnatal development (Crawford & Connor, 1972; Wolf, Schütte & Römhild, 1984), coincidently, spontaneous GDPs observed in CA3 neurones gradually disappeared. The zinc content in the rat hippocampus increased substantially during the first 3 weeks after birth and reached 15μg/g in fresh tissues, which is close to the adult levels of 16μg/g (Szerdahelyi & Kása, 1983). However, in adult hippocampal slices, 'normal' neurotransmission does not exhibit any equivalent innate large depolarizing potential and also the zinc chelators *per se* have no detectable effect, unless exogenous zinc is first applied. An interesting and perplexing issue for future work is why a lower content of zinc in the young hippocampus is able to induce innate GDPs and why such potentials are not observed in adult neurones under physiological conditions. Whether this is because Zn^{2+} distribution in interstitial fluid is higher in neonates than in the adult, or because zinc release is reduced in the adult mossy fibre system compared with neonates is presently unknown. This could be addressed by measuring the release of zinc in the immature hippocampus.

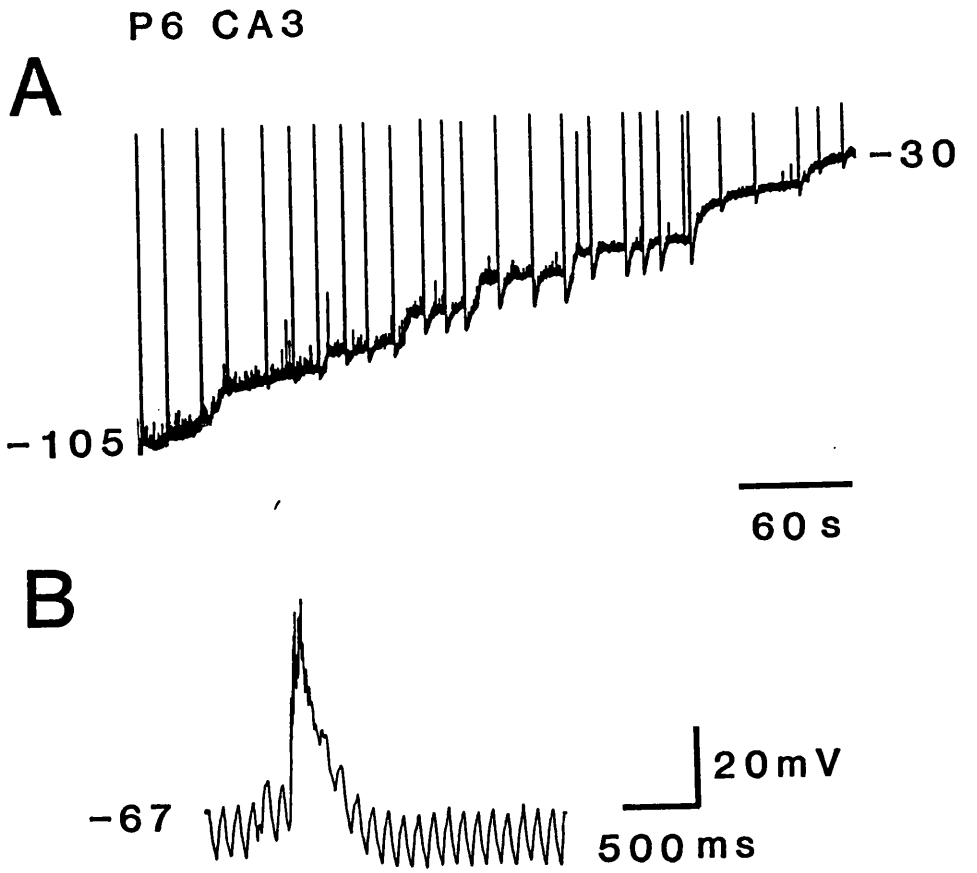

Fig. 4.1. Immature CA3 pyramidal neurones exhibit regularly occurring spontaneous GDPs independent of the membrane potential. **A**, Chart record of an intracellular recording from a CA3 neurone (P6) at a resting membrane potential of -56mV. Upward deflections are spontaneous giant depolarizations (GDPs). The frequency of spontaneous GDPs is independent of the membrane potential from -105 to -30mV adjusted by DC current injection, but the amplitude of the GDPs was increased at more negative membrane potentials. **B**, In a different CA3 neurone (P6), the spontaneous GDP was associated with an increased input conductance. Downward deflections are hyperpolarizing electrotonic potentials evoked by -0.3nA, 10ms, 10Hz constant current pulses. The resting potential was -67mV.

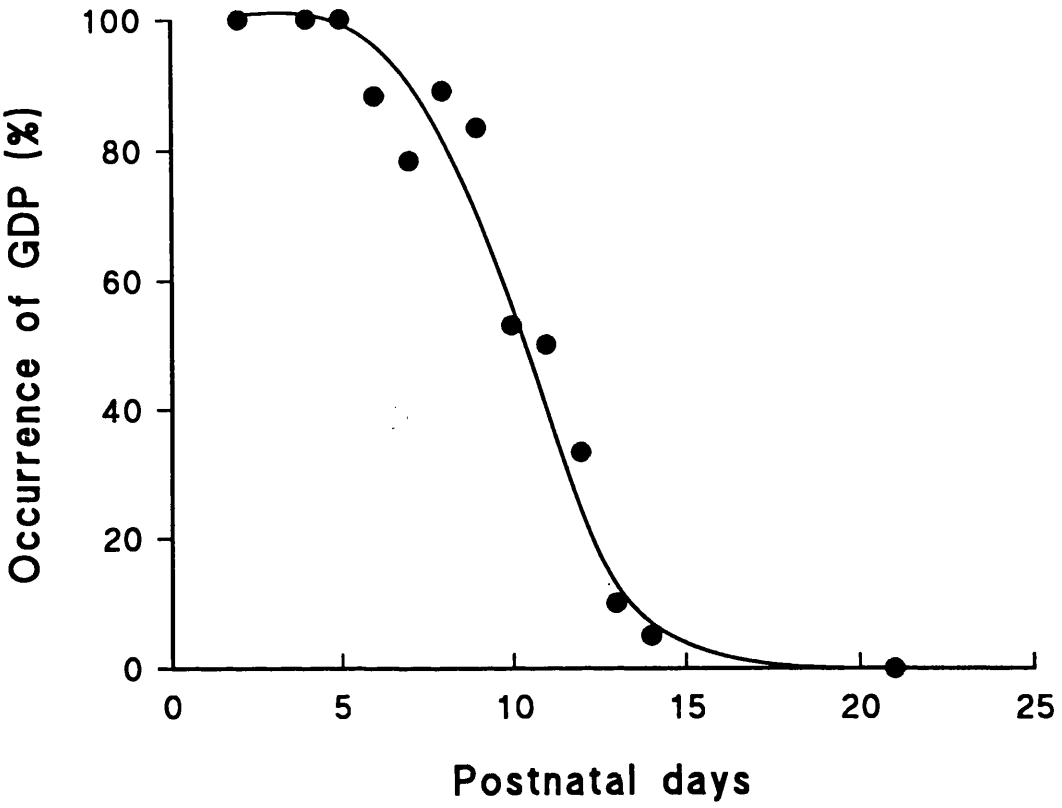

Fig. 4.2. Spontaneous GDPs in immature CA3 neurones waned with development. The percentage of neurones displaying spontaneous GDPs (ordinate) are plotted against the number of postnatal days (abscissa). Data were collected from young CA3 neurones (P2-21, n=168). Each point is obtained from 8-34 cells. The probability of a neurone exhibiting spontaneous GDPs decreased to 0.5 by 10 days after birth.

Fig. 4.3. Mossy fibre stimulation evokes GDPs in immature CA3 neurones. **A**, An evoked-GDP was recorded from a P7 CA3 neurone by stimulation of the mossy fibre pathway (▲, 7V, 60μs). Superimposed hyperpolarizing electrotonic potentials were evoked by -0.3nA, 10ms, 10Hz current pulses. Note the membrane input conductance increased during the peak of the evoked GDP. **B**, Evoked-GDPs occurred in an all-or-none manner. Superimposed oscilloscope records illustrate responses to different stimulus intensities in another P7 CA3 neurone. 6V failed to evoke a GDP (base line). 7V triggered a GDP with long latency (a); 8V (b), 10 and 15V (c) triggered three GDPs respectively, with shorter latencies. The stimulating electrode was placed in the hilar region and the duration of all stimuli was 60μs. Note that the latency of onset became shorter and the duration of the GDP was prolonged by using high intensity stimuli. **C**, in the same cell as B, the amplitude of the second evoked GDP was graded on repeated stimulation of the mossy fibre (▲, 8V, 60μs) with time intervals of 50-2000ms. An interval of approximately 10s was required to evoke a full size GDP (not shown). Membrane potential -60mV adjusted with DC current injection. Voltage calibration in C applied to A and B.

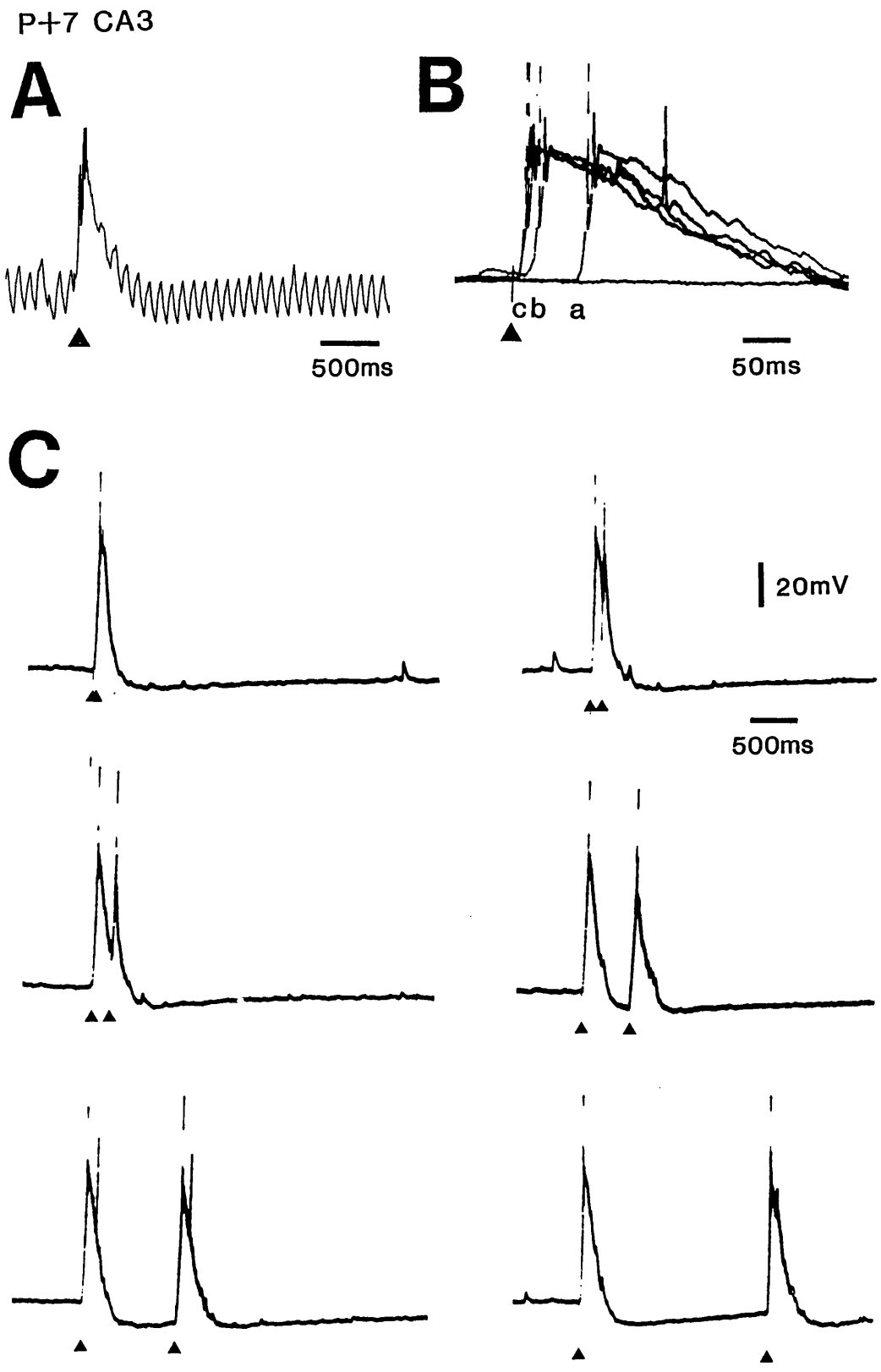
P+7 CA3
A
500ms
B
cb a
50ms
C
20mV
500ms

Fig. 4.4. Spontaneous and evoked GDPs in immature CA3 neurones are blocked by tetrodotoxin or high Ca^{2+}/Mg^{2+}. **A**, Chart record of an intracellular recording from a CA3 neurone (P7) at a membrane potential -65mV (adjusted with DC current injection). Superimposed hyperpolarizing electrotonic potentials evoked by -0.2nA, 230ms, 0.2Hz constant current pulses. Spontaneous GDPs (upward deflections) were blocked by 1μM tetrodotoxin (TTX, solid bar) and recovered after a 30min washout. **B**, Spontaneous and evoked (▲) GDPs recorded from another P7 cell disappeared in Krebs containing 4mM Ca^{2+} and 6mM Mg^{2+}. Membrane potential was -70mV with DC current injection. **C**, In the same neurone as in B, three evoked GDPs triggered by mossy fibre stimulation (▲, 10V, 60μs) before, during and after superfusing with high Ca^{2+}/Mg^{2+}. Hyperpolarizing electrotonic potentials (-0.3nA, 300ms) were used to monitor membrane resistance. Time and voltage calibrations in A apply to B.

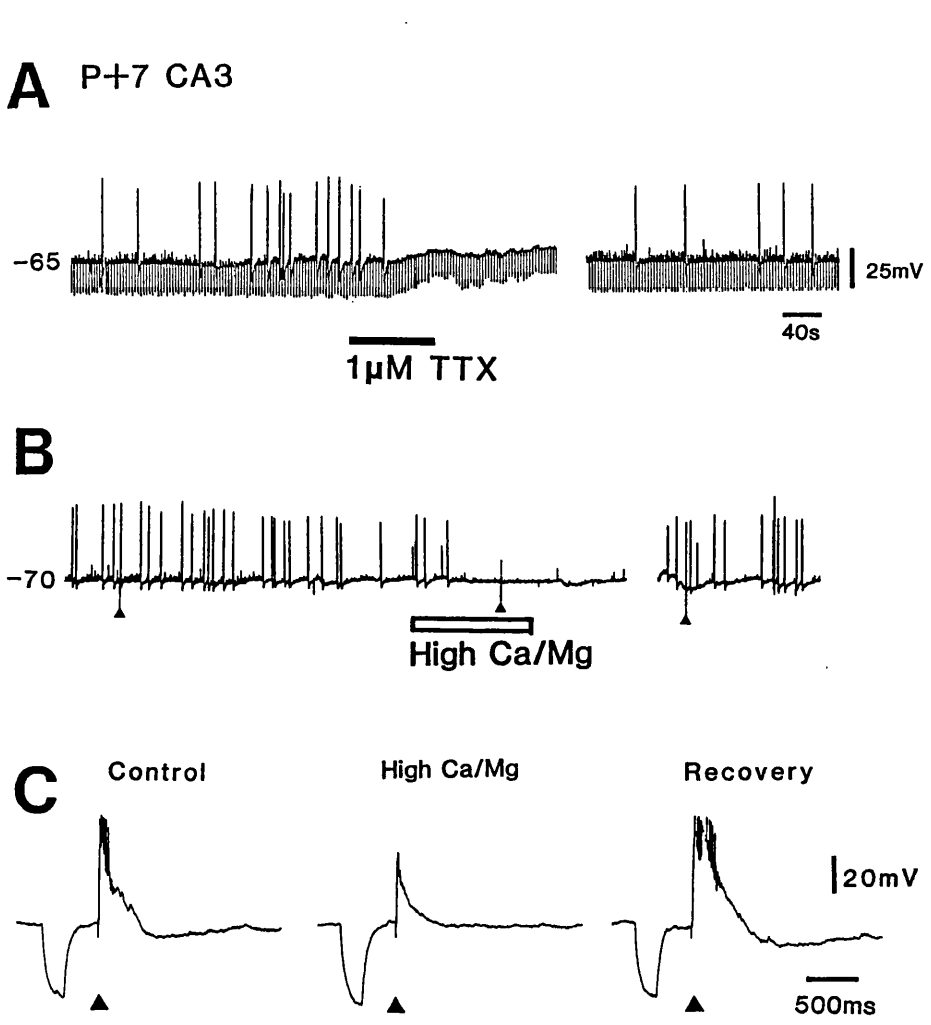
A
P+7 CA3
-65
25mV
40s
1μM TTX
B
-70
High Ca/Mg
C
Control
High Ca/Mg
Recovery
20mV
500ms

Fig. 4.5. Spontaneous and threshold stimulus evoked GDPs in immature CA3 neurones are blocked by bicuculline. **A**, Spontaneous GDPs were recorded from a P7 CA3 neurone at a membrane potential -70mV (adjusted with DC current injection) with superimposed hyperpolarizing electrotonic potentials (-0.2nA, 300ms, 0.2Hz). Spontaneous GDPs (upward deflections) were blocked by 10μM bicuculline (open triangles), which was reversed after a 20min washout. Note that bicuculline also blocked the synaptic 'noise' and induced a seizure-like discharge (see text). **B**, In a different CA3 cell (P7), four pairs of evoked synaptic potentials were triggered by stimulation of the mossy fibre pathway with two stimulus intensities, using threshold (4V) and supra-threshold stimuli (8V; ▲, 60μs). Bath-applied 10μM bicuculline (BIC) blocked the threshold evoked GDP but slightly enhanced the supra-threshold evoked synaptic response. In the presence of BIC, the addition of 40μM APV depressed the later component of the synaptic response. Co-application of 20μM CNQX completely blocked the residual potential triggered by the supra-threshold stimulation. Hyperpolarizing electrotonic potentials (-0.3nA, 300ms, 1 pulse per 20s) were used to monitor membrane resistance. Membrane potential -70mV was adjusted with DC current injection.

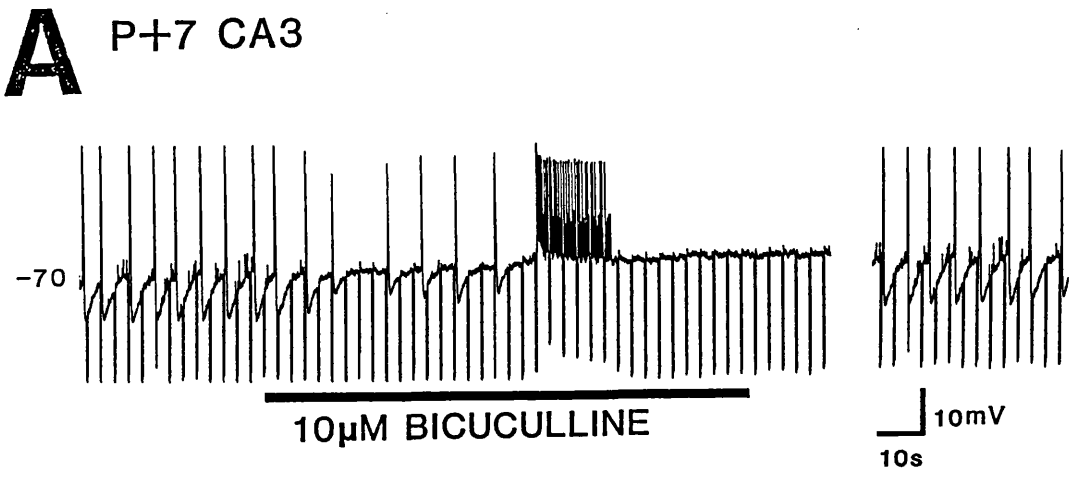
A
P+7 CA3
-70
10μM BICUCULLINE
10mV
10s

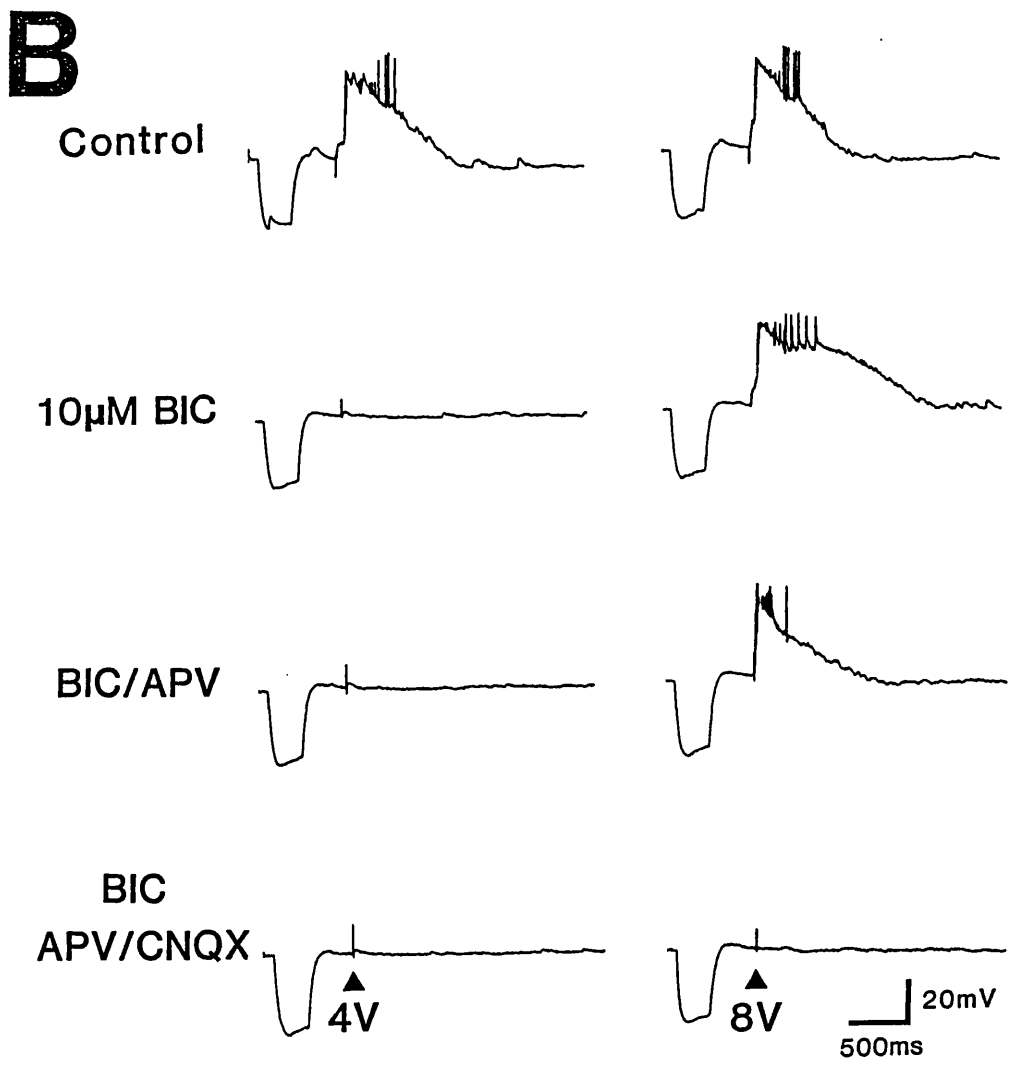
B
Control
10μM BIC
BIC/APV
BIC
APV/CNQX
4V
8V
20mV
500ms

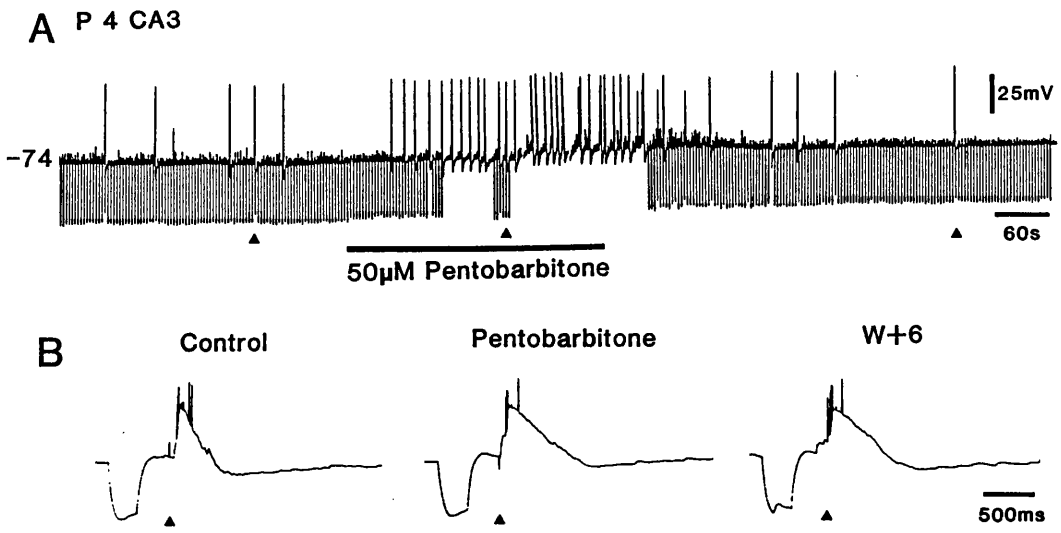

Fig. 4.6. Spontaneous and evoked GDPs in immature CA3 neurones are enhanced by pentobarbitone. **A**, Spontaneous GDPs (upward deflections) were recorded from a P4 CA3 neurone at a resting membrane potential -74mV with superimposed hyperpolarizing electrotonic potentials (-0.2nA, 300ms, 0.3Hz). The frequency of spontaneous GDPs was increased in the presence of 50μM pentobarbitone (solid bar). **B**, Three evoked GDPs triggered by mossy fibre stimulation (▲, 6V, 60μs) were taken before, during and following washout (W+ 6min) of pentobarbitone from the same cell in A. Note that the GDP duration, but not the amplitude, was prolonged by pentobarbitone.

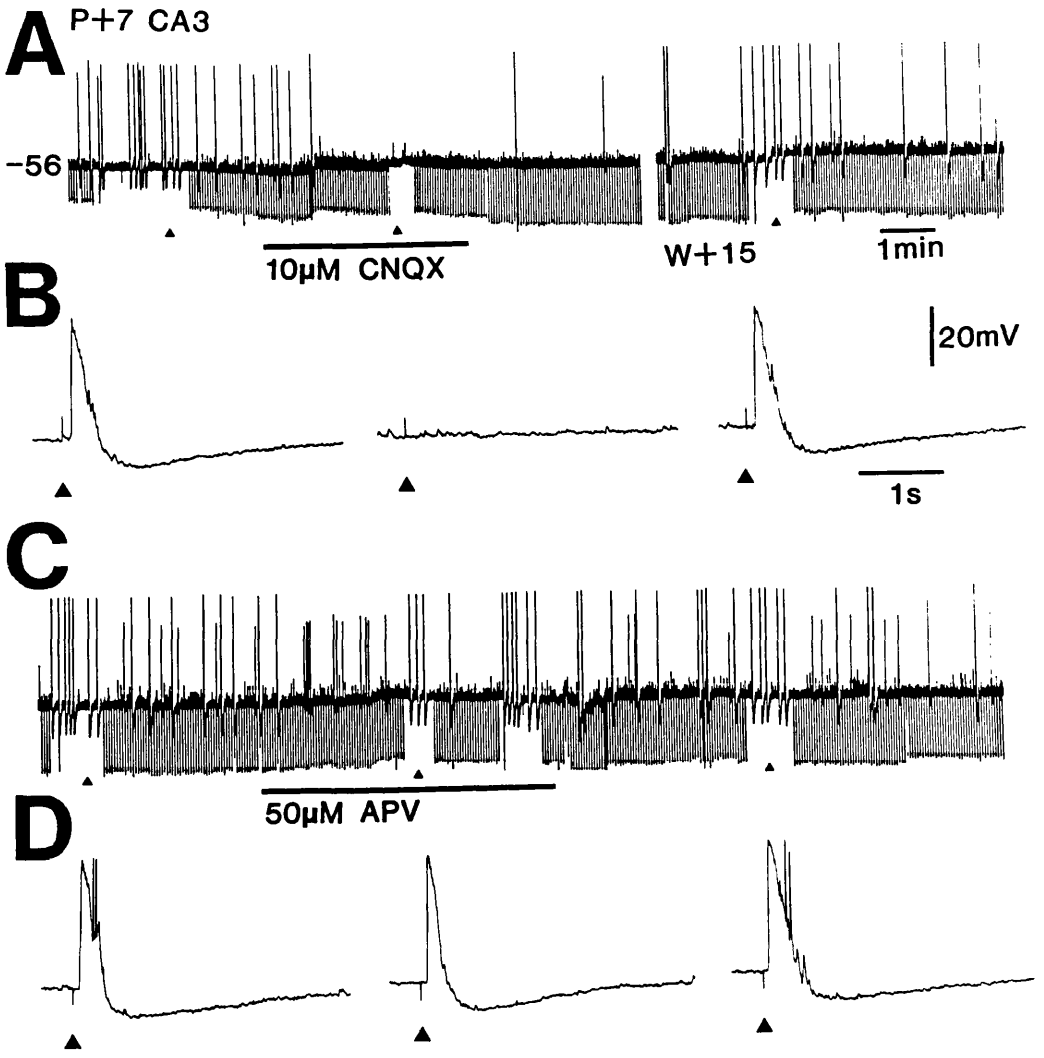

Fig. 4.7. Influence of excitatory transmitter antagonists on the GDPs in young CA3 neurones. Chart recording from a P7 cell at a membrane potential -56mV. Upward deflections are spontaneous and evoked (▲) GDPs and downward deflections, hyperpolarizing electrotonic potentials (-0.3nA, 300ms, 0.3Hz). **A**, Spontaneous GDPs are reversibly blocked by 10μM CNQX (solid bar). **B** illustrates the effect of CNQX on the evoked-GDPs, records taken from A on an expanded timescale. **C**, Following washout of CNQX for 20min, the cell exhibits spontaneous GDPs coupled with the firing of some action potentials (note, spike amplitudes are truncated and without a large AHP). APV (50μM) reduces the frequency of spontaneous GDPs. **D**, APV depressed the later component of the evoked-GDPs, records taken from trace C. The stimulating electrode was placed in the mossy fibre pathway and supplied a 7V, 0.1ms stimulus.

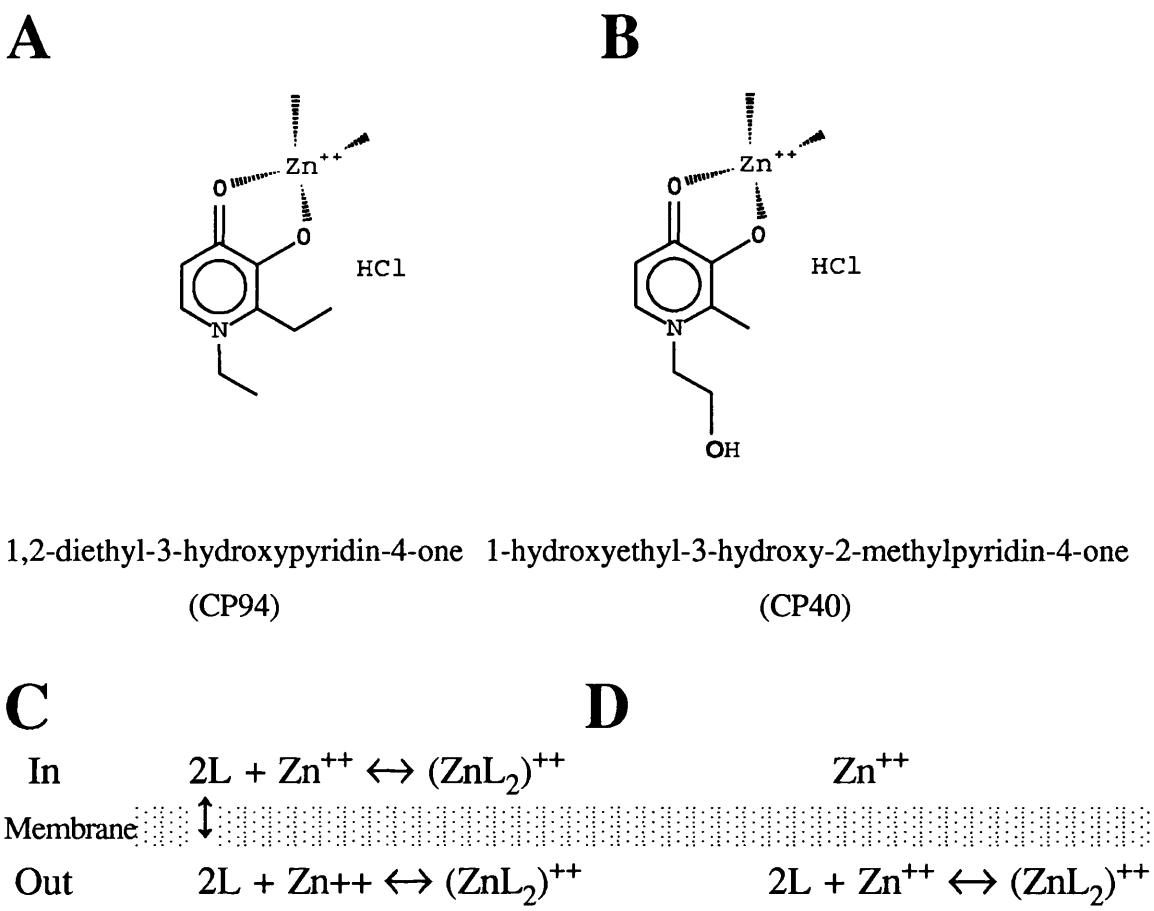

Fig. 4.8. Chemical structures of zinc-chelating compounds and schematic representation of the chelators interacting with zinc. Chemical structures of 1,2-diethyl-3-hydroxypyridin-4-one (CP94, **A**) and 1-hydroxyethyl-3-hydroxy-2-methylpyridin-4-one (CP40, **B**) which form biliganded complexes with Zn^{2+}. **C**, CP94 can permeate cell membranes to chelate intracellular zinc as well as extracellular zinc, but the zinc-chelator complex cannot cross the membrane. **D**, CP40 does not penetrate the membrane and remains extracellular. In C and D, L represents the chelating compound. The chelators are quite selective for zinc under physiological conditions and form water soluble zinc-chelator complexes (cf. Hider et al., 1990).

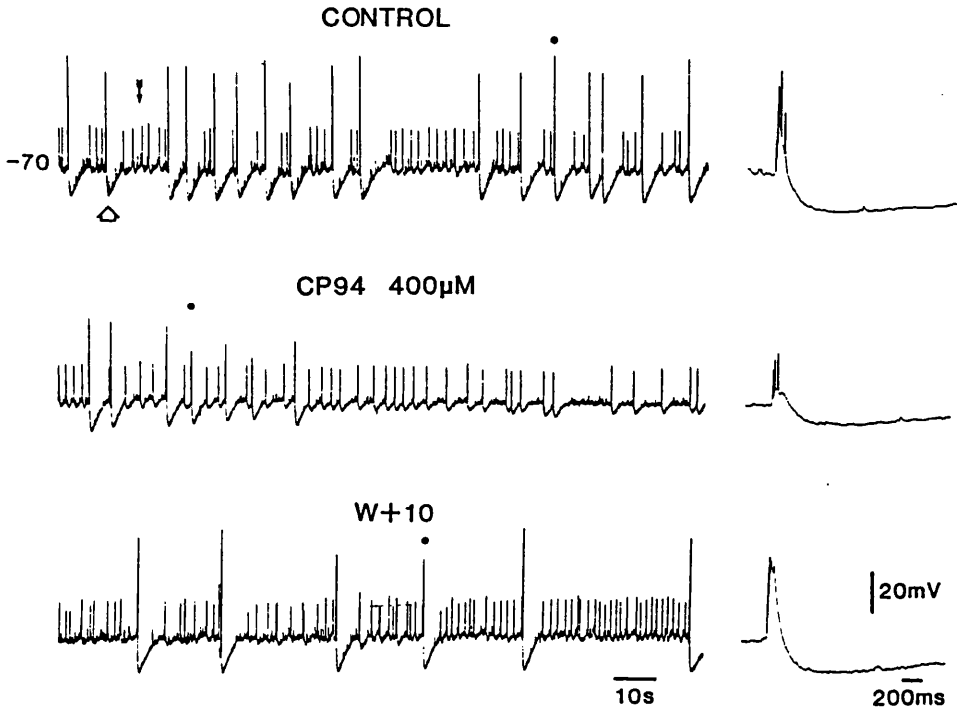

Fig. 4.9. Zinc-chelating agent, CP94 reduces the frequency of spontaneous GDPs in a young (P12) CA3 neurone. Intracellular recording of spontaneous GDPs (open arrow) which occurred with occasional action potential firing (filled arrow, top trace; spike amplitudes are truncated and without a large AHP). CP94 (400µM) reduced the amplitude and frequency of the spontaneous GDPs without affecting the action potentials (middle trace). Recovery was obtained following a 10-min wash (bottom trace). Selected GDPs from each trace (●) are shown on an expanded timescale in the righthand column.

Fig. 4.10. Spontaneous GDPs in immature CA3 neurones are inhibited by CP94 in a dose-related manner. **A**, Sequential recording from a P7 neurone at a membrane potential of -70mV (adjusted with DC current injection) with superimposed hyperpolarizing electrotonic potentials (-0.2nA, 300ms, 0.3Hz). The frequency of spontaneous GDPs (sampled time over 5min) are inhibited by CP94 at various concentrations (10, 25 and 100μM, solid bars). **B**, Relationship between the inhibition (%) of GDP frequency and the concentration of CP94. Data were collected from 153 applications of CP94 at different concentrations. Each point was the mean value of 2-14 applications.

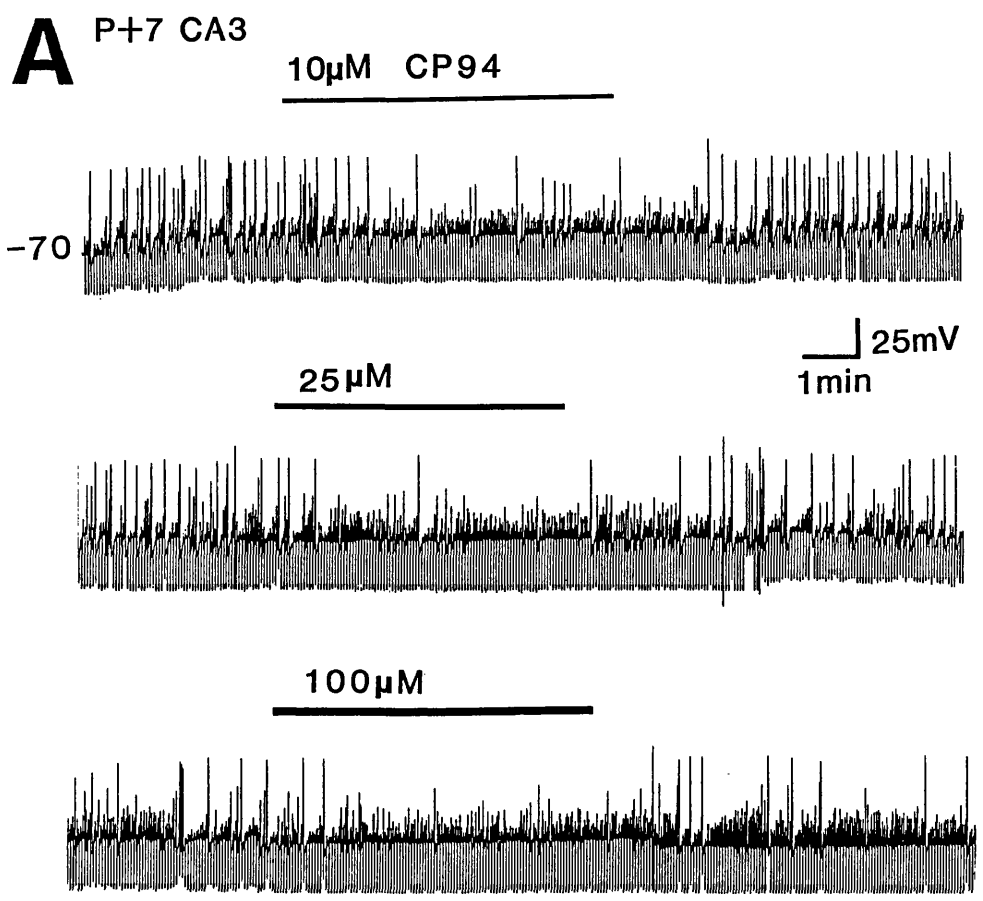
A
P+7 CA3
10μM CP94
-70
25mV
1min
25μM
100μM

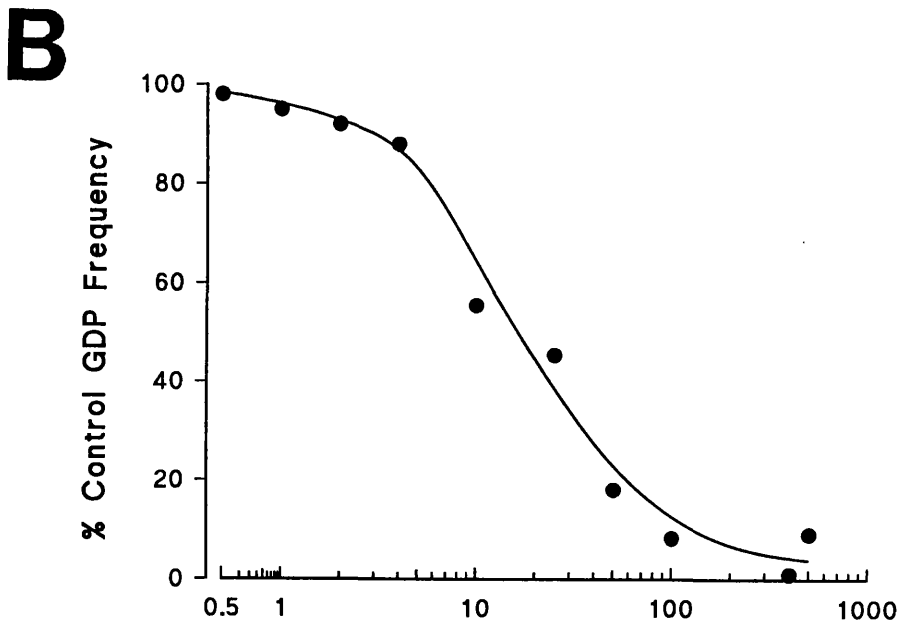
B
% Control GDP Frequency
100
80
60
40
20
0
0.5
1
10
100
1000

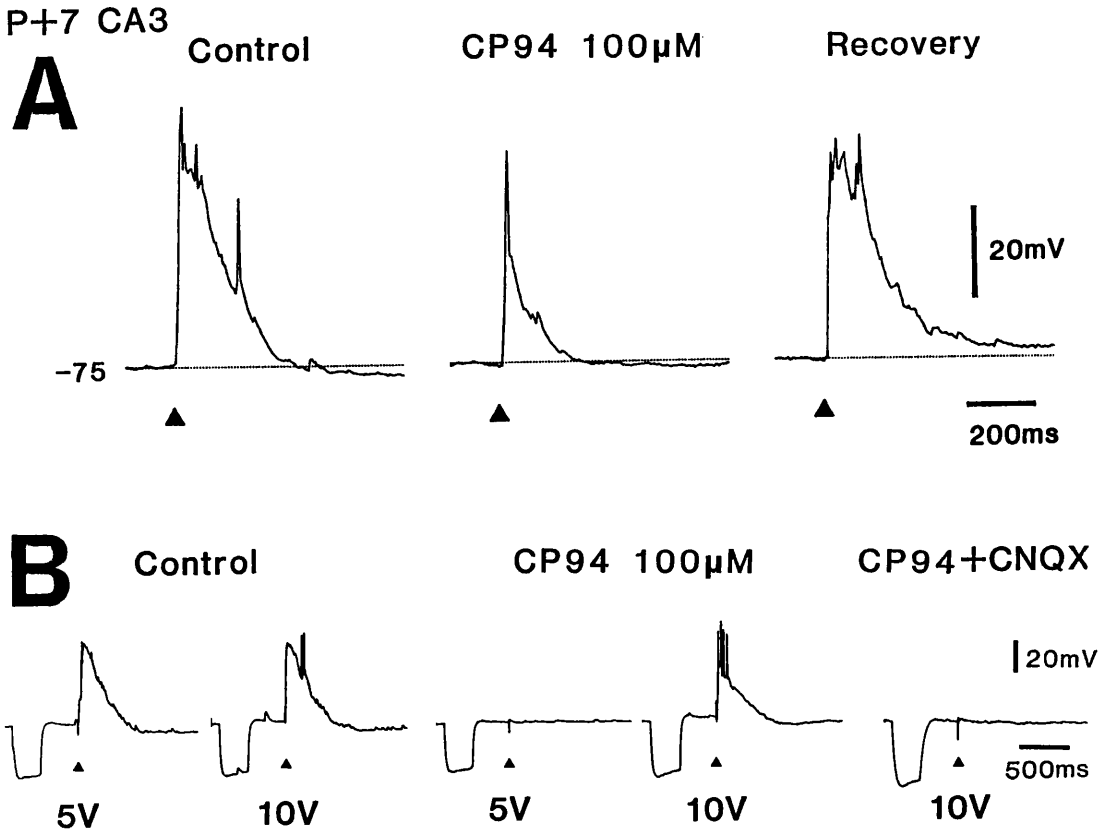

Fig. 4.11. Evoked-GDPs in immature CA3 neurones are depressed by CP94. **A**, Averaged evoked-GDPs recorded from a P7 CA3 neurone following stimulation of the mossy fibres with 8V, 0.1ms, 0.1Hz stimuli (▲) in the absence and presence of 100μM CP94. Each average was constructed from five consecutively evoked GDPs using a synaptic current analysis program (SCAN, version 3.0). The dotted line indicates the resting membrane potential, adjusted with DC current injection to -75mV. **B**, Recording from a different CA3 neurone (P7) at a membrane potential of -70mV adjusted with DC current injection. Stimulating electrodes were placed in the mossy fibre pathway. Stimulus pulses (▲, 5 or 10V, 60μs) were delivered at 0.05Hz. In normal Krebs (control), 5V was the threshold to evoke a GDP. CP94 (100μM) blocked the evoked-GDP triggered by the threshold stimulation, but only slightly suppressed the synaptic potential evoked by a supra-threshold stimulus (10V). The residual potential which persisted in the presence of CP94 was blocked by the addition of 10μM CNQX. Hyperpolarizing electrotonic potentials (-0.2nA, 300ms, 0.05Hz) were applied to monitor membrane resistance.

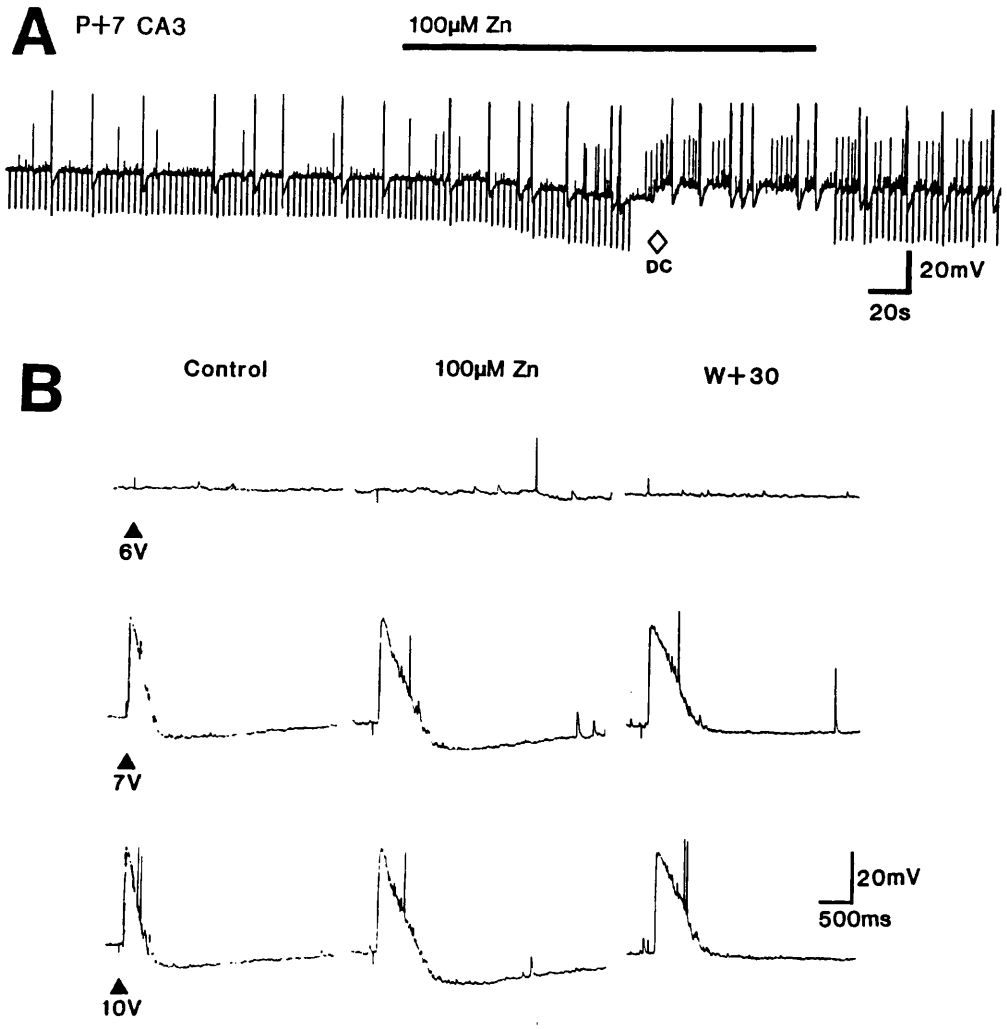

Fig. 4.12. Innate GDPs in immature CA3 neurones are enhanced by exogenous zinc. **A**, Recording from a P7 CA3 neurone which initially exhibited spontaneous GDPs. Application of 100µM zinc (solid line) induced a slow hyperpolarization and an increase in the membrane resistance. The frequency of spontaneous GDPs was slightly increased. Hyperpolarizing electrotonic potentials (-0.2nA, 300ms, 0.3Hz) were applied to monitor membrane resistance. **B**, In the same cell, exogenous zinc prolonged the evoked GDPs, but did not change the stimulus threshold. Stimulating electrodes were placed in the mossy fibre pathway. Stimuli were delivered at 60µs, 0.05Hz, at 6, 7 and 10V intensities (▲). In normal Krebs (control, or washout for 30min, W+30) and in the presence of zinc, 6V was a sub-threshold stimulus and 7V the threshold to evoke a GDP. The membrane potential was adjusted with DC current injection (◊) to -70mV during the application of zinc.

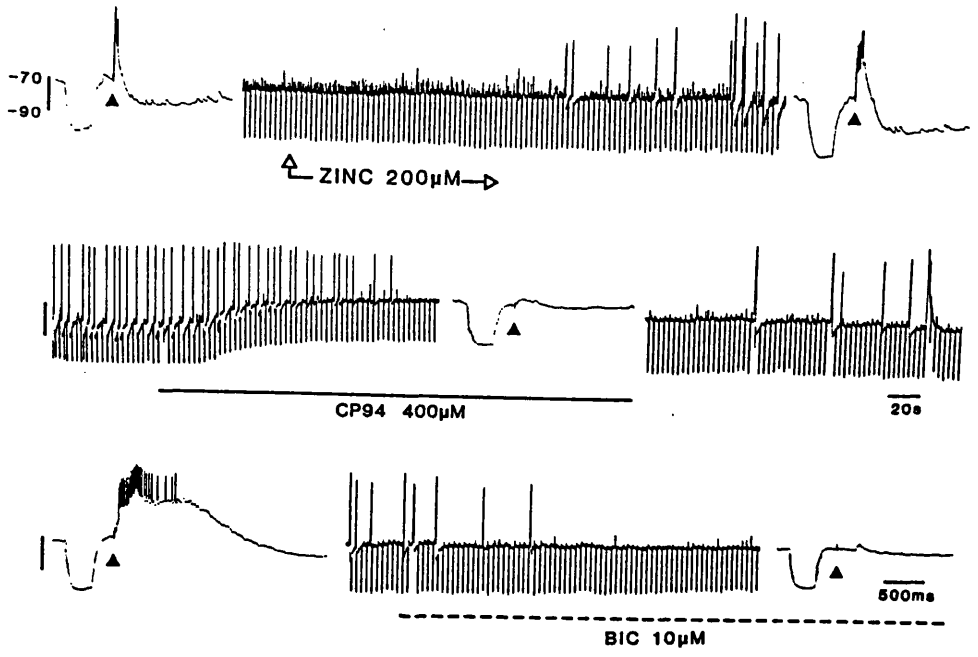

Fig. 4.13. Effects of CP94 on exogenous zinc-induced GDPs in the young hippocampus. Recording from a P13 CA3 neurone which did not initially exhibit any spontaneous GDPs. Stimulation of the mossy fibres in Krebs solution before the addition of zinc, produced a small evoked GDP (▲, top trace). Application of 200μM zinc (open triangle) throughout the experiment induced the appearance of spontaneous GDPs after 6-min incubation and prolonged the evoked GDP response (top trace). Co-application of CP94 (400μM, solid line), reversed the zinc-induced hyperpolarization and membrane resistance increase, and also inhibited both spontaneous and evoked GDPs (middle trace). Spontaneous GDPs recovered after washout of CP94 with zinc-containing Krebs solution. The evoked GDP exhibited an 'over-recovery' (bottom trace). Both spontaneous and evoked GDPs were blocked by 10μM bicuculline (BIC) (bottom trace, broken line). The lefthand calibration indicates the membrane potential (mV) of the cell. Hyperpolarizing electrotonic potentials (-0.3nA, 300ms, 0.3Hz) were applied throughout to monitor the membrane resistance.

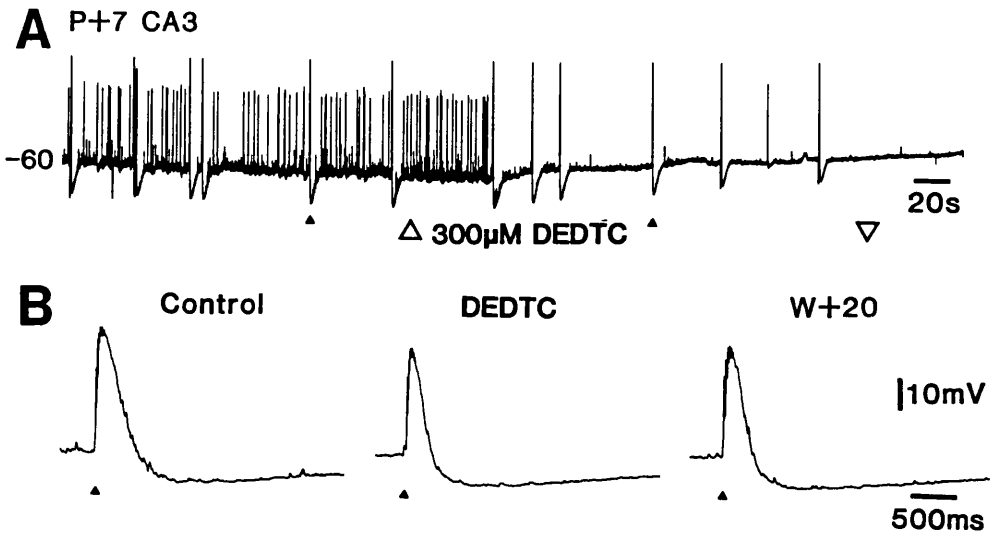

Fig. 4.14. Effects of the metal chelating agent, DEDTC on GDPs in young CA3 neurones. **A**, Chart record of a P7 cell with spontaneous GDPs (with large AHPs) and action potentials (upward deflections). 300μM DEDTC (open triangle) had no effect on the GDP frequency, but inhibited the spontaneous action potentials. **B**, In the same cell, three evoked GDPs triggered by the mossy fibre stimulation (▲, 8V, 60μs) before, during and after (wash 20min, W+20) application of DEDTC. Note that DEDTC slightly reduced the GDP duration. Membrane potential -60mV adjusted with DC current injection.

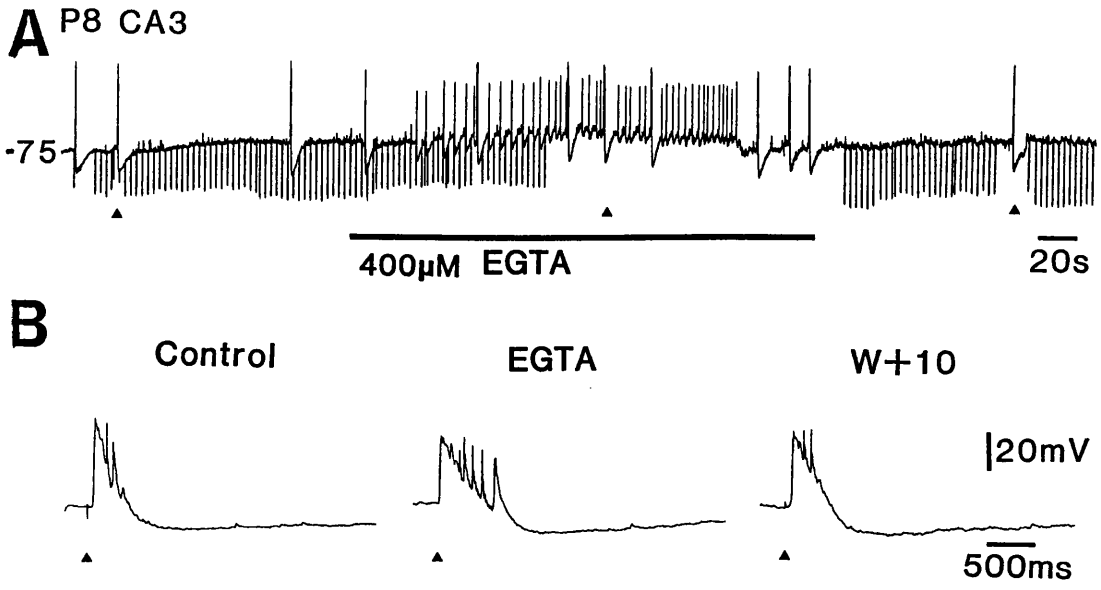

Fig. 4.15. Effects of the divalent cation chelator, EGTA, on GDPs in young CA3 neurones. **A**, Chart record of a P8 cell with spontaneous GDPs (upward deflections) and superimposed hyperpolarizing electrotonic potentials (downward deflections, -0.3nA, 300ms, 0.3Hz). EGTA (400μM, solid line) caused a membrane depolarization and an increase in the spontaneous GDP frequency, associated with firing single action potentials (with small spike-AHP). **B**, In the same cell, three evoked GDPs were triggered by mossy fibre stimulation (▲, 6V, 60μs) before, during and after (wash for 10min, W+10) application of EGTA. Membrane potential -75mV adjusted with DC current injection.

Fig. 4.16. Effect of CP94 on GABA and excitatory amino acid receptors. Recording from a young CA3 neurone (P11) at a membrane potential -70mV (adjusted with DC current injection) with superimposed hyperpolarizing electrotonic potentials (-0.5nA, 300ms, 0.5Hz). GABA (**A**, solid bar) and glutamate (**B**, open bar) were applied for 10s (+ and -60nA ejection currents respectively) from a double-barrelled ionophoretic pipette to the apical dendrites. A 10nA holding current was used on each barrel. Both GABA and glutamate produced reproducible depolarizations and conductance increases which were unaffected by 400μM CP94. **C**, In the same cell, the frequency of spontaneous GDPs was reduced in the presence of CP94. **D**, Current clamp records of membrane potential (lower traces) obtained from a different CA3 neurone (P12) at a resting membrane potential of -63mV (spike amplitude 92mV). Superimposed electrotonic potentials produced by hyperpolarizing and depolarizing current pulses (upper traces; 300ms, 0.25Hz) were recorded in the presence and absence of 400μM CP94.

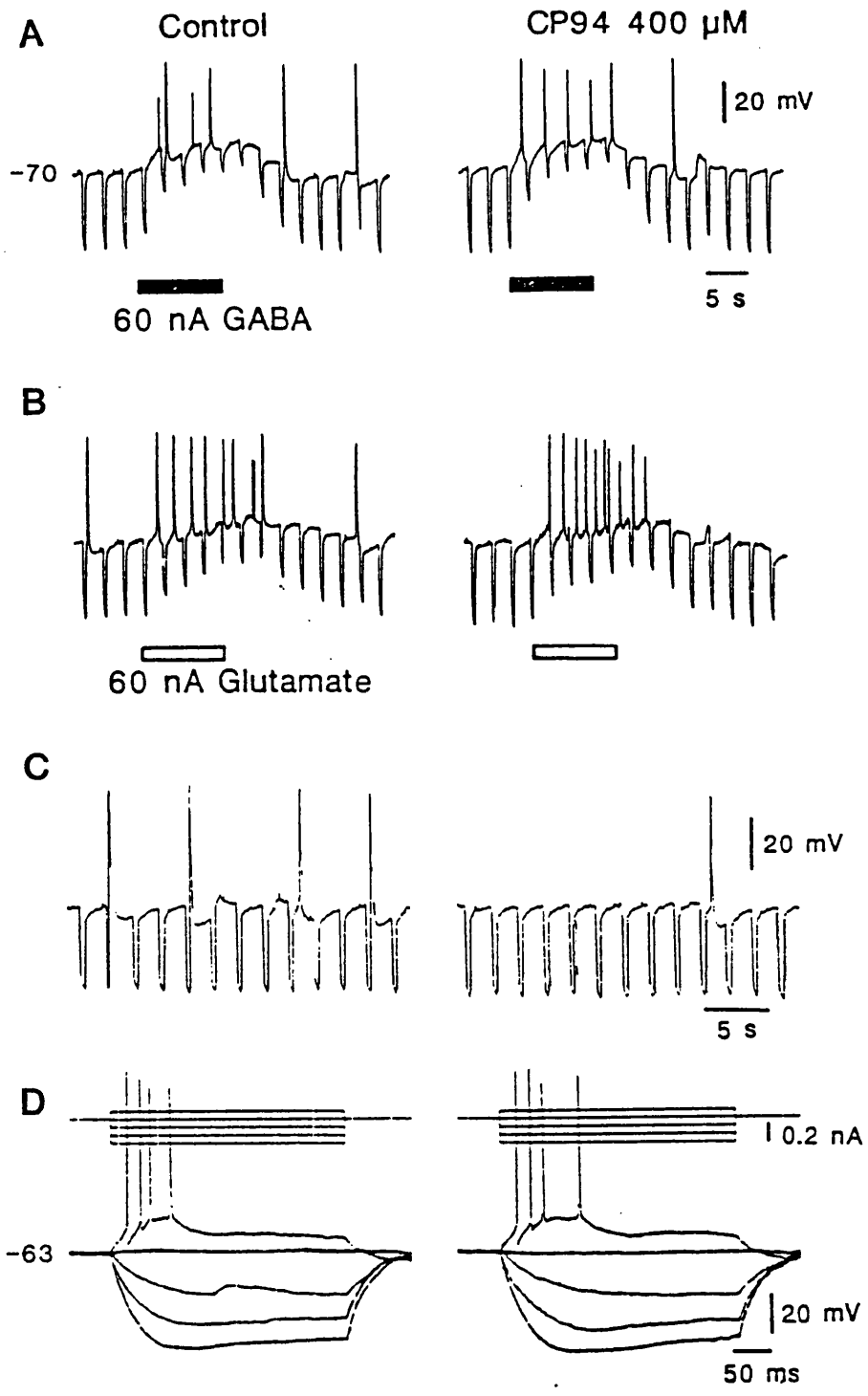
A
Control
CP94 400 µM
20 mV
-70
5 s
60 nA GABA
B
60 nA Glutamate
C
20 mV
5 s
D
0.2 nA
-63
20 mV
50 ms

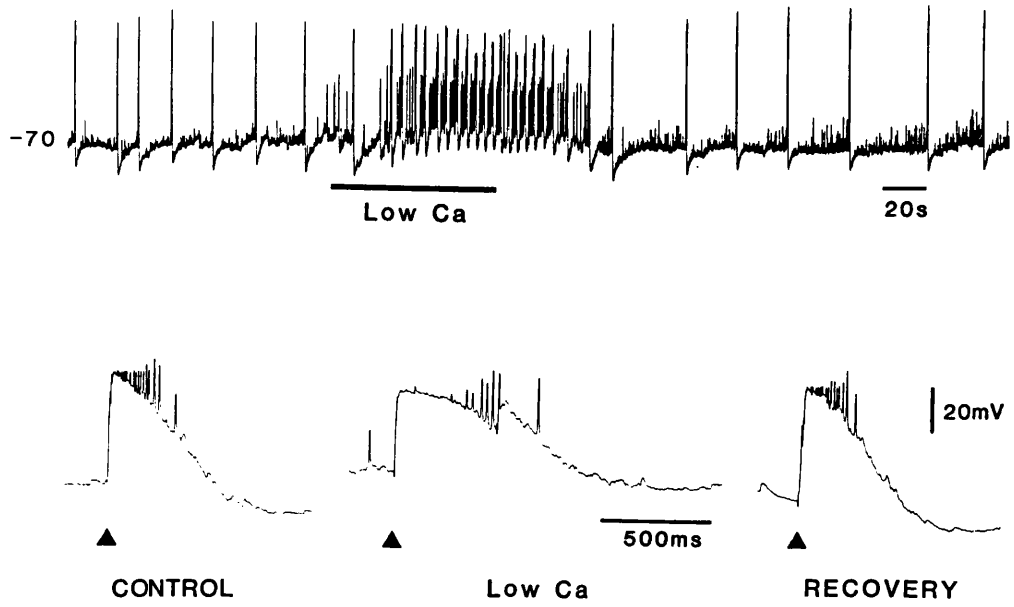

Fig. 4.17. Effects of low Ca^{2+} on the GDPs in immature CA3 neurones. Recording from a P7 neurone at a resting membrane potential of -70mV. Reducing the extracellular calcium concentration from 2mM to 1.5mM (low Ca, solid line) caused a depolarization and increased the frequency of spontaneous GDPs. Lower traces illustrate three evoked (▲) GDPs taken before, during and after perfusing the low Ca^{2+} solution. Note the phasic increase in spontaneous IPSP activity prior to the discharge of some of the GDPs. Stimulating electrodes were placed in the hilar region and supplied a 7V, 60μs stimulus.

Fig. 4.18. Effect of CP94 on membrane properties and synaptic transmission in **adult** hippocampal slices. **A**, Current clamp records of membrane potential (lower traces) obtained from a CA3 pyramidal neurone at a resting potential of -64mV (spike amplitude 95mV). Superimposed electrotonic potentials, elicited by hyperpolarizing and depolarizing current pulses (upper traces; 300ms, 0.5Hz), were recorded in the presence and absence of 400μM CP94. **B**, An EPSP followed by fast and slow IPSPs were recorded in another CA3 cell following stimulation of the mossy fibres (▲, 35V, 0.1ms). CP94 (400μM) was applied for 10min. Membrane potential -70mV (adjusted with DC current injection) **C**, Intracellular and simultaneous extracellular recording from another adult slice. Upper traces are extracellular records of orthodromically-evoked population spikes (OPS). Lower traces illustrate intracellular recording from a CA3 pyramidal cell at a membrane potential of -70mV (adjusted with DC current injection) with two evoked action potentials in the presence and absence of 400μM CP94. Stimulating electrodes were placed in the mossy fibre pathway applying 45V, 0.1ms stimuli. In A a 3M KCl-filled microelectrode was used. In B and C intracellular recordings were performed with 4 M K acetate-filled microelectrodes and extracellular recording using a 2 M NaCl-filled microelectrode.

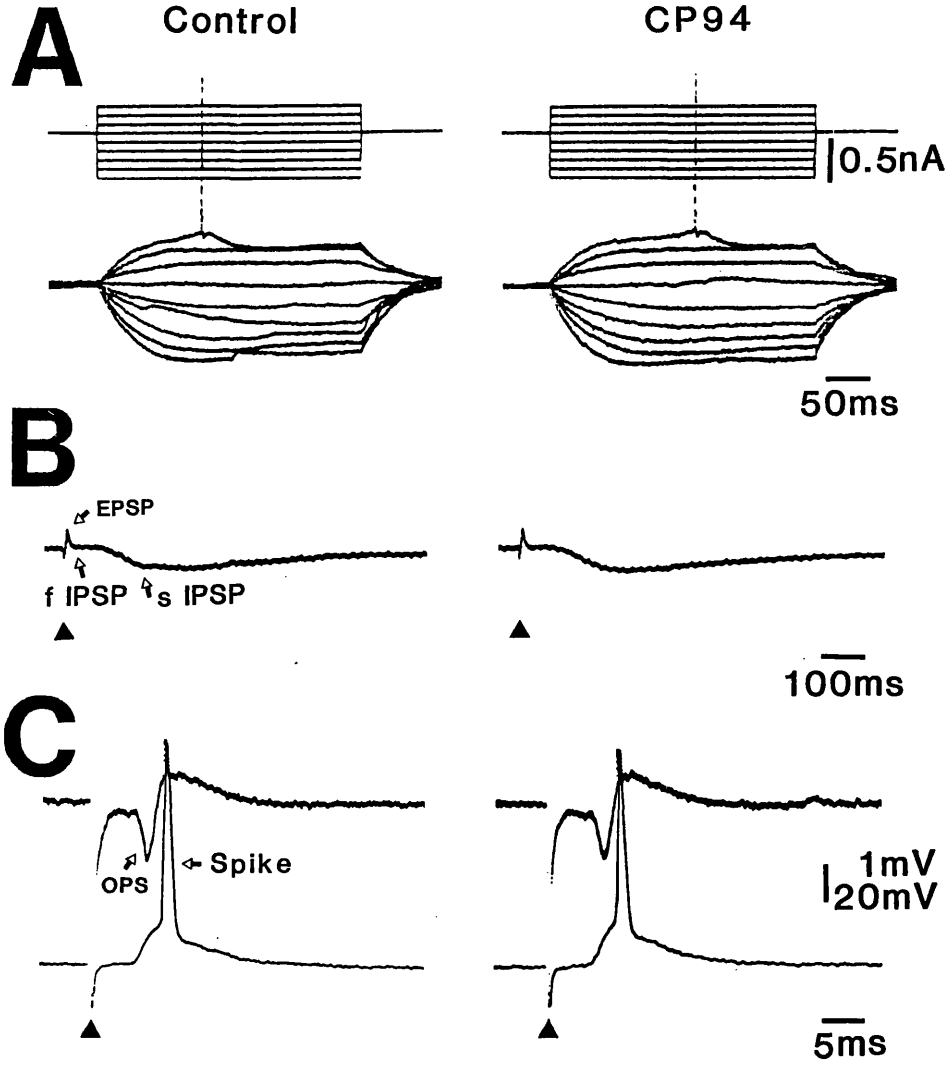
Adult CA3
A
Control
CP94
0.5nA
50ms
B
EPSP
f IPSP
s IPSP
100ms
C
OPS
Spike
1mV
20mV
5ms

Chapter 5

EFFECTS OF ZINC ON MEMBRANE PROPERTIES AND CELL EXCITABILITY: A COMPARISON WITH OTHER CATIONS

INTRODUCTION

Although the zinc-induced GDPs in both young and adult hippocampal pyramidal cells appeared to be synaptic events, it was also important to determine whether the postsynaptic membrane properties of these neurones were altered by zinc and whether any changes could contribute to the generation of GDPs in the mature rat hippocampus.

A large body of studies have demonstrated that zinc has some consistent, direct effects on membrane properties and voltage-activated membrane currents in a variety of species. However, studies of zinc on the resting membrane potential yielded conflicting results. At 50-500μM, zinc caused a small but maintained hyperpolarization and an increase in the input resistance in rat sympathetic ganglion and cortical neurones (Smart & Constanti, 1983, 1990). In contrast, very low concentrations of zinc (0.5-10μM) produced a small membrane depolarization associated with an increase in input resistance in hippocampal slices (Sim & Cherubini, 1990), whereas no obvious changes in membrane potential and input resistance were induced by zinc (50-500μM) in cultured cortical cells or hippocampal neurones (Peters, Koh & Choi, 1987; Mayer & Vyklicky, 1989). Single channel studies on cultured sympathetic neurones reported that zinc reduced the opening probability of calcium-activated potassium channels, defined as I_C (Constanti & Smart, 1987; Smart, 1987). Studies on hippocampal neurones in cultures or in brain slices also demonstrated that zinc blocks afterhyperpolarizations (AHPs) or the current underlying the AHP (I_{AHP}), and reduces accommodation of firing elicited by depolarizing current injection (Mayer & Vyklicky, 1989; Sim & Cherubini, 1990). These observations suggested that zinc might depress Ca^{2+}-activated K^+ currents in there preparations. Zinc also blocks a variety of K^+ channels in squid axons (Begenisich & Lynch, 1974; Begeisich, 1988) and frog sartorius muscle (Stanfield, 1975). Furthermore, zinc like 4-AP

can block a transient outward potassium current in cultured rat sympathetic neurones (Constanti & Smart, 1987), defined as an A-current (I_A, Gustafsson et al., 1982), but the non-inactivating muscarine-sensitive M-current (I_M, Brown & Adams, 1980; Halliwell & Adams, 1982) was unaffected. All these actions of zinc seem to be relatively non-specific effects since several calcium-dependent potassium currents are readily blocked by other divalent cations such as Cd^{2+}, Co^{2+} and Mn^{2+} which all interfere with Ca^{2+} entry (Lancaster & Adams, 1986).

In extracellular studies *in vivo* on rat cortex, zinc inhibited the calcium-induced depression of neuronal firing frequency (Wright, 1984). Zinc also blocked paired-pulse potentiation in rat hippocampal slices, another calcium-dependent phenomenon (Khulusi, Brown & Wright, 1986), suggesting that zinc may interfere with calcium entry into neurones. This is supported by voltage clamp experiments where zinc reduces the slow inactivating voltage-dependent calcium current in hippocampal neurones (Sim & Cherubini, 1990). Studies in mouse myotubes further reveal that zinc blocking calcium currents is voltage-dependent and probably occurs by binding to a site within the calcium channel pore (Winegar & Lansman, 1990). In contrast, studies on Helix neurones demonstrate that zinc is able to pass through some calcium channels and induce an inward membrane current (Oyama et al., 1982). Zinc also depresses fast sodium currents in calf purkinje fibres and isolated guinea-pig ventricular cells. This action is shared with Cd^{2+}, Mn^{2+} and Hg^{2+} (Visentin, et al., 1990). As other divalent cations (e.g. Ba^{2+}, Cd^{2+} Co^{2+} and Mn^{2+}) produce similar effects to zinc on neuronal membrane properties, such as a small hyperpolarization, an increase in the input resistance, reduction in cell firing accommodation and an inhibition of AHPs (Krnjević et al., 1979; Smart & Constanti, 1983, 1990; Lancaster & Adams, 1986; Westbrook & Mayer, 1989; Harris, Webb & Greenfield, 1989; Gerber & Gähwiler, 1991), it was of interest to examine such cations are capable of inducing GDPs in adult CA1 or CA3 neurones.

RESULTS

1. Zinc and pyramidal neuronal membrane properties

In most hippocampal pyramidal neurones exposure to 50-300μM zinc induced a small, maintained hyperpolarization in the membrane potential (3-10mV, n=70) which was observed before and during the generation of GDPs (see Fig. 3.1 and 4, in Chapter 3). The membrane input resistance (42±12 MΩ) of adult neurones was consistently increased by up to 20 % by zinc (51±15 MΩ, n=70; $P<0.01$), which was determined at the control membrane potential prior to zinc application with D.C. current injection. In the presence of TTX (0.5-1μM), the current-voltage relationship (I-V) under current clamp conditions indicated that zinc (300μM) increased the membrane resistance in an essentially voltage-independent fashion (Fig. 5.1A and C). Under corresponding voltage clamp conditions at a holding potential of -70mV, zinc induced a small outward current, and reduced the leakage current evoked following small hyperpolarizing voltage commands in a voltage-independent manner (Fig. 5.1B and D). If neurones were exposed to zinc for far longer than 1h, following the washout of zinc, a continuous membrane depolarization with a decrease in the input resistance was often observed. This indicated that the cells deteriorated on washout of zinc and implied that zinc might have toxic effects.

The delay in excitation following injection of depolarizing current into hippocampal pyramidal neurones is due to at least two outward potassium currents with different activation/inactivation kinetics. The A-current (I_A) is a brief transient current which is usually rapidly activated at depolarized potentials above -60mV (Gustafsson et al., 1982; Adams & Galvan, 1986; Storm, 1988). The current is also rapidly inactivated and blocked by a high dose of 4-AP (> 1mM). Under current clamp, if the resting membrane potential is sufficiently hyperpolarized to remove a large proportion of the steady state inactivation, a brief injection of depolarizing current elicited an electrotonic potential with a short delay (approximately 0.1s) before the first action potential (Fig. 5.2A). In hippocampal pyramidal neurones, the latency for firing action potentials is generally larger than that accounted for by the passive membrane time constant, or by activation of an A-current. Storm (1988) defined a new slow-inactivating 'delay' current,

termed I_D, which activates within 20ms but inactivates slowly over several seconds. I_D is more sensitive to 4-AP being blocked at 30-40μM. A long delay (0.5-1s) to the first action potential, during which the membrane depolarized slowly, was induced by a long depolarizing current pulse. (Fig. 5.1B). This usually reflected I_D activation (Storm, 1988). This delay in excitation, probably resulting from the activation of I_A and I_D, was removed by zinc (100-300μM) (Fig. 5.2A and B). The appearance of an anodal break spike (or rebound excitation) from a hyperpolarizing pulse in the presence of 300μM zinc (Fig. 5.2A) also suggests that zinc may inhibit the activation of I_A.

Single action potentials and more obviously, bursts of action potentials elicited by short depolarizing current pulses (1nA, 50-100ms) in pyramidal cells are followed by biphasic afterhyperpolarizations (AHPs). The fast, short phase of the AHP is proposed to be due to the activation of a large, calcium and voltage-dependent potassium current, termed I_C (Brown & Griffith, 1983). The longer lasting component is attributed to another calcium dependent potassium current, termed I_{AHP} (Alger & Nicoll, 1980; Nicoll & Alger, 1981; Lancaster & Adams, 1986). Both the single spike-AHP and the AHP following a burst of spikes were inhibited by 10-300μM of zinc (Fig. 5.2A and D, n=12). Interestingly, zinc not only blocked the single spike-AHP but also often induced an after-depolarizing potential (Fig. 5.2A). The onset of the zinc effect (approximately 5-min) was similar to the latency of inducing the GDP, but the generation of the GDP was not always associated with the blockade of AHPs and vice versa. In some neurones (n=5) spontaneous GDPs were induced by zinc (300μM) but the AHP following a burst of spikes elicited by a depolarizing current pulse was still observed (Fig. 5.4; cf. Sim & Cherubini, 1990). This suggested that the appearance of the GDP was not due to the blockade of AHPs, though inhibition of the AHP would greatly increase cell excitability. GDPs usually disappeared quickly following the washout of zinc, but the effect of zinc on AHPs was fairly resistant to washing, even after prolonged periods (1-3h). AHPs were further characterized by being inhibited with Cd^{2+} or Ba^{2+} (see also below).

The decline in firing and eventual cessation of action potentials during a spike train induced by a steady depolarization has been termed accommodation (Madison & Nicoll, 1984). Accommodation of firing is determined, in part, by calcium-dependent potassium currents (e.g. I_{AHP}) in hippocampal neurones (Alger & Nicoll, 1980; Nicoll & Alger, 1981; Lancaster & Adams, 1986) and is reinforced by other potassium currents,

such as the non-inactivating, voltage-dependent I_M (Brown & Adams, 1980). Zinc (100-300μM, n=24) clearly reduced action potential accommodation following a direct constant current pulse (Fig. 5.2C).

A hyperpolarization induced inwardly rectifying sodium/potassium current in hippocampal pyramidal neurones has also been previously described as the Q-current (I_Q). I_Q serves to resist hyperpolarizing deviations from the resting potential and hence stabilise the membrane potential (Halliwell & Adams, 1982). Under voltage clamp conditions, I_Q was seen as a slow inwardly relaxing current when the membrane was hyperpolarized to -80mV or more (Fig. 5.1B). Under current clamp recordings, the activation of I_Q by hyperpolarizing current injection produced a repolarizing sag in the electrotonic potential and a rebound depolarization at the end of the current pulse (Fig. 5.1A and 5.2A). Under voltage clamp, I_Q was unaffected by 300μM zinc (Fig. 5.1A).

2. Actions of other divalent cations and Al^{3+} on pyramidal neurones

2.1. Barium

Superfusion of Ba^{2+} (300-1000μM; n=6) over adult CA1 neurones caused a membrane depolarization with an increased membrane input resistance and burst firing of action potentials (Fig. 5.3). Ba^{2+} had a dramatic effect on action potential shape, causing an increase in the spike half-width to more than double the control value (control, 1.67±0.05ms; Ba^{2+} 3.89±0.08ms, n=6) and increased the cell excitability (Fig. 5.3B). Ba^{2+} blocked both the single spike-AHP and the burst-AHP elicited by depolarizing current pulses (Fig. 5.3B and C). Both the spontaneous synaptic 'noise' and stimulation-evoked synaptic responses were markedly enhanced by Ba^{2+}. Stimulation of the Schaffer collateral pathway evoked a large and long-lasting depolarizing potential. This indicated that Ba^{2+} increased synaptic neurotransmission. Most of these actions were resistant to 10μM bicuculline, except the later component of the evoked synaptic potential which was blocked (Fig. 5.3D). This suggests that a GDP-like potential induced by Ba^{+} may be partly mediated by $GABA_A$ receptor activation. Bicuculline also blocked the majority of spontaneous synaptic potentials which were enhanced by Ba^{2+}, suggesting that they are mainly IPSPs.

2.2. Cadmium, Cobalt and Manganese

Bath application of Cd^{2+} (100-300μM, n=8), induced a small hyperpolarization with a small increase in the resting input resistance (Fig. 5.4A), whereas Co^{2+}(100-300μM, n=4; Fig. 5.5A) and Mn^{2+} (300-1000μM, n=3; Fig. 5.6A) had no obvious effect on the membrane potential and input resistance. However all these elements increased the spike threshold (5.5B and 5.6B) and effectively blocked the slow component of burst-AHPs elicited by short depolarizing current pulses (Fig. 5.4C, 5.6C). Also these three metals had the same effect on synaptic neurotransmission, depressing spontaneous synaptic activity and the evoked synaptic responses (EPSP-IPSP) triggered by orthodromic stimulation of the Schaffer-collaterals (Fig. 5.4B, 5.5C and 5.6D). Neither Cd^{2+}, Co^{2+} nor Mn^{2+} induced any GDPs after application for over 10-20min, whereas zinc at the same range of concentrations (300-1000μM) routinely induced GDPs in the same neurones after washout of the previously applied metals (Fig. 5.4 and 5.5).

Co^{2+} has an epileptogenic action in the rat like Zn^{2+}, when injected intracerebroventricularly or placed directly on the cortical surface (Balcar et al., 1978). But at the doses used in this study no seizure-like activity was induced in the hippocampal neurones *in vitro* (Fig. 5.5).

2.3. Copper and Iron

Adult hippocampal neurones responded to Cu^{2+} (100-500μM, n=11), with a depolarization, an increased synaptic 'noise' and increased firing of action potentials (Fig. 5.7). Cu^{2+} had a more pronounced effect on cell excitability compared with zinc in the same cell and induced a particularly strong depression of the burst-AHP elicited by direct current injection (Fig. 5.7D). Although Cu^{2+} increased neurotransmitter release, manifest by increased spontaneous synaptic activity and by an enhanced evoked synaptic response (Fig. 5.7C), spontaneous or evoked GDP-like events were never observed in the presence of Cu^{2+}. In contrast, zinc (100μM) induced relatively small amplitude spontaneous and evoked GDPs (Fig. 5.7A and C).

Compared to Cu^{2+}, Fe^{2+} at concentrations of 100-300μM seemed less active in affecting the membrane potential and synaptic activity and was also unable to induce any GDPs. Again zinc (300μM) induced spontaneous and evoked GDPs in the same neurones (Fig. 5.8).

In the immature hippocampus, the levels of abundance for the essential trace metals are in the following order: zinc, iron, copper and manganese (Szerdahelyi & Kása, 1983). Zinc-chelating agents, CP94 and CP40 can complex with Fe^{2+} and Cu^{2+} under normal physiological conditions (Hider, personal communication). However, these two elements are usually very tightly bound to enzymes and currently these is no evidence to suggest that they can be released following neuronal activity in the hippocampus, although evidence for Cu^{2+} release in the rat hypothalamus has been presented by Hartter and Barnea (1988). Application of Cu^{2+} (100-300μM) or Fe^{2+} (100-300μM) to young hippocampal slices (P5-8; n=9) did not increase the naturally occurring innate GDPs observed in immature CA3 neurones.

2.4. Aluminum

Al^{3+}, a trivalent cation, also has an epileptogenic action in animals when implanted onto the cerebral cortex of rats (Balcar et al., 1978; Reynolds et al., 1981; Macdonald & Martin, 1988). Bath application of Al^{3+} (300-500μM) to adult pyramidal neurones had no obvious effects on the membrane potential or the input resistance. Although Al^{3+} increased the cell excitability, GDPs were not induced (n=5). Al^{3+} could induce seizure-like activity when applied to younger pyramidal neurones (P15-20; n=3). In this context, Al^{3+} (500μM) initially caused a slight hyperpolarization and then induced sudden large depolarizations superimposed with action potentials lasting for 2-3min. This seizure-like activity could be blocked by applying hyperpolarizing current. Al^{3+} also enhanced immature neuronal excitability but slightly depressed the evoked synaptic responses (Fig. 5.9B and C).

DISCUSSION

1. Zinc has multiple effects on membrane properties

The observation that zinc caused a small but maintained membrane hyperpolarization and significantly increased the input resistance or reduced the leakage currents (under voltage-clamp) was in agreement with previous studies in rat ganglion and cortical neurones (Smart & Constanti, 1982, 1983, 1990). The reason for the discrepancy between zinc causing a hyperpolarization in this study and a depolarization in the study by Sim & Cherubini (1990) using the same hippocampal slice preparation is unclear. Previous studies in cultured neurones failed to detect any changes in membrane potential and the input resistance (Peters, Koh & Choi, 1987; Mayer & Vyklicky, 1989). This may be explained by the use of different preparations and patch clamp recording techniques and also the generally brief application of zinc in these later studies. Neurones in the brain slice will have extensive dendrites, whereas cells in culture will initially lose these on dissociation. It is possible that some types of K^+ channels that are blockable by zinc are located on the dendrites. Also the effect of zinc on the intrinsic membrane properties in the present study were only observed after application of zinc for more than 5min. Considerable evidence suggests that zinc increases the stability of biological membranes by acting on both membrane proteins and lipids. Certain cytotoxic agents (such as haemolytic bacterial toxins) damage cells by the induction of pores across their plasma membrane, termed leakage (Chvapil, 1973). Zinc protects against such damage by preventing non-specific leakage including an influx of Ca^{2+} (Pasternak, 1988). This biological effect of zinc may be linked to the action of zinc in reducing the leak current and hyperpolarizing the neurone. Presumably the cell would then depolarize and the input resistance decrease following washout of zinc after re-establishing the leak conductances.

The input resistance of adult pyramidal neurones were significantly increased in the presence of exogenous zinc. Interestingly, young immature neurones (P2-14) show exceedingly high input resistances (83±39 MΩ) in normal Krebs solution (see Table 2.1, Chapter 2). An increased input resistance and a small hyperpolarization by zinc could lead to a facilitation in dendritic/somatic coupling and also synaptic coupling, whereby

small currents generated at a few distal synapses or single synapse, could be magnified into larger voltage events. Such events may travel further along the cell as a decreased input conductance would make the cell electrotonically more compact.

Zinc reduced the delay in excitation following an injection of depolarizing current probably as a result of blocking I_A and I_D currents (cf. Constanti & Smart, 1987; Smart & Constanti, 1990; Storm, 1988). Zinc also blocked the AHP supporting the notion that zinc inhibits Ca^{2+}-dependent K^+ currents (Constanti & Smart, 1987; Mayer & Vyklicky, 1989; Sim & Cherubini, 1990). These effects of zinc on Ca^{2+}-dependent and other K^+ channels would greatly potentiate the response to a synaptic input and thus contribute to the generation of the GDP in pyramidal cells. The passive membrane properties of neurones were altered by zinc at concentrations which also induced the appearance of GDPs. If zinc inhibits such a variety of potassium channels in the presynaptic nerve terminal or presynaptic GABAergic interneurones present in the hippocampus (Lacaille & Schwartzkroin, 1988b), it could also increase the presynaptic cell excitability and consequently enhance the release of neurotransmitter(s).

2. Induction of GDPs is an action unique to zinc in comparison with other cations

To examine whether other ions, like zinc, were capable of inducing GDPs, a variety of divalent cations were applied to the hippocampal slice. Ba^{2+}, Cd^{2+}, Co^{2+}, Cu^{2+}, Fe^{2+} and Mn^{2+} were tested and all showed blocking activity against AHPs following bursts of action potentials elicited by depolarizing current injection. This suggests that they might interfere with Ca^{2+} entry or block Ca^{2+}-dependent K^+ channels (Lancaster & Adams, 1986). However, these ions had different effects on the membrane properties and synaptic transmission in pyramidal neurones. Ba^{2+} and Cu^{2+} caused a small membrane depolarization and markedly increased cell excitability and enhanced synaptic transmission, whereas Cd^{2+}, Co^{2+} and Mn^{2+} apparently did not affect the membrane potential but decreased neuronal excitability and blocked spontaneous and evoked synaptic activity. In agreement with this observation, Cd^{2+}, Co^{2+} and Mn^{2+} have also been found to block synaptic transmission in the CNS (Krnjević et al., 1979; Gerber & Gähwiler, 1991) and at the neuromuscular junction (Brodie, Shefner & Levy, 1982; Cooper, Suszkiw & Manalis, 1984). Ba^{2+} and Cd^{2+} consistently increased the input

resistance, but Cu^{2+} slightly reduced the resistance, while the other three ions, Co^{2+}, Fe^{2+} and Mn^{2+} apparently had no effect. Al^{3+}, a trivalent cation, also increased membrane excitability and was capable of inducing seizure-like activity in young neurones. The seizure activity could be aborted with direct hyperpolarzing current injection, suggesting that it might result, in part, from the intrinsic properties of the postsynaptic neurone. This is in agreement with a previous study *in vivo* (Reynolds et al., 1981).

All these metal ions, at comparable concentrations to zinc, could not induce GABA-mediated GDPs in hippocampal neurones. An exception to this was Ba^{2+}, which to a certain degree like zinc, induced a $GABA_A$ mediated late depolarizing potential following orthodromic stimulation. Ba^{2+} partly reproduced the effect of zinc implying a further dimension to the actions of zinc which is shared by Ba^{2+}, but not by the other divalent cations studied. Interestingly, zinc and Ba^{2+} can enhance $GABA_A$ responses recorded in brain slices, probably due to an increase in the resting input resistance (Smart & Constanti, 1990).

Those ions (Cd^{2+}, Co^{2+}, Mn^{2+} and Al^{3+}) which inhibited neurotransmission will certainly not induce any GDPs. Although Cu^{2+} enhanced transmitter release and increased cell excitability, Cu^{2+} did not induced any GDPs, possibly due to a decreased cell input resistance. In contrast, in most neurones either before application or after washing out the various metal ions, zinc always induced GDPs in the same cells. Therefore, it is concluded that this action of Zn^{2+} in inducing GDPs is highly specific and so far unique. This is unusual as zinc has multiple effects on many voltage-operated or Ca^{2+}- dependent ion channels which are shared by the other cations.

Fig. 5.1. Effect of zinc on neuronal membrane properties in the presence of TTX (0.5μM). **A**, Current clamp records of membrane potential (lower traces) obtained from an adult CA1 neurone. Superimposed electrotonic potentials were produced by hyperpolarizing and depolarizing current pulses (upper traces; 300ms, 0.25Hz) and recorded before, during and after washing (60min) of 300μM zinc. Note zinc caused a hyperpolarization (5mV) in the membrane potential which had been adjusted back to the resting potential level with DC current injection. **B**, Corresponding voltage clamp recording from the same cell as in A, superimposed membrane currents (upper traces) evoked by hyperpolarizing and depolarizing voltage commands (5mV/step, 300ms, 0.25Hz, lower traces) from a holding potential of -70mV in the absence and presence of 300μM zinc. **C**, Current-voltage (I-V) curves constructed from the records in A by measuring the steady state electrotonic potential amplitudes before (○), during (▲) and after recovery from zinc (△). Note that zinc increased the input resistance more so at hyperpolarized membrane potentials. **D**, The steady state I-V relationships are plotted for the records in B by measuring steady state currents at the end of the voltage steps in control (○), in the presence of zinc (▲) and following the washout of zinc (△). The resting membrane potential was -72mV and its spike amplitude prior to TTX was 103mV.

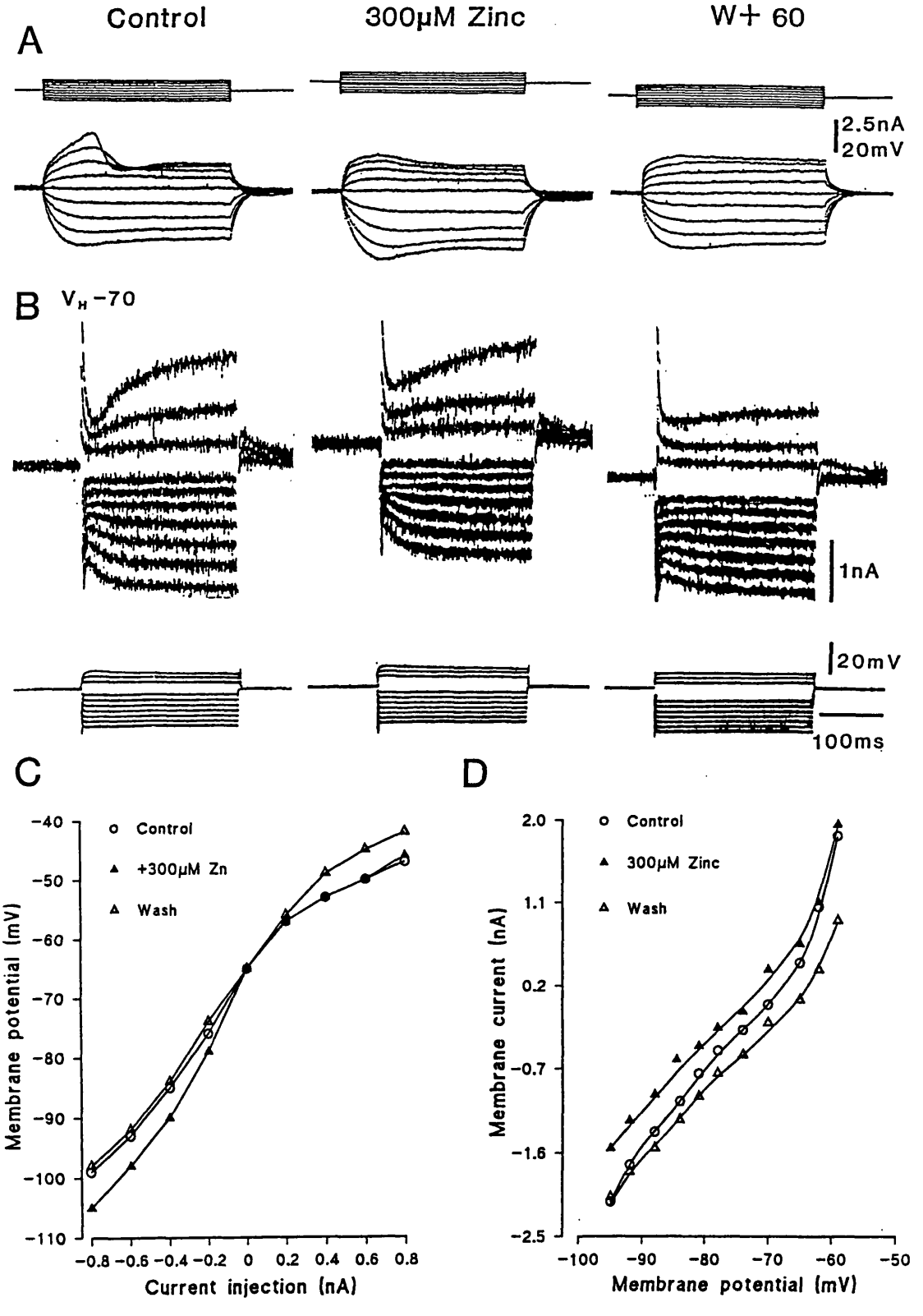
A
Control
300μM Zinc
W+ 60
2.5nA
20mV
B
V_H -70
1nA
20mV
100ms
C
Control
+300μM Zn
Wash
Membrane potential (mV)
Current injection (nA)
D
Control
300μM Zinc
Wash
Membrane current (nA)
Membrane potential (mV)

Fig. 5.2. Effects of zinc on action potential latency, accommodation and afterhyperpolarization (AHP). Current clamp records of membrane potential (lower traces in each row) were obtained from an adult CA1 neurone. Superimposed electrotonic potentials were produced by hyperpolarizing or depolarizing current pulses (upper traces in each row). **A**, Electrotonic potentials were evoked by 300ms, 0.2Hz current pulses. A short delay occurred before an action potential was seen in control. In the presence of zinc (300μM), the spike threshold was reduced, the latency for firing the first spike became shorter and the spike-AHP was blocked being replaced by an after-depolarizing potential (arrow). **B**, A long duration (800ms) small depolarizing (0.2nA) current pulse elicited a long delay to the first action potential in control. Zinc reduced the delay and induced multiple action potentials. **C**, Zinc reduced the accommodation of firing evoked by a large amplitude (0.4nA, 800ms) depolarizing current injection. **D**, Zinc depressed burst-AHPs elicited by short duration, large amplitude depolarizing current pulses (1nA, 50ms, 0.05Hz). Records in A, B, C and D are from the same neurone with a resting membrane potential of -68mV in A. Recordings in B, C and D the membrane potential was maintained at -75mV with DC current injection in the absence and presence of zinc. The slice was perfused with Krebs containing 4mM Mg to reduce spontaneous synaptic potentials. Voltage calibration is 20mV for all rows. Current calibrations are 1nA (A, B), and 2nA (C). Time calibrations are 100ms (A), 200ms (B, C) and 400ms (D).

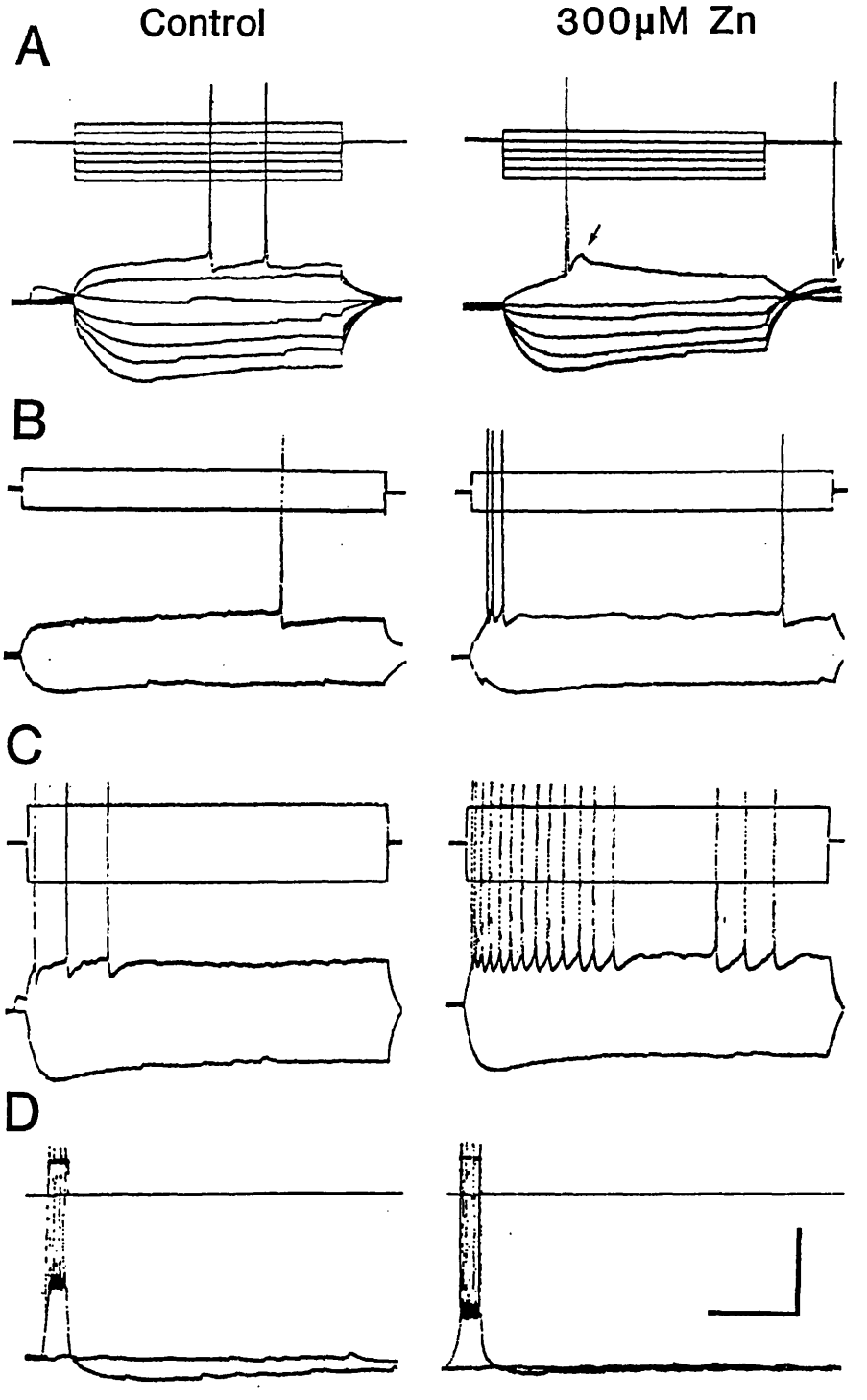
Control
300μM Zn
A
B
C
D

Fig. 5.3. Ba^{2+} induced a depolarization and bursts of action potentials in adult CA1 neurones. **A**, Chart record of an intracellular recording of membrane potential with superimposed hyperpolarizing electrotonic potentials (downward deflections) evoked by -0.3nA, 300ms, 0.3Hz current pulses. Bath application of 1mM Ba^{2+} (Δ) caused spontaneous depolarizations which were resistant to 10μM bicuculline (solid line). **B**, Current clamp records of superimposed electrotonic potentials (lower traces) produced by hyperpolarizing and depolarizing current pulses (upper traces; 300ms, 0.25Hz) recorded in the absence and presence of 1mM Ba^{2+}, and also in Ba^{2+} plus 10μM bicuculline (Ba/BIC). Ba^{2+} increased cell excitability and prolonged the durations of the spikes. **C**, Ba^{2+} blocked the AHP elicited by a depolarizing current pulse (1nA, 100ms). **D**, Ba^{2+} induced a large and prolonged potential following stimulation of the Schaffer-collateral pathway (▲, 15V, 0.1ms). A brief hyperpolarizing electrotonic potential was used to monitor membrane resistance (-0.3nA, 300ms). Most of the effects of Ba^{2+} were resistant to bicuculline (10μM), but bicuculline blocked the spontaneous synaptic potentials (B) and reduced the spontaneous firing of action potentials (C). Also the later component of the evoked synaptic response was inhibited by 10μM bicuculline. A, B, C and D are from the same neurone. The membrane potential was adjusted at -70mV with DC current injection. Voltage calibration in A is 10mV, in B, C and D, 20mV. Current calibration is 1nA for B, C and D. Time calibration in A is 40s, in B, 100ms, in C, 400ms and in D, 1s.

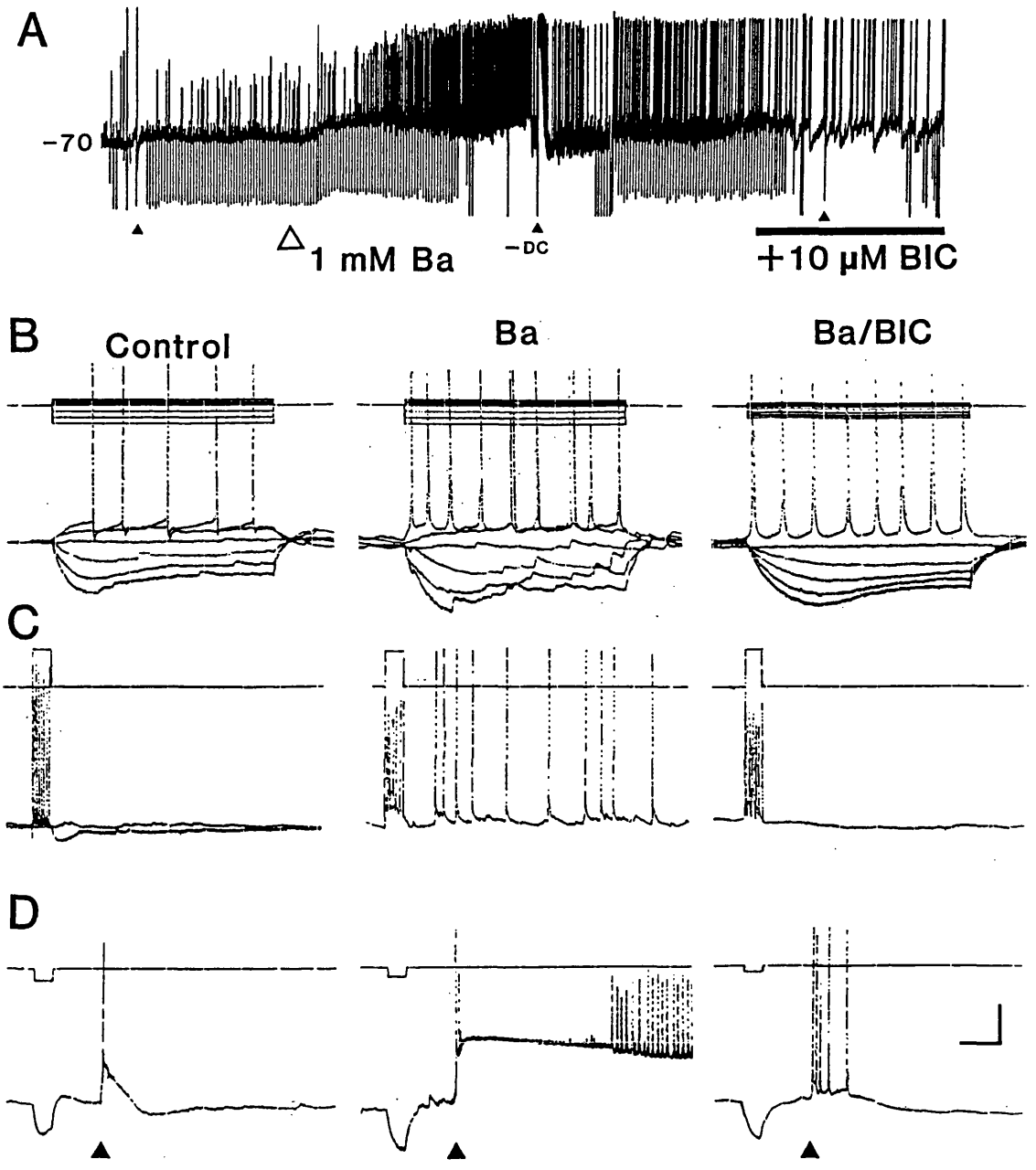
A
-70
1 mM Ba
-DC
+10 µM BIC
B
Control
Ba
Ba/BIC
C
D

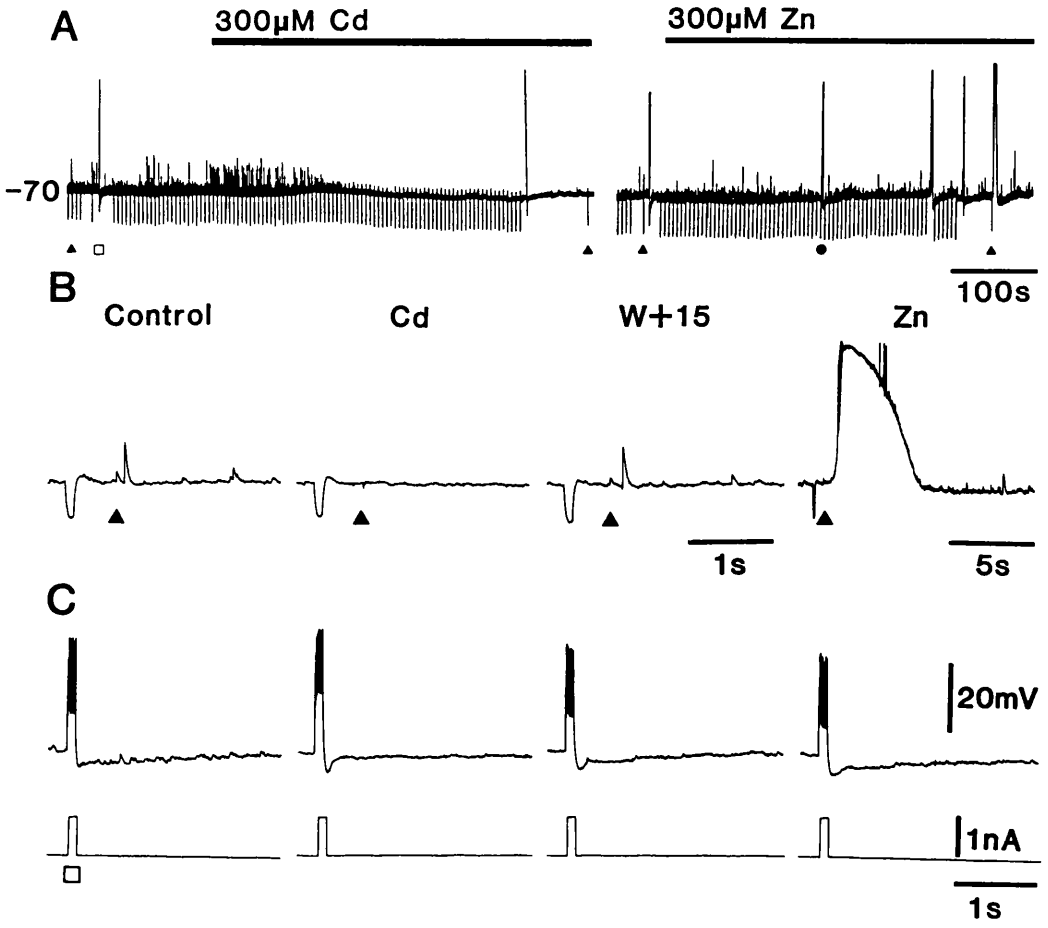

Fig. 5.4. Comparison between Cd^{2+} and Zn^{2+} effects on synaptic activity and AHPs in adult CA1 neurones. **A**, Chart record of an intracellular recording of membrane potential adjusted to -70mV with superimposed hyperpolarizing electrotonic potentials (-0.3nA, 300ms, 0.5Hz). Bath application of 300μM Cd^{2+} depressed spontaneous and evoked (▲) synaptic potentials and slightly hyperpolarized the membrane potential associated with a small increase in the input resistance. After recovery from Cd^{2+} (washing for 15min, W+15), 300μM Zn induced spontaneous (●) and evoked GDPs (▲). **B**, Cd^{2+} (300μM) and Zn^{2+} (300μM) effects on evoked synaptic potentials on an expanded timescale. The Schaffer-collateral pathway was stimulated with 15V, 0.1ms pulses. **C**, Effects of Cd^{2+} and Zn^{2+} on AHPs following bursts of action potentials elicited by short depolarizing current pulses (1nA, 100ms) in the same neurone. Note in this particular cell Zn^{2+} did not block the AHP but still induced GDPs.

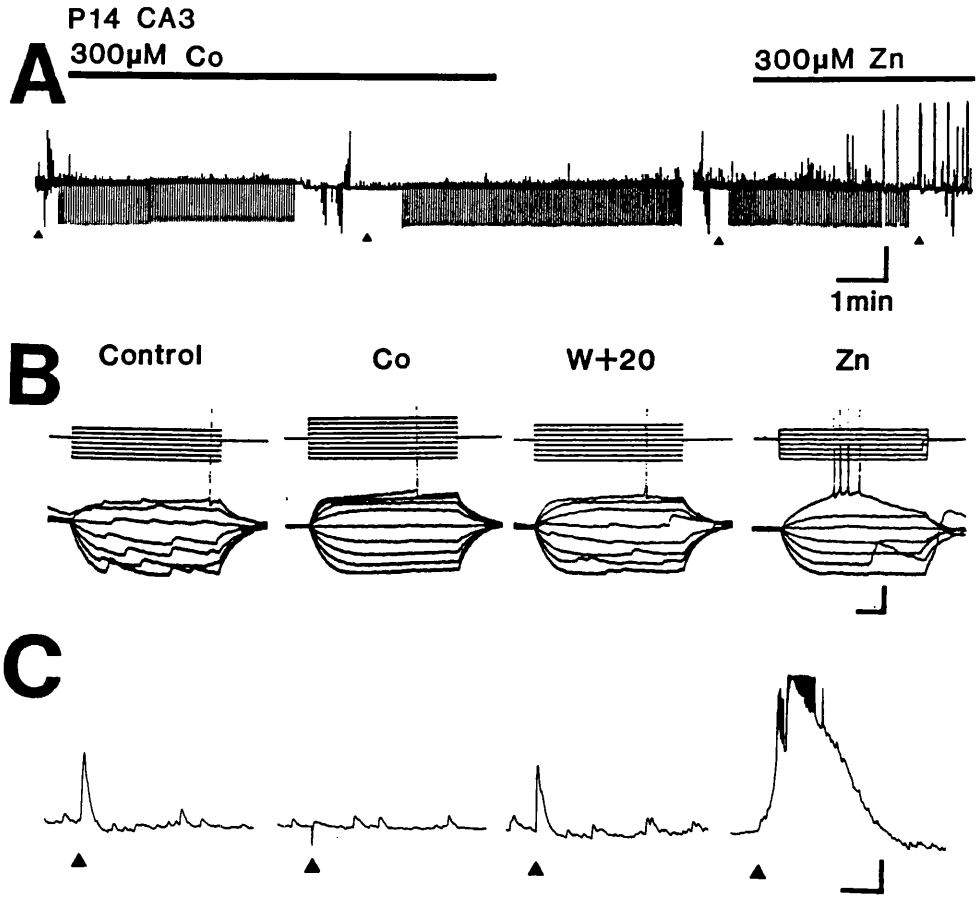

Fig. 5.5. Comparison between Co^{2+} and Zn^{2+} effects on the membrane properties and synaptic activity of a young (P14) CA3 neurone. **A**, Chart record of an intracellular recording of the resting membrane potential at -87mV with superimposed hyperpolarizing electrotonic potentials (-0.3nA, 300ms, 0.3Hz). Bath application of 300μM Co^{2+} depressed spontaneous and evoked (▲) synaptic potentials. After washout of Co^{2+} for 20-min, 300μM Zn^{2+} induced spontaneous and evoked GDPs (▲). **B**, Current clamp records of membrane potential (lower traces) obtained from the same neurone. Superimposed electrotonic potentials produced by hyperpolarizing and depolarizing current pulses (upper traces; 300ms, 0.25Hz) were recorded before, during and 20min after application (W+20) of Co^{2+} (300μM), and in the presence of Zn^{2+} (300μM). **C** illustrates the effects of Co^{2+} and Zn^{2+} on evoked synaptic potentials (▲) following stimulation of the mossy fibres (10V, 60μs). Time calibration in B is 50ms, in C, 100ms. Voltage calibration in A and C is 10mV, in B, 20mV. Current calibration in B is 0.5nA.

Fig. 5.6. Effects of Mn^{2+} on the membrane properties, burst-afterhyperpolarization (AHP) and synaptic activity in an adult CA1 neurone. **A**, Chart record of an intracellular recording of membrane potential adjusted to -70mV with superimposed hyperpolarizing electrotonic potentials (-0.3nA, 300ms, 0.3Hz). Bath application of 300μM Mn^{2+} depressed spontaneous and evoked (▲) synaptic potentials. **B**, Current clamp records of membrane potential (lower traces) obtained from the same neurone. Superimposed electrotonic potentials produced by hyperpolarizing and depolarizing current pulses (upper traces; 300ms, 0.25Hz) were recorded before, during and 15min after application (W+15) of Mn^{2+} (1mM). **C**, Mn^{2+} inhibited the AHP following a train of action potentials (lower traces) elicited by a short depolarizing current pulse (1nA, 100ms, upper traces). **D** illustrates Mn^{2+} blocking evoked synaptic potentials (▲) following stimulation (10V, 0.1ms) of the Schaffer-collateral pathway on an expanded timescale. Voltage and current calibrations in D apply to B and C. Time calibration is 50ms for B, 200ms for C, and 500ms for D.

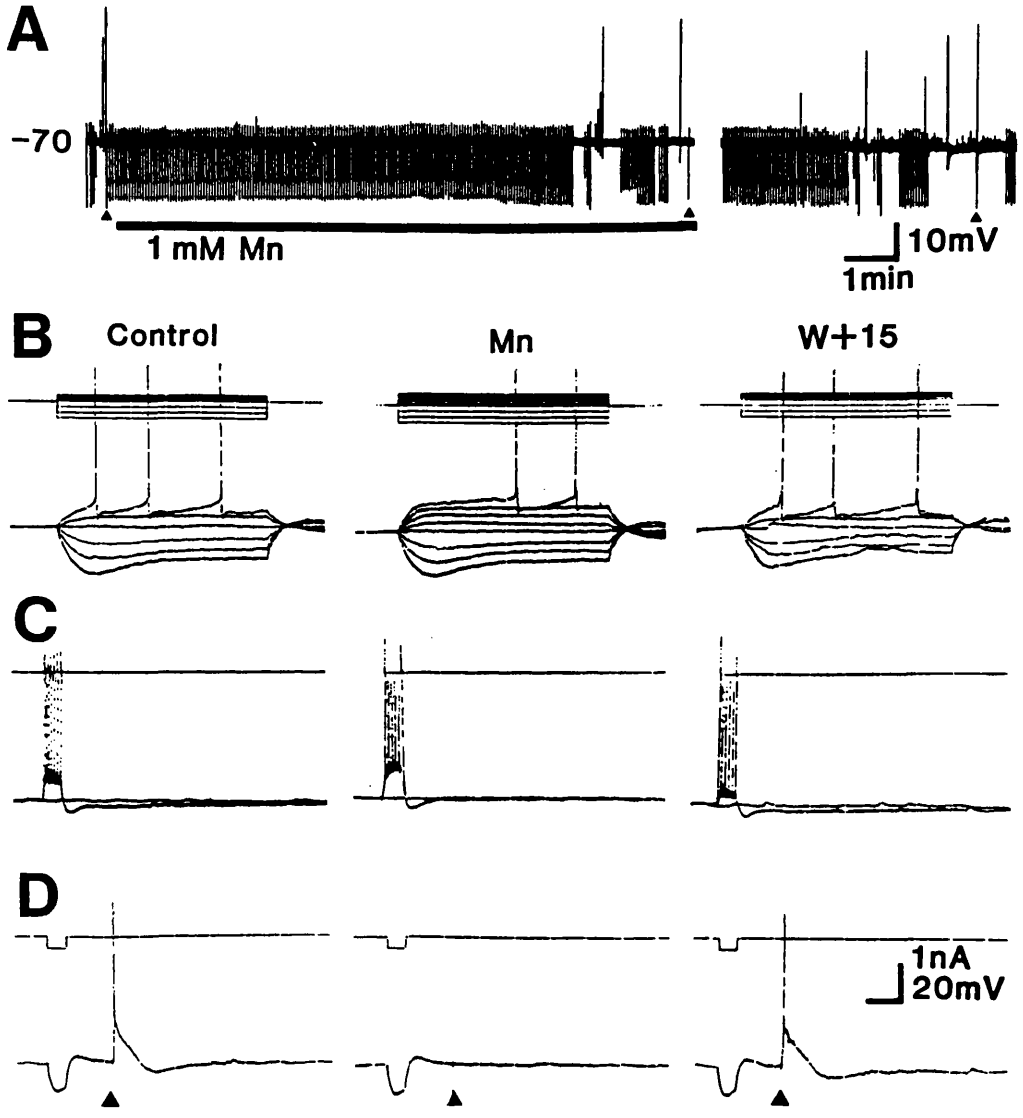
A
-70
1 mM Mn
10mV
1min
B
Control
Mn
W+15
C
D
1nA
20mV

Fig. 5.7. A comparison of the action of Cu^{2+} and Zn^{2+} on the membrane properties and synaptic activity in adult CA1 neurones. **A**, Chart record of an intracellular recording of membrane potential with superimposed hyperpolarizing electrotonic potentials (downward deflections) evoked by -0.3nA, 300ms, 0.3Hz current pulses. Bath application of 100μM Zn^{2+} induced spontaneous (●) and evoked (▲) GDPs. After recovery from Zn^{2+} (washing Zn^{2+} for 20-min), bath application of 100μM Cu^{2+} markedly increased both spontaneous and evoked (▲) synaptic potentials. **B**, Current clamp records of membrane potential (lower traces) obtained from the same neurone shown in A at -70mV (with DC current injection). Superimposed electrotonic potentials produced by hyperpolarizing and depolarizing current pulses (upper traces; 300ms, 0.25Hz) were recorded during and 20min after application (W+20) of Zn^{2+} (100μM), and in the presence of Cu^{2+} (100μM). **C** illustrates the effect of Zn^{2+} and Cu^{2+} on evoked synaptic potentials (▲) on an expanded timescale. 15V, 0.1ms stimuli were applied to the Schaffer-collateral pathway. Note in the presence of Zn^{2+} a GDP was evoked, while in the presence of Cu^{2+}, an enhanced EPSP with superimposed action potentials was triggered in addition to an increase in spontaneous synaptic potentials. **D**, Both Zn^{2+} and Cu^{2+} depressed the afterhyperpolarizations following trains of action potentials (upper traces) elicited by short depolarizing current pulses (1nA, 100ms, lower traces). Time calibration is 40s for A, 50ms for B, 500ms for C and D. Voltage calibration is 10mV for A, C and D; 20mV for B. Current calibration in D applies to B.

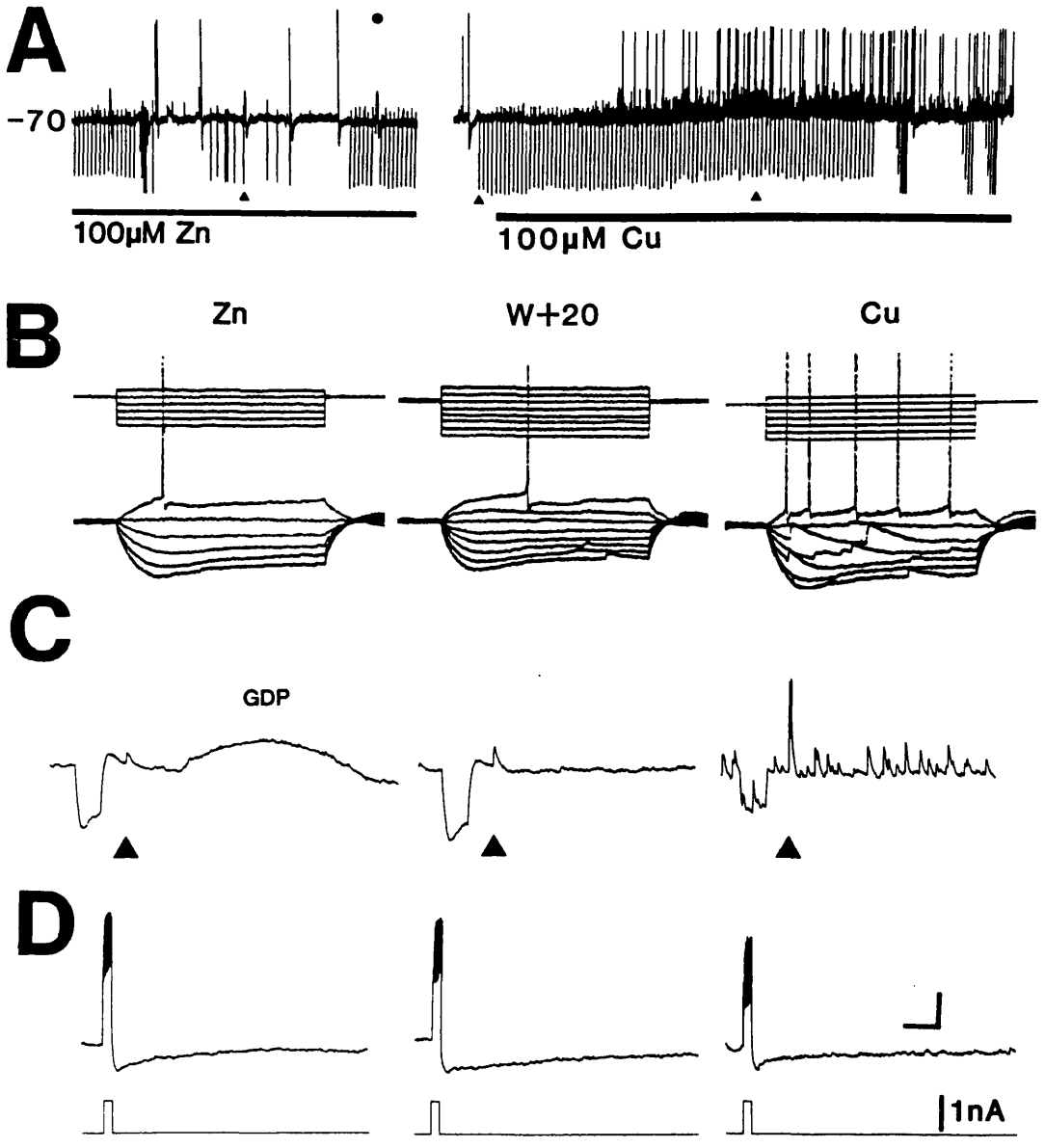
A
-70
100μM Zn
100μM Cu
B
Zn
W+20
Cu
C
GDP
D
1nA

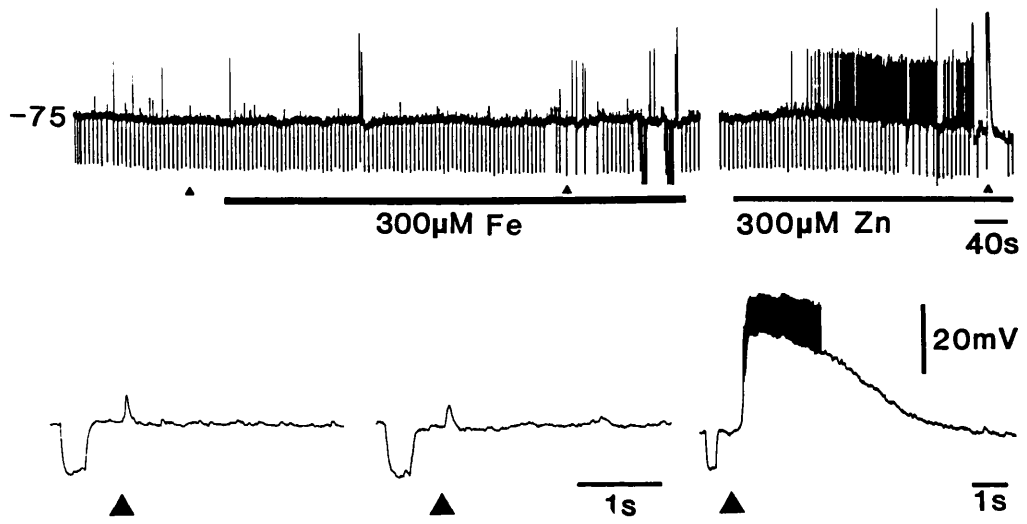

Fig. 5.8. Effects of Fe^{2+} and Zn^{2+} on the membrane potential and synaptic activity in an adult CA1 neurone. **A**, Chart record of an intracellular recording of the resting membrane potential at -75mV with superimposed hyperpolarizing electrotonic potentials (-0.3nA, 300ms, 0.3Hz). Bath application of 300μM Fe^{2+} had no obvious effect on the membrane potential or spontaneous and evoked (▲) synaptic activity. In the same cell after washing Fe^{2+} for 20-min, Zn (300μM) induced spontaneous and evoked (▲) GDPs. **B** illustrates Fe^{2+} and Zn^{2+} effects on evoked synaptic potentials (▲) on an expanded timescale. The Schaffer-collateral pathway was stimulated with 18V, 0.1ms stimuli. Hyperpolarizing electrotonic potentials were evoked by -0.3nA, 300ms current pulses.

Fig. 5.9. Al^{3+} modulates membrane properties and synaptic potentials in a young (P20) CA1 neurone. **A**, Chart record of an intracellular recording of membrane potential adjusted to -70mV with superimposed hyperpolarizing electrotonic potentials (-0.3nA, 300ms, 0.3Hz). Bath application of 500μM Al^{3+} for 12min caused two seizure-like prolonged depolarizing events. During the period of the second seizure, the hyperpolarizing current pulses were stopped and injecting hyperpolarizing DC current caused the cessation of action potentials firing (◊). **B**, Current clamp records of superimposed electrotonic potentials (lower traces) produced by hyperpolarizing and depolarizing current pulses (upper traces; 300ms, 0.25Hz) were recorded in the presence and absence of Al^{3+}. **C**, Al^{3+} depressed the evoked synaptic potentials (▲) triggered by stimuli at different intensities applied to the Schaffer-collateral pathway (15V, 0.1ms).

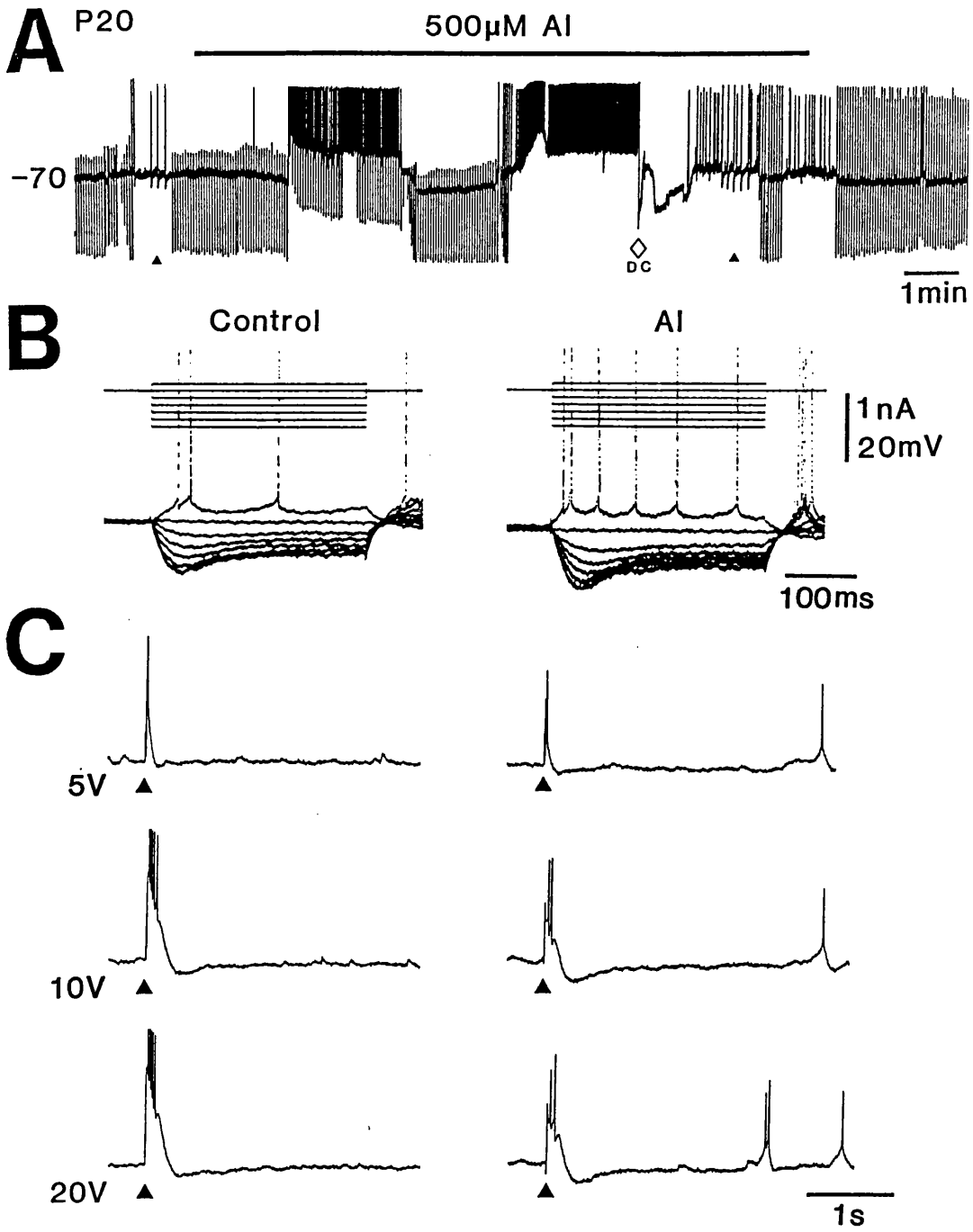
A
P20
500μM Al
-70
DC
1min
B
Control
Al
1nA
20mV
100ms
C
5V
10V
20V
1s

Chapter 6

ZINC MODULATION OF $GABA_A$ AND $GABA_B$ RECEPTORS AND INHIBITORY SYNAPTIC TRANSMISSION

INTRODUCTION

Although zinc does have some direct actions on membrane properties and ion channels, particularly various K^+ channels (Constanti & Smart, 1987; Mayer & Vyklicky, 1989; Sim & Cherubini, 1990), it is unlikely to be the sole cause of the GDPs. To elucidate the mechanism(s) underlying GDP generation and reveal which receptors were involved, this study first concentrated on the GABAergic system since the mediation of GDPs was apparently due to the release of the inhibitory transmitter GABA.

Pharmacological evidence suggests that the mammalian CNS contains two major classes of receptors mediating GABA responses: the bicuculline-sensitive $GABA_A$ receptors which selectively increase chloride conductance (Curtis et al,, 1971; Krnjević, 1976; Bormann, 1988), and the bicuculline-insensitive $GABA_B$ receptors, which involve an increase in K^+ conductance or a block of calcium conductance (Bowery et al., 1980; Hill & Bowery, 1981; Inoue, Matsuo & Ogata, 1985b; Dutar & Nicoll, 1988a; Bowery, 1989). $GABA_B$-mediated responses are also blocked by specific antagonists, such as phaclofen (Kerr et al., 1987), 2-hydroxy-saclofen (2-OH-saclofen, Lambert et al., 1989) and more recently by CGP 35348 (Olpe et al., 1990).

The $GABA_A$ receptor complex is a multimeric protein comprising allosteric sites for $GABA_A$ receptor modulators, including the benzodiazepines (BDZ), barbiturates (Study & Barker, 1981), and the sedative steroids (Simmonds, Turner & Harrison, 1984; Lambert, Peters & Cottrell, 1987). Zinc was also suggested to be a $GABA_A$ receptor modulator or antagonist following the original observation of zinc inhibiting GABA-evoked responses recorded from crustacean muscle (Smart & Constanti, 1982). This suggestion was confirmed by zinc producing a block of GABA responses on frog dorsal root ganglia neurones (Yakushiji et al., 1987) and on cultured mouse embryonic hippocampal neurones, in which the $GABA_A$-receptor mediated IPSPs were also blocked

by zinc (Westbrook & Mayer, 1987; Mayer & Vyklicky, 1989). Recently, patch clamp recordings from cultured superior cervical ganglion, cerebellar neurones or hippocampal neurones have revealed zinc blocks GABA-mediated ion channels by reducing the frequency of single channel opening (Smart, 1990, 1992; Legendre & Westbrook, 1991).

However, interestingly the $GABA_A$ receptors resident on **adult** rat sympathetic ganglia are entirely resistant to a blockade by zinc (Smart & Constanti, 1982) and GABA responses recorded from CNS pyramidal neurones in **adult** cortical and hippocampal brain slices displayed an enhancement in the presence of zinc (Smart & Constanti, 1983, 1990; Xie & Smart, 1991b). Other studies both *in vivo* and *in vitro* have also confirmed this insensitivity in adult neurones (Wright, 1984; Hori et al., 1987). Recently, a comparative study has further demonstrated that zinc blocking $GABA_A$ receptors does not occur in older mammalian neurones, irrespective of whether one uses intact preparations or tissue cultures, but appears to depend critically on the stage of neuronal development (Smart & Constanti, 1990).

Whether zinc inhibits or enhances GABA responses in rat neonatal hippocampal neurones has currently not been shown. Since zinc can also inhibit K^+ and Ca^{2+} conductances, it was of interest to test whether zinc could modulate $GABA_B$ receptors, either at the receptor or channel level. To date there are no endogenous substances which have been found to modulate $GABA_B$ receptor function (Bowery, 1989). It has been reported that K^+ channel blockers, such as Ba^{2+} and 4-AP depress baclofen (a selective $GABA_B$ agonist) responses in hippocampal neurones (Gähwiler & Brown, 1985; Inoue, Matsuo & Ogata, 1985a). The present experiments were undertaken to address these questions, through which it may be possible to gain insight into the mechanism of zinc-induced GDPs.

RESULTS

1. Exogenous GABA-evoked responses are augmented by zinc

In contrast to zinc blocking GABA responses in cultured embryonic hippocampal neurones, bath-applied or ionophoretically-applied GABA responses recorded from young postnatal (P11) and adult (P>90) hippocampal CA1 or CA3 neurones were not blocked by zinc (100-300μM), but actually slightly enhanced (Fig. 6.1,2 and 3). Adult hippocampal neurones responded to bath-applied GABA (1mM) with a slow depolarization and associated conductance increase (Alger & Nicoll, 1982). These responses were slightly enhanced (but never blocked) in the presence of 20-300μM zinc (Fig. 6.1; n=6). Curiously, in young slices, flurazepam (0.5-10μM; n=6) did not produce any enhancement of the GABA responses, but in adult slices, the sensitivity of the GABA response to flurazepam became readily apparent (Fig. 6.2). The result with young CA3 neurones confirmed that these GABA responses are apparently insensitive to BDZ (Rovira & Ben-Ari, 1990; Smart et al., 1991); however, $GABA_A$ receptors in these young postnatal neurones were still resistant to zinc antagonism.

The enhancement of GABA responses by zinc was probably not due to an effect on the $GABA_A$ receptor affinity since analysis of ionophoretic GABA dose-response curves revealed that all GABA responses evoked by different ejection currents were increased equally in the presence of 300μM zinc suggesting that the dose-response curve is not shifted laterally to the left (Fig. 6.3). Ionophoretically-applied GABA responses were blocked by bath-applied 20μM bicuculline or by co-ionophoretically-applied picrotoxin, confirming they were mediated by $GABA_A$ receptor activation (see Fig. 3.14, Chapter 3). However it was noted that the GABA response evoked by ionophoresis when the ionophoretic pipette was positioned in the dendritic region in stratum radiatum is more obviously enhanced by zinc than GABA responses induced by bath application, which acts on both the soma and dendrites of the recorded neurone.

2. Zinc enhances the $GABA_A$ receptor-mediated fast IPSP

Since zinc potentiated responses to exogenous GABA in postnatal hippocampal

neurones, it was of interest to consider whether zinc might enhance the $GABA_A$-mediated component of inhibitory transmission. Orthodromic stimulation of input afferents evoked an EPSP followed by fast and slow IPSPs. The fast IPSP was mediated by $GABA_A$ receptor activation (Alger & Nicoll, 1982) and the slow IPSP was mediated by $GABA_B$ receptors (Dutar & Nicoll, 1988a). The $GABA_A$-mediated IPSP could be clearly resolved by first blocking the slow IPSP with a $GABA_B$ antagonist, CGP 35348 (100-300μM) as shown in Fig. 6.4A,B. The fast $GABA_A$-mediated IPSP, which has a likely somatic localization (Andersen et al., 1980; Alger & Nicoll, 1982) (where few $GABA_B$ receptors are thought to reside, cf. Bowery, Hudson & Price, 1987; Bowery, 1989), was not blocked, but slightly enhanced by 300μM zinc. Furthermore, a late depolarizing potential (GDP) was also revealed in the presence of zinc (Fig. 6.4C,D). This may indicate that zinc has increased the amplitude and duration of $GABA_A$-mediated **depolarizing IPSPs** which occur in the dendrites (Avoli, 1988). Both the early hyperpolarizing (fast IPSP) and late depolarizing potentials were blocked by 20μM bicuculline (Fig. 6.4D; n=3). However, the enhancement of the fast IPSPs is sometimes difficult to resolve, because the latent GDP increases in amplitude and tends to obscure the fast hyperpolarizing IPSP.

3. Postsynaptic $GABA_B$ receptor-mediated responses are inhibited by zinc

An analysis of the synaptic responses in CA3 neurones implied that the late, long-lasting giant depolarizing potential induced by zinc had a similar time course to the slow $GABA_B$-mediated IPSP observed prior to zinc administration (Fig. 6.4). This was the first indication that zinc might inhibit $GABA_B$ receptors. An inhibition of postsynaptic $GABA_B$ responses by zinc could be directly demonstrated in both adult and young postnatal neurones by using the specific $GABA_B$ receptor agonist, baclofen (Hill & Bowery, 1981). Repeated application of (-)-baclofen (10-20μM) often produced an apparent desensitization. Therefore, baclofen doses and the application intervals were carefully selected to give reproducible submaximal responses with minimal desensitization. Zinc (50-300μM) reversibly inhibited the baclofen-induced hyperpolarization (reduced to 30-80%, n=9) and conductance increase (Fig. 6.5A; n=9). For comparison, 50-100μM CGP 35348, the specific $GABA_B$ receptor antagonist (Olpe et al., 1990), also reversibly blocked the baclofen-evoked responses (Fig. 6.5B),

confirming that these responses were mediated by $GABA_B$ receptors in pyramidal cells. In addition, it also showed that CGP 35348 is a more potent inhibitor of $GABA_B$ receptors compared to zinc. Pyramidal neurones voltage-clamped at or near their resting potential (-60 to -70mV) responded to baclofen (10-20μM) with an outward (hyperpolarizing) membrane current which was also reversibly inhibited by zinc (300μM, n=3).

In order to further confirm the differential effect of zinc on $GABA_A$- and $GABA_B$-responses, it was necessary to make recordings from the same cell. As shown in Fig. 6.6, zinc (300μM) selectively enhanced GABA-evoked depolarizing responses, with the appearance of spontaneous and evoked-GDPs and inhibited baclofen-induced hyperpolarizing responses. However, during the action of baclofen even in zinc, spontaneous and evoked GDPs were abolished, suggesting that zinc is a weak inhibitor at $GABA_B$ receptors. Furthermore, exogenous GABA (4mM) induced a hyperpolarization and conductance increase in the presence of bicuculline (50μM) and picrotoxin (40μM), suggesting activation of postsynaptic $GABA_B$ receptors (Dutar & Nicoll, 1988), which was also inhibited by 300μM zinc.

$GABA_B$ receptor activation is reliant upon extracellular Ca^{2+} and Mg^{2+} ions (Hill & Bowery, 1981), it seems unlikely that the zinc inhibition of $GABA_B$ responses is simply due to an interference with the action of Ca^{2+} and Mg^{2+} and therefore baclofen binding, since micromolar concentrations of zinc are capable of antagonizing baclofen responses in perfusing media containing much higher concentrations of Ca^{2+} and Mg^{2+} from 1.5mM to 2.5mM.

4. Zinc induces giant hyperpolarizing synaptic potentials

The results presented thus far indicate that zinc is capable of inhibiting postsynaptic $GABA_B$ receptors. This implies that evoked $GABA_B$-mediated synaptic potentials should also be blocked by zinc. To test the action of zinc on synaptic $GABA_B$ receptors, a protocol of recording 'pure' monosynaptic $GABA_B$-mediated IPSPs in CA3 and CA1 neurones was adopted (Davies, Davies & Collingridge, 1990). Since GABAergic neurones have invariably short axons and they are usually activated indirectly (i.e. by feedback and feed-forward inhibition) following activity in excitatory neurones

(i.e. pyramidal cells), this protocol was designed to provide a possibility of excluding any influences that may come from zinc affecting either excitatory synaptic activity or the fast $GABA_A$-mediated IPSP. In the presence of 20μM CNQX, 40μM APV, 20μM bicuculline and 40μM picrotoxin, blocking EPSPs mediated by NMDA and non-NMDA receptors and also fast $GABA_A$-mediated IPSPs, localized stimulation in stratum radiatum (stimulation electrodes placed close less than approximately 0.5mm from the recording site) evoked slow hyperpolarizing potentials. These potentials were triggered with a consistent latency and were reversibly blocked by 50-150μM CGP 35348, indicating they were probably monosynaptic $GABA_B$-mediated IPSPs ($IPSP_B$s). Their properties, which are presented in Table 6.1, are in general agreement with a previous study by Davies and colleagues (1990).

Table 6.1. Effect of zinc on monosynaptic $GABA_B$-mediated IPSPs in CA3 pyramidal neurones

	Amplitude (mV)	Time to peak (ms)	Duration (ms)	n
Control	-4.8±2.1	216±51	717±203	8
Zinc (300μM)	-8.7±2.7	410±292	1613±708	8

$IPSP_B$s were evoked by localised stimulation in stratum radiatum using a stimulus intensity to evoke a maximum response (30-45V, 0.1ms) in the presence of 20μM CNQX, 40μM APV, 20μM bicuculline and 40μM picrotoxin. Data are presented as mean±S.D. and the differences between control and zinc treated cells are statistically significant (<0.01) using a paired *t* test.

Following the previous results of zinc inhibiting $GABA_B$ receptors, it was surprising to find that bath-applied 300μM zinc induced the appearance of spontaneous slow giant **hyperpolarizing** potentials (GHPs) under these experimental conditions (Fig. 6.7). These GHPs consisted of large (5-12mV amplitude) and long-lasting (1-2s duration) hyperpolarizations from the resting potential. These spontaneous events recurred at approximately every 60 to 100-s. Localized stimulation now evoked a biphasic hyperpolarizing potential. An initial hyperpolarization (presumably an initial $IPSP_B$, since

$GABA_A$ receptors were blocked) was slightly depressed and followed by a slower onset, large amplitude (6-12mV) and long duration (1-2s) hyperpolarizing potential, which was very similar to the spontaneous GHP (Fig. 6.7). Both spontaneous and evoked GHPs were resistant to the addition of 100μM CGP 35348, a concentration shown to completely inhibit the initial $IPSP_B$ (Fig. 6.7B, indicated by the arrow) and usually sufficient to block 10μM bath-applied (-)-baclofen responses (Fig. 6.5B). This at first seemed to resemble the bicuculline- and phaclofen-resistant hyperpolarization evoked by glutamate application to stratum lacunosum-moleculare and recorded in CA1 cells (Williams & Lacaille, 1990). However, as CGP 35348 concentrations were increased up to 300-800μM, these zinc-induced GHPs were depressed and eventually blocked (Fig. 6.7). This suggests that the zinc-induced GHPs are still mediated by released GABA acting on $GABA_B$ receptors.

The paradoxical effect of zinc on the $GABA_B$ agonist-induced postsynaptic responses and the $GABA_B$-mediated synaptic potentials implies that zinc may be inhibiting presynaptic $GABA_B$ receptors, causing large local amounts of GABA to be released which may then nullify postsynaptic zinc inhibition. To test this hypothesis, CGP 35348 was used for comparison, since it is a defined competitive $GABA_B$ antagonist (Olpe et al., 1990). At a low concentration of 10μM, CGP 35348 did not depress but **enhanced** monosynaptic $IPSP_B$s recorded in CA3 neurones (Fig. 6.8A). CGP 35348 at this dose had no direct effect on the membrane potential or general cell properties and presumably no effect on the membrane of GABAergic neurones either. If the latter is true, then this effect is most likely due to the inhibition of presynaptic $GABA_B$ receptors on or near the terminals of the GABAergic neurones, consequently increasing the release of GABA. As the concentration of CGP 35348 increased (50-150μM), the influence of the postsynaptic depressant action was greater than the effect of promoting GABA release, thus the $GABA_B$-mediated IPSPs were inhibited and eventually abolished (Fig. 6.8A). In an analogous manner, the monosynaptic $IPSP_B$ was also initially enhanced by zinc at 50-300μM, but eventually slightly inhibited at 300-1000μM (Fig. 6.8B).

It was of interest to re-investigate whether **endogenous** zinc modulates the presynaptic $GABA_B$ receptor activity in **adult** CA3 neurones, though zinc chelators have been shown to have no obvious effect on intact synaptic transmission in adult slices (see Chapter 4). As shown in Fig. 6.9, when two stimuli of identical strength were applied separated by intervals of 100-800ms, the second monosynaptic $IPSP_B$ was markedly

depressed, which is suggested to be due to presynaptic $GABA_B$ receptor activation (Davies, Davies & Collingridge, 1990). The zinc chelator, CP94 (400μM) had little or no effect on paired-pulse depression (n=3), but after washout of the chelator, exogenous zinc (50μM) also hardly reduced paired-pulse depression. Unfortunately, raising the zinc concentration to 300μM to resolve this effect produced an inhibition in both the first and second $IPSP_B$. However, zinc again induced the spontaneous GHPs with much slower onset and these events were blocked by 300μM CGP 35348. These results suggest if that zinc inhibits presynaptic $GABA_B$ receptors in GABAergic nerve fibres ('autoreceptors'), it is likely to be extremely weak. Furthermore, endogenous zinc concentrations in the synaptic cleft in the mature hippocampal CA3 subfield are probably not high enough to tonically inhibit $GABA_B$ 'autoreceptors'.

Clearly, the interaction of zinc and GABA on the $GABA_B$ receptor is a complex phenomenon dependent on both zinc and agonist concentrations, suggesting that zinc appears to be a weak competitive antagonist acting at the receptor site. This was supported by the observation that an increase in $GABA_B$ receptor activation by baclofen could prevent or block GDPs occurring in both adult and young neurones (Fig. 6.6 and 6.10). Moreover, the inhibition was in a stereoselective manner (cf. Newberry & Nicoll, 1984; Haas et al., 1985). The (+)isomer at a concentration of 2μM had little effect, but the (-)isomer at 0.5-1μM is effective in blocking both spontaneous and evoked GDPs in young CA3 neurones with very small postsynaptic hyperpolarizing responses (Fig. 6.10).

To further determine how zinc inhibits $GABA_B$-mediated responses, the effects of baclofen were compared with serotonin (5-HT), and (±)-8-hydroxy-2-(di-n-propylamino)-tetralin (DPAT), a selective $5\text{-}HT_{1a}$ receptor agonist. 5-HT and DPAT were chosen because $5\text{-}HT_{1a}$ receptors activate a potassium conductance with very similar properties to $GABA_B$ receptors, indeed both receptors are thought to share the same ion channel population (Andrade, Maleka & Nicoll, 1986; Dutar & Nicoll, 1988a). Adult hippocampal CA1 neurones responded to bath-applied 5-HT (10μM) with a membrane hyperpolarization (5-8mV) and conductance increase (Fig. 6.11A), which is mainly mediated by $5\text{-}HT_{1a}$ receptors (Colino & Halliwell, 1987; Dutar & Nicoll, 1988a). This action was resistant to zinc (300μM). During the 5-HT evoked hyperpolarization zinc-induced spontaneous GDPs still occurred, though the frequency of GDPs was slightly reduced (Fig. 6.11A; n=3). Bath application of DPAT (2μM) had a similar but more

pronounced effect on membrane potential and conductance. Again 300μM zinc did not block the DPAT responses, but DPAT markedly decreased the frequency of spontaneous GDPs and IPSPs (Fig. 6.11B; n=3).

5. Comparison of the action of zinc with other $GABA_B$ antagonists

The induction by zinc of spontaneous and evoked GDPs in young and adult hippocampus was possibly due, in part, to an inhibition of $GABA_B$ receptors (Xie & Smart, 1991a). It was therefore, of interest to study whether other proposed $GABA_B$ antagonists could also induce GDPs in pyramidal neurones.

5.1. CGP 35348

Although CGP 35348, at low concentrations (10μM) could increase the release of GABA, manifest by an enhanced monosynaptic $IPSP_B$ following stronger stimulation (Fig. 6.8A), it did not induce any spontaneous GDP- or GHP-like events in adult CA1 or CA3 neurones (n=9). CGP 35348 (10-300μM) had no effects on membrane potentials, input resistance or synaptic 'noise'. At high concentrations (100 - 300μM) CGP 35349 selectively attenuated the slow $GABA_B$-mediated IPSP but it did not reveal a late depolarizing potential (Fig. 6.4), which was consistent with previous studies using other $GABA_B$ antagonists, such as phaclofen, a weaker $GABA_B$ antagonist (Dutar & Nicoll, 1988a), or 2-OH-saclofen, a relatively more potent blocker than phaclofen (Lambert et al., 1989). The specific $GABA_B$ antagonist, CGP 35348 appears to be inert, suggesting the absence of any physiological 'tone' for $GABA_B$ receptor activation in normal neuronal activity in **adult** hippocampus. Indeed, CGP 35348 produced few behavioural changes in normal adult animals at doses which blocked applied baclofen-induced responses *in vivo* (Bittiger et al., 1990; Olpe et al., 1990).

However, when inhibitory synaptic transmission was altered by zinc, manifest by the appearance of GDPs or GHPs in adult neurones, CGP 35348 either slightly prolonged the evoked GDP (Fig. 6.12A) with no effect on the frequency of spontaneous GDPs, or depressed both spontaneous and evoked GHPs (Fig. 6.7). Furthermore, in **immature** CA3 neurones the duration of the evoked innate GDP was also prolonged and the depressant action of baclofen on the evoked GDP was now largely antagonized by CGP 35348

(100μM, Fig. 6.12B, C). These results might suggest the presence of a tonic activation of $GABA_B$ receptors in young neurones.

It was noted that bath application of CGP 35348 (50-200μM) often caused a seizure-like activity in young CA3 neurones (6 out of 8 cells), which was not observed in adult CA3 cells (n=14). Figure 6.13 shows recordings from a P7 CA3 neurone where spontaneous innate GDPs were absent. After bath application of CGP 35348 (100μM) for 10min, only two GDP-like events were seen, but more obviously, a seizure-like discharge occurred. This activity consisted of a sudden depolarization (15-20mV) associated with bursts of action potentials lasting for about 30s followed by an afterhyperpolarization. In contrast, zinc (100μM) induced typical GDPs in the same cell after washout of CGP 35348.

5.2. Barium

Bath application of 300μM Ba^{2+} inhibited a 10μM (-)-baclofen-induced hyperpolarization and conductance increase (Fig. 6.14A), confirming Ba^{2+} inhibition of postsynaptic $GABA_B$-mediated responses (Gähwiler & Brown, 1985). However, Ba^{2+} at this concentration also completely blocked the monosynaptic $GABA_B$-mediated IPSP (n=5). Figure 6.14B illustrates that in the same adult CA3 cell, the duration of the evoked monosynaptic $IPSP_B$ is prolonged by 300μM zinc, but subsequent co-application of 300μM Ba^{2+} reversibly blocked the zinc-enhanced $IPSP_B$. This IPSP was mediated by $GABA_B$ receptors since it was also inhibited by CGP 35348. Taken together with the earlier result that Ba^{2+} (500-1000μM) only induced stimulus-evoked late depolarizing potentials mediated by $GABA_A$ receptors (Fig. 5.3, in Chapter 5), it suggests that the inhibition of $GABA_B$-mediated slow IPSPs probably does not contribute to the generation of spontaneous $GABA_A$-mediated GDPs.

5.3. 4-aminopyidine

Previous studies on the interaction of 4-AP with $GABA_B$-mediated responses have produced conflicting results. Inoue et al, (1985a) showed inwardly rectifying baclofen responses were blocked by 10μM 4-AP, whereas Dutar and Nicoll (1988a) did not find that baclofen responses were sensitive to 4-AP. Moreover, others have reported that 4-AP reveals a novel response to baclofen in the rat interpeduncular nucleus (Docherty &

Halliwell, 1984). Recently two separate groups have reported that 4-AP induces spontaneous and evoked large hyperpolarizing potentials mediated by the release of GABA acting on $GABA_B$ receptors in the neocortex or hippocampus after blockade of $GABA_A$ receptors and excitatory synaptic transmission (Segal, 1990; Aram, Michelson & Wong, 1991). These potentials appear similar to zinc-induced GHPs observed under comparable conditions (Fig. 6.7). 4-AP has also been shown to induce spontaneous and evoked GDP-like events in CA1 neurones (Fig. 3.15, in Chapter 3). Therefore, it was of interest to re-examine whether 4-AP inhibited baclofen responses. Bath application of 4-AP (10-50μM) had little or no inhibitory effect on 10μM baclofen-induced hyperpolarizations in adult CA1 neurones (n=3, not shown), suggesting 4-AP was not an antagonist on postsynaptic $GABA_B$ receptors in this study.

6. β-adrenergic receptors modulate inhibitory synaptic transmission

The appearance of rhythmically occurring spontaneous giant synaptic potentials (GDPs or GHPs) suggested that zinc was capable of inducing interneuronal synchronization in the apparent absence of functional glutamatergic synaptic activity (Fig. 3.10 in Chapter 3 and Fig. 6.7). This raised the possibility that other transmitters might be involved in the activation of GABAergic neurones. It has been observed that noradrenaline increases the amplitude and frequency of spontaneously occurring IPSPs (Madison & Nicoll, 1988). Recently, Andreasen & Lambert (1991) using a combination of CNQX and APV, found that the small 'residual' IPSPs recorded in the CA1 subfield were completely blocked by the adrenergic β-receptor antagonist, L-propranolol, or more effectively by the specific β_1-receptor antagonist, atenolol. These results provided evidence that noradrenergic receptors could modulate GABAergic synaptic transmission in the hippocampus. It was of interest, therefore, to examine whether adrenergic β_1-receptors participate in the regulation of GABAergic synaptic transmission in the presence of zinc. Bath application of atenolol (50μM, n=4) reversibly blocked zinc-induced spontaneous GDPs in the CA1 subfield where glutamatergic transmission was previously blocked by CNQX (20μM), APV (40μM) and 5mM Mg^{2+} (Fig. 6.15A). Furthermore, in the presence of 20μM bicuculline and 40μM picrotoxin to block $GABA_A$

receptors and again in the absence of excitatory synaptic activity, zinc-induced spontaneous GHPs in CA3 neurones were also abolished by 100μM atenolol (Fig. 5.15B).

DISCUSSION

1. $GABA_A$ receptor-mediated responses are enhanced by zinc

Exogenous GABA-evoked responses and the $GABA_A$-mediated IPSP were clearly not blocked by zinc in both young postnatal and adult hippocampal neurones (Fig. 6.1-4). The insensitivity of the $GABA_A$ receptor to zinc in postnatal hippocampus is in complete agreement with results obtained from adult rat sympathetic ganglia (Smart & Constanti, 1982, 1983) and from adult pyramidal neurones in the cortex (Hori et al., 1987; Smart & Constanti, 1983, 1990). Embryonic neuronal GABA responses and $GABA_A$-mediated IPSPs were consistently antagonized by zinc (Westbrook & Mayer, 1987; Mayer & Vyklicky, 1989; Smart & Constanti, 1990), whereas postnatal neuronal responses were insensitive to zinc block or frequently slightly enhanced by zinc (Smart & Constanti, 1990; Xie & Smart, 1991b). This suggested that zinc inhibition of $GABA_A$ receptors was closely correlated with neuronal development (reviewed in Smart, 1990).

The application of cDNA cloning techniques to $GABA_A$ receptors has revealed a number of different protein subunits (defined as α, β, γ, δ and ρ) which can be subdivided into numerous subtypes (Levitan et al., 1988; Olsen & Tobin, 1990; Verdoorn et al., 1990). The developmental aspect of $GABA_A$ receptor pharmacology, revealed by zinc, was possibly due to different populations of $GABA_A$ receptors existing in embryonic and postnatal neurones, some sensitive and others insensitive to zinc inhibition. By using recombinant GABA receptors expressed in cell lines (Draguhn et al., 1990; Smart et al., 1991) or *Xenopus* oocytes (Krishek, personal communication), receptors composed of α and β subunits were sensitive to zinc inhibition whereas α, β and γ containing receptors were relatively insensitive. On this basis, it would seem that the zinc-induced GDPs recorded in hippocampal neurones are probably mediated by $GABA_A$ receptors containing at least one or more γ subunits.

GABA-responses evoked by ionophoresis on hippocampal neurones (mainly affecting dendrites) were more obviously augmented by zinc compared to bath-applied

GABA responses. Zinc appeared to have no effect on $GABA_A$ receptor affinity (Fig. 6.3), supporting the notion that the zinc enhancement may be mainly due to an increase in the input resistance. Since the reduction of the leak conductance located on dendritic membranes will allow a greater proportion of the dendritic GABA depolarizing response to be resolved back in the soma, where the recording was made. Such an effect could be reproduced by Ba^{2+} and Cd^{2+}, which also reduced leak conductances (Smart & Constanti, 1990). In addition, zinc-induced GDPs, mediated by $GABA_A$ receptors in adult neurones were further enhanced by pentobarbitone and flurazepam (Fig. 3.12, in Chapter 3) suggesting that zinc enhances GABA responses probably not by acting at the modulatory sites for barbiturates or benzodiazepines (Smart, 1992).

2. Paradoxical inhibition of $GABA_B$ receptors by zinc

In contrast to $GABA_A$ receptors, postnatal $GABA_B$ receptors in hippocampal neurones were sensitive to zinc. Divalent cations are known to form complexes with suitable ligands, particularly amino acids (Crawford & McBurney, 1977). However, zinc inhibition of responses to baclofen is probably mediated at the receptor level and not due to complexation of the agonist since zinc also antagonized GABA-evoked, bicuculline-resistant responses (Fig. 6.7).

The following observation further supported the notion that zinc inhibits postsynaptic $GABA_B$ responses acting on receptor sites, rather than affecting the receptor-coupled K^+ channels. (i) Zinc had little effect on 5-HT and DPAT-induced responses, which are mediated by $5\text{-}HT_{1a}$ receptors coupling to the same K^+ channels as $GABA_B$ receptors. (ii) Zinc mimicked the effect of CGP 35348, a recognized competitive antagonist. At low concentrations (50-300μM), zinc enhanced monosynaptic $GABA_B$-mediated IPSPs and at higher concentrations (300-1000μM) depressed these previously enhanced synaptic potentials. In contrast, Ba^{2+}, presumably acting directly on the K^+ channel, always blocked the $IPSP_B$s. (iii) Activation of $GABA_B$ receptors with a specific agonist, such as baclofen, could abolish the induction of GDPs by zinc. Moreover, the (-)isomer of baclofen was much more potent in this respect than the (+)isomer, or 5-HT or DPAT in adult hippocampal neurones. Activation of $5\text{-}HT_{1a}$ receptors with 5-HT, or more specifically with DPAT (2μM) slightly reduced the frequency of spontaneous GDPs

induced by 300μM zinc in adult hippocampus. This raised the possibility that 5-HT_{1a} receptor activation may directly or indirectly inhibit the release of GABA, since it is unlikely that the reduction of zinc-induced GDPs results solely from a chemical interaction between the ligand and zinc. Also zinc did not affect the 5-$HT1_a$ receptor-mediated hyperpolarization of the membrane potential.

Furthermore, γ-hydroxybutyrate, an analogue of GABA (Vayer, Mandel & Maitre, 1987) caused a membrane hyperpolarization in hippocampal neurones via the activation of $GABA_B$ receptors, which is also inhibited by zinc (Xie & Smart, 1992).

However, the effects of zinc on $GABA_B$ receptors are very complex. Zinc (50-300μM) consistently inhibited the postsynaptic effects of baclofen on young and adult pyramidal neurones. On the other hand, zinc could induce spontaneous and evoked GHPs mediated by $GABA_B$ receptors in the presence of high concentrations of bicuculline (20) or a combination of bicuculline with picrotoxin (40μM). The zinc-induced GDPs mediated by $GABA_A$ receptors were readily blocked by 10μM bicuculline (see Fig. 3.11, Chapter 3), but this did not reveal the underlying giant hyperpolarizing potential and may be due to incomplete blockade of $GABA_A$ activation. The monosynaptic $IPSP_B$ was always blocked by barium, but the effects of zinc was variable with some $IPSP_BS$ initially being enhanced by 50-300μM zinc and eventually slightly inhibited by 300-1000μM. This apparent paradoxical effect of zinc on the $GABA_B$ postsynaptic responses and $GABA_B$-mediated IPSPs may be due to higher concentrations of GABA in the synaptic cleft overcoming the zinc inhibition.

The existence of presynaptic $GABA_B$ autoreceptors on GABAergic terminals is suggested by neurochemical studies in brain slices showing $GABA_B$ agonists, such as baclofen decreasing GABA release (Pittaluga et al., 1987; Bonanno et al., 1989). Evidence from electrophysiological studies also suggests GABA-releasing terminals possess $GABA_B$ receptors and GABA acts as a negative feedback on its own release via an action at these 'autoreceptors' (Davies, Davies & Collingridge, 1990). Furthermore, these 'autoreceptors' are sensitive to $GABA_B$ antagonists, including phacolofen, 2-OH-saclofen and CGP 35348 (Harrison, 1990; Harrison, Lambert & Lovinger, 1990; Davies, Davies & Collingridge, 1990; Calabresi et al., 1991; Thompson & Gähwiler, 1992). Zinc probably has little effect at presynaptic $GABA_B$ 'autoreceptors'. An increase in GABA release in the presence of zinc was manifest by the enhancement of the $GABA_A$-mediated

fast IPSP (Fig. 6.4), but zinc failed to significantly reduce the paired-pulse depression of $IPSP_B$s suggesting no presynaptic $GABA_B$ blocking action. Since zinc consistently inhibited (but did not completely block) postsynaptic $GABA_B$ receptor activation, the induction of spontaneous and evoked large $GABA_B$-mediated potentials could only result from an increased and/or synchronized release of GABA. This effect is unlikely to involve an inhibition of presynaptic $GABA_B$ receptors, but the involvement of other neurotransmitters (such as noradrenaline) to increase the release of GABA should not be discounted (*vide infra*).

3. Mechanisms of zinc-induced giant synaptic potentials

The large amplitude of the spontaneous or evoked GABA-mediated synaptic potentials induced by zinc suggested that an increased level of transmitter release was responsible. It is more likely that the generation of rhythmically occurring events required the synchronized activity of a population of GABAergic neurones since the long variable latency of these potentials may represent the time required for a synchronization process to develop (cf. Aram, Michelson & Wong, 1991).

Zinc has many actions in blocking voltage-activated potassium currents (see Chapter 5, cf. Constanti & Smart, 1987; Mayer & Vyklicky, 1989; Sim & Cherubini, 1990) which could result in an increased transmitter release. One possibility would be for zinc to inhibit a variety of potassium channels in the presynaptic nerve terminal which could broaden the duration of the presynaptic action potential and therefore increase the release of GABA. However, 4-AP, a well known A-current blocker, enhances the release of excitatory amino acids in addition to generating GDP-like events (see Chapter 3; see also Buckle & Haas, 1982; Ives & Jefferys, 1990). In contrast, the effect of zinc seems to result in an apparently specific increase in the release of GABA, presumably from interneurones, since bicuculline abolished the vast majority of synaptic potentials. Furthermore, other divalent and trivalent cations, which can interact with a number of voltage-sensitive ion channels and Ca^{2+}-dependent K^+ channels, do not reproduce the action of zinc in generation of GDPs (see Chapter 5). Whether zinc has any specific effect on presynaptic calcium channels in GABAergic nerve fibre terminals remains to be established, although on postsynaptic pyramidal neurones, or myotubes, zinc blocked

calcium channels (Sim & Cherubini, 1990; Winegar & Lansman, 1990). However, a similar effect on GABAergic neurones would be expected to decrease transmitter release.

The action of zinc inhibiting $GABA_B$ receptors and enhancing postsynaptic $GABA_A$-mediated responses could provide an alternative explanation for the mechanism underlying GDP generation. First, a depressant action of zinc at postsynaptic $GABA_B$ sites would remove the overlying $GABA_B$-mediated hyperpolarizing slow IPSP, which might obscure the latent $GABA_A$-mediated depolarizing potential. This was supported by the following observation. Intracellular injection of GTP-γ-s into the recorded single neurone inhibits the G-protein to which $GABA_B$ receptors are coupled and also revealed the $GABA_A$ receptor-mediated GDP (Thalmann, 1988). Secondly, zinc enhancing postsynaptic $GABA_A$ responses would enable responses generated in distal parts of the cell (i.e. dendrites) to be resolved back at the somatic recording site. Barium which inhibited $GABA_B$-mediated responses (Fig. 6.14; cf. Gähwiler & Brown, 1985) and enhanced postsynaptic $GABA_A$ responses (Smart & Constanti, 1990) also partly reproduced the effects of zinc (see Chapter 5). However, the specific competitive $GABA_B$ antagonist, CGP 35348 was ineffective in the generation of GDPs (see also Lambert, Levitin & Harrison, 1992). Whether this is due to a lack of ability to potentiate postsynaptic $GABA_A$-mediated responses is presently unclear. The conclusion from these studies is that blockade of $GABA_B$ receptors by zinc is unlikely to be the sole mechanism of inducing GDPs.

The zinc-induced GDP events clearly were not sustained by glutamatergic transmission, because they could be recorded in the presence of EAA receptor antagonists, which were sufficient to block evoked EPSPs and bath-applied EAA agonist responses (*vide infra*, Chapter 7). Recently, it has been reported that GABAergic synaptic **excitation** mediated by $GABA_A$ receptors synchronized the activity of inhibitory interneurones in the presence of 4-AP (Michelson & Wong, 1991). Zinc-induced interneuronal synchronization in the apparent absence of any glutamatergic transmission could possibly be mediated by the recurrent connections of these neurones using $GABA_A$ receptors. However, in the presence of $GABA_A$ antagonists and EAA blockers, zinc still induced the appearance of large synaptic potentials mediated by GABA acting on $GABA_B$ receptors. Under a comparable condition, 4-AP also induced similar potentials (Segal, 1990; Aram, Michelson & Wong, 1991).

The demonstration that the β_1-antagonist, atenolol reversibly inhibited GABA-mediated giant synaptic potentials induced by zinc not only confirmed that catecholaminergic receptors participate in the regulation of GABAergic inhibition (Andreasen & Lambert, 1991) but also suggests that zinc may enhance noradrenergic transmission which may underlie the synchronized release of GABA.

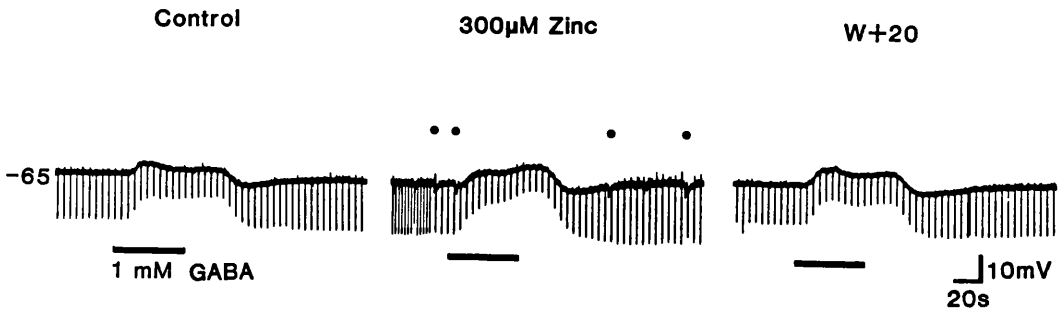

Fig. 6.1. Effect of zinc on GABA-evoked depolarizations in adult hippocampal CA1 neurones. Bath-applied GABA (1mM, solid bars) induced depolarizing responses in the presence and absence of 300µM zinc. Hyperpolarizing electrotonic potentials (-0.3nA, 300ms, 0.3Hz) were used to monitor membrane resistance. Note that zinc-induced spontaneous GDPs (●) are small in amplitudes when using a 4 M K acetate-filled microelectrode. Resting potential -73mV.

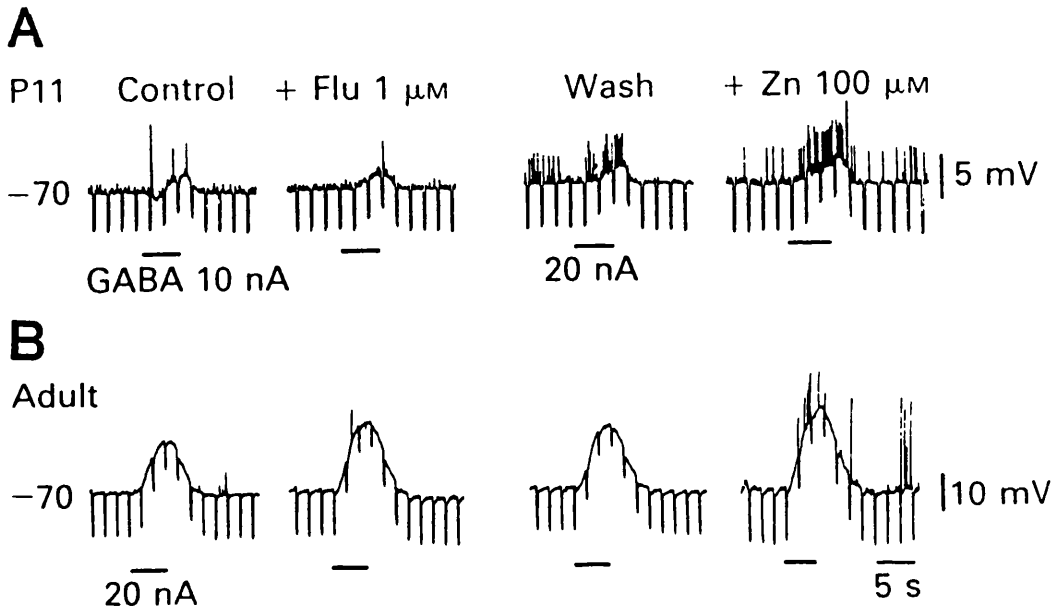

Fig. 6.2. Comparison of zinc and flurazepam effects on GABA-responses in young and adult hippocampal CA3 neurones. Ionophoretically-applied GABA (1M, ejection current 10-20nA, holding current -10nA) to the apical dendrites of young postnatal (P11, **A**) and adult (**B**) CA3 neurones. Flurazepam (Flu, 1μM) and zinc (100μM) were bath-applied. Hyperpolarizing current pulses (-0.4nA; 300ms; 0.5Hz) were applied throughout. Membrane potential adjusted to -70mV. Note Flu produced a clear enhanced GABA response only in the adult neurone and zinc was ineffective as a GABA antagonist in slices of either age.

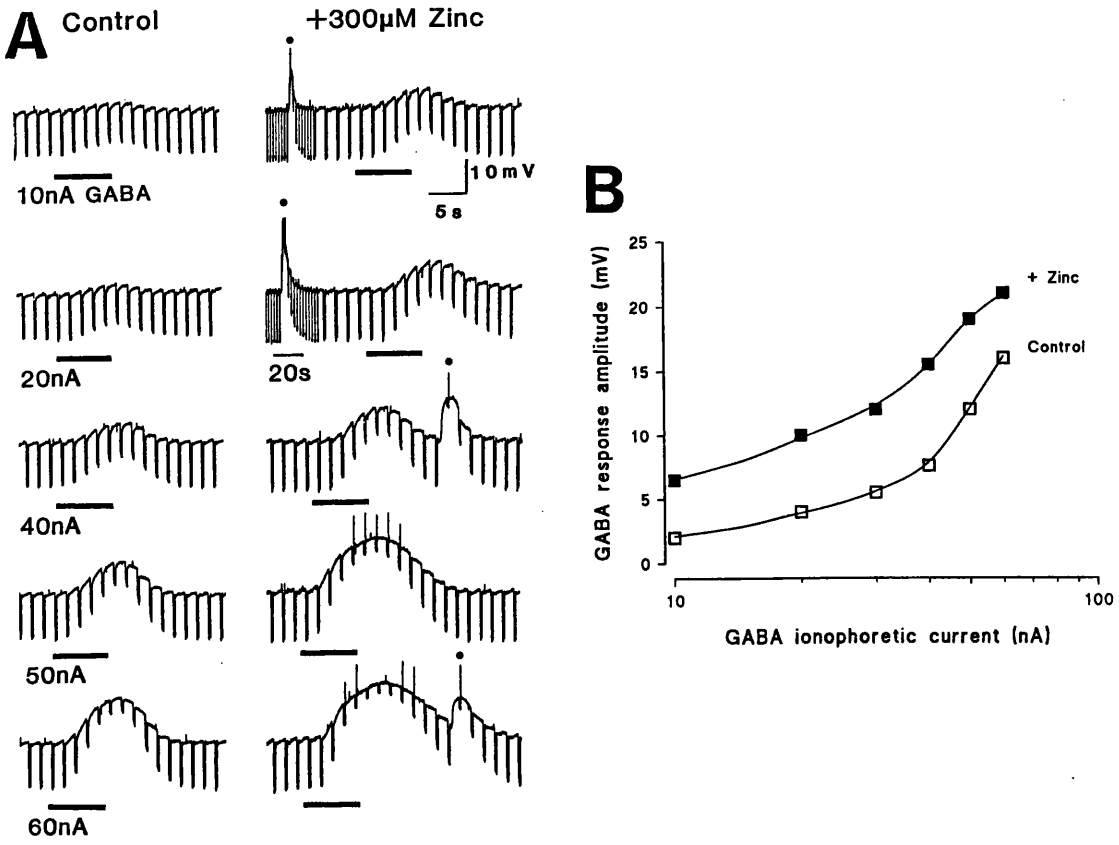

Fig. 6.3. GABA induced dose-responses in an adult CA1 neurone in the presence and absence of zinc. **A**, Ionophoretic application of GABA (1M) to the dendrites of a CA1 neurone using different ejection currents (holding current -10nA). Hyperpolarizing current pulses (-0.5nA; 300ms; 0.5Hz) monitored membrane resistance. Note the appearance of GDPs following the addition of 300μM zinc in the right column (●). Membrane potential -68mV. **B**, peak amplitudes of GABA-responses were plotted against ionophoretic currents in the presence and absence of zinc, data taken from A.

Fig. 6.4. Zinc does not inhibit the $GABA_A$-mediated fast IPSP. Synaptic responses were recorded from a CA3 neurone following stimulation of the mossy fibres (45V, 0.1ms, 1 pulse per 90s) and using a synaptic current analysis program (SCAN, version 3.0).
A, The control stimulation evoked an EPSP followed by fast and slow IPSPs (arrows). **B**, After incubating in 100μM CGP 35348 for 2min, the slow IPSP was reduced. **C**, The addition of 300μM zinc for 4min enhanced the fast IPSP and also revealed a late depolarizing potential (GDP). **D**, Traces B and C are superimposed for clarity indicating the larger fast IPSP. **E**, Both the fast IPSP and GDP in the presence of zinc were blocked by 20μM bicuculline (BIC). Note two spikes are superimposed on the EPSP in the presence of BIC. Resting membrane potential was -64mV using a 4 M K acetate-filled microelectrode.

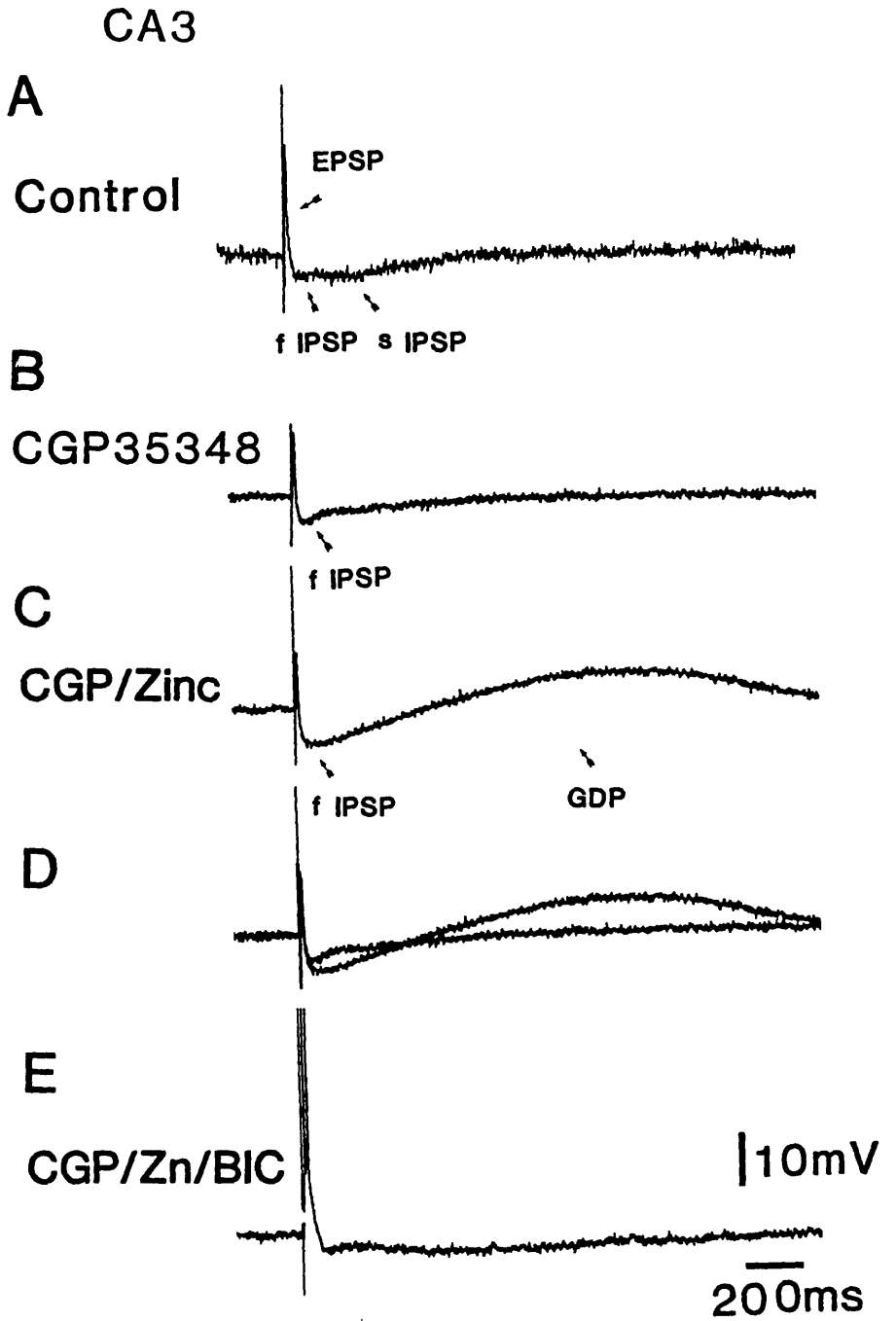
CA3
A
Control
EPSP
f IPSP
s IPSP
B
CGP35348
f IPSP
C
CGP/Zinc
f IPSP
GDP
D
E
CGP/Zn/BIC
10mV
200ms

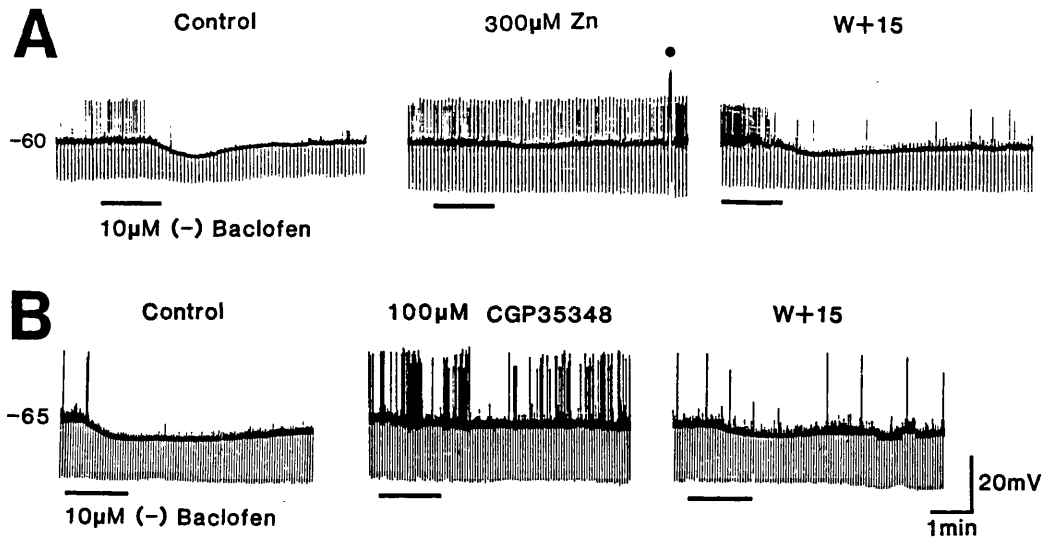

Fig. 6.5. Comparison of the effects of zinc and CGP 35348 on baclofen-evoked responses in CA1 neurones. **A**, Chart records of 10μM (-)-baclofen induced responses before, during (for 5min) and after 300μM-zinc application (washing for 15min, W+15). Downward deflections are hyperpolarizing electrotonic potentials (-0.3nA, 300ms, 0.3Hz) and upward deflections are spontaneous action potentials and anode-break spikes. Membrane potential -60mV maintained with DC current injection. The filled circle indicates a GDP induced by zinc. **B**, Recording from another neurone, (-)-baclofen (10μM) responses in the presence and absence of 100μM CGP 35348. Resting membrane potential -65mV.

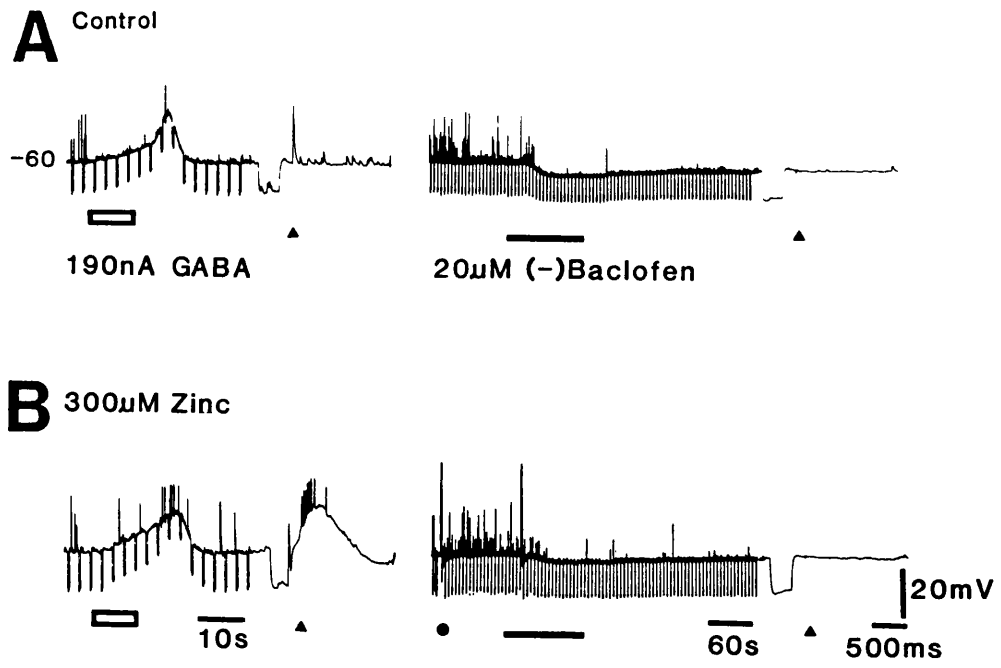

Fig. 6.6. Differential effect of zinc on $GABA_A$ and $GABA_B$-mediated responses in the same neurone. **A** illustrates ionophoretic application of GABA (1M, 190nA; open bar) to the dendrites of a CA1 neurone. A synaptic potential was evoked by stimulation of the Schaffer collateral pathway (▲, 10V, 0.1ms) and (-)-baclofen (20μM, solid bar) was bath applied in control Krebs. **B**, In the presence of 300μM zinc, GABA-responses were slightly enhanced, and stimulation now evoked a GDP (▲), but the baclofen responses were inhibited. Note the appearance of spontaneous GDPs (●) in zinc, and that the spontaneous and evoked GDP were blocked by baclofen even in the presence of zinc. Hyperpolarizing current pulses (-0.5nA, 300ms, 0.3-0.5Hz) were applied to monitor membrane resistance. Membrane potential -60mV.

Fig. 6.7. Zinc induces spontaneous and evoked giant hyperpolarizing potentials (GHPs) in adult CA3 neurones after blockade of $GABA_A$ receptors and excitatory synaptic transmission. Chart records of a CA3 neurone at a membrane potential of -70mV (with DC current injection), superfused with Krebs solution containing 20μM CNQX, 40μM APV, 20μM bicuculline and 40μM picrotoxin to block EPSPs and $GABA_A$-mediated fast IPSPs. Localized stimulation (▲, 37V, 0.1ms) was applied in stratum radiatum (stimulation electrodes placed approximately < 0.5mm to the recording site). **A** illustrates resting potential and an evoked monosynaptic $GABA_B$-mediated IPSP ($IPSP_B$; ▲). Bath-applied 300μM zinc (open triangle) induced the appearance of spontaneous (●) and evoked (▲) GHPs, which were resistant to co-applied 100μM CGP 35348 (open bar), but eventually blocked by 300μM CGP 35348 (solid bar). **B** illustrates evoked synaptic responses in control, during zinc, zinc plus 100μM CGP 35348 and zinc plus 300μM CGP 35348 on an expanded timescale, selected from trace A as denoted by ▲. Note in the presence of zinc, synaptic responses were biphasic, the early component corresponded to the initial $IPSP_B$ (arrow) which was slightly depressed by zinc and more obviously inhibited in zinc plus 100μM CGP 35348. **C**, Two spontaneous GHPs were selected from trace A as denoted by ● during zinc alone and zinc plus 100μM CGP 35348 on an expanded timescale.

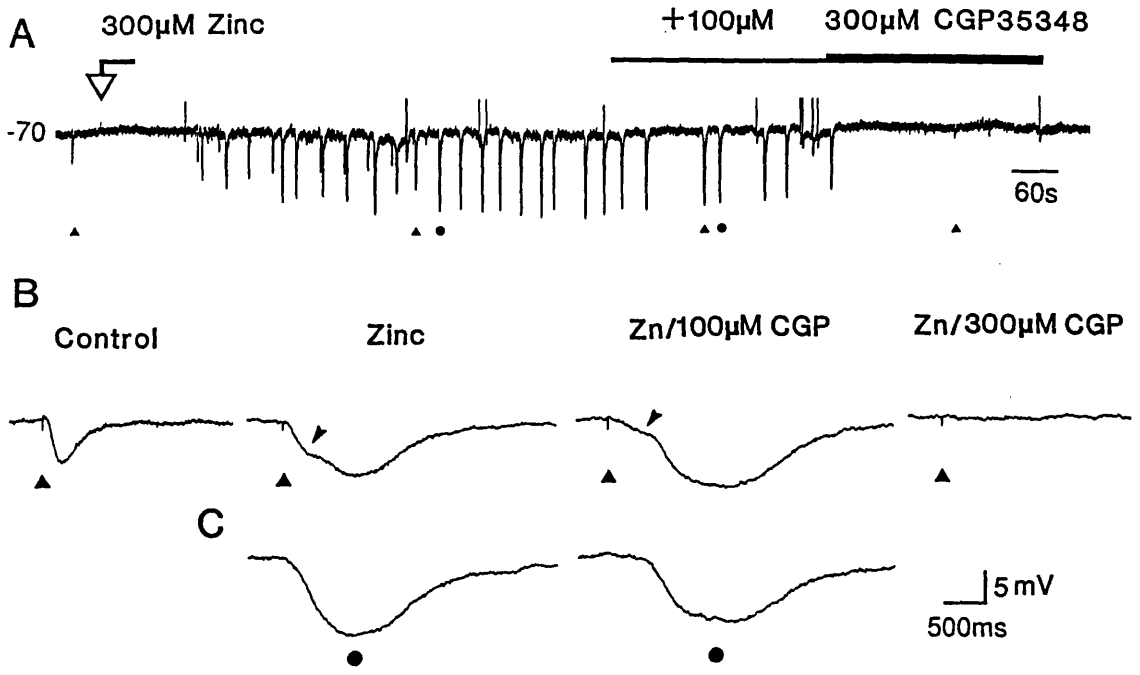
A
300µM Zinc
+100µM
300µM CGP35348
-70
60s
B
Control
Zinc
Zn/100µM CGP
Zn/300µM CGP
C
5 mV
500ms

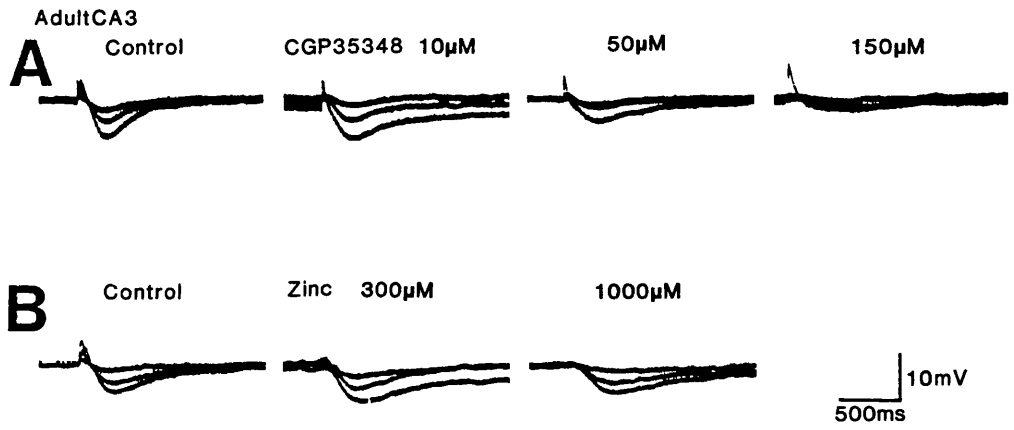

Fig. 6.8. Paradoxical effects of CGP 35348 and zinc on monosynaptic $GABA_B$-mediated IPSPs ($IPSP_B$) in adult CA3 neurones. Slices were perfused with Krebs containing 20μM CNQX, 40μM APV, 20μM bicuculline and 40μM picrotoxin, to block EPSPs and fast $GABA_A$-mediated IPSPs. Localized stimulation at three intensities, 10, 15, and 20V, (0.1ms-duration, 1 pulse per 30s) was applied to the stratum radiatum. **A**, Three superimposed evoked $IPSP_B$s were recorded in control, 10μM, 50μM, and 150μM CGP 35348, respectively. **B**, In a different cell, superimposed $IPSP_B$s were recorded in control, 300μM and 1000μM zinc respectively. Membrane potentials for these two cells were adjusted with DC current injection to -65mV.

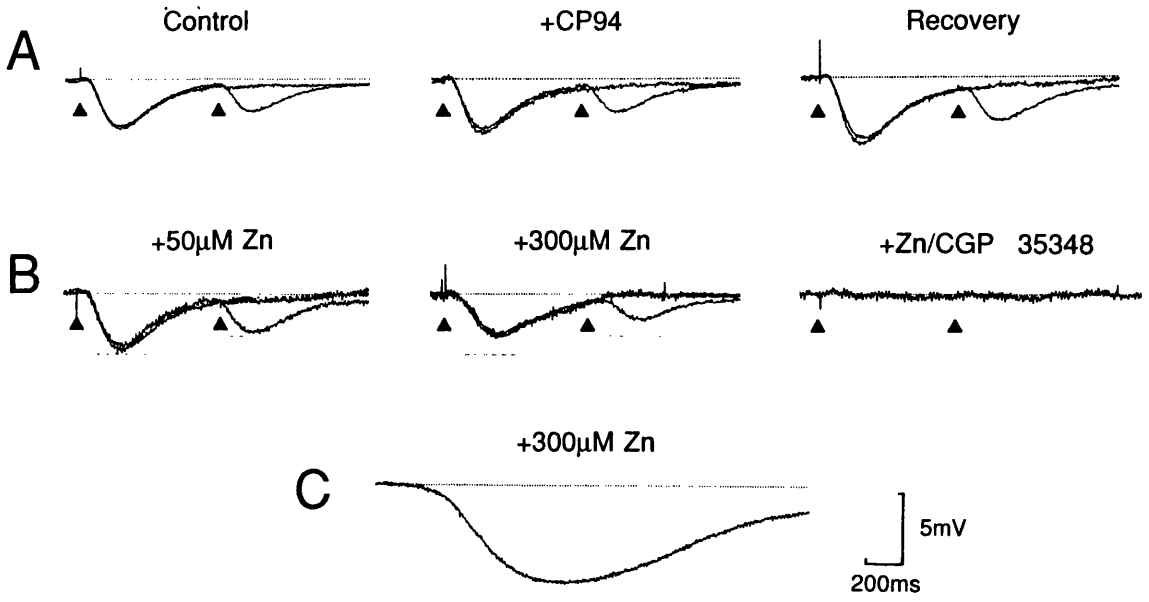

Fig. 6.9. Zinc effect on paired-pulse depression of monosynaptic $GABA_B$-mediated IPSPs in adult CA3 neurones. The brain slice was superfused with Krebs containing 20μM CNQX, 40μM APV, 20μM bicuculline and 40μM picrotoxin to block EPSPs and fast $GABA_A$-mediated IPSPs. Localized stimulation (stimulation electrode placed in stratum lucidum close to the recording site <0.5mm) consisted of a paired-pulse (▲, 15V, 0.1ms, stimulus interval 800ms) and then after a further interval of 30s an equivalent 'recovery' single pulse stimulus. The paired-pulse traces were superimposed upon single-shock responses using a synaptic current analysis program (SCAN, version 3.0). The amplitudes of the first $IPSP_B$ was measured from the peak to the baseline (dotted lines) and the second $IPSP_B$ amplitude was measured from the peak to the decaying tail of the single $IPSP_B$. **A**, Paired-pulse evoked $IPSP_B$s in control, 400μM CP94 (bath-applied for 10min) and recovery (after removal the chelator for 20min). **B**, In the same neurone, 50 and 300μM zinc caused a small depression in both the single and paired $IPSP_B$s with slightly reduced the depression of the second $IPSP_B$. The broken lines indicate the control $IPSP_B$ amplitudes. Both $IPSP_B$s were blocked in 300μM CGP 35348. **C**, Although zinc reduced the amplitude of the evoked $IPSP_B$s, this concentration induced spontaneous GHPs which were also blocked by CGP 35348. Resting membrane potential -67mV.

Fig. 6.10. Comparison of the effects of (+) and (-) isomers of baclofen on spontaneous and evoked GDPs in young CA3 neurones. Chart records from a P5 CA3 neurone exhibit naturally occurring spontaneous GDPs and evoked GDPs following mossy fibre stimulation (▲, 8V, 0.1ms). **A**, Bath-applied (+)-baclofen (2μM) had little effect on the GDPs. Three evoked GDPs taken before, during and after (+)-baclofen application are shown on an expanded timescale (lower traces). **B**, (-)-baclofen (1μM) blocked spontaneous and evoked GDPs in the same cell. Resting membrane potential -65mV. Hyperpolarizing electrotonic potentials were evoked by -0.3nA, 300ms, 0.3Hz current pulses.

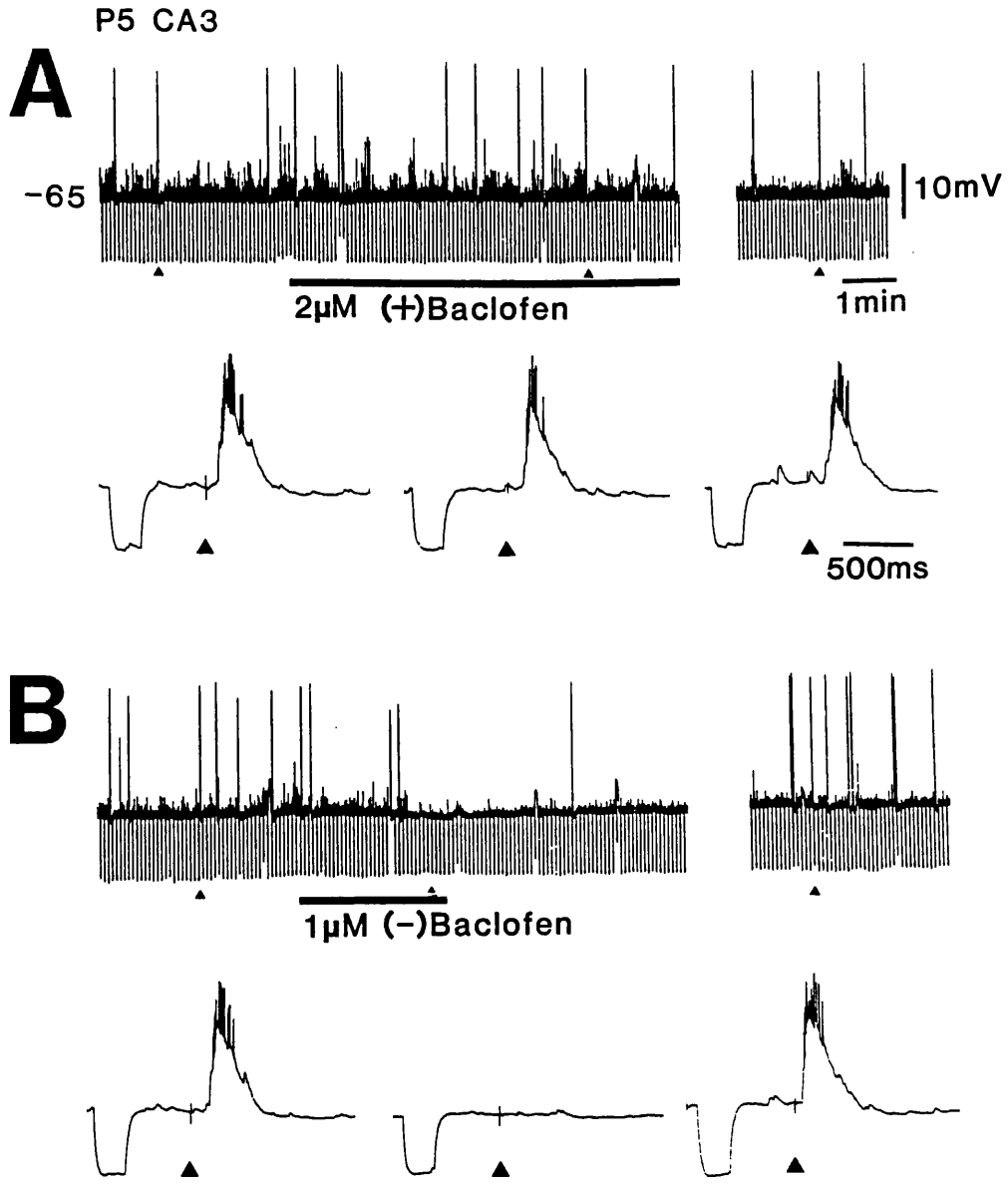
P5 CA3
A
-65
10mV
2μM (+)Baclofen
1min
500ms
B
1μM (−)Baclofen

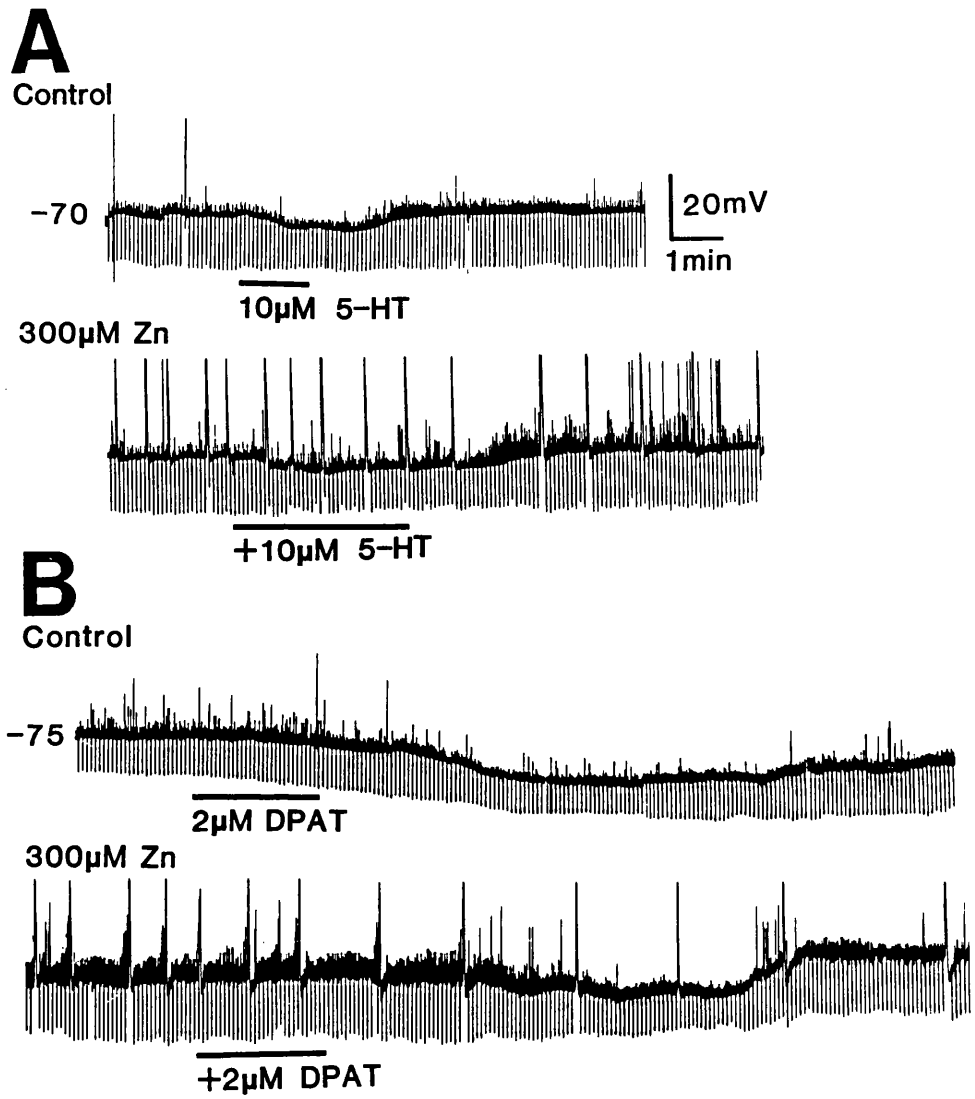

Fig. 6.11. Effects of 5-hydroxytryptamine (5-HT) and (±)-8-hydroxy-2-(di-npropylamino)-tetralin (DPAT) on zinc-induced spontaneous GDPs in adult hippocampus. **A**, Chart records from a CA1 neurone at membrane potential of -70mV (adjusted with DC current injection) with superimposed hyperpolarizing electrotonic potentials evoked by -0.4nA, 300ms, 0.3Hz current pulses. Bath-applied 10 μM 5-HT (solid line) induced a hyperpolarization in the absence (upper trace) and presence of 300μM zinc (lower trace). Note zinc induced the appearance of spontaneous GDPs. **B**, In a different CA1 cell, 2μM DPAT induced a hyperpolarization in the absence (upper trace) and presence of 300μM zinc (lower trace). Note DPAT more clearly reduced the frequency of zinc-induced spontaneous GDPs. Resting membrane potential -75mV.

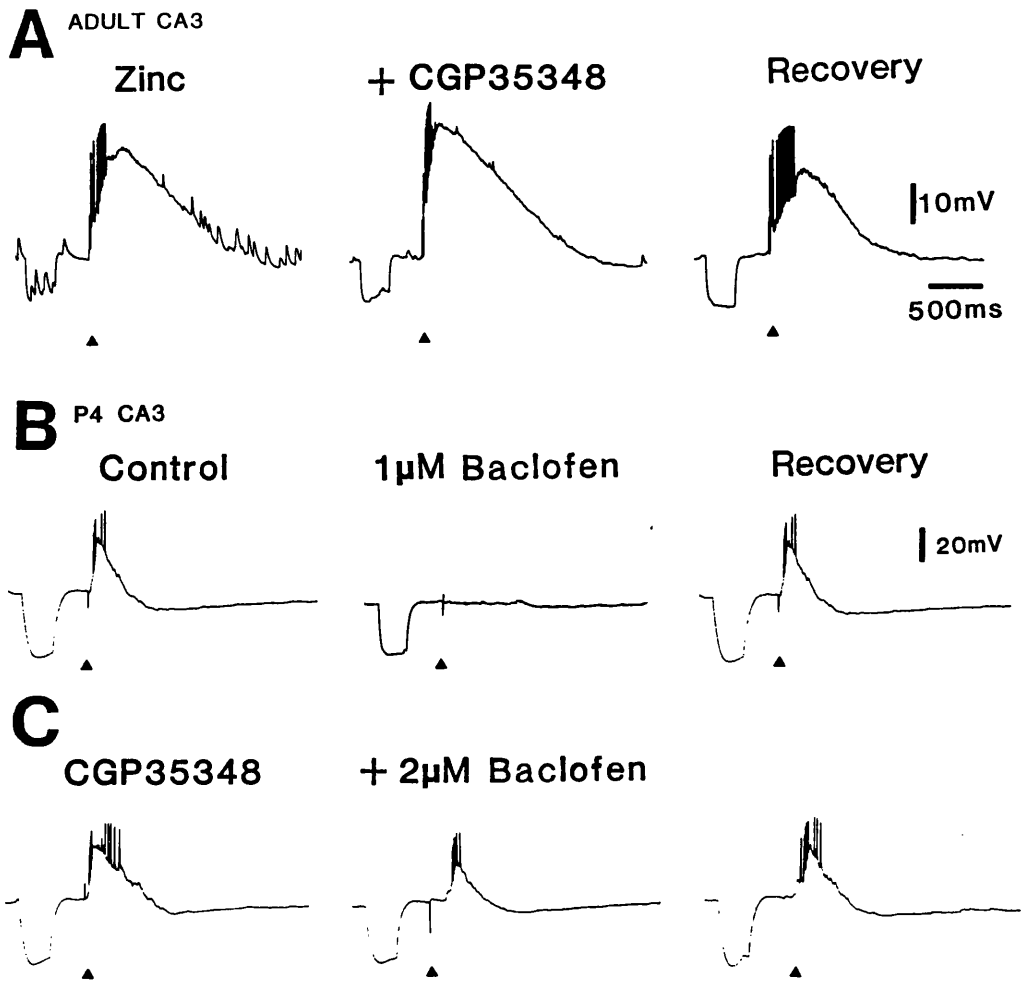

Fig. 6.12. Effects of CGP 35348 on zinc-induced GDPs in adult slices and innate GDPs in the young hippocampus. **A**, Chart records of three evoked GDPs induced by 300μM zinc in an adult CA3 cell following stimulation of the mossy fibres (▲, 10V, 0.1ms, 1 pulse per 90s) taken before, during and after applying 100μM CGP 35348. Membrane potential -70mV. **B**, Records from a young, P4 CA3 neurone. Bath-applied (-)-baclofen (1μM) reversibly blocked the innate GDP evoked by stimulation of the mossy fibre pathway (▲, 5V, 60μs, 1 pulse per 30s). **C**, In the same young neurone, after washing baclofen for 15-min, bath application of 100μM CGP 35348 slightly prolonged the evoked GDP and antagonized the blockade by baclofen (2μM). Resting membrane potential was -66mV. Hyperpolarizing electrotonic potentials (-0.3nA, 300ms) were used to monitor membrane resistance. Time calibration in A applies to B and C.

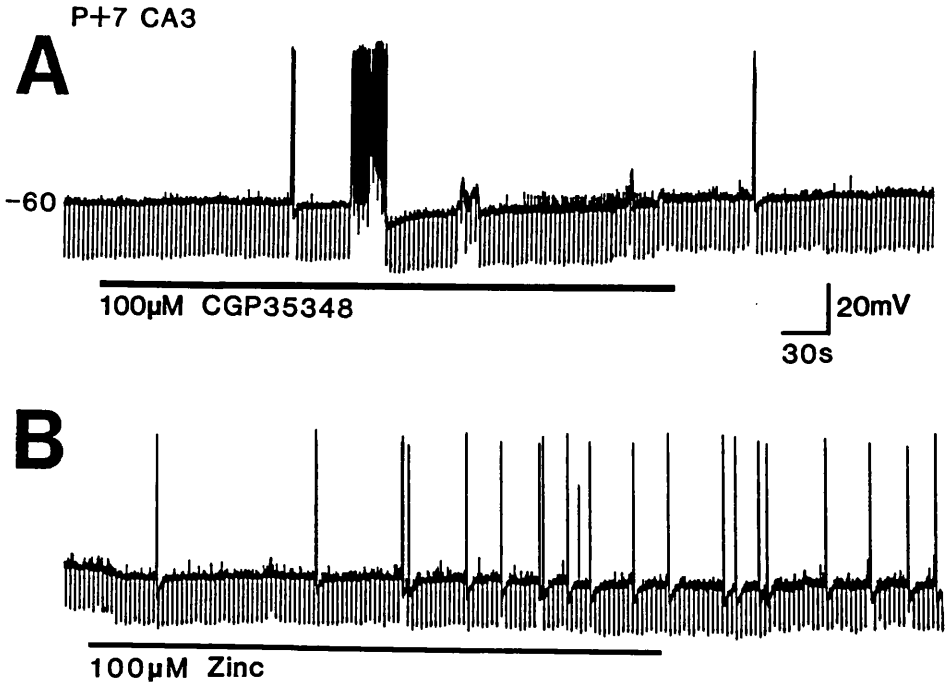

Fig. 6.13. Comparison of the effects of CGP 35348 and zinc on young CA3 neurones. **A**, Chart record of a P7 neurone which did not initially exhibit any spontaneous GDPs, bath application of 100μM CGP 35348 for 10-min induced two GDP-like events and a seizure-like discharge consisting of a sudden depolarization (15-20mV) associated with bursts of action potentials lasting for approximately 30s and followed by an afterhyperpolarization (-8mV amplitude). **B**, In the same cell, after washing CGP 35348 for 15-min, bath-applied 100μM zinc (solid line) induced a high frequency of spontaneous GDPs (upward deflections), which did not disappear after washout of zinc for 20min. Membrane potential was adjusted to -60mV with DC current injection, and superimposed hyperpolarizing electrotonic potentials evoked by -0.3nA, 300ms, 0.3Hz current pulses.

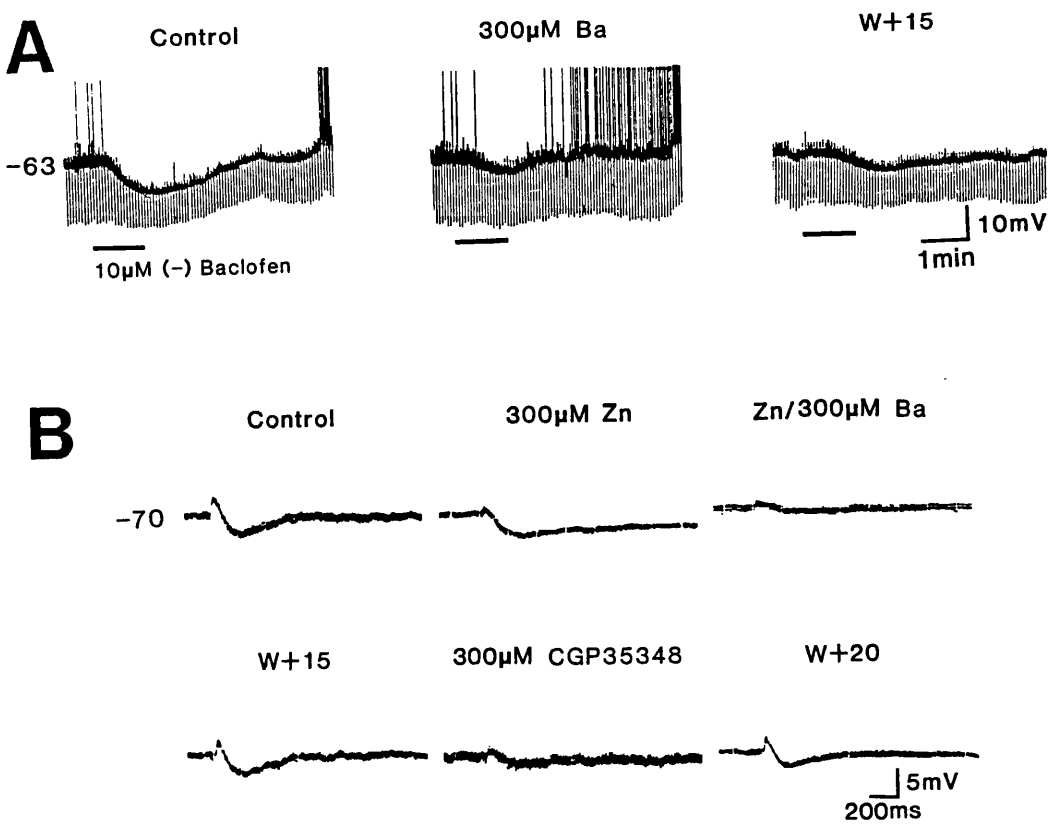

Fig. 6.14. Effect of Ba^{2+} on baclofen-induced responses and monosynaptic $GABA_B$-mediated IPSPs in adult neurones. **A**, Chart records of a CA1 neurone responded to 10μM (-)-baclofen responses before, during and after 300μM-Ba^{2+} application (washing for 15min, W+15). Downward deflections are hyperpolarizing electrotonic potentials (-0.3nA, 300ms, 0.3Hz) and upward deflections are spontaneous action potentials and anode-break spikes. Membrane potential -63mV (with DC current injection). **B**, Effects of Ba^{2+}, zinc and CGP 35348 on monosynaptic $GABA_B$-mediated IPSPs ($IPSP_B$s) in adult CA3 neurones. Slices were perfused with Krebs containing 20μM CNQX, 40μM APV, 20μM bicuculline and 40μM picrotoxin. Localized stimulation (20V, 0.1ms, 1 pulse per 30s) was applied to the stratum radiatum. Bath-applied 300μM zinc prolonged the $IPSP_B$, which was subsequently blocked by the co-application of 300μM Ba^{2+} (upper traces). After washing zinc and Ba^{2+} for 15-min (W+15), the recovered $IPSP_B$ was reversibly inhibited by 300μM CGP 35348. Resting membrane potential -65mV.

Fig. 6.15. Spontaneous GABA-mediated giant synaptic potentials induced by zinc are blocked by the β1-adrenergic antagonist, atenolol. **A**, Chart records of an adult CA1 neurone at the resting membrane potential of -67mV with superimposed hyperpolarizing electrotonic potentials evoked by current injection (-0.4nA, 300ms, 0.2 Hz). In a Krebs solution containing 20μM CNQX, 40μM APV and 5mM Mg^{2+}, bath-applied 300μM zinc (throughout the experiment) induced spontaneous GDPs (upward deflections; upper trace). Co-application of 50μM atenolol (solid line) abolished the GDPs. A partial recovery was obtained after washing with zinc-containing Krebs for 10 min (W+ 10; lower trace). **B**, Chart records of a CA3 neurone at the resting membrane potential of -72mV superfused with a Krebs solution containing 20μM bicuculline, 40μM picrotoxin, 20μM CNQX and 40μM APV. 500μM zinc (also bath-applied throughout the experiment) induced spontaneous GHPs (upper trace). Co-application of 100μM atenolol (solid line) blocked the GHPs which did not recover after washing with zinc-containig Krebs for 10min (lower trace).

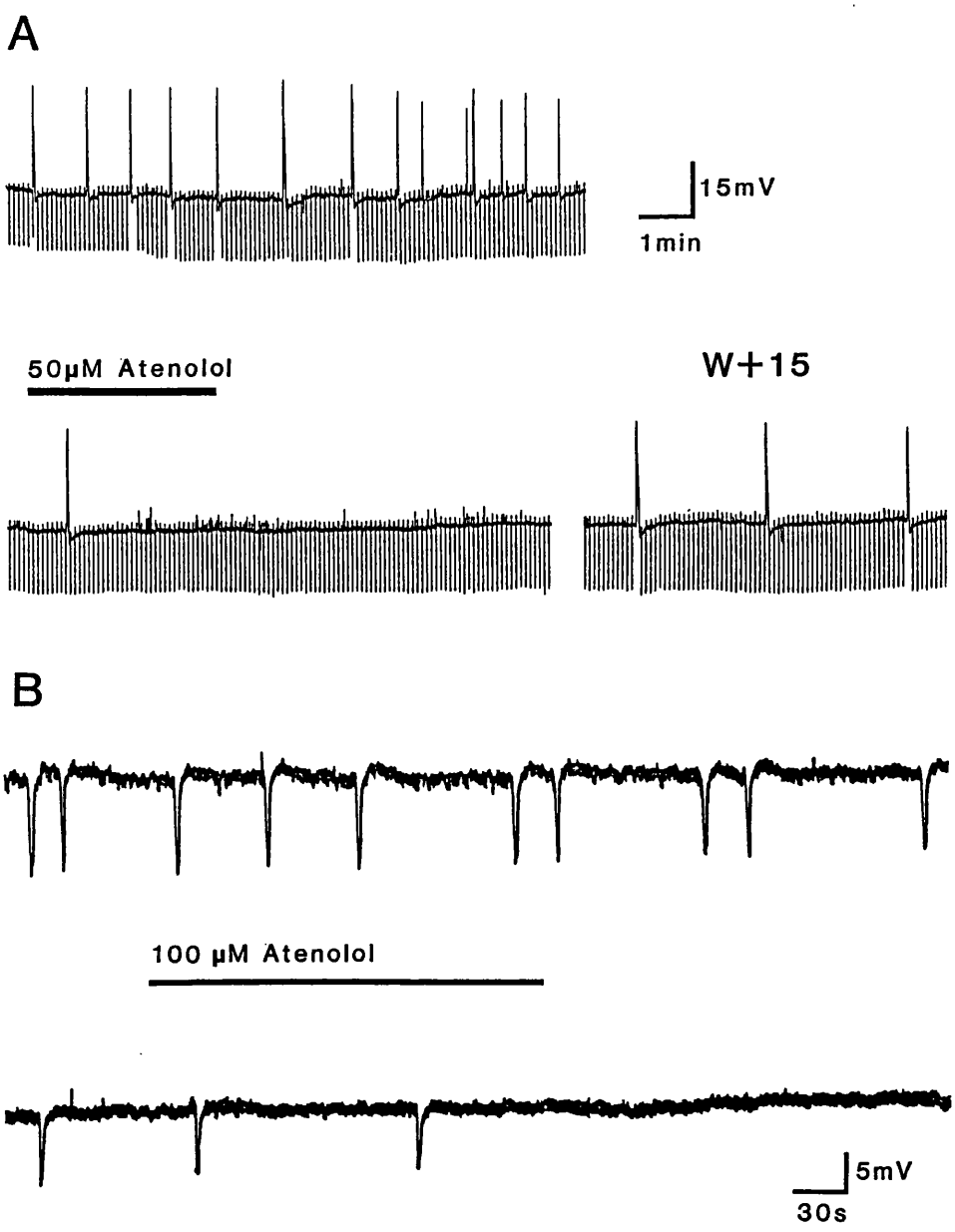
A
15mV
1min
50μM Atenolol
W+15
B
100 μM Atenolol
5mV
30s

Chapter 7

ACTION OF ZINC ON EXCITATORY AMINO ACID RECEPTORS AND EXCITATORY SYNAPTIC TRANSMISSION

INTRODUCTION

Excitatory amino acids (EAA, mainly L-glutamic acid) mediate synaptic transmission and regulate synaptic plasticity in the CNS via the activation of at least two groups of receptors, ionotropic and metabotropic. Ionotropic glutamate receptors contain integral cation-specific ion channels and can be further subdivided into three distinct receptors based on agonist sepecificities, termed α-amino-3-hydroxy-5-methyl-4-isoxazolepropionate (AMPA), kainate (KA) and NMDA receptors (Watkins & Evans, 1981; Mayer & Westbrook, 1984; Davies & Collingridge, 1989; Lambert et al., 1989). In contrast, metabotropic receptors function by intracellular signalling through G proteins and link to inositol phospholipid metabolism (Sladeczek et al., 1985; Sugiyama, Ito & Hirono, 1987; for review, see Smart, 1989; Baskys, 1992). The metabotropic receptors can be selectively activated by trans-1-amino-cyclopentyl-1,3-dicarboxylate (tACPD) (Stratton, Worley & Baraban, 1990; Charpak et al., 1990). Recently, ionotropic and metabotropic receptors have been characterized by molecular cloning and both consist of many different subtypes (Hollmann et al., 1989; Moriyoshi et al., 1991; Kumar et al., 1991; Masu et al., 1991; for review see Dingledine, 1991). For example, six subunits have been identified for non-NMDA receptors and classified as GluR1 to GluR6 (Hollmann et al., 1989; Boulter et al., 1990; Egebjerg et al., 1991; Verdoorn et al., 1991; Werner et al., 1991).

Stored zinc in mossy fibre nerve terminals can be co-released with glutamate (Crawford & Connor, 1973) into the synaptic cleft with neuronal activity, especially at high rates of stimulation (Assaf & Chung, 1984; Howell, Welch & Frederickson, 1984) and has been studied extensively on EAA ionotropic receptors in a variety of preparations, including cultured mouse embryonic cortical and hippocampal neurones, rat cortical brain slices and Xenopus oocytes expressing EAA receptors (Peters, Koh & Choi,

1987; Westbrook & Mayer, 1987; Hori, et al., 1987; Reynolds & Miller, 1988; Kushner et al., 1988; Rassendren, et al., 1990). These studies revealed that zinc selectively antagonized NMDA receptor-mediated responses and potentiated non-NMDA responses. Recently, a study using Xenopus oocytes expressing GluR3 mRNA found that zinc enhanced desensitized KA currents and suggested that GluR3 alone may be responsible for the zinc-induced potentiation of non-NMDA responses (Dreixler & Leonard, 1991).

However, studies in adult rat cortical 'wedge-shape' brain slices either failed to find zinc antagonism of NMDA-induced responses, or showed a non-specific blockade of both NMDA and non-NMDA agonist-induced responses (Joes et al., 1989; Lam et al., 1990). Furthermore, zinc has been shown not to affect the frequency or duration of epileptiform discharges induced by Mg-free medium, a phenomenon usually associated with NMDA receptor activation in the immature neocortex *in vitro* (Hegstad, Langmoen & Hablitz, 1989). Whether NMDA sensitivity to zinc undergoes changes with neuronal development like that associated with the $GABA_A$ receptor (Smart, 1992), or whether other factors produce this discrepancy is unknown. Also whether zinc has any effect on responses induced by the natural excitatory transmitter, L-glutamate, and the selective metabotropic receptor agonist, tACPD under 'physiological conditions' has not yet been demonstrated in a preparation retaining much of its cellular architecture and synaptic connections.

It has been reported that zinc modulates excitatory synaptic transmission, enhancing the amplitude of the EPSP at low concentrations (50μM) and eventually blocking the EPSP at higher concentrations (1mM) in cultured hippocampal neurones (Mayer & Vyklicky, 1989). The later effect was also observed after prolonged application of zinc (500μM) in olfactory cortex slices (Smart & Constanti, 1983). However, the mechanism underlying the zinc modulation of excitatory synaptic transmission, particularly in depressing the EPSP was unclear. In addition, zinc inhibition of NMDA receptors causing a reduction in Ca^{2+} entry through NMDA channels (Peters, Koh & Choi, 1987; Westbrook & Mayer, 1987) may account for the observation that zinc reduces paired-pulse potentiation in the rat hippocampus, a phenomenon indicating a short-term increase in synaptic efficacy (Khulusi, Brown & Wright, 1986). The NMDA receptor has a striking role for inducing long-term potentiation (LTP), an activity-dependent enhancement of synaptic efficacy that is most pronounced in the hippocampus

(Bliss & Lomo, 1973; Schwartzkroin & Wester, 1975; Collingridge, Kehl & McLennan, 1983; Bashir et al., 1991). The LTP phenomenon is putatively linked to memory and learning (Bliss & Gardner-Medwin, 1973; Haas et al., 1988; Laroche, Doyere & Bloch, 1989; Malinow & Tsien, 1990; Zalutsky & Nicoll, 1990). As zinc is particularly important in the early development of the nervous system and can modulate EAA receptors, it was also of interest to investigate whether zinc could influence synaptic plasticity such as LTP following a train of high frequency electrical stimulation in hippocampal CA1 and CA3 neurones.

RESULTS

1. Zinc enhances glutamate-induced responses under physiological conditions

Under normal conditions, at physiological levels of Mg^{2+} (1-2mM) and at the resting membrane potential (-60 to -80mV), the most commonly observed neuronal response to bath-applied glutamate (100-500μM) was a relatively slow and reproducible depolarization associated with the firing of action potentials. Apparently variable changes in the input conductance, both decreases and increases were observed as illustrated in Fig. 7.1. Bath application of zinc (25-300μM) enhanced the glutamate response in a dose-related manner, indicated by a larger depolarization and an increase in the number of spikes (Fig. 7.1A; n=6). However, bath-application of the zinc chelating agent, CP94 (200-400μM; n=4) had no detectable effects on adult CA1 or CA3 neuronal responses to glutamate (Fig. 7.1B), which was consistent with the results obtained from young CA3 neurones (Fig. 4.18, in Chapter 4).

With pharmacological manipulation, it was possible to maximize the action of glutamate at either NMDA or non-NMDA receptors (Mayer & Westbrook, 1984, 1985; Johnson & Ascher, 1987). Figure 7.2 illustrates a typical example from a CA1 neurone under voltage clamp. When superfusing with nominally Mg-free medium containing 1μM TTX to prevent synaptic transmission and adding 10μM glycine and 10μM CNQX a condition allowing NMDA receptor activation and inhibition of non-NMDA receptors, glutamate (200μM) induced a slow inward current reaching a peak at 0.45nA with a

slight increase in conductance. Bath application of zinc (300μM) completely blocked the glutamate response which quickly recovered following washout of zinc (Fig. 7.2A). The recovered responses were further blocked by 10μM APV, confirming their mediation by NMDA receptors. In the same cell, responses to glutamate, recorded in nominally zero glycine and high Mg^{2+} (5mM) solution, which inhibited NMDA receptor activity and allowed preferential activation of non-NMDA receptors, were now **enhanced** by 300μM zinc (Fig. 7.2C). The potentiated responses were not recovered after washing zinc for 30-min, but were subsequently blocked by 10μM CNQX confirming they were mediated by non-NMDA receptors. Current-voltage (I-V) relationships (Fig. 7.2B and D) obtained from this experiment indicated that zinc blockade of the glutamate responses mediated by the NMDA receptor, or enhancement of the responses mediated by non-NMDA receptors was only slightly voltage dependent.

2. Long-lasting enhancement of non-NMDA receptor activation by zinc

CA1 pyramidal neurones responded to bath-applied non-NMDA agonists, AMPA (4μM; n=3), quisqualate (QU, 2-8μM; n=11), or bromowillardiine (BRW, 5-10μM; n=4), with reproducible quick onset but slow offset depolarizations and associated conductance increases. Bath application of zinc (50-1000μM) consistently enhanced neuronal responses to these three agonists by 60-80% (Fig. 7.3,4, and 5), which is in agreement with previous studies on cultured neurones and cortical slices (Peters, Koh & Choi, 1987; Westbrook & Mayer, 1987; Hori, et al., 1987). It was surprising to find that such potentiated responses did not recover, but became further augmented up to 100-300% following washout of zinc for 30 to 120-min. This phenomenon was observed in all neurones tested with these agonists.

To investigate whether the continued augmentation was due to residual zinc bound to the receptors and not removed by washing, the zinc chelator CP94 was added to the Krebs solution. As shown in Fig. 7.3, after washing out zinc for 60-min with normal solution, the addition of 400μM CP94 did not reverse the potentiated AMPA-induced responses, which were even further enhanced. However, the long-lasting potentiated responses were blocked by 20μM CNQX, confirming that they were mediated by non-NMDA receptors.

While zinc consistently augmented AMPA, QU or BRW-induced responses, it was only seen with KA in approximately half of the CA1 neurones examined (5 out of 12 cells; Fig. 7.6). An inconsistent effect of zinc on KA-induced responses was also noted by other investigators in cultured cortical or hippocampal neurones (Peters, Koh & Choi, 1987; Westbrook & Mayer, 1987) and in cortical brain slices (Hori, et al., 1987).

3. Zinc antagonizes NMDA-induced responses

Hippocampal slices were routinely superfused with Mg-free medium containing glycine (5-10μM) for at least 15min before the application of NMDA. Repeated application of 4-8μM NMDA produced reproducible submaximal responses without desensitization. In the presence of TTX (0.5-1μM), zinc (300μM) consistently inhibited NMDA (4-8μM) induced inward currents and conductance increases under voltage clamp (Fig. 7.7, n=5). Aspartate is another excitatory amino acid present in the CNS and thought to act preferentially on NMDA receptor sites (Mayer & Westbrook, 1984). Zinc (300μM) also reversibly inhibited neuronal responses to bath-applied aspartate (200μM, n=3) in the same perfusing solution (Fig. 7.8). These results confirmed that zinc inhibits NMDA-responses and that such an effect is not merely due to the complexation of NMDA (cf. Mayer, Vyklicky & Westbrook, 1989).

However, under conditions where intact synaptic transmission remained functional in the brain slice (superfusing Mg-free containing 10μM Gly Krebs but without adding TTX), the effect of zinc on NMDA-induced responses was more variable. Five out of 13 cells displayed NMDA responses being slight inhibited and in the other cells NMDA responses were either unaffected or slightly enhanced. The 'zinc-resistant' NMDA responses were reversibly blocked by 20μM APV, confirming they were mediated by NMDA receptors. In contrast, zinc potentiating non-NMDA responses was totally unaffected by the application of TTX.

Hippocampal CA1 neurones after being exposed to Mg-free medium containing 10μM glycine and 10μM bicuculline for 15-20min, could occasionally develop spontaneous epileptiform bursts (8 out of 19 cells; Fig. 7.9). This activity consisted of bursts of action potentials superimposed on a low amplitude (5-10mV) and short duration (200-500ms) depolarization and was followed by an afterhyperpolarization (4-8mV

amplitude and 1-1.5s duration). The frequency of the bursts was 0.02-0.1Hz. Bath-applied 50-300μM zinc did not block these bursts, though the frequency of the bursts was slightly reduced (Fig. 7.9). Zinc did not induce the appearance of GDPs in the presence of low concentrations of bicuculline (10μM).

4. Metabotropic action induced by tACPD in the presence of zinc

It has been demonstrated that bath-applied quisqualate, glutamate or tACPD onto hippocampal slices in the presence of ionotropic receptor antagonists, such as CNQX and APV reduces the afterhyperpolarization following a burst of action potentials, slightly depolarizes neurones, increases the membrane input resistance and decreases accommodation of cell firing (Stratton, Worley & Baraban, 1990; Charpak et al., 1990; Baskys, 1992). Bath application of the selective agonist, tACPD (50-100μM) produced a very small depolarization, an increase in the membrane resistance and blockade of AHPs following a burst of spikes in this study. The blockade of the AHP was the most profound effect (Fig. 7.10A). Therefore the AHP was chosen as a parameter to test the interaction between zinc and the metabotropic response induced by tACPD. Bath-applied 300μM zinc slightly reduced the AHP following a depolarizing current injection (see also Chapter 5) and the zinc-induced GDP was also followed by a large AHP. Co-application of 50μM tACPD completely inhibited the AHP following depolarizing current injection and also blocked the AHP following the GDPs without affecting the frequency of spontaneous GDPs. However, it was noted that the membrane input resistance increase by tACPD was reduced in the presence of zinc (Fig. 7.10, n=3).

5. Zinc modulation of excitatory synaptic transmission

Neurotransmission at excitatory synapses in the hippocampus operates through two major classes of ionotropic EAA receptors, non-NMDA and NMDA receptors. These mediate the fast and slow EPSPs respectively (Walkins & Evans, 1981; Nowak et al., 1984; Davies & Collingridge, 1989). Figure 7.11 illustrates typical evoked synaptic responses obtained by intracellular and simultaneous extracellular recordings from the CA1 subfield. The intracellular synaptic potential (EPSP-IPSP sequence) was recorded

from a single neurone at a resting potential of -72mV and the extracellular field potentials (orthodromically-evoked population spikes, OPS) were recorded in the vicinity of the penetrated cell. Single stimuli (1 pulse per 30s) were applied to the Schaffer collateral/commissural pathways. Bath application of 20μM CNQX reversibly blocked both intracellular and extracellular events. After recovery from CNQX, the EPSP and OPS were not depressed in the presence of 50μM APV. This confirmed that under 'physiological' conditions with magnesium in the extracellular fluid at membrane potentials more negative than -70mV and with low frequency stimulation, synaptically released glutamate mainly acts on non-NMDA receptors. Bath application of 10-100μM zinc either had no effect on the EPSP and OPS, or slightly enhanced the EPSP (n=24). In the cell shown in Fig. 7.11, an action potential was evoked in zinc, indicating enhanced excitatory synaptic activity. This may be due to the zinc potentiation of non-NMDA receptor activation, and/or due to zinc increasing cell excitability (see Chapter 5). However, at higher concentrations of zinc (200-300μM), EPSPs and OPSs were gradually depressed (Fig. 7.11), and a late giant depolarizing potential was usually revealed (not illustrated). The EPSP and field potentials were partially recovered after a prolonged (60-90min) washout of zinc; however, the GDP disappeared quickly within 2-min on washout. Furthermore, the depression of EPSPs and OPSs by zinc could not be prevented or reversed by bicuculline at 50μM, a concentration which completely blocked all the intracellular GDP events.

To study the zinc modulation of the EPSP in more detail, EAA antagonists were used to separate the non-NMDA receptor-mediated fast EPSP and NMDA-mediated slow EPSP. Slices were superfused with a Mg-free medium containing 10μM glycine, 10μM CNQX and 20μM bicuculline, a condition allowing NMDA receptor activation and inhibiting non-NMDA and $GABA_A$ receptors. Under these conditions an NMDA-mediated slow EPSP was triggered by stimulation of afferent fibres and was reduced by zinc (50-100μM) within 2-min of bath-application. The EPSP showed little recovery within 10min following washout of zinc (Fig. 7.12). This suggested that zinc could inhibit the synaptic activation of NMDA receptors (Forsythe, Westbrook & Mayer, 1988; Mayer & Vyklicky, 1989). When the perfusing solution contained high Mg^{2+} (4mM) and 40μM APV to inhibit NMDA receptor activation, in addition to 50μM bicuculline and 300μM CGP 35348 to block $GABA_A$ and $GABA_B$ receptors, a 'pure' non-NMDA

receptor mediated fast EPSP was evoked by orthodromic stimulation (Fig. 7.13). The fast EPSP was unaffected by bath-applied 10-100μM zinc and was also initially resistant to a high zinc concentration (300μM) during the first 5-min of zinc administration; however, the EPSP was eventually depressed with time (Fig. 7.13). Interestingly, neuronal responses to exogenous glutamate applied by ionophoresis were not inhibited but slightly potentiated (Fig. 7.13, see also Fig. 7.1). Also, the cell excitability, reflected by the response to a direct depolarizing current injection was not reduced (not shown). This suggested that the action of zinc in depressing excitatory synaptic transmission was mediated largely via presynaptic mechanisms.

6. Zinc blocks long-term potentiation in adult CA1 and CA3 neurones

For studying LTP in the CA1 subfield, a stimulating electrode was placed in stratum radiatum to stimulate Schaffer collateral fibres and simultaneous extracellular recordings were made in the CA1 region of stratum pyramidale and in stratum radiatum to record the OPS and population EPSP (pEPSP). For monitoring LTP in the CA3 subfield, stimulation was applied to the mossy fibres in the hilar region and extracellular recordings were made in the CA3 region of stratum pyramidale.

Control low frequency stimulation (0.01Hz) did not induce LTP, but high frequency stimulation (two 100Hz/1s stimulation trains separated by 30s; cf. Malenka, Madison & Nicoll, 1986) consistently produced a robust LTP in both CA1 and CA3 regions of adult slices lasting for at least 1-2h. The increase in the amplitude of the OPS was 60-100% (n=14), and the increase in the pEPSP slope (expressed as the amplitude of the pEPSP over the time to peak, i.e. mV/ms, cf. Alger & Teyler, 1976) was 100-150% (n=9). After establishing LTP for 20-30min, bath application of zinc at 50-100μM had little or no effect on the LTP, but at 200-500μM, zinc not only blocked the phenomenon of LTP, but also completely abolished the OPS and pEPSP. Following a prolonged washout of zinc, or co-application with a zinc chelator, e.g., CP94 (400-600μM), the OPS and pEPSP only recovered to the level prior to LTP-induction (Fig. 7.14A).

In slices preincubated in 300μM zinc for 5-min before applying the high frequency stimulation, the amplitude of the OPS was reduced and the induction of LTP

completely prevented. Moreover, the brief post-tetanic potentiation was also greatly reduced (Fig. 7.14B; n=4).

To determine whether **endogenous** zinc in the hippocampus had any effect on LTP induction, recordings were obtained from the CA3 region of young postnatal slices (P5-15). Slices taken from P5 rats did not exhibit a robust LTP in the CA3 region (n=5), but slices from P13-15 rats usually showed a significant degree of potentiation in responses following high frequency stimulation of the mossy fibres. The mean increase in the amplitude of the OPS was 65±13%, and in the pEPSP slope, 105±19% (n=6). These observations are in agreement with previous studies which suggested that the ability to generate LTP in hippocampal slices appeared between the first and second week after birth (Baudry, et al., 1981; Harris & Teyler, 1984; Muller, Oliver & Lynch, 1989). It was possible that endogenous zinc was blocking the induction of LTP at P2-5. However, bath application of the zinc chelator, CP94 (200-400μM) to the P5 slices (n=3) did not result in the development of LTP following high frequency stimulation. Furthermore, CP94 (400μM) had no obvious effect on an established LTP in P13-15 slices (n=3).

DISCUSSION

1. Zinc modulation of non-NMDA and NMDA receptor-mediated responses

Exogenous zinc (25-300μM) always enhanced glutamate induced responses in normal Krebs solution containing physiological levels of Mg^{2+} (1-2mM). This action is probably mediated mainly via non-NMDA receptor activation (Collingridge, Kehl & McLennan, 1983; Lambert et al., 1989). The zinc chelator, CP94 had no detectable effect on glutamate-induced responses, suggesting that endogenous zinc in the hippocampus does not influence postsynaptic EAA receptor activation under physiological conditions.

Zinc consistently enhanced non-NMDA receptor-mediated responses in mature pyramidal neurones as well as in cultured immature neurones (Peters, Koh & Choi, 1987; Westbrook & Mayer, 1987). However, the potentiation by zinc was considerably more long-lasting in hippocampal brain slices compared to cultured cells. This maintained

change was not due to residual zinc ions in the membrane, since it was not reversed by the zinc chelator CP94. It could be explained by an increased sensitivity of the postsynaptic receptors to glutamate or non-NMDA receptor agonists, but intracellular processes via second massagers and also receptor up-regulation involvement could not be excluded. Unlike the NMDA receptor ion channels, non-NMDA receptor ion channels are usually thought to conduct Na^+ and K^+ ions only. However, under current clamp, neuronal depolarization via activation of non-NMDA receptors will activate voltage-gated Ca^{2+} channels, so that Ca^{2+} can also enter by this route (Williams & Johnson, 1989). Furthermore, recent studies on recombinant EAA receptors found that AMPA and KA induced inward calcium currents in oocytes expressing GluR1 or GluR3 or GluR1 plus GluR3 subunits, whereas oocytes expressing receptors containing GluR2 subunits showed no such Ca^{2+} permeability (Hollmann, Hartley & Heinemann, 1991; Miller, 1991). It is possible that the neuronal depolarization caused by activation of native non-NMDA receptors in the hippocampus could be a source of Ca^{2+} entry. Whether zinc modulates intracellular Ca^{2+} activity by, for example, affecting calcium stores producing long lasting effects is at present unknown.

Previous studies showed that some properties of NMDA receptors undergo developmental changes, e.g. changes in voltage dependence of NMDA-induced currents and in their sensitivity to modulation by glycine during early postnatal development (Ben-Ari, Cherubini & Krnjević, 1988; Gaiarsa et al., 1990). However, the mature NMDA receptor in adult neurones remains sensitive to zinc inhibition. With pharmacological manipulation to preferentially activate particular EAA receptor subtypes, it has been convincingly demonstrated that zinc selectively inhibited NMDA receptor-mediated responses and enhanced non-NMDA receptor activation by the natural mixed agonist glutamate (Fig. 7.2). However, there was variability in the effect of zinc on KA or NMDA-induced responses in this apparently homogeneous pyramidal cell population. It was quite often difficult to obtain stable responses to KA, this may be related to its well known neurotoxicity (Watkins & Evans, 1981). A number of other studies using intracellular recordings have also failed to obtain reproducible responses to KA (Constanti et al., 1980; Hori, ffrench-Mullen & Carpenter, 1985; Hori & Carpenter, 1988). The failure of zinc to block epileptiform bursts in adult CA1 neurones induced by Mg-free medium was consistent with an observation from the immature neocortex preparation

(Hegstad, Langmoen & Hablitz, 1989). Recent studies also reported that zinc either could not inhibit NMDA responses or non-selectively blocked non-NMDA and NMDA-mediated responses in cortical wedge-slices (Jones et al., 1989; Lam et al., 1991). However, in the present study, zinc consistently inhibited NMDA-induced responses in the **absence** of synaptic transmission, implying that on-going synaptic activity in intact neural circuitry could interfere with the apparent ability of zinc to antagonize NMDA receptors. Although the morphology of the excitatory synapses onto interneurones differs considerably from those onto pyramidal cells, their electrophysiological and pharmacological properties are very similar (Sah, Hestrin & Nicoll, 1990). Zinc at the doses (50-300μM) used here usually partially inhibited pyramidal cell responses to NMDA. Therefore, NMDA receptors in interneurones could still be partially activated by NMDA in the presence of zinc. Neurochemical studies revealed that activation of NMDA receptors could cause interneurones to release GABA (Harris & Miller, 1989), which mainly produced a depolarization in the pyramidal cells when recordings were made using KCl-filled microelectrodes. This response was enhanced by zinc (see Chapter 6). Thus, it may complicate the pattern of zinc effects on NMDA-induced responses. In addition, recent cloning data revealed that the molecular heterogeneity in EAA receptors could well be matched by equally diverse functional properties. How many different subunit combinations actually existed the composition of native EAA receptors are currently unknown.

The apparent no interaction between zinc and the metabotropic response induced by tACPD indicated that zinc at 300μM did not block the metabotropic receptors and that the tACPD-induced metabotropic action did not reduce GABAergic transmission. But it is possible that some ion channels closed by the effects of tACPD were re-opened by zinc. Thus, zinc apparently reduced the membrane resistance in the presence of tACPD. However, such an effect could also occur if zinc open another discrete population of ion channels, but usually, on hippocampal neurones zinc **increases** membrane resistance.

2. Zinc selectively depresses excitatory synaptic transmission

Although synaptically released glutamate normally acts on both non-NMDA and NMDA receptors, the NMDA receptor channels are usually inhibited by extracellular

Mg^{2+} at the resting membrane potential (Nowak et al., 1984; Mayer & Westbrook, 1984). Thus, EPSPs recorded in intact slices are mainly mediated by non-NMDA receptor activation as confirmed in the present study. Although zinc can be co-released with glutamate in neuronal activity (Assaf & Chung, 1984; Howell, Welch & Frederickson, 1984), the zinc chelator CP94 had no obvious effects on excitatory synaptic transmission, suggesting endogenous zinc probably does not modify excitatory transmission under normal 'physiological' conditions and during low frequency stimulation. Exogenously-applied zinc at 10-100μM, also had little effect on intact EPSPs. However, at higher concentrations (300-500μM), zinc not only blocked the EPSP, but also depressed the non-NMDA receptor-mediated fast EPSP without inhibiting postsynaptic glutamate-induced responses or by reducing cell excitability. Furthermore, the zinc-induced depression of EPSPs and the OPS were not blocked or prevented in the presence of bicuculline. These results suggested that the zinc depressant effect on glutamatergic transmission occurs not by enhancing synaptic inhibitory function, but probably occurs due to a reduction in excitatory transmitter release at the presynaptic nerve terminals (*vide infra*, Chapter 8). This was supported by a neurochemical study which demonstrated zinc selectively inhibiting [^{3}H]-glutamate release without affecting the release of [^{3}H]-GABA and [^{3}H]-acetylcholine in rat hippocampal slices (Kihara et al., 1990). A blockade of excitatory transmission by high dose of zinc in the hippocampus was consistent with the results obtained from olfactory cortex slices (Smart & Constanti, 1983) and cultured hippocampal neurones (Mayer & Vyklicky, 1989). Also chronic exposure of cultured neurones to high levels of zinc has been observed to be neurotoxic (Yokoyama, Koh & Choi, 1986). This may partly explain why the inhibition of the EPSP was often irreversible and also why zinc blocked both NMDA and non-NMDA responses in cortical wedges (Lam et al., 1990). Interestingly, in the neuromuscular junction, it has been reported that zinc has multiple actions, decreasing and also increasing transmitter release (Nishimura, 1987, 1988; Wang & Quastel, 1990).

3. Zinc and long-term potentiation

The long-term potentiation of synaptic transmission in the hippocampus following brief trains of high frequency stimulation is one characteristic likely to be involved in

memory and learning (Bliss & Gardner-medwin, 1973; Bliss & Lomo, 1973; Schwartzkroin & Wester, 1975; Haas et al., 1988; Malinow & Tsien, 1990). The presence of zinc in the mossy fibres of granule cells, the major neurones involved in the potentiated responses to repeated stimuli in the perforant pathway, may provide a key to understanding whether there is any physiological role for zinc in synaptic plasticity. Also there may be pathophysiological consequences following changes in zinc content within the hippocampus. A decrease in the spike firing threshold (Chavez-Noriega, Holliwell & Bliss, 1990) and a persistent enhanced non-NMDA mediated EPSP (Kauer, Malenka & Nicoll, 1988) have been observed after induction of LTP in the hippocampal brain slice. Zinc binding sites have been found in protein kinase C (PKC) (Hubbard et al., 1991) and zinc can activate PKC inducing translocation to the membrane (Csermely et al., 1988). Activation of PKC is also associated with the induction of LTP in the hippocampus (Malenka, Madison & Nicoll, 1986). It has been postulated that zinc may enter the postsynaptic neurone via NMDA channels, activating PKC and inducing LTP (Wiss et al., 1989). Indeed, the present study demonstrated that zinc could reduce the spike firing threshold (see Chapter 5) and induce a long-lasting enhancement on non-NMDA mediated postsynaptic responses. However, the application of zinc did not induce LTP, nor enhanced the established LTP following high frequency stimulation in adult neurones.

Activation of NMDA receptors is essential for the induction of LTP in CA1 neurones (Collingridge, Kehl & Mclennan, 1983; Nicoll, Kauer & Malenka, 1988; Bashir et al., 1991). Since zinc inhibits NMDA receptors, it was not surprising to find that zinc blocked LTP in the CA1 region of adult neurones. In contrast to LTP produced in CA1 neurones, the LTP in CA3 neurones, is not blocked by selective NMDA antagonists and is due, in part, to a rise in the intracellular concentration of Ca^{2+}, probably mediated by the activation of voltage-dependent Ca^{2+} channels (Williams & Johnston, 1989; Griffith, 1990; Zalutsky & Nicoll, 1990) or possibly through non-NMDA channels (Miller et al., 1991). However, zinc (200-500μM) still blocked LTP in the CA3 region. Postsynaptic calcium alone has been proposed to be sufficient for the induction of LTP in CA3 neurones (Malenka et al., 1988, 1989). As zinc inhibits some Ca^{2+} currents (Sim & Cherubini, 1990), it may contribute to the blockade of LTP.

Inhibitory postsynaptic potentials are not reduced but enhanced in CA1 pyramidal neurones during the induction of LTP (Haas & Rose, 1982, 1984). This observation was

confirmed by a study using intracellular recording from hippocampal interneurones. It showed that interneurone excitability is increased after the development of LTP (Taube & schwartzkroin, 1987). Thus, although zinc could enhance inhibitory activity, this alone would probably not be responsible for the blockade of LTP. Furthermore the same results were observed in some experiments using the Krebs containing 100μM bicuculline and 500μM CGP 35348 to eliminate the influence from inhibitory synaptic activity.

A recent study suggested that LTP induced in the CA3 region is contributed by an increased release of excitatory transmitter (Hirata, Sawada & Yamamoto, 1991). Since zinc depressed intact EPSPs and the non-NMDA receptor-mediated fast EPSP and also inhibited the phenomenon of post-tetanic potentiation which is usually regarded as a presynaptic phenomenon (Reymann et al., 1988), it is more likely that zinc blocking LTP in the hippocampus is due to a presynaptic block of excitatory transmitter release.

An LTP-like phenomenon could not be observed in P5 slices and the treatment with the zinc chelator, CP94, or application of exogenous zinc did not result in the development of lasting synaptic changes, suggesting that this form of plasticity not present in early development of neonatal rats does not relate to zinc.

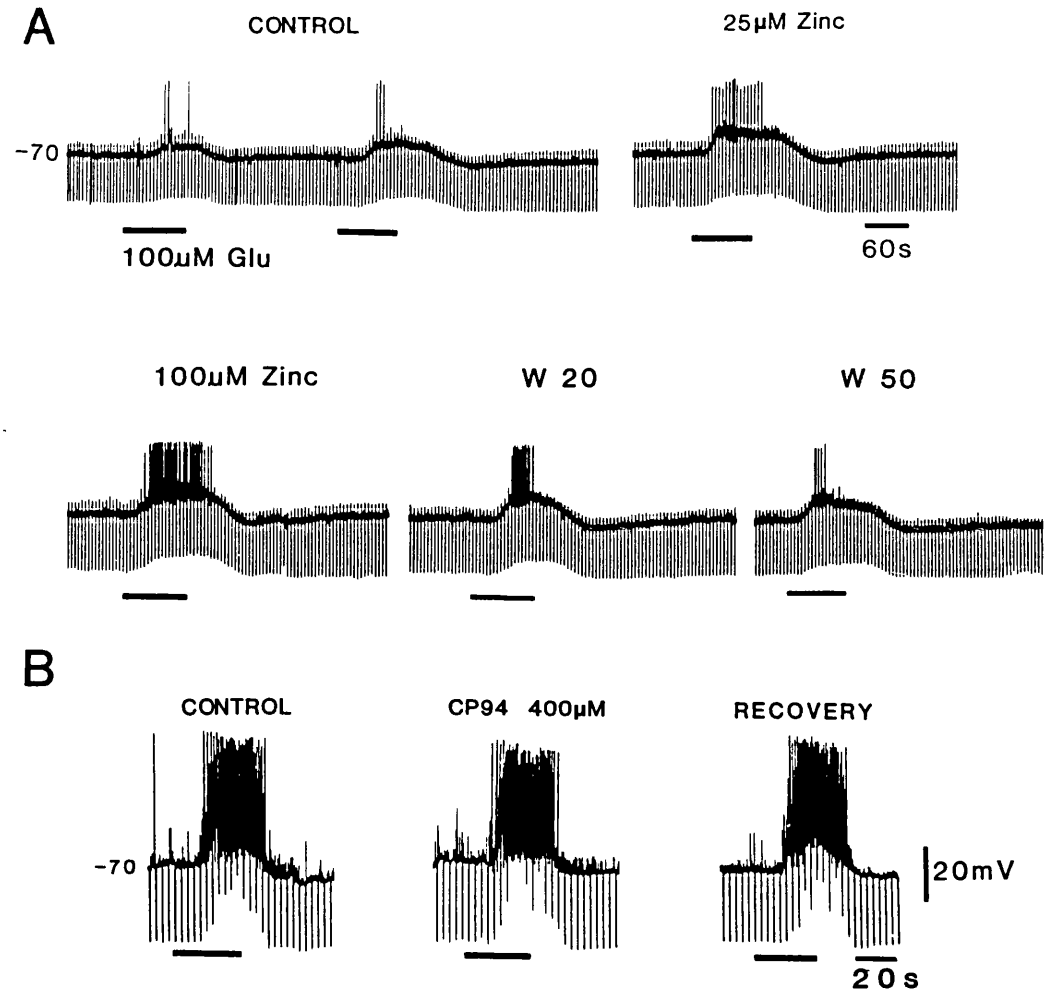

Fig. 7.1. Effects of zinc and the zinc chelator, CP94, on glutamate-induced responses in hippocampal neurones. **A**, Intracellular recording of an adult CA1 cell under current clamp. Responses to bath applied glutamate (solid bars) consistently induced a depolarization with superimposed action potential firing (upward deflections). Hyperpolarizing electrotonic potentials were evoked by -0.3nA, 300ms, 0.3Hz current pulses. Bath application of 25μM or 100μM zinc reversibly enhanced glutamate responses. The slice was superfused in normal Krebs at a membrane potential of -70mV with DC current injection. **B**, In a different cell, glutamate induced similar depolarizations and conductance increases in the absence and presence of 400μM CP94. Membrane potential -70mV.

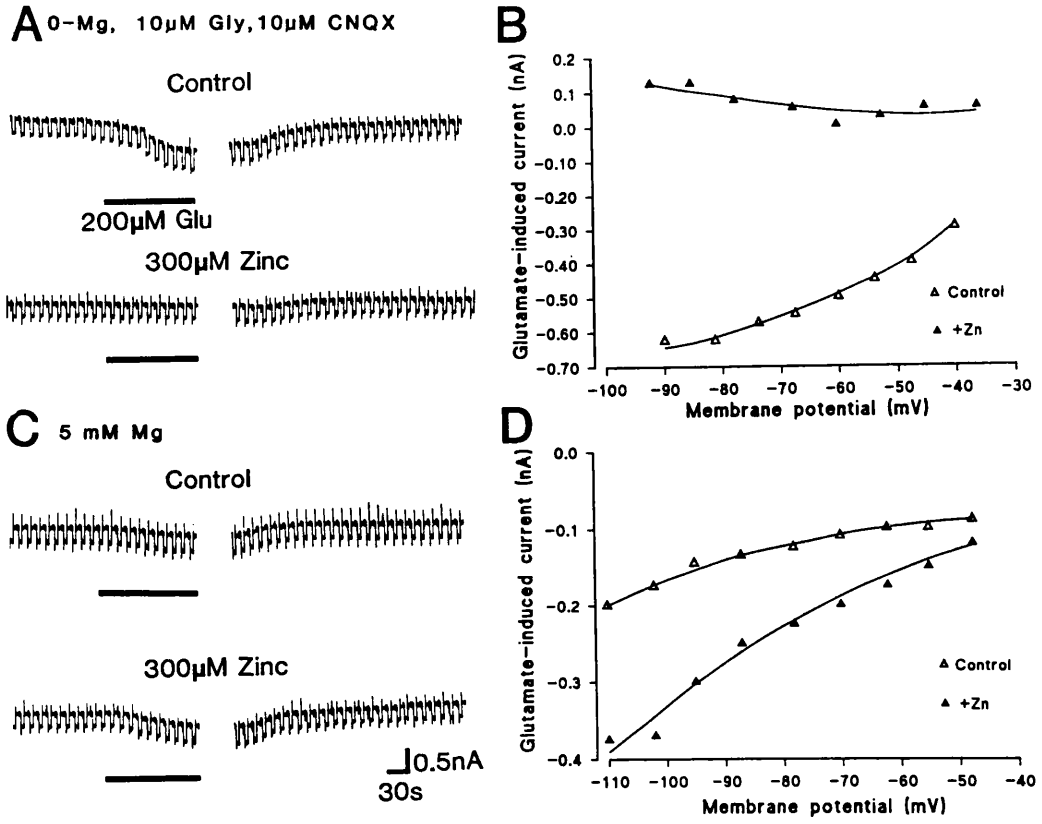

Fig. 7.2. Zinc selectively blocks NMDA receptor-mediated responses and enhances non-NMDA receptor-mediated responses induced by glutamate in the same cell. Recording from a CA1 neurone voltage clamped at -70mV. Downward deflections show leak currents induced by hyperpolarizing voltage commands (-15mV, 250ms, 0.1Hz). During each voltage step, the chart recorder speed was increased to 100 times the time calibration. **A**, Bathing the slice in a Mg-free medium containing 10μM glycine (Gly), 10μM CNQX and 0.5μM TTX, 100μM glutamate (Glu, solid line) induced an inward current which was inhibited by the application of zinc. Gaps in all the chart records refer to intervals where the instantaneous current/voltage (I/V) relationships for Glu were determined in the absence (Δ) and presence (▲) of zinc (plotted in **B**). **C**, In the same cell after washout of zinc for 30-min and superfusion of a Krebs solution containing 5mM Mg, 0.5μM TTX and nominally zero glycine, 200μM Glu induced an inward current which was enhanced by 300μM zinc. The I/V relationships to Glu in the absence (Δ) and presence (▲) of zinc are plotted in **D**.

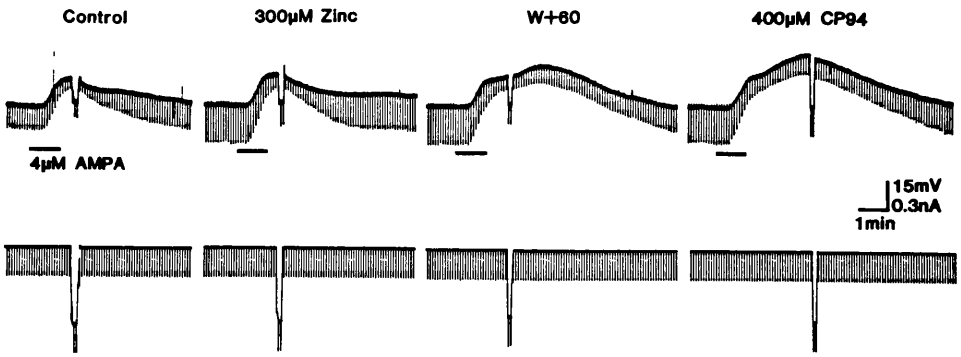

Fig. 7.3. Effects of zinc on AMPA-induced responses in CA1 neurones. Upper traces are chart records of membrane potential showing 4μM-AMPA (solid line) inducing a depolarization and conductance increase in the absence and presence of zinc or the zinc chelator, CP94. DC current injection was applied during the peak of the depolarization to return the membrane potential to the initial pre-agonist level. The conductance was still markedly increased. After washing zinc for 60-min (w+60), or during the addition of 400μM CP94, the AMPA responses were still potentiated. Lower traces are records of constant current pulses (-0.3nA, 300ms. 0.3Hz) used to monitor the membrane input conductance. Membrane potential was -70mV.

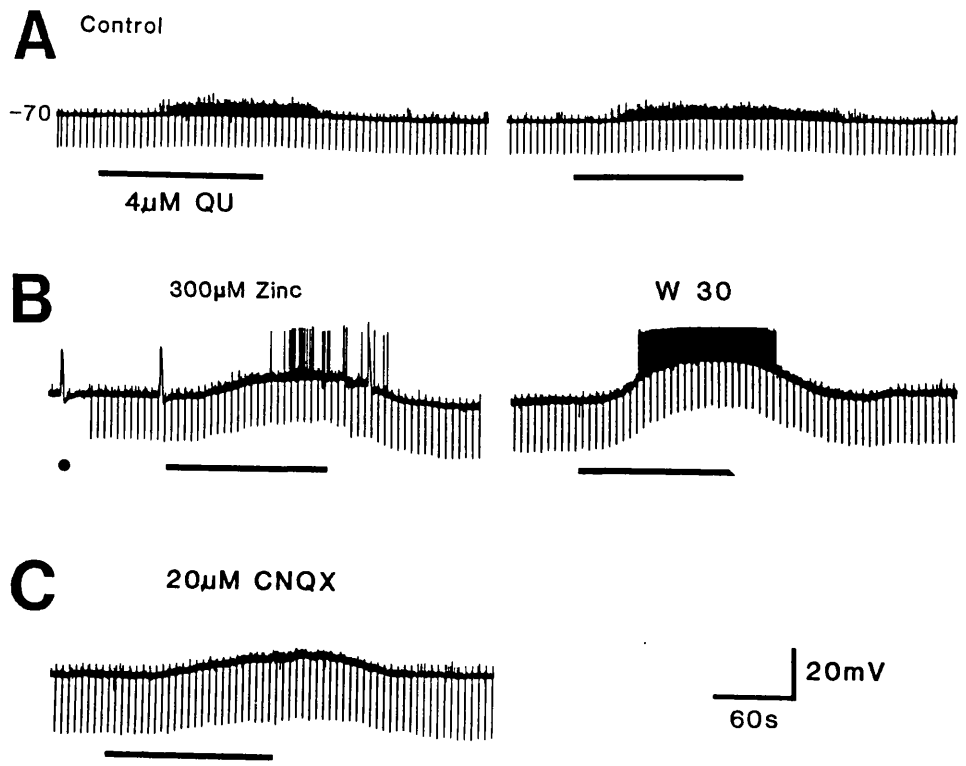

Fig. 7.4. Effects of zinc on quisqualate (QU)-induced responses in CA1 neurones. Chart records of membrane potential and superimposed hyperpolarizing electrotonic potentials evoked by current pulses (-0.3nA, 300ms, 0.3Hz). **A**, Two consecutive responses to 4μM QU (solid line) produced consistently small responses. **B**, Bath applied zinc induced spontaneous GDPs (indicated by ●) and enhanced the QU responses which did not recover after washing zinc for 30-min (W 30). C, in the same cell after washout of zinc, QU-induced responses were reduced by CNQX. Membrane potential -70mV maintained by DC current injection.

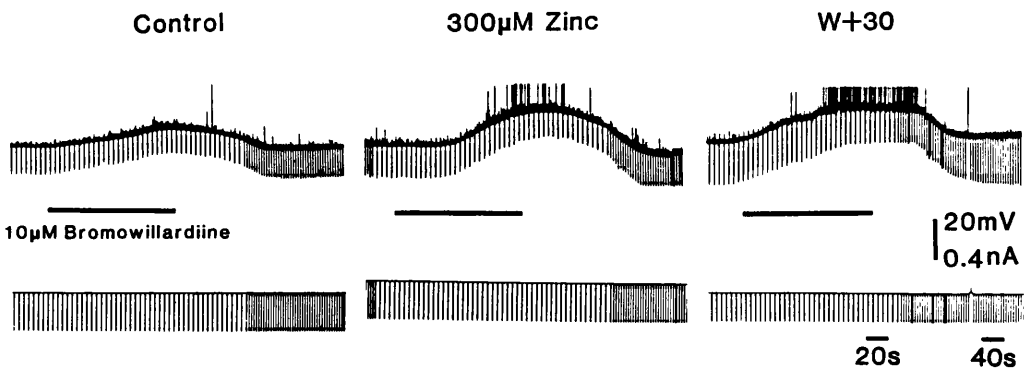

Fig. 7.5. Effects of zinc on bromowillardiine-induced responses in hippocampal neurones. Top traces show current-clamp recordings of a CA1 cell where membrane potential depolarizations and spike firing were induced by 10μM bromowillardiine (solid line) before, during and after application of 300μM zinc. After washout of zinc for 30-min (W+30), bromowillardiine responses were still enhanced. Hyperpolarizing current pulses (lower traces, -0.4 and -0.3nA, 300ms, 0.3Hz) were applied throughout to monitor membrane input resistance. Membrane potential -70mV with DC current injection. Note the membrane potential was manually clamped back to its initial level in the presence of zinc.

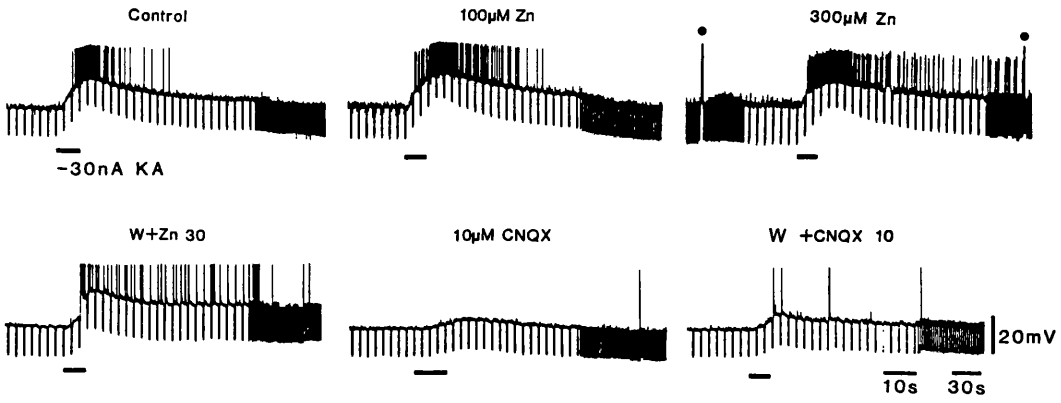

Fig. 7.6. Effects of zinc on kainate-induced responses in CA1 neurones. Continuous chart record of membrane potential from the same neurone showing depolarizations with bursts of action potentials induced by ionophoretically-applied kainate (KA, -30nA; solid bar). These responses were slightly enhanced by 100μM and 300μM zinc (upper traces), and blocked by 10μM CNQX which was only partially reversible (lower traces). In the presence of 300μM zinc spontaneous GDPs (●) occurred. Resting membrane potential was -66mV. Hyperpolarizing current pulses (-0.3nA, 300ms, 0.3Hz) were applied throughout. Holding current for KA was 10nA.

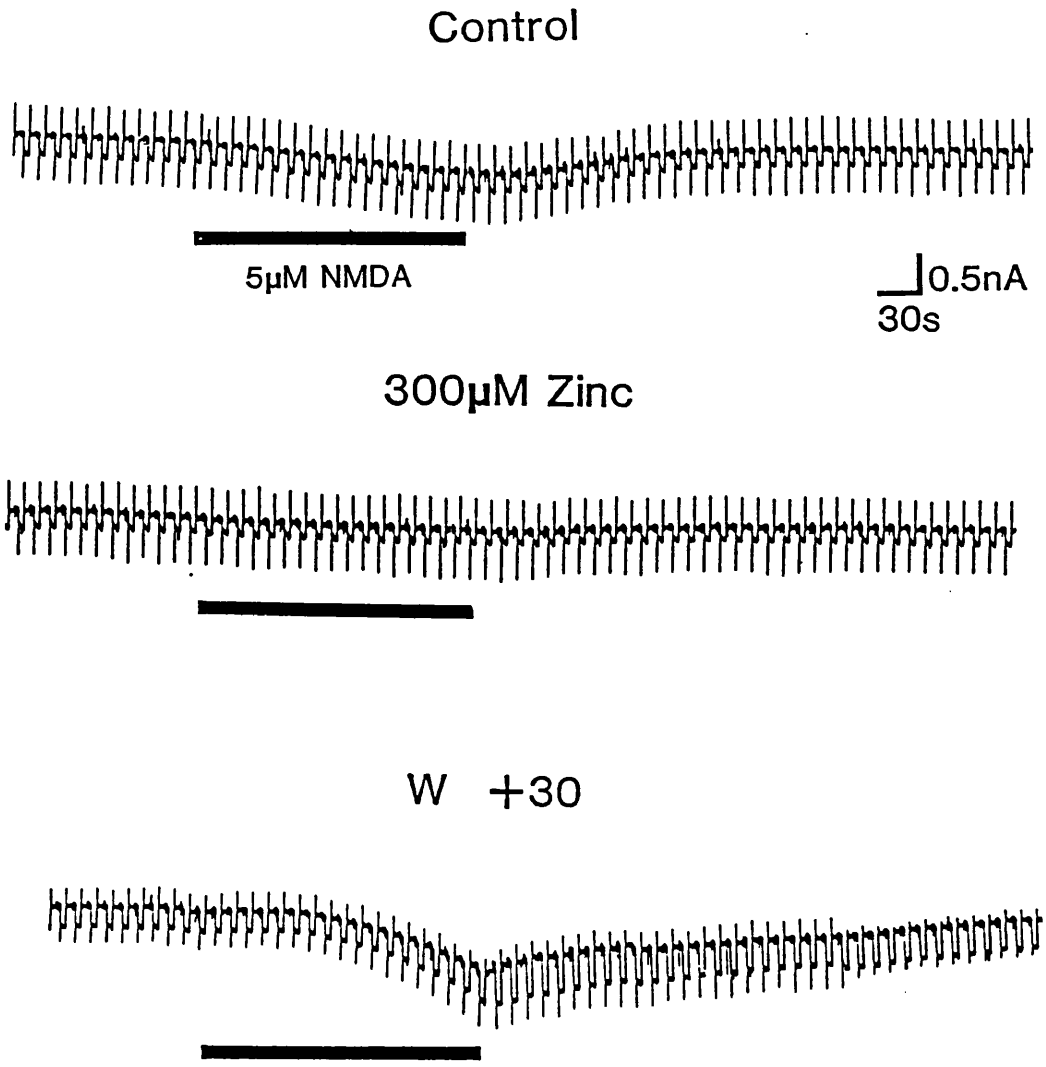

Fig. 7.7. Zinc blocks NMDA-induced responses in the presence of tetrodotoxin (TTX). Voltage clamp recording from a CA1 neurone at a holding potential of -70mV and superfusing with a Mg-free medium containing 10μM glycine (Gly) and 0.5μM TTX. Downward deflections show leak currents induced by hyperpolarizing voltage commands (-15mV, 250ms, 0.1Hz), during which the chart recorder speed was increased to 100 times the time calibration. NMDA (5μM, open bar) induced an inward current and small conductance increases (upper trace). The NMDA-induced response was blocked by the application of 300μM-zinc (middle trace). The response 'over-recovered' after a 30min washout of zinc (W +30, lower trace).

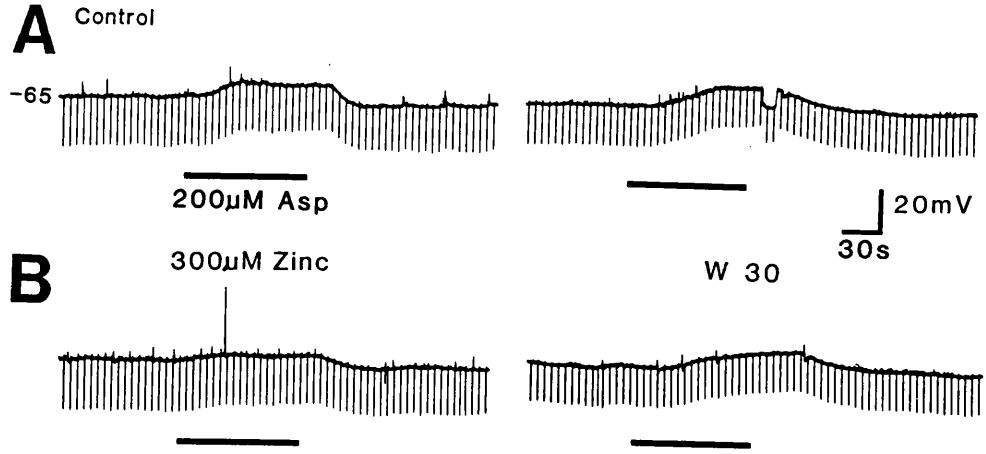

Fig. 7.8. Zinc inhibits aspartate-induced responses in the presence of tetrodotoxin (TTX). Chart records of a CA1 neurone bathed in a Mg-free, 10μM glycine and 1μM TTX containing solution. **A**, Two consecutive responses to 200μM aspartate (Asp, solid line) produced comparable depolarizations with small conductance increases. In the second Asp application, DC current was temporarily injected to adjust the membrane potential back to the resting level. **B**, Asp induced responses in the presence and after washout of zinc (30min, W 30). Hyperpolarizing current pulses (-0.3nA, 300ms, 0.2Hz) were applied throughout. Resting membrane potential -65mV.

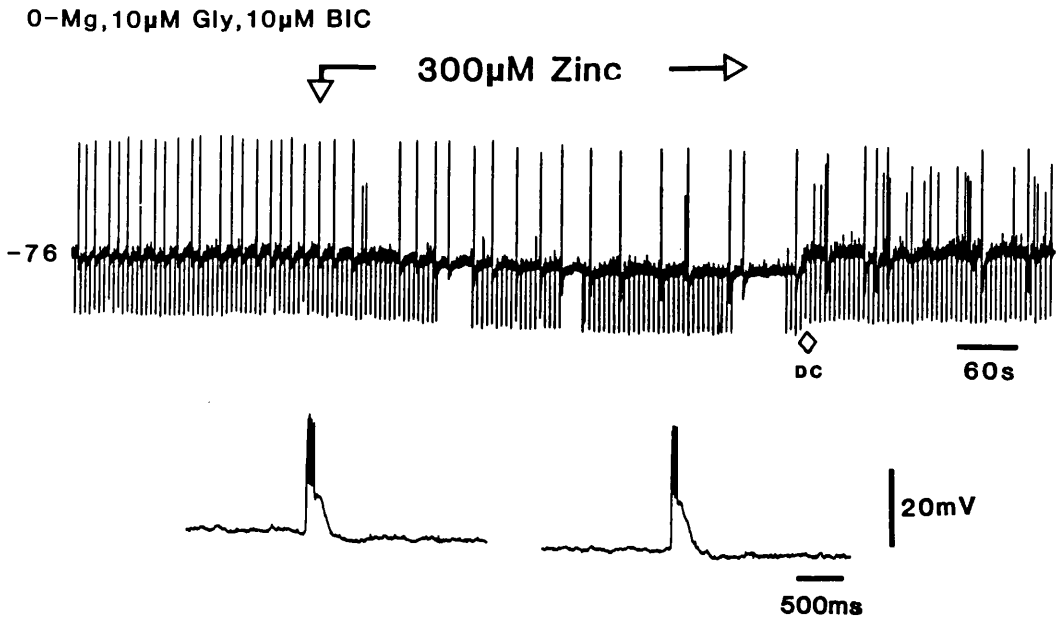

Fig. 7.9. Zinc fails to block spontaneous bursts induced by nominally Mg-free medium in adult pyramidal neurones. Intracellular recording from a CA1 cell at a membrane potential of -76mV. Superfusing Mg-free solution containing 10μM glycine (Gly) and 10μM bicuculline (BIC) for 15-min induced spontaneous bursts (upper traces). Bath-applied 300μM zinc throughout the experiment (open arrow) slightly reduced the frequency of the bursts. The lower traces recorded from the same cell illustrate two bursts before and during application of zinc on a expanded timescale. Hyperpolarizing current pulses (-0.3nA, 300ms, 0.3Hz) were applied throughout. During zinc application the membrane potential was returned to the initial level by DC current injection (◊).

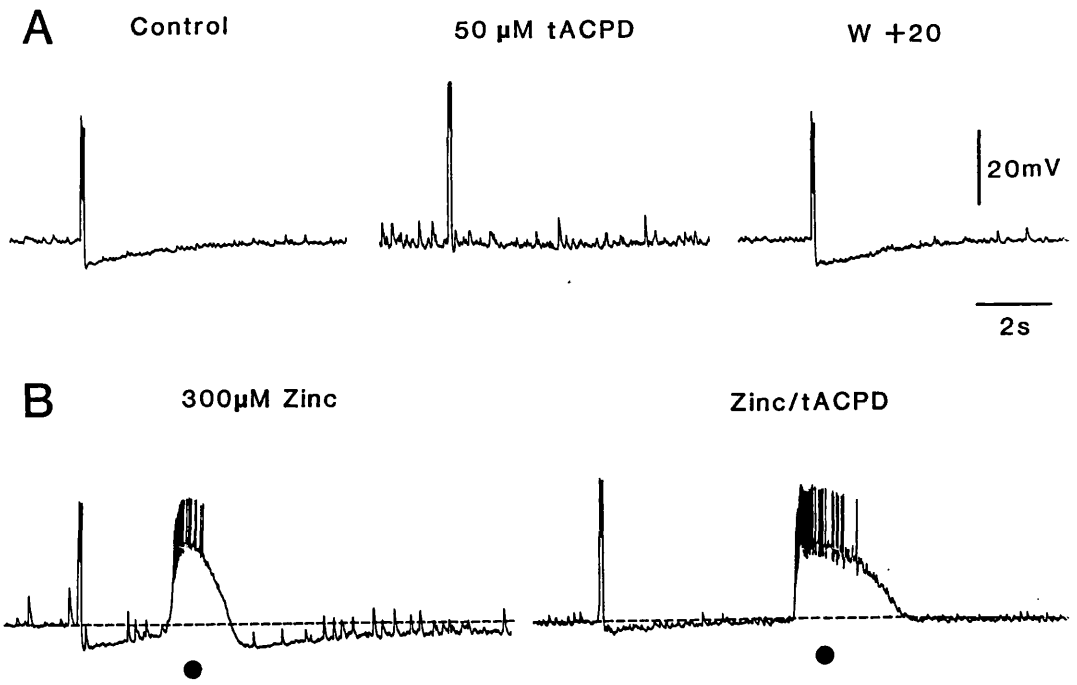

Fig. 7.10. Blockade of the action potential afterhyperpolarization by tACPD in the presence of zinc. **A**, In a CA1 neurone the afterhyperpolarization (AHP) following a burst of spikes elicited by a depolarizing current pulse (0.4nA, 100ms) was blocked by 50µM tACPD and recovered after washing for 20min (W +20). Note that the membrane resistance also increased in the presence of tACPD. **B**, in the same cell, after recovery from tACPD, bath-applied 300µM zinc induced spontaneous GDPs (●) followed by an AHP. The burst elicited by the depolarizing current pulse (0.4nA, 100ms) was also followed by an AHP. Co-application of tACPD with zinc (Zinc/tACPD) for 3min caused both AHPs to be completely blocked. Membrane potential -70mV with DC current injection.

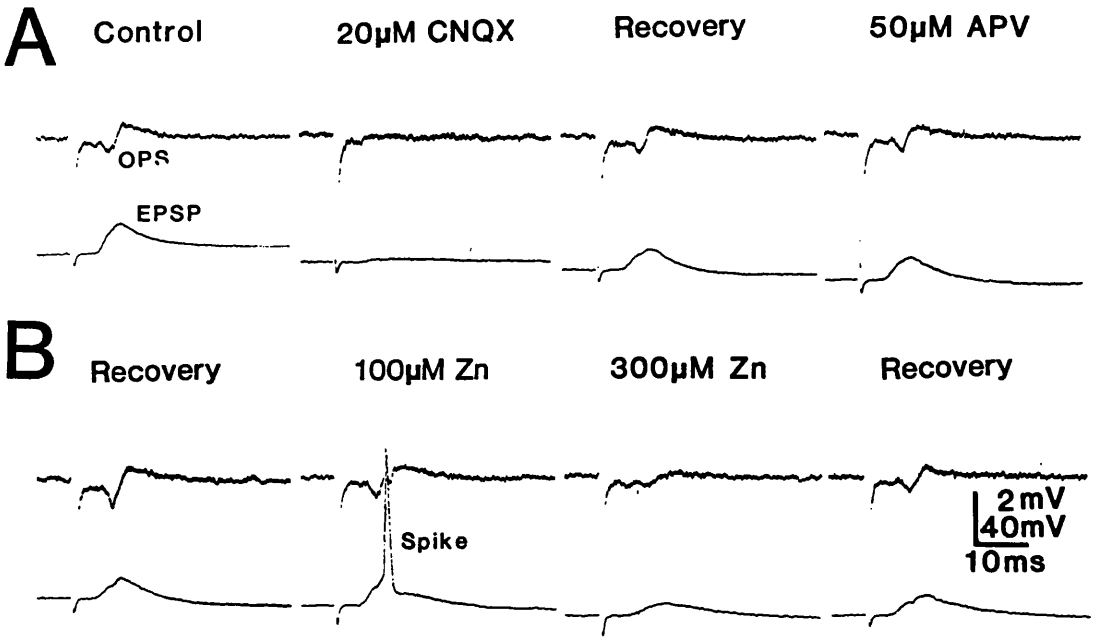

Fig. 7.11. Zinc modulates EPSPs and population spikes. **A**, In control responses, extracellular recordings of orthodromically-evoked population spikes (OPS; upper traces) and simultaneous intracellular recordings of EPSPs (lower traces) were made in the CA1 region following stimuli applied to the Schaffer collateral pathway (35V, 0.1ms, 1 pulse per 30s). All drug applications were bracketed by control recordings indicating full recovery. 20μM CNQX blocked synaptic responses while 50μM APV had no significant effect. **B**, In the same cell, 100μM zinc slightly enhanced synaptic responses, indicated by the appearance of an action potential, whereas 300μM zinc blocked the OPS and EPSP. After washout of zinc for 60min, the OPS and EPSP showed a partial recovery. The resting membrane potential was -72mV. The microelectrode contained 4M K-acetate for intracellular recordings and the extracellular recording electrode contained 2M NaCl.

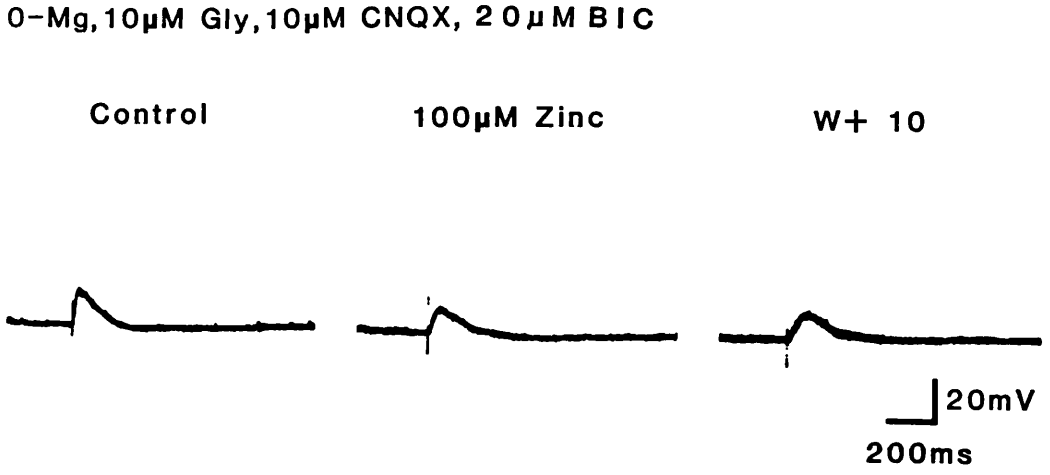

Fig. 7.12. Low concentrations of zinc reduce NMDA receptor-mediated synaptic responses. Intracellular recording from a CA1 neurone bathed in a Mg-free, 10μM glycine (Gly), 10μM CNQX and 20μM bicuculline containing solution. Stimulation of the Schaffer collateral pathway (30V, 0.1ms, 1 pulse per 30s) evoked NMDA receptor-mediated slow EPSPs. Each trace represents superimposed sweeps from three consecutively evoked synaptic responses. Bath-applied 100μM zinc for 2min depressed synaptic responses which only slightly recovered following washout of zinc for 10min (W+ 10). Resting membrane potential was -68mV.

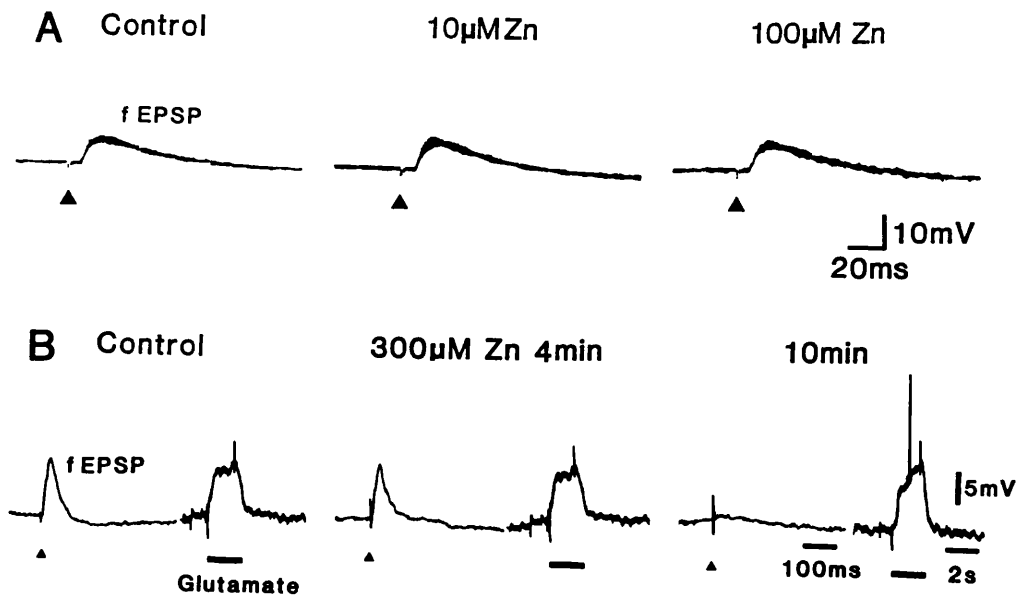

Fig. 7.13. Effects of zinc on non-NMDA receptor-mediated EPSPs and glutamate-induced responses. Intracellular recording from CA1 neurones superfused with a solution containing 4mM Mg, 40μM APV to block NMDA receptors and 50μM bicuculline and 300μM CGP 35348 to inhibit $GABA_A$ and $GABA_B$ receptors. Stimulation of the Schaffer collateral pathway (▲, 35V, 0.1ms, 1 pulse per 30s) evoked non-NMDA receptor-mediated fast EPSPs (f EPSP). **A**, Each trace represents three superimposed sweeps taken from the oscilloscope. Bath-applied 10μM and 100μM zinc had no effects on the synaptic responses. Membrane potential -70mV with DC current injection. **B**, In a different cell, recorded in the same solution as in A, non-NMDA receptor-mediated fast EPSPs were followed by ionophoretically-applied glutamate responses (200mM, pH7, -100nA, solid bar). During the first 5min of bath-applied 300μM zinc, the EPSP and glutamate-responses were unaffected. After application of zinc for 10-min, the EPSP was blocked whereas the glutamate-responses were not inhibited, but slightly enhanced. Membrane potential was -70mV with DC current injection.

Fig. 7.14. Zinc blocks and prevents long-term potentiation in the CA3 region of adult hippocampal slices. **A**, Extracellular recording of orthodromically-evoked population spikes (OPS) evoked by mossy fibre stimulation (▲, 20V, 0.1ms, 1 pulse per 30s). Long-lasting changes in the synaptic responses (LTP 30min) occurred after high frequency stimulation (two 100Hz/1s stimulation trains separated by 30s) of a slice bathed with normal Krebs solution (upper traces). Bath-applied 300μM zinc for 2min began to depress the LTP and after application for 10min in this cell, completely abolished synaptic responses. The OPS was partially recovered by the addition of the zinc chelator, CP94. Each trace represents four consecutive superimposed sweeps taken from the oscilloscope. **B**, The changes in the OPS amplitude (▼, each point is the average of 2-4 consecutive responses) taken from A are plotted against time. The closed circles (●) are the mean value of the amplitudes of OPSs taken from four other experiments. Note pre-incubation of 300μM zinc (thin line) reduced the OPS and post-tetanic potentiation and prevented the slices from generating LTP in the CA3 subfield. Arrow indicates high-frequency stimulation. The OPS amplitude was determined by the method of Alger and Teyler (1976) as shown in the inset in A.

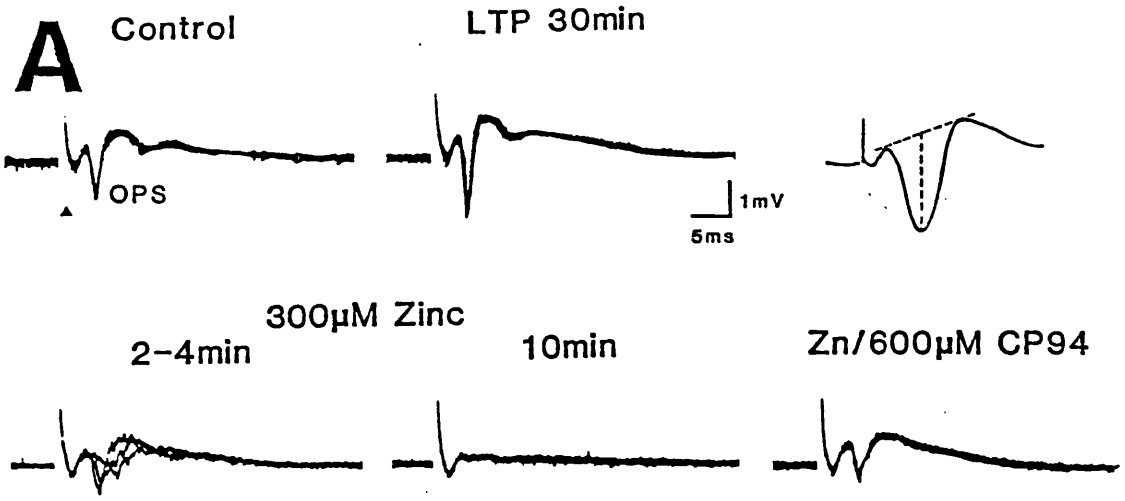
A
Control
LTP 30min
OPS
1mV
5ms
300μM Zinc
2-4min
10min
Zn/600μM CP94

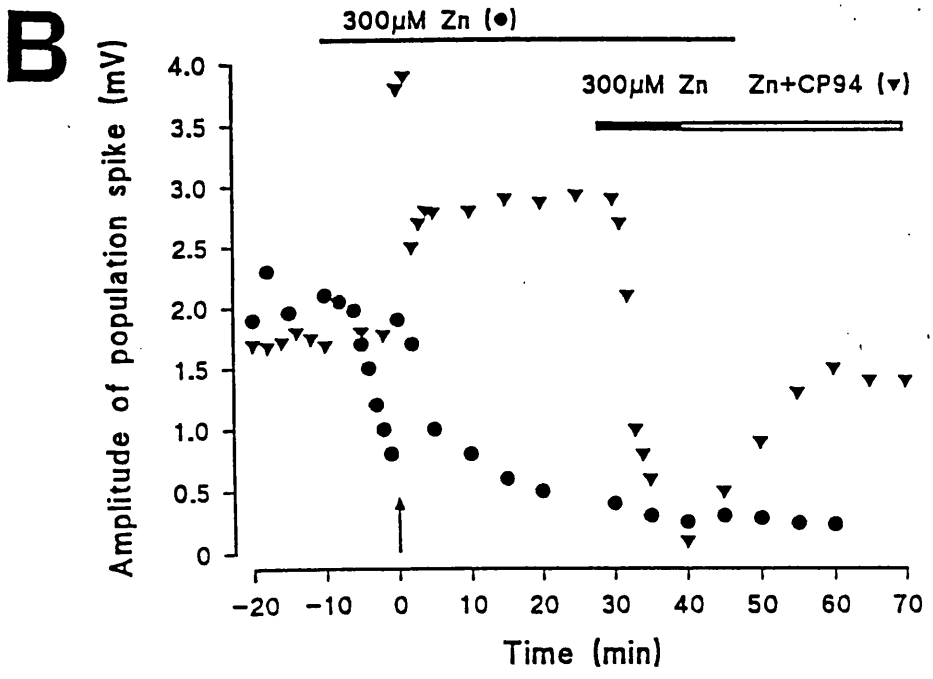
B
300μM Zn (●)
300μM Zn
Zn+CP94 (▼)
Amplitude of population spike (mV)
4.0
3.5
3.0
2.5
2.0
1.5
1.0
0.5
0
−20
−10
0
10
20
30
40
50
60
70
Time (min)

Chapter 8
GENERAL DISCUSSION

1. Choice of preparation for studying the action of zinc

The hippocampus is particularly well suited for investigating the functional role of zinc in synaptic transmission, since it contains the highest amount of zinc in the CNS (Crawford & Connor, 1972; Szerdahelyi & Kása, 1983; Frederickson et al., 1987;) and has been well defined in structure and basic neurophysiology (Schwartzkroin & Prince, 1978; Swanson, 1983; Wong & Traub, 1983; Turner & Schwartzkroin, 1984). The hippocampus has a tri-synaptic relay through which afferent activity from the entorhinal cortex is processed. The three synapses are formed between the entorhinal cortex and dentate granule cells via the perforant path, dentate to CA3 pyramidal neurones via the zinc-rich mossy fibres, and finally CA3 to CA1 pyramidal neurones via the Schaffer collateral fibres, which have a low zinc content (Amaral & Witter, 1989; Savage, Montano & Kasarski, 1989).

Functionally, the hippocampus is widely recognized to be involved in the processing of memory, cognitive function and the integration of emotion (Schwartzkroin & Wester, 1975; Swanson, 1983). In addition, the hippocampus displays a low threshold for epileptic seizures for both experimental animals and humans (Swhwartzkroin & Prince, 1978; Wong & Traub, 1983; Johnston & Brown, 1981, 1984; Ben-Ari & Represa, 1990).

The present study utilized hippocampal brain slices *in vitro*, since they possess an intact synaptic neuronal circuitry and allow a defined analysis of the action of zinc in single cells and neuronal networks (Teyler, 1980; Dingledine, 1984). Pyramidal neurones could also be morphologically identified by a modified histological method (Kata & Armstrong, 1991) using intracellular labelling, based on the avidin-biotin system.

2. Zinc has multiple actions on membrane and neurotransmitter receptors

By increasing input resistance and causing a small hyperpolarization, zinc could

make the cell electrotonically more compact and thereby lead to a facilitation in dendritic/somatic coupling including synaptic coupling. Furthermore, zinc reduced the latency for excitation and action potential accommodation as well as inhibiting AHPs following single spikes or trains of action potentials. These results suggest that zinc inhibits voltage-activated membrane currents probably including I_A, I_D and Ca^{2+}-dependent K^+ currents, i.e., I_C and I_{AHP}. Zinc does inhibit I_A and I_C in cultured sympathetic neurones (Constanti & Smart, 1987) and Ca^{2+} currents in hippocampal neurones or myotubes (Sim & Cherubini, 1990; Wineger & Lansman, 1990). All these actions imply that zinc has a very broad spectrum of pharmacological activity.

Indeed zinc can also interact with the major receptors mediating inhibitory and excitatory synaptic activity. Exogenous GABA-induced responses and the $GABA_A$ receptor mediated IPSP in *embryonic* neurones were consistently inhibited by the application of zinc (Westbrook & Mayer, 1987; Mayer & Vyklicky, 1989; Smart & Constanti, 1990); whereas $GABA_A$-mediated responses in older, more mature postnatal neurones were less sensitive to zinc inhibition. In contrast, the $GABA_B$ receptor maintains a sensitivity to zinc from early postnatal life to adulthood. Zinc consistently inhibited postsynaptic $GABA_B$ receptor mediated responses activated with baclofen or GABA in young and adult neurones. However, paradoxically zinc could also induce spontaneous giant hyperpolarizing potentials mediated by $GABA_B$ receptors after blockade of $GABA_A$ receptors by bicuculline and picrotoxin. The evoked 'pure' $GABA_B$-mediated slow IPSP was prolonged by low concentrations of zinc (50-300μM) and depressed at higher concentrations (300-1000μM), suggesting that zinc increases the amount of GABA released over a long period of time following neuronal activity or upon electrical stimulation. The large release of GABA may be sufficient to initially overcome zinc's postsynaptic inhibitory action at the $GABA_B$ receptor, perhaps by competing for a common receptor binding site. Thus zinc could be classified as a weak $GABA_B$ antagonist.

Excitatory synaptic transmitters generate EPSPs acting primarily on non-NMDA and NMDA receptors. The observation of zinc inhibiting NMDA and potentiating non-NMDA receptor-mediated responses in adult hippocampal neurones is in general agreement with results obtained from cultured embryonic cortical or hippocampal neurones (Peters, Koh & Choi, 1987; Westbrook & Mayer, 1987). Moreover, this study

revealed that on-going synaptic activity in brain slices might interfere with the apparent ability of zinc to inhibit NMDA-induced responses and that the enhancement of non-NMDA-induced responses was long-lasting over many hours. Zinc did not apparently affect the metabotropic response induced by tACPD, suggesting that zinc selectively modulates ionotropic EAA receptors.

3. Differential modulation of GABAergic and glutamatergic release by zinc

Despite the multiple actions of zinc on membrane properties and transmitter receptors, the most profound and striking action of zinc is the induction of GABA-mediated large synaptic potentials associated with an inhibition of EPSPs and population spikes. At low concentrations (50-100μM), zinc only depressed the NMDA-mediated slow EPSP but at higher concentrations (300μM), zinc blocked intact EPSPs and even the 'pure' non-NMDA mediated fast EPSP, without inhibiting postsynaptic membrane responses to exogenously-applied glutamate. This suggests that zinc may depress glutamatergic transmission probably via presynaptic mechanisms. Furthermore, zinc also affected lasting synaptic changes such as LTP induced by trains of high frequency stimulation. Raising extracellular concentrations of zinc (200-300μM) blocked the LTP in both CA1 and CA3 regions of the adult hippocampus which might also result from a presynaptic blockade of excitatory transmission rather than just by inhibiting postsynaptic NMDA receptors. These results suggest that zinc apparently causes a selective increase in GABA release and a decrease in the glutamatergic transmission. Since postsynaptic responses to bath-applied glutamate or GABA are slightly enhanced by zinc and also the uptake of both glutamate and GABA from synaptosomes is severely reduced in the presence of zinc (Gabrielsson et al., 1986), the differential modulation by zinc may result mainly from an effect on the presynaptic release mechanism. There are many possible interpretations for this action.

(i) Zinc depresses a variety of voltage-activated and Ca^{2+}-dependent K^+ currents which could result in an increased transmitter release following broadening of the presynaptic action potential. However, there are many other blockers, including putative neurotransmitters, e.g. acetylcholine acting via muscarinic receptors that block leak conductances, I_A and some Ca^{2+}-dependent K^+ currents, but acetylcholine does not

apparently result in the generation of GDP-like events in the hippocampus (Brown, 1990). Furthermore, 4-AP, a well known I_A blocker, not only increases the release of inhibitory transmitter, but also markedly enhances the release of excitatory transmitter. Also the action of zinc in generation of GDPs could not be reproduced by other cations, such as Cd^{2+}, Co^{2+}, Cu^{2+}, Fe^{2+}, Mn^{2+} and Al^{3+}. So blockade of K^+ channels by zinc in pre- and postsynaptic neurones, is unlikely to be the sole cause of selectively increasing GABA release. Unless a channel exists in inhibitory nerve terminals which is uniquely sensitive to zinc.

(ii) Zinc could inhibit both pre- and postsynaptic $GABA_B$ receptors. This will have two consequences: enhancing the release of GABA and removing the overlying $GABA_B$-mediated slow IPSP which could obscure the latent depolarizing potential mediated by dendritic $GABA_A$ receptor activation. It has been suggested that pre- and postsynaptic $GABA_B$ receptors in the CNS show different pharmacological properties. In the hippocampus, phaclofen blocks the postsynaptic hyperpolarization produced by baclofen, but fails to reverse the baclofen-induced decrease of the glutamatergic synaptic potentials evoked by Schaffer collateral stimulation (Dutar & Nicoll, 1988b, Nicoll & Dutar, 1990). A study on neostriatum further demonstrated that the $GABA_B$ 'autoreceptor' on GABAergic nerve terminals is more sensitive to the $GABA_B$ antagonist 2-hydroxy-saclofen than the heteroreceptors located on glutamatergic afferents (Calabresi et al., 1991). More recently another study in cultured hippocampal slices revealed that postsynaptic and presynaptic $GABA_B$ receptors on interneurones are mediated by a pertussis and Ba^{2+}-sensitive K^+ conductance, while presynaptic $GABA_B$ receptors on excitatory axons work through some other unknown mechanism (Thompson & Gähwiler, 1992). However, there are many other studies which suggest that pre- and postsynaptic $GABA_B$ receptors are pharmacological indistinguishable at present (Curtis et al., 1988; Stratton et al., 1989; Harrison, 1990; Seabrook, Howson & Lacey, 1990). To establish $GABA_B$ receptors subtypes requires additional experimental approaches including more specific antagonists and molecular cloning. Ba^{2+}, a K^+ channel blocker as well as $GABA_B$ inhibitor, partly reproduced the effect of zinc inducing the $GABA_A$-mediated late depolarizing potential following orthodromic stimulation. However, the specific $GABA_B$ antagonists, including phaclofen, 2-OH-saclofen and CGP 35348 were ineffective (Dutar & Nicoll, 1988b; Soltesz et al., 1988; Davies, Davies & Collingridge, 1990; Xie & Smart,

1991c; Lambert, Levitin & Harrison, 1992), indicating that the underlying mechanism is more complex and not explicable by zinc acting solely at $GABA_B$ receptors. Furthermore, the data in this present study indicates that zinc is unlikely to be a presynaptic $GABA_B$ receptor blocker since it did not affect the paired-pulse inhibition of the $IPSP_B$.

(iii) It has been reported that glutamate induces a depression of excitatory monosynaptic transmission via presynaptic non-NMDA receptors (Forsythe & Clements, 1990). As zinc potentiated postsynaptic non-NMDA receptor activation, it is possible that zinc may also enhance presynaptic non-NMDA receptors and therefore increase the feedback inhibition of glutamate release. In addition, zinc inhibits postsynaptic Ca^{2+} currents in hippocampal pyramidal neurones (Sim & Cherubini, 1990). It might be postulated that zinc could also inhibit Ca^{2+} channels in presynaptic glutamatergic nerve terminals, thereby reducing the Ca^{2+} entry and depressing transmitter release. But why does such an action of zinc not suppress the GABAergic transmission? The release of GABA from immature CNS synaptosomes is proposed to be non-vesicular and calcium-independent (Taylor & Gordon-Weeks, 1989; Taylor, Docherty & Gordon-Weeks, 1990). However, whether GABA release in the mature hippocampus is less dependent on Ca^{2+} compared with the release of glutamate, or whether calcium channels located in GABAergic and in glutamatergic nerve terminals possess a different sensitivity to zinc is presently unknown. What would be convenient is to have a suitable model of a CNS synapse which is amenable to intracellular recording from the **presynaptic** terminal to test the action of zinc.

(iv) The induction of GDPs by zinc could be observed in the apparent absence of any functional glutamatergic synaptic transmission, suggesting that either zinc may have direct actions on interneurones inducing GABA release, or other transmitters may be involved. One of the most likely candidates is a catecholamine transmitter, since the specific β_1-adrenergic receptor antagonist, atenolol, reversibly blocked zinc-induced GDPs.

Although the generation of GDPs may involve more than one of the possible mechanisms discussed above, the differential modulation of inhibitory and excitatory synaptic transmission is quite unique to zinc. This specificity suggests that zinc may play a physiological role in rat hippocampal synaptic neurotransmission.

4. A physiological role for zinc in synaptic neurotransmission

The suggestion that zinc has a neuromodulatory role requires the fulfilment of several stringent criteria including the identification of defined zinc-containing neuronal pathways (Crawford & Connor, 1972; Frederickson, 1984), the localization of zinc in synaptic vesicles (Haug, 1967, 1973; Ibata & Otsuka, 1969; Pérez-Clausell & Danscher, 1985; Holm et al., 1988; Claiborne, Rea & Terrian, 1989), a demonstration of calcium-dependent release (Assaf & Chung, 1984; Howell, Welch & Frederickson, 1984; Aniksztejn & Ben-Ari, 1987), an interaction with neurotransmitter receptors/ion channels (Peters, Koh & Choi, 1987; Westbrook & Mayer, 1987; Smart & Constanti, 1990), and the presence of uptake mechanisms (Wolf, Shütte & Römhild, 1984; Wensink et al., 1988).

Evidence of a physiological role was provided by the demonstration of giant synaptic potentials induced by zinc in the adult CNS and the inhibition of a similar potential occurring spontaneously in immature CNS neurones by complexation of endogenous zinc. Previous studies of endogenous zinc on synaptic transmission have produced conflicting results. Brain zinc levels were modified only in **adult** animals by systemic or intracerebral infusion of metal chelators (von Euler, 1961; Crawford et al., 1973; Crawford & Connor, 1975; Danscher, Shipley & Andersen, 1975), or by using dietary zinc deficiency (Hesse, 1979). Synaptic transmission was subsequently monitored with extracellular recording techniques *in vivo*. The present study observed a consistent effect of chelation of endogenous zinc but only in young immature animals by recording specifically innate GDPs *in vitro*.

The physiological function of the GDP is probably complex. $GABA_A$-mediated GDPs could be generated in the dendrites, where depolarizing $GABA_A$-mediated IPSPs have previously been demonstrated and suggested to have an inhibitory role (Andersen et al., 1980; Alger & Nicoll, 1982; Avoli, 1988). The large increase in the chloride conductance associated with the GDP in the dendrites could be inhibitory by providing a 'shunt' across the membrane for excitatory inputs. Indeed, at the peak and during the repolarizing phase of zinc-induced GDPs, action potentials firing was frequently shunted. However, the depolarization would also spread electrotonically towards the soma where some facilitation of excitatory input may also occur (Andersen et al., 1980). Thus, the

action of GABA underlying the GDPs, could have multiple roles causing inhibition and excitation in different parts of the cell. The degree and balance of inhibition-excitation would then be expected to be closely related to the extracellular levels of zinc which may modulate synaptic transmission and postsynaptic membrane excitability. This might explain why previous studies have often reported apparently conflicting results for the effects of zinc in neuronal excitability.

Endogenous zinc-induced spontaneous GDP in the young hippocampus is a normal, physiological synaptic response. The production of the zinc-induced $GABA_A$-mediated GDPs could be involved in rudimentary dendritic synaptic inhibition in this 'seizure-prone' area of the CNS. If all the GABA 'tone' and the GABA-mediated GDPs are blocked by bicuculline, some excitatory burst-discharges of action potentials often become apparent even in these young neurones. There are many reports suggesting that a decrease in brain zinc levels may be implicated in susceptibility to epilepsy in whole animal experiments. For example, zinc content in the dentate area of the hippocampus was found to be significantly lower in epilepsy-prone mice (E1) compared with normal strains. The seizure susceptibility of the epilepsy-prone mouse is increased by zinc deficiency and decreased by a zinc loading diet (Fukahori et al., 1988; Fukahori & Itoh, 1990). Furthermore, systemic zinc adminstration can also inhibit seizure development in some animal models (Porsche, 1983; Sterman et al., 1986; Morton, Howell & Frederickson, 1990). Interestingly, very young children (4-6 days old) can suffer from benign postnatal seizures (fifth day fits) which have been correlated with low levels of zinc in their cerebrospinal fluid (Goldberg & Sheehy, 1982).

It has been reported that prenatal alcohol exposure decreases zinc in the rat hippocampal mossy fibres (Savage et al., 1989) and injection of alcohol into rats or humans also reduces zinc content in the CNS (Kasarskis et al., 1985). Zinc deficiency in adult humans has been postulated to contribute to the development of epileptic seizures occurring in alcoholism and this deficiency may be corrected by an adequate dietary zinc intake (Ebadi & Pfeiffer, 1984).

In addition, lead intoxication in humans and other species causes seizures, which are thought to be partly due to an inhibition of GABAergic transmission (Audesirk, 1985). High levels of dietary zinc can protect against the toxic effect of lead (Petit, 1984). Zinc-induced GDPs, mediated by the release of GABA and associated with an

inhibition of excitatory synaptic transmission, may 'functionally antagonize' the toxicity of lead on synaptic transmission particularly if taking into account histochemical evidence that shows zinc and lead are distributed in the same areas of the CNS, especially within the hippocampus (Timm, 1958; Danscher et al., 1976; Petit, 1984; Frederickson et al., 1987).

Furthermore, the depolarizing effects of GABA and even zinc alone can influence neuronal development. GABA has been demonstrated to act as a growth signal for neurite outgrowth/synaptogenesis in cultured neurones (Dames et al., 1985; Mattson, 1988) and zinc deficiency caused a poor growth of basket cell dendrites in the cerebellum (Dvergsten, Johnson & Sandstead, 1984). A syndrome of zinc deficiency is also associated with cerebellar dysfunction (Henkin et al., 1975; Sandyk, 1991). Therefore, zinc-induced GDPs in the immature hippocampus could also influence growth and differentiation during neuronal development (cf. Dreosti et al., 1981; Prasad, 1988) and clearly have the potential for multiple roles.

5. Pathological relevance of zinc in the brain

The naturally occurring GDPs in young hippocampal CA3 neurones gradually disappear with development. From postnatal day 14 to adulthood no such equivalent synaptic potentials could be recorded in CA3 and CA1 regions, but application of exogenous zinc routinely reproduced this phenomenon. Although this effect of exogenous zinc mimics the physiological action of zinc observed in the young hippocampus, the zinc-induced GDP in mature neurones is probably representative of an abnormal synaptic behaviour and may have pathological relevance.

Although there are conflicting reports in the literature regarding the association of zinc content in the brain with the induction of seizures, in a variety of experimental animals, when zinc is applied directly to the brain (injected intracerebroventricularly or intrahippocampally) epileptiform seizures are **routinely** observed *in vivo* (Donaldson et al., 1971; Itoh & Ebadi, 1982; Pei et al., 1983). Some biochemical studies have suggested that zinc-induced seizures might result from an inhibition of Na^+-K^+-ATPase or from a selective inhibition of glutamic acid decarboxylase by which GABA is synthesized (Donaldson et al., 1971; Barbeau & Donaldson, 1974; Itoh & Ebadi, 1982). In addition,

a selective **loss** of zinc in the hippocampal mossy fibre system accompanies granule cell seizure activity induced by electrical stimulation or by kainate-induced seizures (Sloviter, 1985; Charlton et al., 1985; Frederickson et al., 1988). These results were used to provide evidence *in vivo* for a possible role of zinc in seizure generation, but the mechanism underlying this action of zinc is unclear. Also, rather importantly, these studies did not demonstrate that the disappearance of zinc implied by the Timm stain was due to zinc being released and having a functional effect on the synaptic neurotransmission and postsynaptic neurones. A brief epileptiform episode can produce a long-lasting potentiation of synaptic transmission, which is similar to a 'classical LTP' induced by trains of high frequency stimulation (Ben-Ari & Represa, 1990). As a large amount of zinc can be released during seizure-like activity (Assaf & Chung, 1984) and based on the finding of zinc blocking LTP in CA3 neurones, it is suggested from the present study that zinc may have a pathophysiological role in the regulation of synaptic plasticity by its ability to reduce glutamate release whilst enhancing GABAergic transmission. Thus synaptically released zinc during seizure activity may actually contribute to the limitation of seizure development rather than being a cause of seizures. Although both a deficiency and an excess of zinc may alter synaptic function and cause hyperexcitability or epileptiform seizures through poorly and unidentified mechanisms, it is clearly important to be aware of how the zinc is applied and at what stage of development animals are used for the experiment. Both factors seem to influence whether zinc is pro- or anticonvulsant.

In summary, zinc ions have multiple effects on voltage-activated and ligand-gated membrane proteins. Exogenous zinc induced the appearance of novel GABA-mediated giant synaptic potentials in adult hippocampal neurones, while selective zinc-chelating agents inhibited similar synaptic potentials which occur naturally in immature CA3 neurones. This study suggests that zinc can differentially modulate inhibitory and excitatory synaptic transmission and for the first time demonstrated a physiological role for endogenous zinc in hippocampal synaptic transmission in young rats.

ACKNOWLEDGEMENTS

I would express my gratitude to my supervisor, Dr. Trevor Smart, for his invaluable guidance and encouragement throughout the course of my work for this thesis. In addition, not only am I indebted to him for the detailed critical reading of the manuscript of this thesis but also for his unstinting support outside my academic work.

I am grateful to the Medical Research Council for financial support.

I would like to thank Professor Norman Bowery for allowing me to work in the Department of Pharmacology and for his accessability as well as providing a good source for $GABA_B$ ideas.

I thank all my colleagues, particularly Derek Bowie, Chris Magnus and Belinda Krishek for their help and for the pleasant atmosphere that they created. My especial thanks are due to Professor Mike Simmonds and Dr. Andy Constanti for their helpful advice and discussion.

This study would not have been achieved without the help of the technical expertise of the Department: Chris Courtice (Electronics), Dave Tullett (Workshop), Derek King and Dave McCarthy (Photography), Steve Coppard (Animal House), Dave Khan (Teaching technician), Graham Withers (Laboratory Superintendent) and Angela Marshall (secretary).

I wish to thank Professor R.C. Hider (Kings College, London) for the kind provision of the zinc chelating agents.

I would like to take this opportunity to thank my M.Sc. supervisor, Professor Hu Benrong (Sun Yat-sen University of Medical Sciences, China), my M.D. supervisor, Professor Mike Bickel (University of Berne, Switzerland) and Professor Helmut Haas (Heinrich-Heine-Universität, Germany) for encouraging me to pursue a Ph.D. in London and showing continuous interest in my work and future career. I am also considerably indebted to Professor Haas for originally introducing me to hippocampal brain slice techniques.

Last, but by no means least, I thank my parents, Zhirong and Yuqin, my wife, Xiaosu and her parents, Li Zhenbang and Deng Shaoxian for their wholehearted support and encouragement at all times.

REFERENCES

Adams, P.R. & Galvan, M. (1986). Voltage-dependent current of vertebrate neurons and their role in membrane excitability. Advances in Neurology, **44**, 137-170.

Akaike, N., Yakushiji, T., Tokutomi, N. & Carpenter, D.O. (1987). Multiple mechanisms of antagonism of γ-aminobutyric acid (GABA) responses. Cell. Mol. Neurobiol., **7**, 97-103.

Alger, B.E. & Nicoll, R.A. (1980). Epileptiform burst afterhyperpolarization: calcium-dependent potassium potential in hippocampal CA1 pyramidal cells. Science, **210**, 1122-1124.

Alger, B.E. & Nicoll, R.A. (1982). Feed-forward dendritic inhibition in rat hippocampal pyramidal cells studied in vitro. J. Physiol., **328**, 105-123.

Alger, B.E. & Teyler, T.J. (1976). Long-term and short-term plasticity in the CA1, CA3 and dentate regions of the rat hippocampal slice. Brain Res. **110**, 463-480.

Amaral, D.G. & Witter, M.P. (1989). The three-dimensional organization of the hippocampal formation: a review of anatomical data. Neuroscience, **31**, 571-591.

Andersen, P., Eccles, J.C. & Løyning, Y. (1964). Pathway of postsynaptic inhibition in the hippocampus. J. Physiol. **27**, 608-619.

Andersen, P., Dingledine, R., Gjerstad, L., Langmoen, I.A. & Laursen, A.M. (1980). Two different responses of hippocampal pyramidal cells to application of gamma-amino butyric acid. J. Physiol., **305**, 279-296.

Anderson, W.W., Lewis, D.V. Swartzwelder, H.S. & Wilson, W.A. (1986). Magnesium-free medium activates seizure-like events in the rat hippocampal slice. Brain Res., **398**, 215-219.

Andrade, R., Malenka, R.C. & Nicoll, R.A. (1986). A G protein couples serotonin and $GABA_B$ receptors to the same channels in hippocampus. Science, **234**, 1261-1265.

Andreasen, M. & Lambert, J.D.C. (1991). Noradrenaline receptors participate in the regulation of GABAergic inhibition in area CA1 of the rat hippocampus. J. Physiol., **439**, 649-669.

Aniksztejn, L., Charton, G. & Ben-Ari, Y. (1987). Selective release of endogenous zinc from the hippocampal mossy fibres in situ. Brain Res., **404**, 58-64.

Aram, J.A., Michelson, H.B. & Wong, R.K.S. (1991). Synchronized GABAergic IPSPs recorded in the neocortex after blockade of synaptic transmission mediated by excitatory amino acids. J. Neurophysiol., **65**, 1034-1041.

Assaf, S.Y. & Chung S.H. (1984). Release of endogenous Zn^{2+} from brain tissue during activity. Nature, **308**, 734-736.

Audesirk, G. (1985). Effects of lead exposure on the physiology of neurons. Progress in Neurobiology. **24**, 199-231.

Avoli, M. (1988). GABAergic mechanisms and epileptic discharges. In: Avoli, M., Reader, T.A., Dykes, R.W. & Gloor, P. (eds) Neurotransmitters and cortical function. Plerum Press, New York, pp. 187-205.

Avoli, M. & Perreault, P. (1987). A GABAergic depolarizing potential in the hippocampus disclosed by the convulsant 4-aminopyridine. Brain Res., **400**, 191-195.

Ayala, G.F., Dichter, M. Gumnit, R.J., Matsumoto, H. & Spencer, W.A. (1973). Genesis of epileptic interictal spikes. New knowledge of cortical feedback systems suggests a neurophysiological explanation of brief paroxysms. Brain Res., **52**, 1-17.

Balcar, V.J., Pumain, R., Mark, J., Borg, J. & Mandel, P. (1978). GABA-mediated inhibition in the epileptogenic focus, a process which may be involved in the mechanism of the cobalt-induced epilepsy. Brain Res., **154**, 182-185.

Baranyi, A. & Fehér, O. (1979). Convulsive effects of 4-aminopyridine on cortical neurones. Electroencephalogr. Clin. Neurophysiol., **47**, 745-751.

Barbeau, A. & Donaldson, J. (1974). Zinc, taurine, and epilepsy. Arch Neurol., **30**, 52-58.

Bashir, Z.I., Alford, S., Davies, S.N., Randall, A.D. & Collingridge, G.L. (1991). Long-term potentiation of NMDA receptor-mediated synaptic transmission in the hippocampus. Nature, **349**, 156-158.

Baskys, A. (1992). Metabotropic receptors and 'slow' excitatory actions of glutamate agonists in the hippocampus. TINS., **3**, 92-96

Baudry, M., Arst, D., Oliver, M. & Lynch, G. (1981). Development of glutamate binding sites and their regulation by calcium in rat hippocampus. Dev. Brain Res., **1**, 37-48.

Begenisich, T. & Lynch, C. (1974). Effects of internal divalent cations on voltage-clamped squid axons. J. Gen. Physiol., **63**, 675-689.

Begenisich, T. (1988). The role of divalent cations in potassium channels. TINS., **11**, 270-273.

Ben-Ari, Y., Cherubini, E., Corradetti, R. & Gaiarsa, J.L. (1989). Giant Synaptic Potentials in immature rat CA3 hippocampal neurones. J. Physiol., **416**, 303-325.

Ben-Ari, Y., Cherubini, E. & Krnjević, K. (1988). Changes in voltage dependence of NMDA currents during development. Neurosci. Lett., **94**, 88-92.

Ben-Ari, Y., Krnjević, K. & Reinhardt, W. (1990). Hippocampal seizures and failure of inhibition. Canadian J. Physiol. Pharmacol., **57**, 1462-1466.

Ben-Ari, Y. & Represa, A. (1990). Brief seizure episodes induce long-term potentiation and mossy fibre sprouting in the hippocampus. TINS., **13**, 312-318.

Berry, M.S. & Pentreath, V.W. (1976). Criteria for distinguishing between monosynaptic and polysynaptic transmission. Brain Res., **105**, 1-20.

Bettger, W.J. & O'Dell, B.L. (1981). A critical physiological role of zinc in the structure and function of biomembranes. Life Sci., **28**, 1425-1438.

Bittiger, H., Froestl, W., Hall, R., Karlsson, G., Klebs, K., Olpe, H.-R., Pozza, M.F., Steinmann, M.W., van Riezen, H. (1990). Biochemistry, Electrophysiology and pharmacology of a new $GABA_B$ antagonist: CGP 35348. In: Bowery, N.G., Bittiger, H. & Olpe, H.-R. (eds) $GABA_B$ receptors in mammalian function. John Wiley & Sons, Chichester, New York, Brisbane, Toronto, Singapore, pp. 47-62.

Bliss, T.V.P. & Gardner-medwin, A.R. (1973). Long lasting potentiation of synaptic transmission in the dentate area of the unanaesthetized rabbit following stimulation of the perforant path. J. Physiol., **232**, 357-374.

Bliss, T.V.P. & Lomo, T. (1973). Long lasting potentiation of synaptic transmission in the dentate area of the anaesthetized rabbit following stimulation of the perforant path. J. Physiol., **232**, 331-356.

Bormann, J. (1988). Electrophysiology of $GABA_A$ and $GABA_B$ receptor subtypes. TINS., **11**, 112-116.

Bonanno, G., Cavazzani, P., Andrioli, G.C., Asaro, G., Pellegrini, G. & Raiteri, M. (1989). Release-regulating autoreceptors of the $GABA_B$ type in human cerebral cortex. Br. J. Pharmacol., **96**, 314-346.

Boulter, J., Hollmann, M. O'Shea-Greenfield, A., Hartley, M., Deneris, E., Maron, C. & Heinemann, S. (1990). Molecular cloning and functional expression of glutamate receptor subunit genes. Science, **249**, 1033-1037.

Bowery, N.G. (1989). $GABA_B$ receptors and their significance in mammalian pharmacology. TIPS., **10**, 401-407.

Bowery, N.G., Hill, G.R., Hudson, A.L., Doble, A., Middlemiss, D.N., Shaw, J. & Turnbull, M. (1980). (-)Baclofen decreases neurotransmitter release in the mammalian CNS by an action at a novel GABA receptor. Nature, **283**, 92-94.

Bowery, N.G., Hudson, A.L. & Price, G.W. (1987). $GABA_A$ and $GABA_B$ receptor site distribution in the rat central nervous system. Neuroscience, **20**, 365-383.

Brodie, M.S., Shefner, S.A. & Levy, R.A. (1982). Elevated divalent cation concentration decreases potassium-induced depolarization of bullfrog primary afferent fibres. Brain Res., **240**, 181-185.

Brown, D.A. (1990). G-proteins and potassium currents in neurones. Annu. Rev. Physiol., **52**, 215-242.

Brown, D.A. & Adams, P.R. (1980). Muscarinic suppression of a novel voltage-sensitive K^+ current in a vertebrate neurone. Nature, **283**, 673-676.

Brown, D.A. & Griffith, W.A. (1983). Calcium-activated outward current in voltage-clamped hippocampal neurones. J. Physiol. **337**, 287-301.

Buckle, P.J. & Haas, H.L. (1982). Enhancement of synaptic transmission by 4-aminopyridine in hippocampal slices if the rat. J. Physiol., **326**, 109-122.

Calabresi, P., Mercuri, N.B., Murtas, M.De. & Bernardi, G. (1991). Involvement of GABA systems in feedback regulation of glutamate- and GABA-mediated synaptic potentials in rat neostriatum. J. Physiol., **440**, 581-599.

Chamberlin, N.L. & Dingledine, R. (1988). GABAergic inhibition and the induction of spontaneous epileptiform activity by low chloride and high potassium in the hippocampal slice. Brain Res., **445**, 12-18.

Charpak, S. & Gähwiler, B.H., Do, K.Q. & Knöpfel, T. (1990). Potassium conductances in hippocampal neurons blocked by excitatory amino-acid transmitters. Nature, **347**, 765-767.

Charton, G., Rovira, C., Ben-Ari, Y. & Leviel, V. (1985). Spontaneous and evoked release of endogenous Zn^{2+} in the hippocampal mossy fibres zone of the rat in situ. Exp. Brain Res., **58**, 202-205.

Chavez-Noriega, L.E., Halliwell, J.V. & Bliss, T.V.P. (1990). A decrease in firing threshold observed after induction of the EPSP-spike (E-S) component of long-term potentiation in rat hippocampal slices. Exp. Brain Res., **79**, 633-641.

Chung, S.H. & Johnson, M.S. (1983a). Divalent transition-metal ions (Cu^{2+} and Zn^{2+})in the brains of epileptogenic and normal mice. Brain Res., **280**, 323-334.

Chung, S.H. & Johnson, M.S. (1983b). Experimentally induced susceptibility to audiogenic seizure. Exp. Neurol., **82**, 89-107.

Chvapil, M. (1973). New aspects in the biological role of zinc: a stabilizer of macromolecules and biological membranes. Life Sci., **13**, 1041-1049.

Claiborne, B.J., Rea, M.A. & Terrian, D.M. (1989). Detection of zinc in isolated nerve terminals using a modified Timm's sulfide-silver method. J. Neurosci. Meth., **30**, 17-22.

Colino, A. & Halliwell, J.V. (1987). Differential modulation of three separate K-conductances in hippocampal CA1 neurons by serotonin. Nature, **327**, 73-77.

Collingridge, G.L., Kehl. S.J. & McLennan, H. (1983). Excitatory amino acids in synaptic transmission in the Schaffer-collateral commissural pathway of the rat hippocampus. J. Physiol., **334**, 33-46.

Collins, G.G.S., Anson, J. & Surtees, L. (1983). Presynaptic kainate and N-methyl-$_D$-aspartate receptors regulate excitatory amino acid release in the olfactory cortex. Brain Res., **265**, 157-159.

Constanti, A., Connor, J.D., Galvan, M. & Nistri, A. (1980). Intracellularly-recorded effects of glutamate and aspartate on neurones in the guinea-pig olfactory cortex slice. Brain Res., **195**, 403-420.

Constanti, A. & Smart, T.G. (1987). Zinc blocks the A-current in cultured rat sympathetic neurones. J. Physiol., **396**, 159p.

Cooper, G.P., Suszkiw, J.B. & Manalis, R.S. (1984). Heavy metals: effects on synaptic transmission. Neuro. Toxicol. **5**, 247-266.

Crawford, I.L. (1983). Zinc and the hippocampus, Histology, neurochemistry, pharmacology and putative functional relevance. In: Dreosti, I.E. & Smith, R.M. (eds) Neurobiology of the trace elements. Volume 1, Trace element neurobiology and deficiencies. Humana Press, Clifton, New Jersey, pp. 163-211.

Crawford, I.L., Doller, H.J. & Connor, J.D. (1973). Diphenylthiocarbazone effects on evoked waves and zinc in the rat hippocampus. Pharmacologist, **15**, 197p.

Crawford, I.L. & Connor, J.D. (1972). Zinc in maturing rat brain: hippocampal concentration and localization. J. Neurochem., **19**, 1451-1458.

Crawford, I.L. & Connor, J.D (1973). Localization and release of glutamic acid in relation to the hippocampal mossy fibre pathway. Nature, **244**, 442-443.

Crawford, I.L. & Connor, J.D. (1975). Zinc and hippocampal function. Orthomolecular Psychiatry, **4**, 39-52.

Crawford, A.C. & McBurncy, R.N. (1977). The synergistic action of L-glutamate and L-aspartate at crustacean excitatory neuromuscular junctions. J. Physiol., **268**, 697-709.

Croucher, M.J., Collins, J.F. & Meldrum, B.S. (1982). Anticonvulsant action of excitatory amino acid antagonists. Science, **216**, 899-901.

Csermely, P., Szamel, M., Resch, K. & Somogyi, J. (1988). Zinc increases the activity of protein kinase C and contributes to its binding to plasma membrane in T lymphocytes. J. Biol. Chem., **263**, 6487-6490.

Curtis, D.R., Duggan, A.W., Felix, D. & Johnston, G.A.R. (1971). Bicuculline, an antagonist of GABA and synaptic inhibition in the spinal cord of the cat. Brain Res., **32**, 69-96.

Curtis, D.R., Gynther, B.D., Beattie, D.T., Kerr, D.I.B. & Prager, R.H. (1988). Baclofen antagonism by 2 hydroxy-saclofen in the cat spinal cord. Neurosci. Lett., **92**, 97-101.

Dames, W., Joo, F., Feher, O., Toldi, J. & Wolff, J.R. (1985). γ-aminobutyric acid enables synaptogenesis in the intact superior cervical ganglion of the adult rat. Neurosci. Lett., **54**, 159-164.

Danscher, G., Fjerdingstad, E.J., Fjerdingstad, E. & Fredens, K. (1976). Heavy metal content in subdivisions of the rat hippocampus (zinc, lead and copper). Brain Res., **112**, 442-446.

Danscher, G., Shipley, M.T. & Andersen, P. (1975). Persistent function of mossy fibre synapses after metal chelation with DEDTC (Antabuse). Brain Res., **85**, 522-526.

Davies, C.H., Davies, S.N. & Collingridge, G.L. (1990). Paired-pulse depression of monosynaptic GABA-mediated inhibitory postsynaptic responses in rat hippocampus. J. Physiol., **424**, 513-531.

Davies, J., Francis, A.A., Jones, A.W. & Watkins, J.C. (1981). 2-Amino-5-phosphonovalerate (2APV), a potent and selective antagonist of amino acid-induced and synaptic excitation. Neurosci. Lett., **21**, 77-81.

Davies, S.N. & Collingridge, G.L. (1989). Role of excitatory amino acid receptors in synaptic transmission in area CA1 of rat hippocampus. Proc. R. Soc. Lond. B, **236**, 373-384.

Dencker, L & Tjalve, H. (1979). An autoradiographic study on the fate of Zn-65 in zinc-rich tissues in some rodents. Med. Biol., **57**, 391-397.

Deisz, R.A. & Prince, D.A. (1989). Frequency-dependent depression of inhibition in guinea-pig neocortex *in vitro* by $GABA_B$ receptor feed-back on GABA release. J. Physiol., **402**, 513-541.

Dencker, L. & Tjalve, H. (1979). An autoradiographic study on the fate of Zn^{65} in zinc-rich tissues in some rodents. Med. Biol., **57**, 391-397.

Dingledine, R. (1984). Hippocampus: Synaptic pharmacology. In: Dingledine, R. (eds) Brain slices. Plenum Press. New York and London, pp: 87-112.

Dingledine, R. (1991). New wave of non-NMDA excitatory amino acid receptors. TiPS. **12**, 360-362.

Dingledine, R. & Gjerstad, L. (1980). Reduced inhibition during epileptiform activity in the in vitro hippocampal slice. J. Physiol., **305**, 297-313.

Dingledine, R., Hynes, M.A. & King, G.L. (1986). Involvement of N-methyl-D-aspartate receptors in epileptiform bursting in the rat hippocampal slice. J. Physiol., **380**, 175-189.

Docherty, R.J. & Halliwell, J.V. (1984). 4-Aminopyridine reveals a novel response to baclofen in the rat interpeduncular nucleus in vitro. J. Physiol., **357**, 18p.

Domann, R., Dorn, T. & Witte O.W. (1989). Calcium-dependent potassium current following penicillin-induced epileptiform discharges in the hippocampal slice. Exp. Brain Res., **78**, 646-648.

Donaldson, J., St-Pierre, T., Minnich, J. & Barbeau, A. (1971). Seizures in rats associated with divalent cation inhibition of Na^+-K^+-ATP'ase. Canadian J. Biochemistry, **49**, 1217-1224.

Donaldson, J., St-Pierre, T., Minnich, J. & Barbeau, A. (1973) Determination of Na^+, K^+, Cu^{2+}, Zn^{2+} and Mn^{2+} in rat brain regions. Can. J. Biochem., **51**, 87-92.

Draguhn, A., Verdorn, T.A., Ewert, M., Seeburg, P.H. & Sakmann, B. (1990). Functional and molecular distinction between recombinant rat $GABA_A$ receptor subtypes by Zn^{2+}. Neuron, **5**, 781-788.

Dreixler & Leonard. (1991). Zinc potentiates desensitized kainate currents of a glutamate receptor clone (GluR3). Neuroscience, **17**, 33.13P.

Dreosti, I.E. (1989). Neurobiology of zinc. In: Mills, C.F. (eds) Zinc in human biology. Springer-Verlag, London, Berlin, Heidelberg, New York, Paris, Tokyo, pp. 235-248.

Dreosti, I.E., Manuel, S.J., Buckley, R.A., Fraser, F.S. & Record, I.R. (1981). The effect of late prenatal and/or early postnatal zinc deficiency on the development and some biochemical aspects of the cerebellum and hippocampus in rats. Life Sci., **28**, 2133-2141.

Dutar, P. & Nicoll, R.A. (1988a). A physiological role for $GABA_B$ receptors in the central nervous system. Nature, **332**, 156-158.

Dutar, P. & Nicoll, R.A. (1988b). Pre- and postsynaptic $GABA_B$ receptors in the hippocampus have different pharmacological properties. Neuron, **1**, 585-591.

Dvergsten, C.L., Johnson, L.A. & Sandstead, H.H. (1984). Alteration in the postnatal development of the cerebellar cortex due to zinc deficiency. Dev. Brain Res., **16**, 21-26.

Ebadi, M. & Pfeiffer, R.F. (1984). Zinc in neurological disorders and experimentally induced epileptiform seizures. In: Frederickson, C.J., Howell, G.A. & Kasarskis, E.J. (eds) The Neurobiology of zinc. Part B: Deficiency, toxicity and pathology, Alan R. Liss, Inc., New York, pp. 307-324.

Egebjerg, J., Bettler, B., Hermans-Borgmeyer, I. & Heinemann, S. (1991). Cloning of a cDNA for a glutamate receptor subunit activated by kainate but not AMPA. Nature, **351**, 745-748.

Euler, C. von. (1961). On the significance of the high zinc content in the hippocampal formation. In: Passonant, P. (eds) Physiologie de I'hippocampe. Editions du centre national de la recherche scientifique, Paris, pp. 135-345.

Forsythe, I.D. & Clements, J.D. (1990). Presynaptic glutamate receptors depress excitatory monosynaptic transmission between mouse hippocampal neurones. J. Physiol., **429**, 1-16.

Forsythe, I.D., Westbrook, G.L. & Mayer, M.L. (1988). Modulation of excitatory synaptic transmission by glycine and zinc in cultures of mouse hippocampal neurons. J. Neurosci., **8**, 3733-3741.

Frederickson, C.J. (1989). Neurobiology of zinc and zinc-containing neurones. Inter. Rew. Neurobiol., **31**, 145-328.

Frederickson, C.J., Hernandez, M.D. Goik, S.A., Morton, J.D. & McGinty, J.F. (1988). Loss of zinc staining from hippocampal mossy fibres during kainic acid induced seizures: a histofluorescence study. Brain Res., **446**, 383-386.

Frederickson, C.J., Howell, G.A. & Frederickson, M.H. (1981). Zinc dithizonate staining in the cat hippocampus: relationship to the mossy-fiber neuropil and postnatal development. Exp. Neurology, **73**, 812-823.

Frederickson, C.J., Kasarskis, E.J., Ringo, D. & Frederickson, R.E. (1987). A quinoline fluorescence method for visualizing and assaying the histochemically reactive zinc (bouton zinc)in the brain. J. Neurosci. Meth., **20**, 91-103.

Frederickson, C.J., Klitenick, M.A., Manton, W.I. & Kirkpatrick, J.B. (1983). Cytoarchitectonic distribution of zinc in the hippocampus of man and rat. Brain Res., **273**, 335-339.

Frotscher, M. (1985). Mossy fibres form synapses with identified pyramidal basket cells in the CA3 region of the guinea-pig hippocampus: a combined Golgi-electron microscope study. J. Neurocytol., **14**, 245-259.

Fukahori, M. & Itoh, M. (1990). Effects of dietary zinc status on seizure susceptibility and hippocampal zinc content in the El (epilepsy) mouse. Brain Res., **529**, 16-22.

Fukahori, M., Itoh, M., Oomagari, K. & Kawasaki, H. (1988). Zinc content in discrete hippocampal and amygdaloid areas of the epilepsy (EI) mouse and normal mice. Brain Res., **455**, 381-384.

Gabrielsson, B., Robson, T., Norris, D. & Chung S.H. (1986). Effects of divalent metal ions on the uptake of glutamate and GABA from synaptosomal fractions. Brain Res., **384**, 218-223.

Gähwiler, B.H. & Brown, D.A. (1985). $GABA_B$-receptor-activated K^+ current in voltage-clamped CA_3 pyramidal cells in hippocampal cultures. Proc. Natl. Acad. Sci. USA, **82**, 1558-1562.

Gaiarsa, J.L., Corradetti, R., Cherubini, E. & Ben-Ari, Y. (1990). The allosteric glycine site of the N-methyl-D-aspartate receptor modulates GABAergic-mediated synaptic events in neonatal rat CA3 hippocampal neurons. Proc. Natl. Acad. Sci. USA, **87**, 343-346.

Gerber, U. & Gähwiler, B.H. (1991). Cobalt blocks postsynaptic responses induced by neurotransmitters in the hippocampus *in vitro*. Neurosci. Lett., **134**, 53-56.

Gilbertson, T.A., Scobey, R. & Wilson, M. (1991). Permeation of calcium ions through non-NMDA glutamate channels in retinal bipolar cells. Science, **251**, 1613-1615

Goldberg, H.J. & Sheehy, E.M. (1982). Fifth day fits: an acute zinc deficiency syndrome? Arch. Dis. Child, **57**, 633-635.

Griffith, W.H. (1990). Voltage-clamp analysis of post-tetanic potentiation of the mossy fiber to CA3 synapse in hippocampus. J. Neurophysiol., **63**, 491-501.

Gustafsson, B., Galvan, M., Grafe, P., & Wigström, H. (1982). A transient outward current in a mammalian central neurone blocked by 4-aminopyridine. Nature, **299**, 252-254.

Haas, H.L. & Greene, R.W. (1986). Effects of histamine on hippocampal pyramidal cells of the rat in vitro. Exp Brain Res., **62**, 123-130.

Haas, H.L., Greene, R.W. Heimrich, B. & Xie, X. (1988). Long-term potentiation in slices from human hippocampus. In: Haas, H.L. & Buzsáki, G. (eds) Synaptic Plasticity in the hippocampus. Springer-Verlag Berlin Heidelberg, pp. 77-80.

Haas, H.L., Grenn, K.W. & Olpe, H.-R. (1985). Stereoselectivity of L-baclofen in hippocampal slices of rat. Neurosci. Lett., **55**, 1-4.

Haas, H.L. & Rose, G. (1982). Long-term potentiation of excitatory synaptic transmission in the hippocampus: the role of inhibitory processes. J. Physiol., **329**, 541-552.

Haas, H.L. & Rose, G. (1984). The role of inhibitory mechanisms in hippocampal long-term potentiation. Neurosci. Lett., **47**, 301-306.

Haas, H.L., Xie, X. & Lui, S.Y. (1986). Analysis of the actions of stepping inducing substance II (SIS-II) on hippocampal slices of the rat. Chinese J. Physiol. Sci., **2**, 350-355.

Hablitz, J.J. (1985). Action of excitatory amino acids and their antagonists on hippocampal neurons. Cell. Mol. Neurobiol., **5**, 389-405.

Halliwell, J.V. & Adams, P.R. (1982). Voltage-clamp analysis of muscarinic excitation in hippocampal neurons. Brain Res., **250**, 71-92.

Harris, K.M. & Miller, R.J. (1988). Excitatory amino acid-evoked release of [^{3}H] GABA from hippocampal neurons in primary culture. Brain Res., **482**, 23-33.

Harris, K.M. & Teyler, T.J. (1983). Evidence for late development of inhibition in area CA1 of the rat hippocampus. Brain Res., **268**, 339-343.

Harris, K.M. & Teyler T.J. (1984). Developmental onset of long-term potentiation in area CA1 of the rat hippocampus. J. Physiol., **346**, 27-48.

Harris, N.C., Webb, C. & Greenfield, S.A. (1989). A possible pacemaker mechanism in pars compacta neurons of the guinea-pig substantia nigra revealed by various ion channel blocking agents. Neuroscience, **31**, 355-362.

Harrison, N.L. (1990). On the presynaptic action of baclofen at inhibitory synapses between cultured rat hippocampal neurones. J. Physiol., **422**, 433-446.

Harrison, N.L., Lambert, N.A. & Lovinger, D.M. (1990). Presynaptic $GABA_B$ receptors on rat hippocampal neurons. In: Bowery, N.G., Bittiger, H. & Olpe, H.-R. (eds) $GABA_B$ receptors in mammalian function. John Wiley & Sons, Chichester, New York, Brisbane, Toronto, Singapore, pp. 207-221.

Hartter, D.E. & Barnea, A. (1988). Evidence for release of copper in the brain: depolarization-induced release of newly take-up ^{67}copper. Synapse, **2**, 412-415.

Hassler, O. & Söremark, R. (1988). Accumulation of zinc in mouse brain. Arch. Neurol., **19**, 117-120.

Haug, F.M. (1967). Electron microscopical localization of the zinc in hippocampal mossy fibre synapses by a modified sulphide sliver procedure. Histochemie., **8**, 355-368.

Haug, F.M. (1973). Heavy metals in the brain. A light microscopic study of the rat with Timm's sulphide silver dendritic morphology of pyramidal neurones in the rat hippocampal CA3 area. I. Cell types. Brain Res., **479**, 105-114.

Hegstad, E., Langmoen, I.A. & Hablitz, J.J. (1989). Zinc and glycine do not modify low-magnesium-induced epileptiform activity in the immature neocortex in vitro. Epilepsy Res., **3**, 174-177.

Heidelberger, R. & Matthews, G. (1991). Inhibition of calcium influx and calcium current by γ-aminobutyric acid in single synaptic terminals. Proc. Natl. Acad. Sci. USA., **88**, 7135-7139.

Henkin, R .I. Patten, B.M., Re, P.K. & Bronzert, D.A. (1975). A Syndrome of acute zinc loss. Cerebellar dysfunction, mental changes, anorexia and taste and smell dysfunction. Arch. Neurol., **32**, 745-752.

Hesse, G.W. (1979). Chronic zinc deficiency alters neuronal function of hippocampal mossy fibres. Science, **205**, 1005-1007.

Hesse, G.W., Hesse, K.A. & Catalanotlo, F.A. (1979). Behavioral characteristics of rats experiencing chronic zinc deficiency. Physiology & Behavior, **22**, 211-215.

Hider, R.C., Ejim, L., Taylor, P.D., Gale, R., Huehns, E. & Porter, J.B. (1990). Facilitated uptake of zinc into human erythrocytes. Relevance to the treatment of sickle-cell anaemia. Biochem. Pharmacol., **39**, 1005-1012.

Hill, D.R. & Bowery, N.G. (1981). ^{3}H-baclofen and ^{3}H-GABA bind to bicuculline-insensitive $GABA_B$ sites in rat brain. Nature, **290**, 149-152.

Hirata, K., Sawada, S. & Yamanoto, C. (1991). Enhancement of transmitter release accompanying with long-term potentiation in synapses between mossy fibers and CA3 neurones in hippocampus. Neurosci. Lett., **123**, 73-76.

Hollmann, M., Hartley, M. & Heinemann, S. (1991). Ca^{2+} permeability of KA-AMPA-gated glutamate receptor channels depends on subunit composition. Science, **252**, 851-853.

Hollmann, M., O'Shea-Greenfield, A., Rogers, S.W. & Heinemann, S. (1989). Cloning by functional expression of a member of the glutamate receptor family. Nature, **342**, 643-648.

Holm, I.H., Andreasen, A., Danscher, G., Pérez-Clausell, J. & Nielsen, H. (1988). Quantification of vesicular zinc in the rat brain. Histochemistry, **89**, 289-293.

Honoré, T., Davies, S.N., Drejer, J., Fletcher, E.J., Jacobsen, P., Lodge, D. & Nielsen, E. (1988). Quinoxalinediones: potent competitive non-N-mehtyl-D-aspartate glutamate receptor antagonists. Science, **241**701-703.

Hori, N. & Carpenter, D.O. (1988). Excitatory amino acid receptors in piriform cortex do not show receptor desensitization. Brain Res., **457**, 350-354.

Hori, N., ffrench-Mullen, J.M.H. & Carpenter, D.O. (1985). Kainic acid responses and toxicity show pronounced Ca^{2+} dependence. Brain Res., **358**, 380-384.

Hori, N., Galeno, T., & Carpenter, D.O. (1987). Responses of Pyriform cortex neurons to excitatory amino acids: voltage dependence, conductance changes, and effects of divalent cations. Cell. and Mol. Neurobiol., **7**, 73-90.

Horikawa, K. & Armstrong, W.E. (1988). A versatile means of intracellular labeling: injection of biocytin and its detection with avidin conjugates. J. Neurosci. Meth., **25**, 1-11

Horne, A.L., Harrison, N.L., Turner, J.P. & Simmonds, M.A. (1986). Spontaneous paroxysmal activity induced by zero magnesium and bicuculline: suppression by NMDA antagonists and GABA mimetics. Eur. J. Pharmacol., **122**, 231-238.

Howell, G.A., Welch, M.G. & Frederickson, C.J. (1984). Stimulation-induced uptake and release of zinc in hippocampal slices. Nature, **308**, 736-738.

Hu, K.H. & Friede, R.L. (1968). Topographic determination of zinc in human brain by atomic absorption spectrophotometry. J. Neurol., **15**, 677-685.

Hubbard, S.R., Bishop, W.R., Kirschmeier, P., George, S.J., Cramer, S.P. & Hendrickson, W.A. (1991). Identification and characterization of zinc binding sites in protein kinase C. Science, **254**, 1776-1779.

Ibata, Y. & Otsuka, N. (1969). Electron microscopic demonstration of zinc in the hippocampal formation using Timm's sulphide silver technique. J. Histochem. Cytochem. **17**, 171-175.

Inoue, M., Matsuo, T. & Ogata, N. (1985a). Baclofen activates voltage-dependent and 4-aminopyridine sensitive K^+ conductance in guinea-pig hippocampal pyramidal cells maintained in vitro. Br. J. Pharmacol., **84**, 833-841.

Inoue, M., Matsuo, T. & Ogata, N. (1985b). Possible involvement of K^+-conductance in the action of γ-aminobutyric acid in the guinea-pig hippocampus. Br. J. Pharmacol., **86**, 515-524.

Itoh, M. & Ebadi, M. (1982). The selective inhibition hippocampal glutamic acid decarbaxylase (BAb) in Zinc-induced epileptic seizures. Neurochem. Res., **7**, 1287-1290.

Itoh, M., Ebadi, M. & Swanson, S. (1983). The presence of Zinc binding proteins in brain. J. Neurochem., **41**, 823-833.

Ives, A.E. & Jefferys, J.G.R. (1990). Synchronization of epileptiform bursts induced by 4-aminopyridine in the vitro hippocampal slice. Neurosci. lett., **112**, 239-245.

Iyengar, G.V. (1987). Reference values for the concentrations of As, Cd, Co, Cr, Cu, Fe, I, Hg, Mn, Mo, Ni, Pb, Se, and Zn in selected human tissues and body fluids. Biological Trace Element Research, **12**, 263-295.

Jackson, M.J. (1989). Physiology of zinc: general aspects. In: Mills, C.F. (eds) Zinc in human biology. Springer-Verlag, London, Berlin, Heidelberg, New York, Paris, Tokyo, pp. 1-14.

Johnson, J.W. & Ascher, P. (1987). Glycine potentiates the NMDA response in cultured mouse brain neurons. Nature, **325**, 529-531.

Johnston, D. & Brown, T.H. (1981). Giant synaptic potential hypothesis for epileptiform activity. Science, **211**, 294-297

Johnston, D. & Brown, T.H. (1984). Mechanisms of neuronal burst generation. In: Schwartzkroin, P.A. & Wheal, H.V. (eds) Electrophysiology of epilepsy. Academic Press, London, Orlando, San Diego, San Francisco, New York, Toronto, Montreal, Tokyo, São Paulo, pp. 277-301.

Jones, R.S.G. & Heinemann, U. (1989). Spontaneous activity mediated by NMDA receptors in immature rat entorhinal cortex in vitro. Neurosci. Lett., **104**, 93-98.

Jones, M.G., Li, Y., Lodge, D. & Millar, J.A. (1989). Failure of tricyclic antidepressants and zinc to produce selective antagonism of nmda in rat brain in vitro and in vivo. Br. J. Pharmacol., **97**, 376p.

Kasarskis, E.J., Manton, W.I., Devenport, L.D., Kirkpatrick, J.B., Howell, G.A., Klitenick, M.A. & Frederickson, C.J. (1985). Effects of alcohol injection on zinc content of human and rat central nervous system. Exp. Neurol., **90**, 81-95.

Kauer, J.A., Malenka, R.C. & Nicoll, R.A. (1988). A persistent postsynaptic modification mediates long-term potentiation in the hippocampus. Neuron, **1**, 911-917.

Kawaguchi, Y. & Wilson, C.J. & Emson, P.C. (1989). Intracellular recording of identified neostriatal patch and matrix spiny cells in a slice preparation preserving cortical inputs. J. Neurophysiol., **62**, 1052-1068.

Kerr, D.I.B., Ong, J., Prager, R.H. Gynther, B.D. & Curtis, D.R. (1987). Phaclofen: a peripheral and central baclofen antagonist. Brain Res., **405**, 150-154.

Khulusi, S.S., Brown, M.W. & Wright, D.M. (1986). Zinc and paired-pulse potentiation in the hippocampus. Brain Res., **363**, 152-155.

Kihara, T., Baba, A., Koyama, Y., Ishihara, T. & Iwata, H. (1990). Inhibition of [^{3}H] glutamate release by Zn^{2+} in rat hippocampal slices. J. Pharmacobio-Dyn., **13**, 321-326.

Kita, H. & Armastrong, W. (1991). A biotin-containing N-(2-aminoethyl) biotinamide for intracellular labelling and neuronal tracing studies: comparison with biocytin. J. Neurosci. Meth., **37**, 141-150.

Krnjević, K. (1976). Inhibitory action of GABA and GABA-mimetics on vertebrate neurones. In: Roberts, E., Chase, T.N. & Tower, D.B. (eds) GABA in nervous system function. Raven Press, New York, pp. 269-382.

Krnjević, K., Lamour, Y., Macdonald, J.F. & Nistri, A. (1979). Depression of monosynaptic excitatory postsynaptic potentials by Mn^{2+} and Co^{2+} in cat spinal cord. Neuroscience, **4**, 1331-1339.

Kumar, K.N., Tilakaratne, N., Johnson, P.S., Allen, A.E. & Michaelis, E.K. (1991). Cloning of cDNA for the glutamate-binding subunit of an NMDA receptor complex. Nature, **354**, 70-73.

Kushner, L., Lerma, J., Zukin, R.S. & Bennett, M.V.L. (1988). Coexpression of N-methyl-D-aspartate and phencyclidine receptors in Xenopus oocytes injected with rat brain mRNA. Proc. Natl. Acad. Sci. USA, **85**, 3250-3254.

Lacaille, J-C. Schwartzkroin, P.A. (1988a). Stratum Lacunosum-Moleculare interneurones of hippocampal CA1 region. I. Intracellular response characteristics, synaptic responses, and morphology. J. Neuroscience **8**, 1400-1410.

Lacaille, J-C. Schwartzkroin, P.A. (1988b). Stratum Lacunosum-Moleculare interneurones of hippocampal CA1 region. II. Intrasomatic and intradendritic recordings of local circuit synaptic interactions. J. Neuroscience **8**, 1411-1424.

Lam, K.H.K., Palmer, A.J., Millar, J.D. & Lodge, D. (1991). Effects of lead, zinc, and other divalent cations on responses of cortical slices to excitatory amino acids. Br. J. Pharmacol. **102**, 134P.

Lambert, J.D.C., Jones, R.S.G., Andreasen, M., Jensen, M.S. & Heinemann, U. (1989). The role of excitatory amino acids in synaptic transmission in the hippocampus. Comp. Biochem. Physiol., **93A**, 195-201.

Lambert, J.J., Peters, J.A. & Cottrell, G.A. (1987). Actions of synthetic and endogenous steroids on the $GABA_A$ receptor. TIPS, **8**, 224-227.

Lambert, N.A., Harrison, N.L., Kerr, D.I.B., Ong, J., Prager, R.H. & Teyler, T.J. (1989). Blockade of the late IPSP in the rat CA1 hippocampal neurons by 2-hydroxy-saclofen. Neurosci. Lett., **107**, 125-128.

Lambert, N.A., Levitin, M. & Harrison, N.L. (1992). Induction of giant depolarizing potentials by zinc in area CA1 of the rat hippocampus does not result from block of $GABA_B$ receptors. Neurosci. Lett., **135**, 215-218.

Lancaster, B. & Adams, P.R. (1986). Calcium-dependent current generating the afterhyperpolarization of hippocampal neurons. J. Neurophysiol., **55**, 1268-1282.

Laroche, S., Doyere, V. & Bloch, V. (1989). Linear relation between the magnitude of long-term potentiation in the dentate gyrus and associative learning in the rat. A demonstration using commissural inhibition and local infusion of an N-methyl-D-aspartate receptor antagonist. Neuroscience, **28**, 375-386.

Lee, W.L. & Hablitz, J.J. (1989). Involvement of non-NMDA receptors in picrotoxin-induced epileptiform activity in the hippocampus. Neurosci. Lett., 129-134.

Legendre, P. & Westbrook, G.L. (1991). Noncompetitive inhibition of γ-aminobutyric $acid_A$ channels by Zn. Mol. Pharmacol., **39**, 267-274.

Levitan, E.S., Schofield, P.R., Burt, D.R., Rhees, L.M., Wisden, W., Köhler, M., Fujita, N., Rodriguez, H.F., Stephenson, A., Darlison, M.G. Barnard, E.A., & Seeburg, P.H. (1988). Structural and functional basis for $GABA_A$ receptor heterogeneity. Nature, **335**, 76-79.

Macdonald, T.L. & Martin, R.B. (1988). Aluminum ion in biological systems. TIBS., **13**, 15-19.

Madison, D.V. & Nicoll. R.A. (1984). Control of the repetitive discharge of rat CA1 pyramidal neurones *in vitro*. J. Physiol., **354**, 319-331.

Madison, D.V. & Nicoll. R.A. (1988). Norepinephrine decreases synaptic inhibition in the rat hippocampus. Brain Res., **442**, 131-138.

Malenka, R.C., Kauer, J.A., Zucker, R.S. & Nicoll, R.A. (1988). Postsynaptic calcium is sufficient for potentiation of hippocampal synaptic transmission. Science, **242**, 81-84.

Malenka, R.C., Kauer, J.A. Perkel, D.J. & Nicoll, R.A. (1989). The impact of postsynaptic calcium on synaptic transmission-its role in long-term potentiation. Tins, **12**, 444-450.

Malenka, R.C., Madison, D.V. & Nicoll, R.A. (1986). Potentiation of synaptic transmission in the hippocampus by phorbol esters. Nature, **321**, 175-177.

Malinow, R. & Tsien, R.W. (1990). Presynaptic enhancement shown by whole-cell recordings of long-term potentiation in hippocampal slices. Nature, **346**, 177-180.

Maske, H. (1955). Über den topochemischen Nachweis von Zink im Ammonshorn verschiedener Säugetiere, Naturwissenschaften, **42**, 424.

Masu, M., Tanabe, Y., Tsuchida, K., Shigemoto, R. & Nakanishi, S. (1991). Sequence and expression of a metabotropic glutamate receptor. Nature, 349, 760-765.

Matsumoto, H & Marsan, C.A. (1964). Cortical cellular phenomena in experimental epilepsy: ictal manifestations. Exp. Neurol., **9**, 305-326.

Mattson, M.P. (1988). Neurotransmitters in the regulation of neuronal cytoarchitecture. Brain Res. Rev., **13**, 179-212.

Mayer, M.L. & Westbrook, G.L. (1984). Mixed-agonist action of excitatory amino acids on mouse spinal cord neurones under voltage clamp. J. Physiol., **354**, 29-53.

Mayer, M.L. & Westbrook, G.L. (1985). The action of N-methyl-D-aspartic acid on mouse spinal neurones in culture. J. Physiol., **361**, 65-90.

Mayer, M.L., Westbrook, G.L. & Guthrie, P.B. (1984). Voltage-dependent block by Mg^{2+} of NMDA responses in spinal cord neurones. Nature, **309**, 261-263.

Mayer, M.L. & Vyklicky J_R, L. (1989). The action of zinc on synaptic transmission and neuronal excitability in cultures of mouse hippocampus. J. Physiol., **415**, 351-365.

Mayer, M.L., Vyklicky J_R, L. & Westbrook, G.L. (1989). Modulation of excitatory amino acid receptors by group IIB metal cations in cultured mouse hippocampal neurones. J. Physiol., **415**, 329-350.

McCarren, M. & Alger, B.E. (1985). Use-dependent depression of IPSPs in rat hippocampal pyramidal cells *in vitro*. J. Neurophysiol., **53**, 557-571.

Mesher, R.A. & Schwartzkroin, P.A. (1980). Can CA3 epileptiform discharge induce bursting in normal CA1 hippocampal neurons? Brain Res., **183**, 472-476.

Michelson, H.B. & Wong, R.K.W. (1991). Excitatory synaptic responses mediated by $GABA_A$ receptors in the hippocampus. Science, **253**, 1420-1423.

Miles, R. & Wong, R.K.S. (1984). Unitary inhibitory synaptic potentials in the guinea-pig hippocampus in vitro. J. Physiol., **356**, 97-113.

Miles, R & Wong, R.K.S. (1986). Excitatory synaptic interactions between CA3 neurones in the guinea-pig hippocampus. J. Physiol., **373**, 397-418.

Miller, R.J. (1991). The revenge of the kainate receptor. TINS, **14**, 477-479.

Mody, I., Lambert, J.D.C. & Heinemann, U. (1987). Low extracellular magnesium induces epileptiform activity and spreading depression in rat hippocampal slices. J. Neurophysiol., **57**, 869-888.

Mody, I. & Miller, J.J. (1984). Levels of hippocampal calcium and zinc following kindling-induced epilepsy. Canadian. J. Physiol. Pharmacol., **63**, 159-161.

Moriyoshi, K., Masu, M., Ishii, T., Shigemoto, R., Mizuno, N. & Nakanishi, S. (1991). Molecular cloning and characterization of the rat NMDA receptor. Nature, **354**, 31-37.

Morton, J.D., Howell, G.A. & Frederickson, C.J. (1990). Effects of subcutaneous injections of zinc chloride on seizures induced by noise and by kainic acid. Epilepsia, **31**, 139-144.

Muller, W. & Misgeld, U. (1991). Picrotoxin- and 4-aminopyridine-induced activity in hilar neurons in the guinea-pig hippocampal slice. J. Neurophysiol., **65**, 141-147.

Mueller, A.L., Taube, J.S. & Schwartzkroin, P.A. (1983). Development of hyperpolarizing inhibitory postsynaptic potentials and hyperpolarizing response to γ-aminobutyric acid in rabbit hippocampus studied in vitro. J. Neurosci., **4**, 860-867.

Muller, D., Oliver, M. & Lynch, G. (1989). Developmental changes in synaptic properties in hippocampus of neonatal rats. Dev. Brain Res., **49**, 105-114.

Neuman, R., Cherubini, E. & Ben-Ari, Y. (1988). Epileptiform bursts elicited in CA3 hippocampal neurons by a variety of convulsants are not blocked by N-methyl-D-aspartate antagonists. Brain Res., **459**, 265-274.

Neuman, R.S. Cherubini, E. & Ben-Ari, Y. (1989). Endogenous and network bursts induced by N-methyl-D-aspartate and magnesium free medium in the CA3 region of the hippocampal slice. Neuroscience, **28**, 393-399.

Newberry, N.R. & Nicoll, R.A. (1984). Direct hyperpolarizing action of baclofen on hippocampal pyramidal cells. Nature, **308**, 450-452.

Nicoll, R.A. & Alger, B.E. (1981). Synaptic excitation may activate a calcium-dependent potassium conductance in hippocampal pyramidal cells. Science, **212**, 957-959.

Nicoll, R.A., Kauer, J.A. & Malenka, R.C. (1988). The current excitement in LTP. Neuron, **1**, 97-103.

Nicoll, R.A. & Dutar, P. (1990). Pre- and postsynaptic $GABA_B$ responses in the hippocampus. In: Bowery, N.G., Bittiger, H. & Olpe, H.-R. (eds) $GABA_B$ receptors in mammalian function. John Wiley & Sons, Chichester, New York, Brisbane, Toronto, Singapore, pp. 197-205.

Nishimura, M. (1987). Zinc competitively inhibits calcium-dependent release of transmitter at the mouse neuromuscular junction. Pflügers Arch., **410**, 623-626.

Nishimura, M. (1988). Zn^{2+} stimulates spontaneous transmitter release at mouse neuromuscular junctions. Br. J. Pharmacol., **93**, 430-436.

Nitsch, R., Soriano, E. & Frotscher, M. (1990). The parvalbumin-containing nonpyramidal neurons in the rat hippocampus. Anatomy and Embryology **181**, 413-425.

Nowak, L., Bregestovski, P., Ascher, P., Herbet, A.& Prochiantz, A. (1984). Magnesium gates glutamate-activated channels in mouse central neurones. Nature, **307**, 462-465.

Ochiai, E-I. (1988). Uniqueness of zinc as a bioelement. Journal of Chemical Education, **65**, 943-947.

Olpe, H.-R., Karlsson, G., Pozza, M.F., Brugger, F., Steinmann, M., Riezen, H.V., Fagg, G., Hall, R.G., Froestl, W. & Bittiger. H. (1990). CGP 35348: a centrally active blocker of $GABA_B$ receptors. Eur. J. Pharmacol., **187**, 27-38.

Olsen, R.W. & Tobin, A.J. (1990). Molecular biology of $GABA_A$ receptors. FASEB., **4**, 1469-1479.

Oyama, Y., Nishi, K., Yatani, A. & Akaike, N. (1982). Zinc current in helix soma membrane. Comp. Biochem. Physiol., **72C**, 403-410.

Pasternak, C.A. (1988). A novel role of Ca^{2+} and Zn^{2+}: protection of cells against membrane damage. Biosci. Rep., **8**, 579-683.

Peet, M.J., Curry, K., Magnuson, D.S. & Mclennan, H. (1986). Ca^{2+}-dependent depolarization and burst firing of rat CA1 pyramidal neurones induced by N-methyl-D-aspartic acid and quinolinic acid: antagonism by 2-amino-5-phosphonovaleric and kynurenic acids. Can. J. Physiol. Pharmacol., **64**, 163-168.

Pei, Y., Zhao, D., Huang, J. & Cao, L. (1983). Zinc-induced seizures: A new experimental model of epilepsy. Epilepsia, **24**, 169-176.

Pérez-Clausell, J. & Danscher, G. (1985). Intravesicular localïzation of zinc in rat telencephalic boutons. A histochemical study. Brain Res., **337**, 91-98.

Pérez-Clausell, J. & Danscher, G. (1986). Release of zinc sulphide accumulations into synaptic clefts after in vitro injection of sodium sulphide. Brain Res., **362**, 358-361.

Perreault, P. & Avoli, M. (1988). A depolarizing inhibitory postsynaptic potential activated by synaptically released γ-aminobutyric acid under physiological conditions in rat hippocampal pyramidal cells. Canadian J. Physiol. Pharmacol. **66**, 1100-1102.

Perreault, P. & Avoli, M. (1989). Effects of low concentrations of 4-aminopyridine on CA1 pyramidal cells of the hippocampus. J. Neurophysiol., **61**, 953-970.

Peters, S., Koh, J. & Choi, D.W. (1987). Zinc selectively blocks the action of N-methyl-D-aspartate on cortical neurons. Science, **236**, 589-593.

Petit, T.L. (1984). Lead-zinc interactions in the central nervous system, with particular reference to the hippocampus. In: Frederickson, C.J., Howell, G.A. & Kasarskis, E.J. (eds) The neurobiology of zinc Part B: deficiency, toxicity, and pathology. Alan R. Liss, Inc., New York, pp. 251-273.

Pittaluga, A., Asaro, D., Pellegrini, G. & Raiteri, M. (1987). Studies on [^{3}H]GABA and endogenous GABA release in rat cerebral cortex suggest the presence of autoreceptors of the $GABA_B$ type. Eur. J. Pharmacol., **144**, 45-52.

Porsche, E. (1983). Zinc prevents kainic acid seizures in rats. IRCS. Med. Sci., **11**, 599.

Prasad, A. S. (1988). Zinc in growth and development and spectrum of human zinc deficiency. Journal of the American College of Nutrition, **7**, 377-384.

Rassendren, F-A., Lory, P., Pin, J-P. & Nargeot, J. (1990). Zinc has opposite effects on NMDA and non-NMDA receptors expressed in xenopus oocytes. Neuron, **4**, 733-740.

Reymann, K.G., Brödemann, R., Kase, H. & Matthies, H. (1988). Inhibitors of calmodulin and protein kinase C block different phases of hippocampal long-term potentiation. Brain Res. **461**, 388-392.

Reynolds, A. F., Ojemann, G.A. & Ward, Jr. A.A. (1981). Intracellular records from chronic alumina epileptogenic foci in the monkey. Epilepsia, **22**, 147-152.

Reynolds, I.J. & Miller, R.J. (1988). Tricyclic antidepressants block N-methyl-D-aspartate receptors: similarities to the action of zinc. Br. J. Pharmacol., **95**, 95-102.

Rovira, C. & Ben-Ari, Y. (1990). Benzodiazepine fails to potentiate GABA responses in immature CA3 hippocampal neurons. Eur, J. Neurosci., Suppl., **3**, p.24.

Rutecki, P.A., Lebeda, F.J. & Johnston, D. (1987). 4-aminopyridine produces epileptiform activity in hippocampus and enhances synaptic excitation and inhibition. J. Neurophysiol., **57**, 1911-1924.

Sah, P., Hestrin, S. & Nicoll, R.A. (1990). Properties of excitatory postsynaptic currents recorded in vitro from rat hippocampal interneurones. J. Physiol., **430**, 605-616.

Sandler, R. & Smith, D.A. (1991). Coexistence of GABA and glutamate in mossy fiber terminals of the primate hippocampus: An ultrastructural study. J. Comparative Neurology **303**, 177-192.

Sandyk, R. (1991). Zinc deficiency and cerebellar disease. Inter. J. Neurosci. **60**, 21-26.

Savage, D.D., Montano, C.Y. & Kasarskis, E.J. (1989). Quantitative histofluorescence of hippocampal mossy fiber zinc. Brain Res., **49**, 257-267.

Savage, D.D., Montano, C.Y., Paxton, L.L. & Kasarskis, E.J. (1989). Prenatal ethanol exposure decreases hippocampal mossy fiber zinc in 45-day-old rat. Alcoholism (NY), **13**, 588-593.

Scharfman, H.E. & Schwartzkroin, P.A. (1988). Electrophysiology of morphologically identified mossy cells of the dentate hilus recorded in guinea pig hippocampal slices. J. Neurosci., **8**, 3812-3821.

Schneiderman, J.H. & MacDonald, J.F. (1989). Excitatory amino acid blockers differentially affect bursting of in vitro hippocampal neurons in two pharmacological models of epilepsy. Neuroscience, **31**, 593-603.

Schwartzkroin, P.A. (1975). Characteristics of CA1 neurons recorded intracellularly in the hippocampal in vitro slice preparation. Brain Res., **85**, 423-436.

Schwartzkroin, P.A. (1977). Further characteristics of hippocampal CA1 cells in vitro. Brain Res., **128**, 53-68.

Schwartzkroin, P.A. (1982). Development of rabbit hippocampus: physiology. Dev. Brain Res., **2**, 469-486.

Schwartzkroin, P.A. (1990). $GABA_B$ receptor function in the hippocampus: development and control of excitability. In: Bowery, N.G., Bittiger, H. & Olpe, H.-R. (eds) $GABA_B$ receptors in mammalian function. John Wiley & Sons, Chichester, New York, Brisbane, Toronto, Singapore, pp. 223-238.

Schwartzkroin, P.A. & Kunkel, D.D. (1982). Electrophysiology and morphology of the developing hippocampus of fetal rabbits. J. Neurosci., **2**, 448-462.

Schwartzkroin, P.A., Kunkel, D.D. & Mathers, L.H. (1982). Development of rabbit hippocampus: Anatomy. Dev. Brain Res., **2**, 453-468.

Schwarztkroin, P.A. & Mathers, L.H. (1978). Physiological and morphological identification of a non-pyramidal hippocampal cell type. Brain Res. **157**, 1-10.

Schwartzkroin, P.A. & Prince, D.A. (1978). Cellular and field potential properties of epileptogenic hippocampal slices. Brain Res., **147**, 117-130.

Schwartzkroin, P.A. & Wester, K. (1975). Long-lasting facilitation of a synaptic potential following tetanization in the in vitro hippocampal slice. Brain Res., **89**, 107-119.

Seabrook, G.R., Howson, W. & Lacey, M.G. (1990). Electrophysiological characterization of potent agonists and antagonists at pre- and postsynaptic

$GABA_B$ receptors on neurones in rat brain slices. Br. J. Pharmacol., **101**, 949-957.

Segal, M. (1990). A subset of local interneurons generate slow inhibitory postsynaptic potentials in hippocampal neurons. Brain Res., **511**, 163-164.

Seress, L. & Ribak, C.E. (1985). A combined Golgi-electron microscopic study of non-pyramidal neurons in the CA1 area of the hippocampus. J. Neurocytology **14**, 717-730.

Sim, J.A. & Cherubini, E. (1990). Submicromolar concentrations of zinc irreversibly reduce a calcium-dependent potassium current in rat hippocampal neurons in vitro. Neuroscience, **36**, 623-629.

Simmonds, M.A., Turner, J.P. & Harrison, N.L. (1984). Interaction of steroids with the $GABA_A$ receptor complex. Neuropharmacol. **23**, 877-878.

Sladeczek, F., Pin, J-P., Recasens, M., Bockaert, J. & Weiss, S. (1985). Glutamate stimulates inositol phosphate formation in striatal neurones. Nature, **317**, 716-719.

Slevin J.T. & Kasarskis, E.J. (1985). Effects of zinc markers of glutamate and aspartate neurotransmission in rat hippocampus. Brain Res., **334**, 281-186.

Sloviter, R.S. (1985). A selective loss of hippocampal mossy fiber Timm stain accompanies granule cell seizure activity induced by perforant path stimulation. Brain Res., **330**, 150-153.

Smart, T.G. (1987). Single calcium-activated potassium channels recorded from cultured rat sympathetic neurones. J. Physiol., **389**, 337-360.

Smart, T.G. (1989). Excitatory amino acids: the involvement of second messengers in the signal transduction process. Cell. Mol. Neurobiol., **9**, 193-206.

Smart, T.G. (1990). Uncultured lobster muscle, cultured neurons and brain slices: the neurophysiology of zinc. J. Pharm. Pharmacol., **42**, 377-387.

Smart, T.G. (1992). A novel modulatory binding site for zinc on the $GABA_A$ receptor complex in cultured rat neurones. J. Physiol. **447**, 587-625.

Smart, T.G. & Constanti, A. (1982). A novel effect of zinc on the lobster muscle GABA receptor. Proc. R. Soc. Lond. B, **215**,

Smart, T.G. & Constanti, A. (1983). Pre- and postsynaptic effects of zinc on in vitro prepyriform neurones. Neurosci. Lett., **40**, 205-211.

Smart, T.G. & Constanti, A. (1990). Differential effect of zinc on the vertebrate $GABA_A$-receptor complex. Br. J. Pharmacol., **99**, 643-654.

Smart, T.G., Moss, S.J., Xie, X. & Huganir, R.L. (1991). $GABA_A$ receptor are differentially sensitive to zinc: dependence on subunit composition. Br. J. Pharmacol., **103**, 1837-1839.

Soltesz, I., Haby, M., Leresche, N & Crunelli, V. (1988). The $GABA_B$ antagonist phaclofen inhibits the late K^+-dependent IPSP in cat and rat thalamic and hippocampal neurones. Brain Res., **448**, 251-354.

Spyker, D.A., Linch, C., Shabanowitz, J. & Sinn, J.A. (1980). Poisoning with 4-aminopyridine: report of three cases. Clin. Toxicol., **16**, 487-497.

Stanfield, P.R. (1975). The effect of zinc ion on the gating of the delayed potassium conductance of frog sartorius muscle. J. Physiol., **251**, 711-735.

Stengaard-Pedersen, K., Fredens, K. & Larsson, L.-I. (1981). Enkephalin and zinc in the hippocampal mossy fiber system. Brain Res., **212**, 230-233.

Sterman, M.B., Shouse, M.N., Fairchild, M.D. & Belsito, O. (1986). Kindled seizure induction alters and is altered by zinc absorption. Brain Res., **383**, 382-386.

Stone, T.W. & Connick, J.H. (1985). Quinolinic acid and other kynurenines in the central nervous system. Neuroscience, **15**, 597-617.

Storm, J.F. (1988). Temporal integration by a slowly inactivating K^+ current in hippocampal neurons. Nature, **336**, 379-381.

Stratton, K.R., Cole, A.J., Pritchett, J., Eccles, C.U., Worley, P.F. & Baraban, J.M. (1989). Intrahippocampal injection of pertussis toxin blocks adenosine suppression of synaptic responses. Brain Res., **494**, 359-364.

Stratton, K.R., Worley, P. & Baraban, M. (1990). Pharmacological characterization of phosphoinositide-liked glutamate receptor excitation of hippocampal neurones. Eur. J. Pharmacol., **186**, 357-361.

Study, R.E. & Barker, J.L. (1981). Diazepam and (-)- pentobarbital: Fluctuation analysis reveals different mechanisms for potentiation of γ-aminobutyric acid responses in cultured central neurons. Proc. Natl. Acad. Sci. USA. **78**, 7180-7184.

Sugiyama, H., Ito, I. & Hirono, C. (1987). A new type of glutamate receptor linked to inositol phospholipid metabolism. Nature, **325**, 531-533.

Swann, J.W. & Brady, R.J. (1984). Penicillin-induced epileptogenesis in immature rat CA3 hippocampal pyramidal cells. Dev. Brain Res., **12**, 243-254.

Swann, J.W. Brady, R.J. & Martin, D.L. (1989). Postnatal development of GABA-mediated synaptic inhibition in rat hippocampus. Neuroscience, **28**, 551-561.

Swanson, L.W. (1983). The hippocampus and the concept of the limbic system. In: Seifert, W. (eds) Neurobiology of the hippocampus. Academic Press, London,

New York, Paris, San Diego, San Francisco, Sáo Paulo, Sydney, Tokyo, Toronto, pp. 3-19.

Swartzwelder, H.S., Anderson, W.W. & Wilson, W.A. (1988). Mechanism of electrographic seizure generation in the hippocampal slice in Mg^{2+}-free medium: the role of $GABA_A$ inhibition. Epilepsy Res., **2**, 239-245.

Szerdahelyi, P. & Kása, P. (1983). Variations in trace metal levels in rat hippocampus during ontogenetic development. Anat. Embryol., **167**, 141-149.

Szerdahelyi, P. & Kása, P. (1987). Partial depletion and altered distribution of synaptic zinc in the rat hippocampus after treatment with sodium diethydithiocarbamate. Brain Res., **422**, 287-294.

Tancredi, V. & Avoli, M. (1987). Control of spontaneous epileptiform discharges by extracellular potassium: an "in vitro" study in the CA1 subfield of the hippocampal slice. Exp. Brain Res., **67**, 363-372.

Tancredi, V., Hwa, G.G.C., Zona, C., Brancati, A. & Avoli, M. (1989). Low magnesium epileptogenesis in the rat hippocampal slice electrophysiological and pharmacological features. Brain Res., **511**, 280-290.

Taube, J.S. & Schwartzkroin, P.A. (1987). Intracellular recording from hippocampal CA1 interneurons before and after development of long-term potentiation. Brain Res., **419**, 32-38.

Taylor, J. & Gordon-Weeks, P.R. (1989). Developmental changes in the calcium dependency of γ-aminobutyric acid release from isolated growth cones: correlation with growth cone morphology. J. Neurochem., **53**, 834-843.

Taylor, J., Docherty, M. & Gordon-Weeks, P.R. (1990). GABAergic growth cones: release of endogenous γ-aminobutyric acid precedes the expression of synaptic vesicle antigens. J. Neurochem., **54**, 1689-1699.

Teyler, T.J. (1980). Brain slice preparation: hippocampus. Brain. Res. Bull., **5**, 391-403.

Thalmann, R.H. (1988). Blockade of a late inhibitory postsynaptic potential in hippocampal CA3 neurons in vitro reveal a late depolarizing potential that is augmented by pentobarbital. Neurosci. Lett., **95**, 155-160.

Thesleff, S. (1980). Aminopyridines and synaptic transmission. Neuroscience, **5**, 1413-1419.

Thompson, S.M. & Gähwiler, B.H. (1989a). Activity-dependent disinhibition. I. Repetitive stimulation reduces IPSP driving force and conductance in the hippocampus in vitro. J. Neurophysiol., **61**, 501-511.

Thompson, S.M. & Gähwiler, B.H. (1989b). Activity-dependent Disinhibition. II. Effects of extracellular potassium, furosemide, and membrane potential on E_{Cl}^- in hippocampal CA3 neurons. J. Neurophysiol., **61**, 512-523.

Thompson, S.M. & Gähwiler, B.H. (1989c). Activity-dependent Disinhibition. III. Desensitization and $GABA_B$ receptor-mediated presynaptic inhibition in the hippocampus in vitro. J. Neurophysiol., **61**, 524-533.

Thompson, S.M. & Gähwiler, B.H. (1992). Comparison of the action of baclofen at pre- and postsynaptic receptors in the hippocampus *in vitro*. J. Physiol. in press.

Timm, F. (1958). Sur histochemie der Schwermetalle, das sulfid-silber-ferfahren. Otsch. Z. Gesamte Gerichtl. Med. **46**, 706.

Thomson, A.M. & West, D.C. (1986). N-methylaspartate receptors mediate epileptiform activity evoked in some, but not all, conditions in rat neocortical slices. Neuroscience, **19**, 1161-1177.

Tokuoka, S., Fuchimoto, T., Hiraoka, H., Takashima, M., Fujii, M. & Watanabe, M. (1967). Neurochemical considerations on the alleviating effect of caudal resection of the pancreas on epileptic seizures: relationship of zinc metabolism to brain excitability. Bull Yamaguchi Med. School, **14**, 1-19.

Todd, W.R., Elvehjem, C.A. & Hart, E.B. (1934). Zinc in the nutrition of the rat. Am. J. Physiol., **146**, 146-256.

Traub, R.D. & Wong, R.K.S. (1983). Synchronised burst discharge in disinhibited hippocampal slice. II. Model of cellular mechanism. J. Neurophysiol., **49**, 459-471.

Turner, D.A. (1990). Feed-forward inhibitory potentials and excitatory interactions in guinea-pig hippocampal pyramidal cells. J. Physiol., **422**, 333-350.

Turner, D.A. & Schwartzkroin, P.A. (1984). Passive electrotonic structure and dendritic properties of hippocampal neurons. In: Dingledine, R. (eds) Brain slices. Plenum Press. New York and London, pp. 25-50.

Vallee, B.L. & Auld, D.S. (1990). Zinc coordination, function, and structure of zinc enzymes and other proteins. Biochem., **29**, 5647-5659.

Vallee, B.L. & Galdes, A. (1984). The metallobiochemistry of zinc enzymes. Adv. Enzymol. Relat. Mol. Biol., **56**, 283-430.

Vayer, P., Mandel, P. & Maitre, M. (1987). Gamma-Hydroxybutyrate, a possible neurotransmitter. Life Sci., **41**, 1547-1557.

Verdoorn, T.A. Burnashev, N., Monyer, H., Seeburg, P.H. & Sakmann, B. (1991). Structural determinants of ion flow through recombinant glutamate receptor channels. Science, **252**, 1715-1718.

Verdoorn, T.A., Draguhn, A., Ymer, S., Seeburg, P.H. & Sakmann, B. (1990). Functional properties of recombinant rat $GABA_A$ receptors depend upon subunit composition. Neuron, **4**. 919-928.

Visentin, S., Zaza, A., Ferroni, A. Tromba, C. & DiFrancesco, C. (1990). Sodium current block caused by group IIb in calf Purkinje fibres and in guinea-pig ventricular myocytes. Pflügers Arch., **417**, 213-222.

Wallwork, J. & Crawford, L. (1987). Effect of zinc nutriture on amygdala kindling in the adult rat. Fed. Proc., **46**, 885.

Wang, Y.X. & Quastel, D.M.J. (1990). Multiple actions of zinc on transmitter release at mouse end-plates. Pflügers Arch., **415**, 582-587.

Watkins, J.C. & Evans, R.H. (1981). Excitatory amino acid transmitters. Ann. Rev. Pharmacol. Toxicol., **21**, 165-204.

Watson, G.B., Rader, R.K. & Lanthorn, T.H. (1989). Epileptiform activity in vitro can produce long-term synaptic failure and persistent neuronal depolarization. Brain Res., **498**, 81-88.

Weiss, J.H., Koh, J.Y., Christina, C.W. & Choi, D.W. (1989). Zinc and LTP. Nature, **338**, 212.

Wensink, J., Molenaar, A.J., Woroniecka, U.D. & Van den Hamer, C.J.A. (1988). Zinc uptake into synaptosomes. J. Neurochem., **50**, 782-789.

Werner, P., Voigt, M., Keinänen, K., Wisden, W. & Seeburg, P.H. (1991). Cloning of a putative high-affinity kainate receptor expressed predominantly in hippocampal CA3 cells. Nature, **351**. 742-744.

Westbrook, G.L. & Mayer, M.L. (1987). Micromolar concentration of Zn^{2+} antagonize NMDA and GABA responses of hippocampal neurons. Nature, **328**, 640-643.

Williams, S & Johnston, D. (1989). Long-term potentiation of hippocampal mossy fiber synapses is blocked by postsynaptic injection of calcium chelators. Neuron, **3**, 583-588.

Williams, S & Lacaille, J-C. (1990). Bicuculline- and phaclofen-resistant hyperpolarizations evoked by glutamate applications to stratum lacunosum-moleculare in CA1 pyramidal cells of the rat hippocampus in vitro. Eur. J. Neurosci., **2**, 993-1003.

Wilson, W.A. & Goldner, M.M. (1975). Voltage clamping with a single microelectrode. J. Neurobiol. **6**, 411-422.

Winegar, B.D. & Lansman, J.B. (1990). Voltage-dependent block by zinc of single calcium channels in mouse myotubes. J. Physiol., **425**, 563-578.

Wolf, G., Schütte, M. & Römhild, W. (1984). Uptake and Subcellular distribution of zinc in brain structures during the postnatal development of the rat. Neurosci. Lett., **51**, 277-280.

Wong, R.K.S. & Traub, R.D. (1983). Synchronized burst discharge in disinhibited hippocampal slice. I. Initiation in CA2-CA3 region. J. Neurophysiol., **49**, 442-458.

Wright, D.M. (1984). Zinc: effect and interaction with other cations in the cortex of the rat. Brain Res., **311**, 343-347.

Xie, X. & Smart, T.G. (1991a). A physiological role for endogenous zinc in rat hippocampal synaptic neurotransmission. Nature, **349**, 521-524.

Xie, X. & Smart, T.G. (1991b). GABA-mediated giant depolarizing synaptic potentials induced by zinc in adult rat hippocampal pyramidal neurones. Br. J. Pharmacol. **102**, 300P.

Xie, X. & Smart, T.G. (1991c). Paradoxical effects of zinc and barium on baclofen-induced postsynaptic responses and $GABA_B$-mediated IPSPs in rat hippocampus. Eur. J. Neuroscience suppl., **4**, 3235P.

Xie, X. & Smart, T.G. (1992). γ-hydroxybutyrate hyperpolarizes hippocampal neurones by activating $GABA_B$ receptors. Eur. J. Pharmacol., **212**, 291-294.

Yakushiji, T., Tokutomi, N., Akaike, N. & Carpenter, D.O. (1987). Antagonists of GABA responses, studied using internally perfused frog dorsal root ganglion neurons. Neuroscience, **22**, 1123-1133.

Yokoyama, M., Koh, J & Choi, D.W. (1986). Brief exposure to zinc is toxic to cortical neurons. Neurosci. Lett., **71**, 351-355.

Zalutsky, R.A. & Nicoll, R.A. (1990). Comparison of two forms of long-term potentiation in single hippocampal neurons. Science, **248**, 1619-1624.

Zimmer, J. & Haug, F.S. (1978). laminar differentiation of the hippocampus, fascia dentatae and subiculum in developing rats, observed with the Timm sulphide silver method. J. Comp. Neur., **179**, 581-618.

PUBLICATIONS

Xie, X. & Smart, T.G. (1991). A physiological role for endogenous zinc in rat hippocampal synaptic neurotransmission. Nature, **349**, 521-524.

Smart, T.G., Moss, S.J., Xie, X. & Huganir, R.L. (1991). $GABA_A$ receptor are differentially sensitive to zinc: dependence on subunit composition. Br. J. Pharmacol., **103**, 1837-1839.

Xie, X. & Smart, T.G. (1992a). γ-hydroxybutyrate hyperpolarizes hippocampal neurones by activating $GABA_B$ receptors. Eur. J. Pharmacol., **212**, 291-294.

Xie, X. & Smart, T.G. (1991a). GABA-mediated giant depolarizing synaptic potentials induced by zinc in adult rat hippocampal pyramidal neurones. Br. J. Pharmacol. **102**, 300P.

Xie, X. & Smart, T.G. (1991b). Paradoxical effects of zinc and barium on baclofen-induced postsynaptic responses and $GABA_B$-mediated IPSPs in rat hippocampus. Eur. J. Neuroscience suppl., **4**, 3235P.

Smart, T.G., Xie, X., Bowie, D., Moss, S.J. & Huganir, R.L. (1991). $GABA_A$ receptor subunit composition underlies the differential sensitivity to inhibition by zinc. Eur. J. Neuroscience suppl., **4**, 3234P.